

The molecular basis of peroxisome proliferation

by

Alex R. Bell, B.Sc.

Being a thesis presented in accordance with the regulations
governing the award of the degree of Doctor of Philosophy at
the University of Nottingham

April 1998

Abstract

Characterisation of expression of functional Peroxisome Proliferator Activated Receptor α (PPAR α) receptor in rodent species responsive and non-responsive to peroxisome proliferators is important for our understanding of the molecular mechanism of peroxisome proliferation and peroxisome proliferator induced hepatocarcinogenesis. In vitro electromobility shift assays, demonstrated that rodent liver nuclear proteins (LNP) bound to a Peroxisome Proliferator Response Element (PPRE) in a sequence specific manner and that LNP from methyldclofenapate (MCP) treated mice do not have enhanced binding to a PPRE. These results demonstrate that in MCP treated mice, PPAR α levels with functional DNA binding do not increase. The diurnal expression of mouse PPAR α (mPPAR α) protein in liver was examined by western blotting. There was no observable difference in the expression of mPPAR α across a 24 hour period. In C57 BL/6 mice, PPAR α protein levels are not regulated in a diurnal manner.

A comparison of mouse and guinea pig LNP revealed a PPAR α -immunoreactive protein in guinea pig. Guinea Pig PPAR α (gPPAR α) was cloned and found to encode a 467 amino acid protein. Phylogenetic analysis of gPPAR α showed a high substitution rate: maximum likelihood analysis was consistent with rodent monophyly, but could not exclude rodent polyphyly ($p \sim 0.07$). The gPPAR α cDNA was expressed in 293 cells, and mediated the induction of the luciferase reporter gene by the peroxisome proliferator Wy-14,643, dependent upon the presence of a PPRE. The gPPAR α mRNA and protein was expressed in guinea pig liver, although at lower levels compared to PPAR α expression in mice. The evidence presented here supports the idea that guinea pigs serve as a useful model for human responses to peroxisome proliferators.

mPPAR α DNA binding domain (mPPAR α -DBD) was cloned and expressed as a fusion protein. Both His \star 6-mPPAR α -DBD and thioredoxin-mPPAR α -DBD were produced as insoluble proteins when over expressed in *E.coli*. In vitro translated mPPAR α -DBD did not bind to a PPRE in an electromobility shift assay.

Abbreviations

ACO	Acyl-CoA oxidase
Amp	Ampicillin antibiotic
Chl	Chloramphenicol antibiotic
CoA	Coenzyme
con4A6z	cytochrome P450 4A6 gene PPRE with consensus 5'flanking sequence
COUP-TF	Chicken ovalbumin upstream promoter-transcription factor
DEN	Diethylnitrosoamine
DEPC	Diethyl Pyrocarbonate
DEHA	Di(2-ethylhexyl)adipate
DEHP	Di(2-ethylhexyl)phthalate
DFPS	Dulbecco's modified eagles medium supplemented with foetal calf serum, penicillin and streptomycin
dmACO-PPRE	double mutant Acyl-CoA oxidase peroxisome proliferator response element
DMSO	Dimethyl Sulphoxide
Dope	L- α -phosphatidylethanolamine, dioleoyl(C18:1,[cis]-9)
Dotma	(N-[I-(2,3-dioleyloxy)propyl]-N,N,N-triethylammonium

DR1	Direct Repeat element with a single nucleotide spacer
EDTA	Ethylenediaminetetraacetic acid
EMSA	Electromobility Shift Assay
ER	Estrogen Receptor
GR	Glucocorticoid Receptor
HNF-4	Hepatic Nuclear Factor-4
LB	Luria-Bertani Broth
mACO-PPRE	single mutant Acyl-CoA oxidase peroxisome proliferator response element
MCP	Methylclofenapate
ORF	Open Reading Frame
PAGE	Polyacrylamide Gel Electrophoresis
PCR	Polymerase Chain Reaction
PPAR	Peroxisome Proliferator-Activated Receptor
PPRE	Peroxisome Proliferator Response Element
PVDF	Polyvinylidene difluoride
RAR	Retinoic Acid Receptor
RXR	Retinoid X Receptor

SDS	Sodium Dodecyl Sulphate
SRC	Steroid Coactivator-1 protein
Tet	Tetracyclin antibiotic
TR	Thyroid Hormone Receptor
UHP	Ultra High Pure Water (double-deionised and 0.22 micron-filtered)
VDR	Vitamin D Receptor
Wy-14,643	[4-chloro-6(2,3-xylidino)-2-pyrimidinylthio] acetic acid
X-Gal	5-bromo-4-chloro-3-indolyl- β -D-galactoside
293 cells	Human embryonic kidney cell line

Acknowledgments

I would like to thank David Bell, my supervisor during my Ph.D., for all his enthusiasm, encouragement and dedication in getting me to complete my work. I leave Nottingham knowing that if any of his enthusiasm for science has rubbed off on to me I should be successful in my future career. I wish to acknowledge the Wellcome trust for their funding of this project. I wish to thank Declan Brady (the lab's technician). He has made many a mean gel, buffer or bug culture for me as well as playing a mean game of Doom and Quake with me. Next, I would like to thank Neill Horley for his help in training me to do tissue culture. I must not fail to mention his humour and colourful language. One should endeavor to experience it to understand what I mean. Yee Heng and Alex Gage both get a special mention as they have contributed to my spiritual well being. Our conversations, both in the lab, and in the pub will not be forgotten in a hurry. I say to them both wax your board and catch a big one. There are many other people who have contributed in a positive way during my time at Nottingham, in ways which are too numerous to mention. These people are Sharon Kuo, Simon Thomlinson, Louise Oram, Munim Choudhury, Richard Savory, Paul Jones, Nick Plant and John Keyte.

Lastly, and the most important person to me over the last three and a half years has been my wife Fiona. She has stood by me through thick and thin, constantly supporting and loving me without ever asking for it in return. She has done more than the lions share of work in looking after our daughter Caitlin, making my life as easy as possible, especially during the last 18 months of my Ph. D.

Dedication

This thesis is dedicated to Fiona and Caitlin, for they are the foundation rock upon which I strive to better our lives, at work, home and at play.

Table of Contents

Abstract	2
Abbreviations	3
Acknowledgments	6
Dedication	6
Table of Contents	7
List of Figures	13
List of Tables	15
I Introduction	16
I.1 Peroxisome proliferation	16
I.1.1 Peroxisomes and their general function	16
I.1.2 Morphology of mammalian peroxisomes	16
I.1.3 Peroxisomal β-Oxidation	17
I.1.4 Peroxisomal diseases and disorders	18
I.1.5 Peroxisome proliferating chemicals	18
I.1.6 Peroxisome proliferation	20
I.1.7 Peroxisome proliferators are hepatocellular carcinogens	22
I.1.8 Peroxisome proliferators are non-genotoxins	22
I.1.9 Peroxisome proliferators and tumour promotion	23
I.1.10 Peroxisome proliferators induce cell transformation	24
I.1.11 Peroxisome proliferator induced oxidative damage to DNA	24
I.1.12 Peroxisome proliferator-induced hepatic DNA lesions	25
I.1.13 Human hazard risk assessment of peroxisome proliferators	26
I.1.14 Peroxisome proliferation in hamster	27
I.1.15 Peroxisome proliferation in guinea pig	28
I.1.16 Peroxisome proliferation in primates	29
I.1.17 Peroxisome proliferation in humans	30
I.1.18 Models of peroxisome proliferation in non-responsive species	31
I.2 Peroxisome proliferated activated receptor	32
I.2.1 Cloning of a receptor which mediates peroxisome proliferation	32
I.2.2 Cloning of PPAR genes	33
I.2.3 Guinea pigs as a model for peroxisome proliferation in humans	33
I.2.4 Expression of PPARα gene	34
I.2.5 Peroxisome proliferators and PPARα gene expression	34
I.2.6 Hormonal regulation of PPARα gene expression	36
I.2.7 Expression of PPARδ and PPARγ genes	37

1.2.8 Peroxisome Proliferators are ligands for PPAR α	37
1.2.9 Peroxisome Proliferator Response Elements (PPREs)	39
1.2.10 PPAR α binds to PPREs with Retinoid X Receptor as a heterodimer	41
1.3 Nuclear steroid hormone receptors	43
1.3.1 Nuclear receptors bind DNA in a polarity specific manner	43
1.3.2 Nuclear receptor cross talk regulates transcription.	43
1.3.3 Phosphorylation regulates nuclear steroid hormone receptor function	45
1.3.4 DNA binding domains define specific DNA interactions	45
1.3.5 DNA binding domains contain important dimerisation sequences	47
1.3.6 Ligand binding domains contain important dimerisation sequences	47
1.3.7 LBDs interact with basal transcription machinery	48
1.3.8 Nuclear steroid hormone receptors contain two transcriptional activation domains	
48	
1.3.9 Nuclear receptors interact with co-activator proteins	49
1.3.10 Differential promoter usage and alternative splicing	50
1.4 Summary	53
1.5 Experimental objectives	54
2 Methods	55
2.1 Laboratory animals	55
2.2 General Molecular Biology Techniques.	55
2.2.1 Bacterial growth media	55
2.2.2 Preparation of CaCl ₂ competent XL1 Blue E.coli and BL21 (DE3) pLys S E.coli	55
2.2.3 Transformation of DNA into CaCl ₂ competent <i>E.coli</i>	56
2.2.4 Preparation of electro-competent <i>E.coli</i>	56
2.2.5 Transformation of electro- competent <i>E.coli</i>	57
2.2.6 Phenol:Chloroform treatment of nucleic acids.	57
2.2.7 Precipitation of nucleic acids using the ethanol / sodium acetate protocol.	58
2.2.8 Plasmid DNA purification by Alkaline lysis method	58
2.2.9 Purification of plasmid DNA on Qiagen Mini-prep and Maxi-prep columns . . .	59
2.2.9.1 Mini-prep method	60
2.2.9.2 Maxi-prep method.	61
2.2.10 Purification of PCR products	61
2.2.11 Restriction endonuclease digests of DNA samples	62

2.2.12	Shrimp Alkaline Phosphatase (SAP) treatment of vectors.	63
2.2.13	Purification of DNA excised from an agarose gel,	63
2.2.14	Non denaturing electrophoresis in agarose gels.	64
2.2.15	DNA sequencing method	65
2.2.16	Purification of total RNA	66
2.2.17	Purification of polyA ⁺ RNA	67
2.2.18	Incorporation of [³² P]-labelled nucleotides	68
2.3	Protein methodologies	69
2.3.1	Purification of liver nuclear proteins.	69
2.3.2	Bradford (Coomassie Blue) Protein Assay	70
2.3.3	Polyacrylamide gel electrophoresis of proteins (PAGE)	71
2.3.4	Immunoblotting analysis of liver nuclear protein extracts	72
2.4	cDNA cloning methodologies	74
2.4.1	Synthesis of 1st strand cDNA by reverse transcription	74
2.4.1.1	1st strand cDNA synthesised using total RNA as a template.	74
2.4.1.2	1st strand cDNA synthesised using poly A ⁺ RNA.	75
2.4.2	PCR Amplification of guinea pig cDNA's.	75
2.4.3	Ligation of amplified putative guinea pig PPAR α cDNA fragments.	76
2.5	Amplification of 5'-cDNA ends using RACE	77
2.5.1	Purification of cDNA	79
2.5.2	Homopolymeric tailing of cDNA	79
2.5.3	PCR amplification of dC-tailed cDNA	79
2.5.4	Cloning and sequencing of 5' cDNA ends.	80
2.6	Overlapping PCR method	81
2.6.1	Cloning of 1.4kb cDNA into pBK-CMV	84
2.7	In vitro transcription and translation	85
2.8	RNA protection assays	86
2.8.1	Synthesis of RNA probes for RNA protection assay	86
2.8.2	Synthesis of [α - ³² P]dCTP labelled 100 bp DNA ladder	87
2.8.3	Determination of gene expression levels using an RNA protection assay	87
2.8.4	RNase protection assay	89
2.9	Tissue culture procedures	90
2.9.1	Growth and Passage of Human Embryonic Kidney 293 cells	90

2.9.2	Resurrection of frozen 293 cells	90
2.9.3	Passage of 293 cells	91
2.9.4	Synthesis of cationic liposome transfection reagent	92
2.9.5	Synthesis of (ACO-PPRE)2.pGL3-Luc reporter vector	92
2.9.6	293 cell transfection protocol	93
2.9.7	β -galactosidase histochemistry (Sanes, J.R. et al 1986)	94
2.9.8	Cell extract harvesting for reporter assays	95
2.9.9	Chloramphenicol acetyltransferase assay	95
2.9.10	Firefly luciferase assay	96
2.9.11	Dual luciferase assay	97
2.10	Cloning of PPAR α DNA binding domain	97
2.11	Cloning of thioredoxin-mPPAR α fusion	99
2.12	Expression of DBD fusion proteins in <i>E.coli</i>	100
2.12.1	Small scale cultures	100
2.12.2	Large scale culture	100
2.13	Purification of DBD fusion proteins	102
2.13.1	Clontech Talon affinity resin	102
2.13.2	Invitrogen ProBond Resin	103
2.14	<i>In vitro</i> coupled transcription/translation	104
2.15	Electromobility shift assay methodologies	105
2.15.1	Electromobility shift assays	105
3	Results	107
3.1	Rat liver nuclear protein binds specifically to a PPRE	107
3.1.1	Mouse liver nuclear proteins bind specifically to a PPRE	110
3.1.2	Binding of mLNP from MCP-treated mice to a PPRE	112
3.1.3	Isolation of liver nuclear proteins	112
3.1.4	Immunoblotting analysis of mouse LNP	114
3.1.5	Expression of mPPAR α protein in guinea and mouse	116
3.1.6	Expression of PPAR α immuno-reactive protein in guinea pig LNP	117
3.2	Cloning of guinea pig PPAR α cDNA	117
3.2.1	Purification of guinea pig RNA	117
3.2.2	PCR amplification of guinea pig 1st strand cDNA	118
3.2.3	5'RACE of guinea pig RNA	121

3.2.4	Sequence analysis of guinea pig cDNAs	I23
3.2.5	Multiple sequence analysis of PPAR α amino acid sequences.	I25
3.2.6	Phylogenetic analysis of PPAR α genes	I28
3.2.7	gPPAR α cDNA contains an extended 5' ORF	I28
3.2.8	A 436 bp gPPAR α clone (GP4) is differentially spliced	I30
3.3	Cloning of full length gPPAR α cDNA	I32
3.3.1	<i>In vitro</i> synthesis of gPPAR α protein	I34
3.4	Functional characterisation of gPPAR α	I34
3.4.1	Optimisation of transfection.	I34
3.4.2	Construction of (ACO-PPRE) reporter plasmid.	I36
3.4.3	Optimisation of transfection normalisation	I36
3.4.4	Induction of luciferase by PPAR α and peroxisome proliferators	I39
3.5	Expression of gPPAR α and mPPAR α mRNA	I42
3.6	Expression of mPPAR α DNA binding domain	I44
3.6.1	Prokaryotic expression of mPPAR α -DBD	I45
3.6.2	Effect of lower temperature on protein solubility	I47
3.6.3	Affinity purification of mPPAR α -DBD protein	I48
3.6.4	Removal of His \star 6 Tag from mPPAR α -DBD	I49
3.6.5	Electromobility shift assay of mPPAR α -DBD	I50
3.6.6	Cloning of thioredoxin-mPPAR α -DBD	I51
3.6.7	Expression of thioredoxin-mPPAR α -DBD protein	I52
3.6.8	<i>In vitro</i> synthesis of mPPAR α -DBD protein	I54
4	Discussion	I57
4.1	The molecular mechanism of peroxisome proliferation	I57
4.1.1	EMSA of LNP binding to DNA response elements	I57
4.1.2	Sequence-specific protein binding to an acyl-CoA oxidase PPRE	I58
4.1.3	Peroxisome proliferators do not affect LNP binding to a PPRE	I59
4.1.4	Mouse PPAR α protein levels do not change across a 24 hour (diurnal) period .	I61
4.1.5	Anti-mPPAR α antibody detects a protein in guinea pig liver	I64
4.2	Cloning of guinea pig PPAR α cDNA	I66
4.2.1	Design of guinea pig PPAR α PCR primers	I66
4.2.2	Amplification of guinea pig cDNAs	I66
4.3	Sequence analysis of the cloned guinea pig cDNAs	I67

4.4	Phylogenetic analysis of mammalian PPAR α genes	171
4.4.1	Is the guinea pig a rodent?	172
4.5	Evidence for alternative splicing of gPPAR α mRNA	174
4.5.1	GP4 gPPAR α cDNA clone contains differential splicing	176
4.6	Cloning of full length gPPAR α cDNA	177
4.7	Functional testing of gPPAR α in a mammalian cell based reporter system	178
4.7.1	Induction of luciferase by PPAR α and peroxisome proliferators	179
4.7.2	Guinea pig PPAR α is activated by a peroxisome proliferator	180
4.8	Guinea pig PPAR α is expressed in liver tissue	183
4.9	Evidence for a functional PPAR α in guinea pig <i>in vivo</i>	185
4.10	Guinea pigs model the non-responsiveness phenotype in humans	185
4.11	Steroid hormone DNA binding domains	187
4.11.1	Cloning of mPPAR α -DBD	187
4.11.2	Expression of mPPAR α -DBD in BL21 (DE3)pLysS <i>E.coli</i>	188
4.11.3	Purification of denatured mPPAR α -DBD	189
4.11.4	Electromobility shift assays of mPPAR α -DBD	190
4.11.5	Recovery of functional DNA binding domain proteins	190
4.11.6	Cloning and expression of thioredoxin-mPPAR α -DBD fusion protein	191
4.11.7	Prokaryotic expression of thioredoxin-mPPAR α -DBD fusion protein	192
4.11.8	<i>In vitro</i> synthesis of mPPAR α -DBD	194
4.11.8	195
5	References.	196

List of Figures

Figure 1.1 The rat acyl-CoA oxidase PPRE	40
Figure 3.1 Rat liver nuclear protein binds specifically to an acyl-CoA oxidase gene PPRE ..	107
Figure 3.2 Rat LNP binding to ACO-PPRE is saturable	108
Figure 3.3 Effect of incubation temperature on ACO-PPRE EMSA.	109
Figure 3.4 Rat LNP does not bind efficiently to a mutant ACO-PPRE	109
Figure 3.5 rLNP does not bind to a double mutant ACO-PPRE	110
Figure 3.6 Binding of mouse LNP to rat acyl-CoA oxidase PPRE probe	111
Figure 3.7 mLNP from mice dosed with MCP does not bind a double mutant PPRE	111
Figure 3.8 ACO-PPRE EMSA with mLNP from control and MCP treated mice	113
Figure 3.9 SDS-Page analysis of mouse liver nuclear proteins	113
Figure 3.10 SDS-Page analysis of guinea pig liver nuclear proteins	114
Figure 3.11 Western blot analysis of purified recombinant mouse PPAR α protein.	115
Figure 3.12 Western blot analysis of mLNP with anti-mPPAR α antibody.	115
Figure 3.13 Western blot analysis of mouse and guinea pig liver nuclear proteins	116
Figure 3.14 Western blot analysis of guinea pig liver nuclear protein	117
Figure 3.15 Analysis of guinea pig liver RNA by agarose gel electrophoresis.	118
Figure 3.16 Alignment of human, mouse and xenopus PPAR α amino acid sequences	119
Figure 3.17 Amplification of guinea pig cDNA with GPIGP2 and GPIGP3 primers	120
Figure 3.18 Analysis of the PCR amplification of guinea pig liver cDNA	121
Figure 3.19 5'RACE of gPPAR α cDNA ends.	121
Figure 3.20 Diagram showing assembly of guinea pig cDNA clones	122
Figure 3.21 cDNA sequence of gPPAR α	123
Figure 3.22 Amino acid sequence of gPPAR α	124
Figure 3.23 Amino acid sequence alignment of mammalian and <i>Xenopus</i> PPAR α 's.	127
Figure 3.24 Phylogenetic analysis of PPAR α genes	128
Figure 3.25 Alignment of cloned gPPAR α protein with AJ000222	129
Figure 3.26 Comparison of gPPAR α cDNA sequence with mPPAR α exon3	130
Figure 3.27 DNA alignment of GP4 clone with gPPAR α cDNA	130
Figure 3.28 gPPAR α GP4 clone contains differentially spliced exons.	131
Figure 3.29 Cartoon of two stage overlapping PCR strategy.	132
Figure 3.30 PCR amplification of full length gPPAR α cDNA	132
Figure 3.31 Cartoon of the cloning of full length gPPAR α cDNA	133

Figure 3.32 SDS-PAGE analysis of <i>in vitro</i> translated gPPAR α , hPPAR α and mRXR α	134
Figure 3.33 Induction of luciferase requires a PPRE	138
Figure 3.34 Effect of plasmid quantity on luciferase expression.	139
Figure 3.35 Optimisation of quantity of transfected DNAs	140
Figure 3.36 Wy-14,643 induces gPPAR α transcriptional activation.	141
Figure 3.37 Expression of gPPAR α and mPPAR α mRNA in liver.	142
Figure 3.38 Expression of gPPAR α mRNA across a 24 hour period.	143
Figure 3.39 PCR amplification of mPPAR α -DBD DNA.	144
Figure 3.40 Cloning of mPPAR α -DBD into pRSET-A vector	145
Figure 3.41 Induction of mPPAR α -DBD protein	146
Figure 3.42 SDS-PAGE of purified proteins from induced cultures.	147
Figure 3.43 Induction of mPPAR α -DBD at 37 C and 30 C	147
Figure 3.44 Purification of protein using Talon resin.	148
Figure 3.45 Purification of mPPAR α -DBD from resolubilised proteins	149
Figure 3.46 Cleavage of His*6 tag from mPPAR α -DBD.	149
Figure 3.47 Binding of His*6 tagged mPPAR α -DBD to con-4A6z PPRE	150
Figure 3.48 Binding of untagged mPPAR α -DBD to con-4A6z PPRE.	151
Figure 3.49 DNA digests of putative pThio-His.A-mPPAR α -DBD clones.	151
Figure 3.50 Induction of thioredoxin-mPPAR α -DBD protein in <i>E.coli</i>	152
Figure 3.51 Purification of soluble thioredoxin-mPPAR α protein	153
Figure 3.52 Purification of soluble thioredoxin-mPPAR α -DBD protein using Talon resin.	154
Figure 3.53 Invitro expression of mPPAR α , mRXR α and mPPAR α -DBD proteins.	155
Figure 3.54 Binding of <i>in vitro</i> translated proteins to con-4A6-PPRE	155

List of Tables

Table 1.1	Examples of peroxisome proliferators.....	19
Table 1.2	Liver enzymes induced by peroxisome proliferators	21
Table 1.3	Sequences of PPREs identified in peroxisome proliferator responsive genes.....	41
Table 3.1	Methylclofenapate induced liver enlargement in C57 Bl / 6 mice	112
Table 3.2	Amino acid sequence identity between gPPAR α and other PPARs.....	125
Table 3.3	Effect of amount of plasmid DNA on transfection efficiency	135
Table 3.4	Effect of amount of Dotma/Dope (DD) on transfection efficiency.....	136
Table 3.5	Summary of CAT and Luc reporter gene activity	137
Table 4.1	Overview of PPAR α mediated induction of reporter genes.....	182

Chapter 1 Introduction

Section 1.1 Peroxisome proliferation

Section 1.1.1 Peroxisomes and their general function

Peroxisomes were discovered to be a distinct biochemical subcellular organelle by the pioneering studies of Christian De Duve in the 1960s (Baudhuin, P. *et al* 1965 and De Duve, C. and Baudhuin, P. 1966). Peroxisomes were originally characterised on their content of catalase and oxidative enzymes. Initially there was an overlap of terminology between descriptions of microbodies, peroxisomes and glyoxysomes due to structural and biochemical similarities. The development of precise biochemical assays, and more refined structural assay techniques, has allowed peroxisomes to be studied in detail. In general, animal peroxisome functions include fatty acid oxidation, plasmalogen biosynthesis, alcohol oxidation, cholesterol synthesis, transaminations and the metabolism of purines, polyamines and bile acids. Long chain fatty acids, steroids, dicarboxylic acids, prostaglandins, and amino acids are some of the substrates required for these metabolic processes (Masters, C. and Crane, D. 1992, Van den Bosch, H. *et al* 1992 and Masters, C.J. 1996).

Section 1.1.2 Morphology of mammalian peroxisomes

Liver peroxisomes are spherical or ovoid, with a diameter of 0.3–1 μm . They are single membraned organelles with a membrane thickness of 4.5–8 nm, thinner than most other single membrane bound structures. In hepatocytes there can be up to 600 individual peroxisomes, occupying a cell volume of approximately 2%. Hepatic peroxisomes often have a crystalloid core, called a nucleoid, containing urate oxidase. The detection of the presence of peroxisomes is facilitated by 3,3'-diaminobenzidine staining using the peroxidative activity of catalase at alkaline pH. In other tissues catalase positive particles are smaller with diameters of 0.05–0.2 μm and lack crystalloid cores (Masters, C. and Crane, D. 1995).

Section 1.1.3 Peroxisomal β -Oxidation

The discovery of peroxisomal involvement in β -oxidation of fatty acids by Lazarow and De Duve 1976, revealed the broad scope of functions carried out by this organelle. The first step in the peroxisomal β -oxidation pathway is to convert long chain free fatty acids to CoA-esters. The reaction to produce the CoA derivative is carried out in the cytoplasm by a variety of acyl-CoA synthetases, using co-enzyme A and ATP. The peroxisome membrane is permeable to CoA-esters. Fatty acids converted to CoA-ester derivative are subject to oxidation in the peroxisome by acyl-CoA oxidase, a multi-subunit flavoprotein. The oxidation of a CoA-ester requires O_2 and produces H_2O_2 (Schultz, H 1991, Van den Bosch, H. *et al* 1992, and Gibson, G. and Lake, B. 1993). The next two steps in the β -oxidation pathway of peroxisomes are catalysed by bifunctional enzyme. Peroxisomal bifunctional protein from rat liver was found to be a trifunctional protein, possessing 2-enoyl-CoA hydratase, 3-hydroxyacyl-CoA dehydrogenase and Δ^3, Δ^2 -enoyl-CoA isomerase activities (Palosaari and Hiltunen 1990). The last stage in the β -oxidation of long chain fatty acids utilises the oxo-acyl-CoA product of step three to form a medium chain fatty acid and acyl-CoA. This reaction is performed by thiolase enzyme. Medium chain fatty acyl-CoAs can be utilised by carnitine acyltransferases and be transported out of the peroxisome into the cytoplasm. From the cytoplasm medium chain fatty acids can be transported to mitochondria for further oxidation, or they may be used for the synthesis of more complex lipids. The function of catalase in the peroxisome is to remove H_2O_2 . The hydrogen donor for the peroxidatic reaction could come from substrates such as phenols, formate, alcohols, nitrites and primary amines (Schultz, H 1991, Van den Bosch, H. *et al* 1992, and Gibson, G. and Lake, B. 1993)

Section 1.1.4 Peroxisomal diseases and disorders

Zellweger syndrome is an inherited general peroxisomal disorder characterised by the absence of functional peroxisomes. Persons born with Zellweger syndrome will die prematurely. An example of impairment of a peroxisomal biochemical pathway in Zellweger syndrome is lack of β -oxidation of fatty acids. This is due to the deficiency of all peroxisomal β -oxidation enzymes, leading to the accumulation of very long chain fatty acids in tissues and blood (Schutgens, R.B.H. *et al* 1986, Moser H.W. 1987 and Lazarow, P.B. and Moser, H.W. 1989). Other general peroxisomal disorders are infantile Refsums disease, neonatal adrenoleukodystrophy and hyperpipecolic acidaemia. These disorders are characterised by multiple peroxisomal enzyme deficiencies, morphologically abnormal peroxisomes, as well as a reduced number or absence of peroxisomes (Moser, H.W. 1993). Two other categories of peroxisomal disorder have been characterised. One category involves limited impairment of peroxisomal function, found in the rhizomelic type of chondrodysplasia punctata and in Zellweger-like syndrome. The other category contains disorders in which a single peroxisomal enzyme has impaired expression or activity, leading to a disease state (Van den Bosch, H. *et al* 1992). The existence of such serious peroxisomal diseases highlights the essential need for correctly functioning peroxisomes in humans.

Section 1.1.5 Peroxisome proliferating chemicals.

Peroxisome proliferators are a family of compounds which when given to rodent species such as rat or mouse, cause common changes to the morphology and biochemistry of the liver. Peroxisome proliferators (PPs) are structurally diverse with no easily identifiable common molecular structure or physical property. The normal functions of the chemicals which make up the peroxisome proliferator family are diverse, ranging from pharmaceutical agents to agricultural herbicides. Physiological conditions such as temperature acclimatisation and nutritional deficiencies can act in the same manner as a peroxisome proliferator (Nedergaard, J. *et al* 1980

and Neat, C.E *et al* 1980). Table 1.1 shows a list of peroxisome proliferators .

Table 1.1 Examples of peroxisome proliferators.

Abbreviations : Fib-HLD, Fibrate hypolipidaemic drug; Non-Fib-HLD ,Non fibrate hypolipidaemic drug; In-Chem., Industrial and agro-chemical compounds such as herbicide, insecticide, wood preservative, and water treatment by-products; Phys., Physiological condition or endogenous substance.

(Green, S. 1992, and Masters, C. and Crane, D. 1995)

Peroxisome Proliferator (PP)	Type of PP	Peroxisome Proliferator (PP)	Type of PP
Clofibrate	Fib-HLD	2,4-Dichlorophenoxy acetic acid	In-Chem
Nafenopin	Fib-HLD	2,4,5-Trichlorophenoxy acetic acid	In-Chem
methylclofenapate	Fib-HLD	Trichloroacetic acid	In-Chem
Gemfibrozil	Fib-HLD	Lactofen	In-Chem
Bezafibrate	Fib-HLD	Dicamba	In-Chem
Ciprofibrate	Fib-HLD	Cold acclimatization	Phys
Fenofibrate	Fib-HLD	High fat diet	Phys
Clobuzarit	Fib-HLD	Thyroxine	Hormone
Wy-14,643	Non-Fib-HLD	Triiodothyronine	Hormone
Tibric Acid	Non-Fib-HLD	Dehydroepiandrosterone	Hormone
BR-931	Non-Fib-HLD	Dimethrin	In-Chem
Tiadenol	Non-Fib-HLD	Perchloroethylene	In-Chem
Acetylsalicyclic Acid	Drug	Chlorophenolate	In-Chem
Ly-171883	Drug	High phytol diet	Phys
Valproic Acid	Drug	Vitamin E- deficiency	Phys
Di-2-ethylhexylphthalate	In-Chem	Long Chain Fatty Acids	Phys
Di-2-ethylheyladipate	In-Chem	2-Ethylhexanoic acid	In-Chem

Section 1.1.6 Peroxisome proliferation

Peroxisome proliferators cause liver enlargement, an increase in the number of hepatic peroxisomes and an increase in the size and volume of hepatic peroxisomes (Price, R.J. *et al* 1992, Elcombe, C.R. and Mitchell, A.M. 1986, Baumgart, E. *et al* 1990, Lake, B.G. *et al* 1989a, McGuire, E.J. *et al* 1992, Pacot, C. *et al* 1993, Stott, W.T. *et al* 1995, Pacot, C. *et al* 1996, Gray, R.H. *et al* 1984). Liver enlargement occurs a result of both hyperplasia and hypertrophy. Associated with these changes in peroxisome biogenesis are alterations in peroxisomal enzyme activities, microsomal enzyme activities and cytosolic enzyme activites. The enzyme activities and gene expression of acyl-CoA oxidase and cytochrome P450 4A are extensively used as characteristic markers of peroxisome proliferation. See table 1.2 for a list of enyzmes induced by peroxisome proliferators.

Table 1.2 Liver enzymes induced by peroxisome proliferators.

Enzyme	References
cyanide insensitive palmitoyl-CoA oxidase	(Price, R.J. <i>et al</i> 1992, Elcombe, C.R. and Mitchell, A.M. 1986, Lake, B.G. <i>et al</i> 1989a, Blaauboer, B.J. <i>et al</i> 1990, Pacot, C. <i>et al</i> 1993, Lake, B.G., <i>et al</i> 1993, Latruffe, N. <i>et al</i> 1995, Stott, W.T. <i>et al</i> 1995, Sausen, P.J. <i>et al</i> 1995, Cornu, M-C. <i>et al</i> 1992, Sakuma, M. <i>et al</i> 1992, Espandiari, P. <i>et al</i> 1995, Elcombe, C.R. 1985 and Pacot, C. <i>et al</i> 1996)
catalase	(Pacot, C. <i>et al</i> 1993, Stott, W.T. <i>et al</i> 1995, Sakuma, M. <i>et al</i> 1992 and Pacot, C. <i>et al</i> 1996)
bifunctional enzyme	(Baumgart, E. <i>et al</i> 1990).
thiolase	(Baumgart, E. <i>et al</i> 1990).
carnitine palmitoyl-CoA transferase	(Sakuma, M. <i>et al</i> 1992)
palmitoyl-CoA hydrolase	(Oesch, F. <i>et al</i> 1988, Sakuma and M. <i>et al</i> 1992)
enoyl-CoA hydratase	(Pacot, C. <i>et al</i> 1996 and Lake, B.G. <i>et al</i> 1986)
epoxide hydrolase	(Oesch, F. <i>et al</i> 1988)
cytochrome P450 4A (lauric acid ω - and ω -1 hydroxylase)	(Bell, D.R. <i>et al</i> 1991 and 1993, Stott, W.T. <i>et al</i> 1995, Espandiari, P. <i>et al</i> 1995, Lake, B.G. <i>et al</i> 1986, Sato, T. <i>et al</i> 1995 and Sabzevari, O. <i>et al</i> 1995, Close, I. <i>et al</i> 1992, Sakuma, M. <i>et al</i> 1992 and Lake, B.G. <i>et al</i> 1989a)
Δ -9, Δ -6, Δ -5 desaturases	(Alegret, M. <i>et al</i> 1995),
palmitoyl-CoA elongation enzyme	(Alegret, M. <i>et al</i> 1995)
NADPH cytochrome c reductase	(Alegret, M. <i>et al</i> 1995)
malic enzyme	(Sakuma, M. <i>et al</i> 1992)
1-acylglycerophosphocholine acetyltransferase	(Sakuma, M. <i>et al</i> 1992)

Section 1.1.7 Peroxisome proliferators are hepatocellular carcinogens

Long term dosing studies of peroxisome proliferators on rats and mice demonstrated that peroxisome proliferators are tumourigenic substances. Rats and mice dosed with Wy14,643, gemfibrozil, DEHP, clofibrate, methylclofenapate or nafenopin caused liver tumour formation (Lalwani, N.D. *et al* 1981, Fitzgerald, J.E. *et al* 1981, Kluwe, W.M. *et al* 1982, Reddy, J.K. and Qureshi, S.A. 1979, Reddy, J.K. *et al* 1982 and Reddy, J.K. and Rao, M.S. 1977, Cohen, A.J. and Crasso, P. 1981, Reddy, J.K. and Lalwani, N.D, 1983). The mechanism by which peroxisome proliferators cause cancer is not known, but there are several proposed possible mechanisms which could explain their action.

Section 1.1.8 Peroxisome proliferators are non-genotoxins

It was originally considered that peroxisome proliferators act as direct mutagens, that is they can covalently interact with DNA, causing mutations to occur during DNA replication, or transcription of DNA, leading ultimately to tumour formation. The Ames Salmonella mutagenesis assay (Warren, J.R. *et al* 1980), [³²P]-post labelling experiments, chromosomal deletion analysis experiments and DNA repair assays have all been used to examine the genotoxic potential of peroxisome proliferators. Butterworth, B.E. *et al* 1989 used a DNA repair assay in primary human hepatocytes to determine the genotoxic potential of DEHP, MEHP, Wy-14,643 and nafenopin to human liver cells. No DNA repair response was seen for any of the peroxisome proliferators. Ashby *et al* 1994 reviewed the extensive experimental data on the genotoxicity of peroxisome proliferator chemicals, concluding that peroxisome proliferators are predominantly non-genotoxic.

Given that peroxisome proliferators are non-genotoxic, two principle hypotheses have been considered as mechanisms by which peroxisome proliferators cause cancer. One hypothesis proposes that peroxisome proliferators could act as tumour promoting agents. Here peroxisome proliferators would not damage the DNA, but instead cause the promotion of cells that have

already suffered mutational damage, leading to the formation of a tumour cell.

Section 1.1.9 Peroxisome proliferators and tumour promotion

DEHP and clofibrate can act as tumour promoting agents. Ward, J.M. *et al* 1983, 1984 and 1986 showed that DEHP promotes N-nitrosodiethylamine (DEN) initiated hepatocellular proliferative lesions after short term exposure in male B6C3F1 mice. A significant increase in focal hepatocellular proliferative lesions was seen compared to mice dosed with DEN alone. Mochizuki, Y. *et al* 1983 demonstrated that co-administration of DEN and clofibrate to F344 rats resulted in a significant increase in the number of hepatic tumours formed, over rats given DEN alone.

Peroxisome proliferators could act as tumour promoting agents by promoting the expansion of cells through cell proliferation. Nafenopin, BR931, methylclofenapate and Wy14,643 have all been shown to induce hepatocyte cell replication and increase nuclear ploidy. The induction of liver cell proliferation by peroxisome proliferators occurs in periportal hepatocytes. Non-parenchymal liver cells do not undergo proliferation in response to peroxisome proliferators (James, N.H. and Roberts R.A. 1996, Price, R.J. *et al* 1992, Melchiorri, C. *et al* 1993, Ohmura, T. *et al* 1996, Styles, J.A. *et al* 1988, Lake, B.G. *et al* 1993 and Lalwani, N.D. *et al* 1997). The induction of DNA synthesis in the mouse by methylclofenapate peaked after 6 days of dosing in a 10 day long dosing study (Styles, J.A. *et al* 1988). In rat, ciprofibrate was found to significantly induce DNA synthesis in hepatocytes up to 24 days of treatment. At 6, 26 and 54 weeks no significant induction of DNA synthesis was found (Chen, H. *et al* 1994). Price, R.J. *et al* 1992 found that nafenopin could induce replicative DNA synthesis in the rat approximately 10-fold over control after 7 days of dosing and approximately 5-fold over control at 7.5 weeks. The duration at which DNA synthesis can be sustained may be of importance in the tumour promoting properties of peroxisome proliferators.

Peroxisome proliferators not only affect DNA synthesis but also have an impact on the process of apoptosis. The effects of peroxisome proliferators on spontaneous and transforming growth factor-1 (TGF β 1) induced apoptosis were studied in rat and mouse hepatocytes. methylclofenapate and Wy14,643 both suppressed spontaneous and induced apoptosis in rat hepatocytes (James and Roberts 1996). It could be possible that initiated cells, targeted for apoptosis escape this process by the action of peroxisome proliferators. These cells could then undergo proliferation leading to possible tumour formation.

Section 1.1.10 Peroxisome proliferators induce cell transformation

Using an *in vitro* cell culture based assay, Ward, J.M. *et al* 1986 examined the effect of DEHP on promotable mouse epidermis derived JB6 cells. DEHP and MEHP, a metabolite of DEHP, promoted the JB6 cells to an anchorage independent phenotype. The syrian hamster embryo (SHE) cell system has been used to examine the effects of clofibrate and methylclofenapate. Both these peroxisome proliferators were able to induce morphological transformation of SHE colonies (Cruciani, V. *et al* 1997). The JB6 cells and SHE cells are not related to liver cells, thus the relevance of the morphological transforming properties of peroxisome proliferators identified in these experiments, to peroxisome proliferator induced hepatocarcinogenesis is unclear.

Section 1.1.11 Peroxisome proliferator induced oxidative damage to DNA

The other principal hypothesis to explain the carcinogenicity of peroxisome proliferators is the oxidative stress hypothesis. The oxidative stress hypothesis (Reddy, J.K. and Lalwani, N.D. 1983, Reddy, J.K. and Rao, M.S. 1986 and Rao, M.S. and Reddy, J.K. 1991) proposed that peroxisome proliferators could cause tumour formation as a result of DNA damage by high levels of H₂O₂ produced by the induction of acyl-CoA oxidase. The hypothesis proposed that the increased activity of acyl-CoA oxidase (induced by peroxisome proliferators) produces a large increase in the cellular levels of hydrogen peroxide. Reddy, Lalwani and Rao proposed that DNA lesions formed by oxidative damage are critical in the formation of peroxisome proliferator

induced hepatocarcinogenesis. Increased levels of hydrogen peroxide could be produced if the processes of detoxifying hydrogen peroxide are decreased.

Catalase, an enzyme which can remove hydrogen peroxide is only marginally induced by peroxisome proliferators. Therefore the balance of acyl-CoA oxidase and catalase levels after peroxisome proliferator treatment effectively produces a net reduction in the detoxifying capability of the liver. Peroxisome proliferators reduce the expression of other enzymes involved in the removal of hydrogen peroxide, such as cellular GSH peroxidase (Tamura, H. *et al* 1990(a) and 1990(b) and Furukawa, K. *et al* 1985), superoxide dismutase (Ciriolo, M.R. *et al* 1982 and Elliott, B.M and Elcombe, C.R. 1987) and GSH transferase (Foliot, A. *et al* 1986, Lake, B.G. *et al* 1989b, Furukawa, K. *et al* 1985 and Tamura, H. *et al* 1990(b)). The effects of peroxisome proliferators on liver antioxidant status have been studied. It was found that levels of GSH or vitamin E remain unchanged or decrease slightly (Conway, J.G. *et al* 1989, Foliot, A. *et al* 1986, Lake, B.G. *et al* 1989b and Weiss, P. and Bianchine, J.R. 1970). Two types of DNA lesions which can be induced by oxidative damage have been investigated in rats and mice treated with peroxisome proliferators.

Section 1.1.12 Peroxisome proliferator-induced hepatic DNA lesions

Hydrogen peroxide can induce 8-hydro-2'-deoxyguanosine (8-OHdG) lesions in DNA (Clayson, D.B. *et al* 1994). Wy-14,643, clofibric acid, ciprofibrate and perfluorodecanoic acid have been investigated in rat to see if they cause an increase in 8-OHdG lesions in hepatic DNA. 8-OHdG lesions in hepatic DNA have been reported to be increased from 0.5 to 2.5 fold in F344 rats treated with DEHP, DEHA (Takagi, A. *et al* 1990 and 1991), PFOA, PFDA (Takagi, A. *et al* 1991), Ciprofibrate (Kasai, H. *et al* 1989 and Huang, C. *et al* 1994) and Wy-14,643 (Cattley, R.C. and Glover, S.E. 1993). Cattley, R.C and Glover, S.E. 1993 found that when isolated hepatic nuclei were examined, no increase in 8-OHdG levels were found for some peroxisome

proliferators tested. Sausen, P.J. *et al* 1995 found that 8-OHdG lesions in DNA isolated from whole liver homogenate increased 1.5-2 fold following treatment with Wy-14,643 and clofibric acid, but the increase was found to be due to an increase in background levels arising from a 3-fold increase in mitochondrial DNA levels. It is not known if the observed peroxisome proliferator induced levels of 8-OHdG found in other studies were due to peroxisome proliferator induced synthesis of hepatic nuclear or mitochondrial DNA. These small inductions in the amounts of DNA lesions were found to be statistically significant but their biological significance remains unclear. Oxidative damage to DNA can cause DNA strand breaks. The induction of DNA strand breaks by oxidative damage in hepatic DNA by peroxisome proliferators has not been found (Elliott, B.M. and Elcombe, C.R. 1987 and Tamura, H. *et al* 1991). There is little evidence to support the hypothesis that peroxisome proliferators act as DNA damaging agents either directly or indirectly through the induction of oxidative stress. Therefore the carcinogenicity of peroxisome proliferators must be due to another mechanism that has still to be elucidated.

Section 1.1.13 Human hazard risk assessment of peroxisome proliferators

Peroxisome proliferators have been shown to be carcinogenic in rat and mouse studies. It is therefore important to determine if humans exposed to peroxisome proliferators are at any risk of cancer. It should be possible to elucidate the molecular mechanism of peroxisome proliferator induced hepatocarcinogenesis in rats and mice. Once that mechanism is found we can examine humans to see if they have the same molecular components that make up the mechanism of peroxisome proliferator induced hepatocarcinogenesis in rats and mice. It may then be possible to determine if humans face a significant risk of getting hepatic cancer, based on the molecular similarities of rats, mice and humans. Human experimentation is not possible, therefore we must study the effects of peroxisome proliferators in a species which we believe to model the human response to peroxisome proliferators. Experiments in other rodents such as hamster and guinea pig, and in species of new world and old world monkeys, have shown that in many respects these

species have similarities to humans in the way in which they respond to peroxisome proliferators. A greater understanding of species differences and similarities in response to peroxisome proliferators is needed. Analysis of the molecular aspects of species differences in peroxisome proliferation could lead to the development of an animal model which displays the same phenotypic response to peroxisome proliferators as that in humans.

Section 1.1.14 Peroxisome proliferation in hamster

Studies involving hamsters or hamster hepatocyte culture revealed that peroxisome proliferators do not affect all rodent species in the same manner. Where studied the hamster has been shown to be much less sensitive to the effects of peroxisome proliferators, than rats and mice. An increase in liver weight in hamsters has been observed in response to dosing with DEHP, MEHP, clofibrate, Wy-14,643, and nafenopin, though the observed increase was always less than that observed in rat (Lake, B.G. *et al* 1986, 1989a and 1993). The number of peroxisomes in hamster hepatocytes is induced by gemfibrozil, but with a concomitant reduction in peroxisome size (Gray, R.H. *et al* 1984). Peroxisomal β -oxidation is induced by peroxisome proliferators in hamster (Lake, B.G. *et al* 1986, Lhuguenot, J.C. *et al* 1988 and Lake, B.G. *et al* 1989a), along with carnitine acetyltransferase activity, carnitine palmitoyl transferase activity (Lake, B.G. *et al* 1986 and 1989a) and lauric acid ω and ω -1 hydroxylase activity (Lake B.G. *et al* 1989a and Sakuma, M. *et al* 1992). The observed enzyme inductions are smaller than those observed in the rat. There is conflicting evidence for the effects of peroxisome proliferators on replicative DNA synthesis. Styles, J.A. *et al* 1988 demonstrated that in hamster only a high dose of methyclofenopate (25mg/kg body weight) caused induction of hepatic DNA synthesis. Doses of 12 mg / Kg and 5mg / Kg had no effect on hamster hepatic DNA synthesis. Rats at the same dose exhibited 3-fold higher induction. Price, R.J. *et al* 1992 and Lake, B.G. *et al* 1993 using nafenopin (0.25% in the diet) and Wy-14,643 (0.025% in the diet) found no increase in hepatic replicative DNA synthesis as measured by incorporation of labelled nucleotide into liver whole homogenate DNA or by

hepatocyte labelling index. Suppression of spontaneous apoptosis of hamster primary hepatocytes by nafenopin has been observed (James, N.H and Roberts R.A. 1996). Histological examination of hamster livers from long term dosing studies of hamsters dosed with clobuzarit, DEHP, nafenopin or Wy-14,643 revealed no abnormalities. No peroxisome proliferator induced liver foci, nodules, adenomas or carcinomas were observed (Tucker, M.J. and Orton, T.C. 1995, Schmezer, P. *et al* 1988, Lake, B.G. *et al* 1993 and 1995). The hamster is regarded as a species that is intermediate in liver toxicity response to peroxisome proliferators and is non-responsive in hepatocarcinogenesis assays.

Section 1.1.15 Peroxisome proliferation in guinea pig

DEHA, MEHA, fenofibrate, clofibrate, DHEA and nafenopin do not induce peroxisomal β -oxidation, do not increase peroxisomal numbers or increase liver weight (Cornu, M.C. *et al* 1992, Cornu-Chagnon, M.C. *et al* 1995, Reo, N.V. *et al* 1994, Oesch, F. *et al* 1988 and Sakuma, M. *et al* 1992). Guinea pigs dosed with ciprofibrate, that had equivalent plasma concentrations of ciprofibrate to those measured in rats dosed with ciprofibrate, induced peroxisomal palmitoyl-CoA oxidase activity in the guinea pig 1.6 fold. In the rat, peroxisomal palmitoyl-CoA oxidase activity was induced 8.7 fold (Latruffe, N. *et al* 1995 and Pacot, C. *et al* 1996). These experiments show that for ciprofibrate, differences in the extent of peroxisome proliferation are not due to differing pharmacokinetics of ciprofibrate. Studies by Elcombe, C.R. and Mitchell, A.M. 1986 and Lake, B.G. *et al* 1986 found that MEHP or metabolites of MEHP had little or no effect on peroxisome number or peroxisomal β -oxidation. Dirven, H. *et al* 1993 showed that a 30-fold higher concentration of MEHP than that used in rat was needed to induce peroxisomal palmitoyl-CoA oxidase activity 50 % above control levels in guinea pig. Such a small induction is not likely to be biologically significant. Lake, B.G. 1989a *et al* found that peroxisome proliferators could induce a very small increase in microsomal cytochrome P450 content of guinea pig hepatocytes, and Pacot, C. *et al* 1996 demonstrated that cytochrome P450 4A lauric

acid ω -hydroxylase activity could be slightly augmented by ciprofibrate. However Dirven, H. *et al* 1993 and Latruffe, N. *et al* 1995 found no such inducibility of microsomal cytochrome P450 content of guinea pig hepatocytes or induction of lauric acid ω -hydroxylase activity. Bell, D.R. *et al* 1993 demonstrated that methylclofenapate did not induce Cyp 4A13 mRNA in guinea pig liver. The lack of induction of the peroxisomal β -oxidation system by peroxisome proliferators in guinea pig is not due to a lack of components which make up the system. Yamamoto, K. *et al* 1992 demonstrated by immunoblotting and immunohistochemistry that guinea pigs have the same molecular weight subunits and proteins of acyl-CoA oxidase, bifunctional enzyme, thiolase and catalase as in the rat. These enzymes were all exclusively located in the peroxisomal compartment, with the exception of catalase, which was also present in the cytoplasm and nucleus of guinea pig hepatocytes. These data strongly suggest that guinea pigs are non-responsive to peroxisome proliferators.

Section 1.1.16 Peroxisome proliferation in primates

The rhesus monkey, cynomolgus monkey and marmoset monkey have been tested with peroxisome proliferators. Reddy, J.K. *et al* 1984 found that ciprofibrate could cause a 1.3 fold and 1.7 fold induction in relative liver weights of rhesus and cynomolgus monkeys. Lake B.G. *et al* 1989a found no change in the relative liver weight of marmoset monkeys dosed with nafenopin. Gemfibrozil has been shown to increase the number of peroxisomes in rhesus monkey hepatocytes 3-5 fold, along with a concomitant decrease in mean peroxisomal volume (Gray, R.H. *et al* 1984). Reddy, J.K. *et al* 1984 found that ciprofibrate could cause a 3-fold increase in peroxisomal volume in rhesus monkey. Blaauboer, B.J. *et al* 1990, Foxworthy, P.S. *et al* 1990 and Lake B.G. *et al* 1989a observed no increase in the number of peroxisomes or change in their size in rhesus monkey cultured hepatocytes, cynomolgus monkey cultured hepatocytes or marmoset monkey dosed with peroxisome proliferators. The induction of peroxisomal β -oxidation has not been observed in primary hepatocyte culture from cynomolgus, rhesus or

marmoset monkey dosed with ciprofibrate, bezafibrate, LY171883 (Foxworthy, P.S. *et al* 1990 and 1994), clofibric acid, beclobric acid (Blaauboer, B.J. *et al* 1990), DEHA or DEHA metabolites (Cornu, M.C. *et al* 1992), DEHP or DEHP metabolites (Elcombe, C.R. and Mitchell, A.M. 1986). However Reddy, J.K. *et al* 1984, Lake, B.G. *et al* 1989a and Dirven, H. *et al* 1993 observed small inductions in the activities of palmitoyl-CoA oxidase, catalase, enoyl-CoA hydratase and carnitine acetyl transferase in their monkey studies. The majority of published data on peroxisome proliferation in monkey species indicates that they are poorly responsive.

Section 1.1.17 Peroxisome proliferation in humans

Studies with primary human hepatocyte culture, transformed human liver cell lines, and studies of humans exposed to fibrate hypolipidaemic drugs have examined what effects peroxisome proliferators have on human liver cells. Primary human hepatocyte cultures have been tested with peroxisome proliferators that produce a large response in rats and mice. Ciprofibrate, clofibric acid, beclobric acid, trichloroacetic acid, MEHP, Wy-14,643, DEHP and metabolites of DEHP used to dose human hepatocytes do not cause induction of peroxisomal β -oxidation or induction of other fatty acid metabolising enzymes (Duclos, S. *et al* 1997, Blaauboer, B.J. *et al* 1990, Butterworth, B.E. *et al* 1989, Elcombe, C.R. 1985, Elcombe, C.R. and Mitchell, A.M. 1986). Experiments using the human hepatoma cell line HepG2 have demonstrated very small inductions (1.4–2 fold) in palmitoyl-CoA oxidase activity with ciprofibrate (Duclos, S. *et al* 1997 and Latruffe, N. *et al* 1995) and clofibric acid (Chance, D.S. *et al* 1995). In Hep G2 cells clofibrate can induce catalase and acyl-CoA oxidase, but to levels less than 3-fold above control values (Chance, D.S. *et al* 1995 and Scotto, C. *et al* 1995). Also in HepG2 cells clofibric acid has been shown to reduce the activity of the mitochondrial enzymes carnitine palmitoyl-CoA transferase and succinate-iodonitrotetrazolium-reductase (Chance, D.S. *et al* 1995). The extent to which gene expression and peroxisomal metabolism in Hep G2 cells (a transformed cell line) is the same as in human hepatocytes is unknown. Therefore extrapolation of data from Hep G2 cell

experiments to humans must be treated with great caution. Liver biopsies of human volunteers dosed with gemfibrozil exhibited no change in peroxisomal number or size (De La Inglesia, F.A. *et al* 1982, Blumcke, S. *et al* 1983 and Gariot, P. *et al* 1987). Liver biopsies of volunteers dosed with clofibrate showed that a 50% increase in peroxisomal number occurred (Hanefeld, M. *et al* 1983) and with ciprofibrate a 30% increase in peroxisomal volume (Bently, P. *et al* 1993). These biopsy data must be treated with caution as examination of all lobes and sections of the liver cannot be carried out. One must be able to eliminate the possibility of intra-regional variance within the liver before firm conclusions as to the effect of peroxisome proliferators can be measured.

Epidemiological studies have examined the tumour incidence in patients receiving clofibrate and gemfibrozil hypolipidaemic drugs. No significant rise in tumour incidence was found from either study (Oliver, M.F. *et al* 1978 and Frick, H. *et al* 1987). Carcinogenic studies in rats and mice have used dosing regimes which cover the majority of the life span of the animal. These human carcinogenic studies cover patients who have been treated for up to 5 years, limiting the interpretation of the results. Any increases in the incidences of tumour formation could be attributed to the preclinical state of the patients treated with the hypolipidaemic drugs. Present experimental data currently supports the view that humans are non-responsive to peroxisome proliferators.

Section 1.1.18 Models of peroxisome proliferation in non-responsive species

The experimental data indicate that the guinea pig rodent species respond to peroxisome proliferators in a manner very simmilar to humans. It could be proposed that the guinea pig species is the strongest candidate for an animal model to study the non-responsive phenotype exhibited by humans. In order to validate an animal model, the molecular mechanism underlying the responsive nature of that species must be elucidated. The mechanism of non-responsiveness

in guinea pigs is not well characterised, and it is therefore important to elucidate the mechanism of non-responsiveness in guinea pigs and determine whether or not that this species is suitable for modelling peroxisome proliferation in humans.

Section 1.2 Peroxisome proliferated activated receptor

Section 1.2.1 Cloning of a receptor which mediates peroxisome proliferation

In 1990 Issemann and Green screened a mouse cDNA library using a probe derived from the consensus sequence of several steroid hormone receptors. A cDNA was cloned that encoded for a 468 amino acid protein, (molecular weight = 52 kDa) that could be activated by hypolipidaemic drugs and a plasticizer. This receptor was termed Peroxisome Proliferator Activated Receptor alpha (PPAR α). Analysis of the amino acid sequence demonstrated that PPAR α belonged to the steroid hormone receptor superfamily. The PPAR α amino acid sequence displayed high homology to the DNA binding domain of nuclear steroid hormone receptors such as glucocorticoid receptor, estrogen receptor, retinoid X receptor, vitamin D receptor and retinoic acid receptor. Steroid hormone receptors are described as having six distinct regions, A to F (Argos, P. 1985, Krust, A. *et al* 1986, and Laudet, V. *et al* 1992). The regions have been classified into four distinct domains. The A/B domain has transactivational function (Folkers, G.E. *et al* 1996), the C domain is a DNA binding domain and has role in heterodimerisation (Zechel, C. *et al* 1994 and Jiang, G. and Sladek, F.M. 1997), D is a hinge domain and E/F domain has ligand binding activity, transactivational activity and also has a role in heterodimerisation for some receptors (Schulman, I.G. *et al* 1995, Leng, X. *et al* 1995 and Qi, J-S. *et al* 1995). Conclusive proof that PPAR α is required for peroxisome proliferation action came from studying mice that expressed a PPAR α receptor disrupted in the ligand binding domain (Lee, S. S-T. *et al* 1995). Mice homozygous for the mutation lacked expression of the wild type receptor. These homozygous mice when dosed with clofibrate or Wy-14,643 did not exhibit proliferation of peroxisomes or induction of peroxisome proliferation marker enzymes.

Section 1.2.2 Cloning of PPAR genes

Three distinct PPAR isoforms α , β (also known as δ and FAAR), and γ have been cloned from mouse (Issemann, I. and Green, S. 1990, Chen, F. et al 1993, Kliewer, S.A. et al 1994 and Amri, E. et al 1995), rat (Bocos, C. et al 1995 and Xing, G. et al 1995), hamster (Aperlo, C. et al 1995), human (Jow, L. and Mukherjee, R. 1994, Greene, M.E. et al 1995, Lambe, K.G. and Tugwood, J.D. 1996 and Elbrecht, A. et al 1996), and *Xenopus* species (Krey, G. et al 1993). A partial PPAR γ cDNA has been cloned from Atlantic Salmon (Ruyter, B. et al 1997). In mouse alternative promoter use and differential splicing gives rise to two distinct isoforms of PPAR γ . mPPAR γ 1 and mPPAR γ 2 mRNAs differ by 300bp. mPPAR γ 2 mRNA has a different 5' untranslated region and encodes for 30 additional amino acids N-terminal to the ATG translation start of mPPAR γ 1 (Zhu, Y. et al 1995). Human PPAR γ 1 (hPPAR γ 1) and hPPAR γ 2 cDNAs have also been cloned. hPPAR γ 1 and hPPAR γ 2 are homologous to mPPAR γ 1 and mPPAR γ 2 with the exception that the 5' end of hPPAR γ 2 has a 84bp extension (90 for the mouse), encoding an additional 28 amino acids (Elbrecht, A. et al 1996).

Section 1.2.3 Guinea pigs as a model for peroxisome proliferation in humans

The human species is considered to be non-responsive to peroxisome proliferators, yet they possess an expressed PPAR α gene (Mukherjee, R. et al 1994 and Braissant, O. et al 1996). The lack of response observed in humans may be due to lower levels of expression of PPAR α in human hepatocytes compared to rat and mouse hepatocytes (Schoonjans, K. et al 1996). It is not known if guinea pigs, a species proposed to model the human response to peroxisome proliferation has a functionally expressed PPAR α gene. This must be determined in order to strengthen the validation of this species as a proposed model. It is not known if hypolipidaemic drugs can lower serum triglyceride levels in guinea pigs, as they can do in humans (De La Iglesia, F.A. et al 1982 and Hanefeld, M. et al 1983). If hypolipidaemic drugs can lower serum triglyceride levels in guinea pigs, then this would be supporting evidence for the presence of a functional PPAR α .

Section 1.2.4 Expression of PPAR α gene

The expression of rat and mouse PPAR α mRNA has been characterised for several tissues (Issemann, I. and Green, S. 1990, Beck, F. *et al* 1992, Mukherjee, R. *et al* 1994, Kliewer, S. *et al* 1994, Jones, P. *et al* 1995, Mansen, A. *et al* 1996 and Braissant, O. *et al* 1996). The highest levels of expression were found in liver, stomach and kidney, with moderate expression in brown adipose tissue, heart, muscle, small intestine, adrenal gland and retina. Low levels were found in white adipose tissue, spleen, smooth muscle, brain and central nervous system tissue. The pattern of expression of a gene should reflect where that gene is known to function or proposed to function. The high expression of PPAR α in the liver correlates well with the fact that peroxisome proliferators have their greatest effect in liver. The expression of PPAR α in numerous other tissues would indicate that PPAR α possibly plays an important role in biological processes other than peroxisomal metabolism. Human PPAR α has been shown to be highly expressed in liver, heart, skeletal muscle and kidney, and expressed in low levels in the lung and brain (Braissant, O. *et al* 1996). Different strains of mice have been compared for the level of liver PPAR α expression in each strain. Both Jones, P. *et al* 1995 and Motojima, K. *et al* 1997 did not find any differences between the strains examined in the expression of liver PPAR α mRNA.

Section 1.2.5 Peroxisome proliferators and PPAR α gene expression

Jones, P *et al* 1995 found that mice dosed with peroxisome proliferators did not induce PPAR α gene expression. Rats treated with Wy14,643 for 22 weeks and 78 weeks, to induce liver tumours had the expression of PPAR α measured at each time point in non-tumour liver tissue and in tumour liver tissue. In non-tumour tissue peroxisome proliferators did not induce PPAR α gene expression, but in tumorous liver tissue, PPAR α gene expression was induced (Miller, R. *et al* 1996). Schoonjans, K. *et al* 1996, found that in rats dosed with fenofibric acid PPAR α mRNA in the liver was not induced. Primary rat hepatocytes maintained on matrigel and a chemically defined medium have had PPAR α mRNA levels measured in the presence of

peroxisome proliferators. The presence of either clofibric acid or dehydroepiandrosterone caused a less than 2-fold induction in PPAR α mRNA levels (Yamada, J. et al 1995). Such a small induction is probably not biologically significant. McNae, F. et al 1994 found that clofibrate and perflourodecanoic acid induced PPAR α mRNA expression, but other peroxisome proliferators examined in these studies had no effect on PPAR α mRNA expression. Gebel, T. et al 1992 used an antibody raised against a mPPAR α Hinge domain- β -galactosidase fusion protein to examine rat PPAR α protein expression in liver cytosol and nuclear extracts from untreated and fenofibrate treated rats. In untreated rats their antibody did not detect an immunoreactive 52 kDa protein in either cytosolic or nuclear extracts, but in fenofibrate treated rats an immunoreactive 53 kDa protein was detected. They also used a cDNA probe derived from mPPAR α cDNA to probe for rat PPAR α . A single 6 kb mRNA species was detected at very low levels in liver RNA from untreated rats, but was induced in fenofibrate treated rats. Braissant, O. et al 1996 have subsequently shown using an anti ratPPAR α antibody and a riboprobe derived from rat PPAR α cDNA that rat PPAR α mRNA is highly expressed in the liver and that the rat PPAR α protein is almost exclusively located in the nucleus. Sterchele, P.F. et al 1996 found that in rat liver, PPAR α mRNA accumulated after treatment with perfluorodecanoic acid (PFDA). Nuclear run-on experiments demonstrated that the accumulation of PPAR α mRNA was not due to an induction of transcription. Pair-fed control animals, and animals which were nutritionally deprived also accumulated PPAR α mRNA. These results indicate that the increase in PPAR α mRNA levels observed after peroxisome proliferator dosing, were likely to be a result of nutritional based, or stress based induction. The inductions observed by some groups is likely to be due to a stress based induction mechanism, possibly arising from the dose of the peroxisome proliferator used. Lemberger, T et al 1996 demonstrated that PPAR α expression in the liver can be induced by stressing the animals. The effects of clofibrate on the expression of hPPAR α mRNA in human glioblastoma A172 cells has been examined by Pineau, T. et al 1996. They

found that clofibrate greatly induced PPAR α expression in this cell line. Tumour derived cell lines are not representative of normal tissue, and so the significance of this result in relation to the effects of peroxisome proliferators on PPAR α expression in normal tissue is unclear.

Section 1.2.6 Hormonal regulation of PPAR α gene expression

Yamada, J. *et al* 1995 also examined the effects of growth hormone (somatotropin) and thyroid hormone (triiodothyronine) on the expression of PPAR α in hepatocyte culture. After 5 days of incubation with growth hormone the PPAR α mRNA levels decreased to 50% of the control levels. The incubation of hepatocytes with thyroid hormone caused a 50% increase in PPAR α mRNA levels over control values. Similar results were obtained when either growth hormone or thyroid hormone was co cultured with clofibric acid or dehydroepiandrosterone sulphate. Lemberger, T. *et al* 1994 found that glucocorticoid hormones could induce rat PPAR α gene expression in primary hepatocyte culture. PPAR α expression has also been claimed to follow a diurnal pattern of expression, peaking at 5.30 pm (Lemberger, T. *et al* 1996), but the data from these experiments was limited as expression of PPAR α was not measured during the night.

The levels of cytosolic and nuclear located glucocorticoid receptor have been studied in rats. Peak expression of glucocorticoid receptor in both cellular compartments peaks between 11.00pm and 2.00 am (Xu, R.B. *et al* 1991). In rats the secretion of glucocorticoid hormones oscillates with a circadian rhythm, with maximal levels being reached at the light / dark switch in the evening (Dhabhar, F.S *et al* 1993, Holmes, M.C. *et al* 1997, Atkinson, H.C. and Waddell, B.J. 1997). Both the peak release of glucocorticoid hormone and glucocorticoid receptor are out of synchronisation with the circadian rhythm of PPAR α measured by Lemberger, T. *et al* 1996. If the glucocorticoid hormone and receptor circadian rhythms regulate PPAR α gene expression, one would expect PPAR α gene expression to peak late at night or early morning, not early evening.

Section 1.2.7 Expression of PPAR δ and PPAR γ genes

The pattern of expression of other isoforms of PPAR could impinge on the signaling pathways of PPAR α . It is possible that PPAR β and γ could compete for binding to available ligands or compete for binding to regulatory regions of genes controlled by PPAR α . There is also the possibility of competition for binding to other transcription factors. The expression of PPAR β mRNA has been studied in rat, mouse and human tissues and is found to be ubiquitously expressed in all tissues studied. Highest expression is found in brain, placenta, skeletal muscle, adipose tissue and intestine and lowest expression is found in liver, kidney, spleen and testis (Kliwer, S. *et al* 1994, Amri. E-Z, *et al* 1995, Xing. G. *et al* 1995, Jones, P. *et al* 1995 and Braissant, O. *et al* 1996). PPAR γ expression has been studied in rat, mouse, hamster and human tissues. In all the species examined PPAR γ mRNA expression was highest in adipose tissue and spleen. Moderate expression has been observed in heart, skeletal muscle, kidney, liver, lung, bone marrow and testes (Kliwer, S. *et al* 1994, Tontonoz, P. *et al* 1994a and 1994b, Aperlo, C. 1995, Jones, P. *et al* 1995, Braissant, O. *et al* 1996, Elbrecht, A. *et al* 1996 and Mukherjee, R. *et al* 1997). The expression of PPAR γ has been examined in obese mice (gold thioglucose and *ob/ob*), in mice with toxigene-induced brown fat ablation, and in mice with insulin deficient diabetes. mPPAR γ expression was not altered in adipose tissue of obese mice but was increased in adipose tissue of mice with brown fat ablation (Vidal-Puig, A. *et al* 1996). Mice fed high fat diets had adipose expression of PPAR γ induced, but in fasting mice the expression was reduced compared to control mice (Rousseau, V. *et al* 1997).

Section 1.2.8 Peroxisome Proliferators are ligands for PPAR α

Four different experimental strategies have been employed to determine if PPs are ligands for PPAR α . A GST-xPPAR α -Ligand-Binding-Domain fusion protein was used to demonstrate that GW2331 (a novel fibrate), palmitic acid, oleic acid, petroselenic acid, linolenic acid, linoleic acid, arachidonic acid and hydroxyeicosatetraenoic acid are ligands for xPPAR α as well as

activator compounds (Kliwer, S. *et al* 1997). Kliwer *et al* measured the amount of radiolabelled GW2331 bound to the fusion protein and how effective the compounds listed were at competing for binding. GW2331 has a $K_d = 140\text{nm}$ for binding to the GST-xPPAR α -LBD fusion protein. GST-hPPAR α -LBD and GST-mPPAR α -LBD-GST fusion proteins exhibited ≈ 3.5 fold and ≈ 6 -fold weaker binding to GW2331. Forman, B. *et al* 1997 used gel retardation-based assays to indirectly demonstrate that Wy14,643, ciprofibrate, clofibrate, long chain fatty acids and inhibitors of β -oxidation are ligands for PPAR α . PPs in the presence of low levels of mPPAR α and hRXR α receptors induced heterodimer binding to an acyl-CoA oxidase PPRE. At high levels of receptor PPs were not able to increase heterodimer binding to the PPRE. These results indicate that peroxisome proliferators influence PPAR α / RXR α heterodimer function when the levels of receptor are low. LG268, a ligand for RXR α induced RXR α homodimer binding to a PPRE. Further evidence to support the theory that PPs can bind to PPAR α comes from a study which shows that mPPAR α has differential protease sensitivity in the presence of Wy-14,643, clofibric acid, 5,8,11,14-eicosatetraenoic acid or LY-171883, indicating that mPPAR α undergoes a conformational change in the presence of these substances (Dowell, P. *et al* 1997). A novel ligand sensor assay has recently been developed by Krey, G. *et al* 1997, termed coactivator dependent receptor ligand assay to screen for binding of peroxisome proliferators and naturally occurring metabolites to all three xenopus PPAR isoforms. This assay uses a fusion of glutathione S-transferase and PPAR ligand binding domain and the steroid coactivator-1 (SRC-1) protein. The formation of PPAR/SRC-1 interactions occur only if the binding of a ligand to the ligand binding domain of the PPAR is specific. Using this assay Krey, G. *et al* were able to demonstrate specific ligand binding to PPAR α for the following compounds, Wy-14,643, Leukotriene-B₄, ETYA, bezafibrate, clofibrate, eicosapentaenoic acid, linolenic acid, linoleic acid, arachidonic acid, 8(S)-hydroxyeicosatetraenoic acid, petroselinic acid, oleic acid, elaidic acid and erucic acid. Many of these peroxisome proliferators and fatty acids were also specific

ligands for *xenopus* PPAR β and γ isoforms. This coactivator dependent assay has highlighted that PPARs have overlapping ligand recognition.

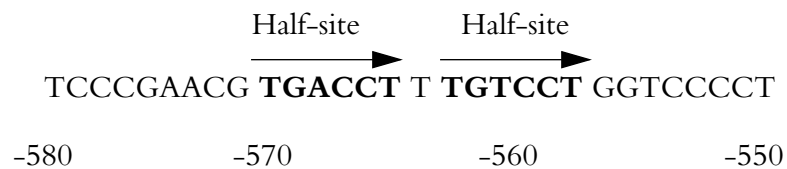
Section 1.2.9 Peroxisome Proliferator Response Elements (PPREs)

Gene transcription is controlled through the interaction of transcription factors with sequence specific motifs in DNA. A functional promoter region containing TATA-box like sequences is often required for the binding of the cells basal transcription machinery. Upstream of gene promoters are regulatory regions which can bind trans-acting factors that control the up-regulation and down-regulation of the transcription of the gene. The third type of sequence specific motif is the enhancer element. Enhancers also bind transcription factors to upregulate the transcription of a gene, in an orientation and position independent manner.

The upstream regions of genes whose expression is modulated by peroxisome proliferators have been examined for regulatory motifs. Rat acyl-CoA oxidase gene (Osumi, T. *et al* 1991, Tugwood, J.D. *et al* 1992 and Green, S. *et al* 1992) and rat peroxisomal enoyl-CoA hydratase/3-hydroxyacyl-CoA dehydrogenase, bifunctional enzyme gene (Zhang, B. *et al* 1992) were investigated first for the presence of regulatory regions which conferred peroxisome proliferator transcriptional responsiveness. DNA containing the rat acyl-CoA oxidase gene upstream region was cloned in front of a β -globin promoter and linked to a CAT reporter gene. The putative response element-reporter gene construct was co-transfected in a mouse hepatoma cell line with an expression plasmid for mouse PPAR α . Dosing of transfected cells with peroxisome proliferator caused the reporter gene to be expressed. In the absence of either PPAR or peroxisome proliferator, stimulation of the reporter gene was much lower. Using deletion analysis of the upstream gene region the localisation of the PPRE was identified. The same molecular strategy was used to identify a PPRE in the bifunctional gene. A distinct motif was found and was termed a Peroxisome Proliferator Response Element (PPRE). PPREs consist of

a tandem repeat of two hexameric nucleotide motifs (half-sites) spaced by a single nucleotide. This motif is known as a direct repeat 1 (DR1). See figure 1.1 for the structure of the rat acyl-CoA oxidase PPRE.

Figure 1.1 The rat acyl-CoA oxidase PPRE.



PPREs from many liver genes have now been identified using similar experiments. Table 1.3 shows PPREs that have been identified to date. Rat bifunctional enzyme, human apolipoprotein A-I and rat acyl-CoA synthetase PPREs all have a third half-site with high homology to the TGACCT consensus half-site either two nucleotides 5' or three nucleotides 3' to the PPRE. The influence of these close half-sites on the function of the PPRE is unclear. The sequence specificity of each PPRE is not strict, as the sequence of the PPRE can deviate from the consensus sequence by as many as 5 nucleotides, but mutations of one or two nucleotides within a particular PPRE can diminish or abolish its peroxisome proliferator responsiveness (Issemann, I. *et al* 1993, Vu-Dac, N. *et al* 1994, Palmer, C.N.A. *et al* 1994 and Chu, R. *et al* 1995).

Gene	PPRE sequence	Reference
Rat acyl-CoA oxidase	TGACCT T TGTCCCT	(Osumi, T. <i>et al</i> 1991 and Tugwood, J.D. <i>et al</i> 1992)
Rat bifunctional enzyme	TGAACT A TTACCT	(Zhang, B. <i>et al</i> 1992, Bardot, O. <i>et al</i> 1993)
Rabbit cytochrome P450 4A6 (z-element)	TCAACT T TGCCCT	(Muerhoff, A.S. <i>et al</i> 1992)
Rabbit cytochrome p450 4A6 (-27 to -1 region)	TGACCC T TGCCCA	(Palmer, C.N.A. <i>et al</i> 1994)
Human peroxisomal fatty acyl-CoA oxidase	TGACCT G TGACCT	(Varanasi, U. <i>et al</i> 1996)
Rat acyl-CoA synthetase	TGACTG A TGCCCT	(Schoonjans, K. <i>et al</i> 1995)
Rat acyl-CoA binding protein	TCACCT T TGCACCT	(Elholm, M. <i>et al</i> 1996)
Human apolipoprotein A-I	TGACCC C TGCCCT	(Vu-Dac, N. <i>et al</i> 1994)
Human lipoprotein lipase	TGCCCT T TCCCCC	(Schoonjans, K. <i>et al</i> 1996)
Rat malic enzyme	GGACCT G TGCCCT	(Castelein, H. <i>et al</i> 1994)
Human apolipoprotein C-III	TGACCT T TGCCCA	(Hertz, R. <i>et al</i> 1995)
Rat apolipoprotein C-III	TGACCT T TGACCA	(Hertz, R. <i>et al</i> 1995)
Rat cytochrome p450 4A1	TCCCCT C TGACCT	(Aldridge, T.C. <i>et al</i> 1995)
Fatty acid binding protein	TGACCT A TGGCCT	(Isseman, I. <i>et al</i> 1992)
3-hydroxy-3-methylglutaryl - CoA synthase (HMG)	AGACCT T TGGCCC	(Rodriguez, J.C. <i>et al</i> 1994)
Human transferrin	CAATCT T TGACCT	(Hertz, R. <i>et al</i> 1996)
Human Hepatitis B virus enhancer 1 element	GAACCT T TACCCC	(Bingfang, H. <i>et al</i> 1995)

Table 1.3 Sequences of PPREs identified in peroxisome proliferator responsive genes.

Section 1.2.10 PPAR α binds to PPREs with Retinoid X Receptor as a heterodimer

It was postulated that PPAR α would bind to a PPRE either as a homodimer or as a heterodimer with retinoid X receptor α (RXR α), a promiscuous binding partner for many steroid hormone nuclear receptors. Using electromobility shift assays (EMSAs) with a labelled PPRE and recombinantly expressed PPAR α and RXR α receptors, it was found that PPAR α only binds to DNA as a heterodimer (Isseman, I. *et al* 1993, Bardot, O. *et al* 1993, Gearing, K.L. *et al* 1993 and Keller, H. *et al* 1993).

Protein-DNA contact points have been identified in the PPREs of the rat acyl-CoA oxidase gene, rat bifunctional enzyme gene, rabbit cytochrome p450 4A6 gene and human lipoprotein lipase gene by DNase I protection mapping and by methylation interference experiments (Tugwood, J.D. *et al* 1992, Bardot, O. *et al* 1993, Palmer, C.N.A. *et al* 1994 and Schoonjans, K. *et al* 1996). These close points of contact are essential for determining the specificity of the protein - DNA binding interaction. The importance of the spacing between the half-sites in a PPRE was investigated by Issemann, I. *et al* 1993. Using a PPRE driven reporter gene system they found that a spacer consisting of one nucleotide between the half-sites was essential for maximal peroxisome proliferator responsiveness. A PPRE containing a spacer greater than or equal to three nucleotides in length was not peroxisome proliferator responsive. PPREs with either zero or two nucleotides as a spacer were very weakly responsive. The importance of the immediate 5' flanking sequence of PPREs has been investigated. Palmer C.N.A. *et al* 1995 determined that mutants in the 5' flanking sequence of the cyp 4A6z PPRE dramatically diminished the binding of PPAR α /RXR α heterodimers, but did not affect the binding of RXR α /RXR α homodimers. Osada, S. *et al* 1997, Juge-Aubrey, C. *et al* 1997 and Ijpenberg, A. *et al* 1997 have also demonstrated the importance of the 5' flanking nucleotide in PPAR α /RXR α heterodimer binding. Castelain, H. *et al* 1997 using a binding site selection assay with PPAR α /RXR α heterodimers found that half of the binding sites recovered contained DR1, DR2, two palindromic half sites with zero spacing (PAL0) and DR3 elements, in diminishing order of frequency. The remaining half of the binding sites recovered contained three half sites with varying spaces from 0 to 7 nucleotides. An element with three half sites spaced by one nucleotide was most efficient at mediating the effects of peroxisome proliferators. These results indicate that the upstream flanking sequence of a DR1 PPRE is important in influencing the binding of PPAR α /RXR α heterodimers.

Section 1.3 Nuclear steroid hormone receptors

Section 1.3.1 Nuclear receptors bind DNA in a polarity specific manner

The binding polarity of PPAR α / RXR α and PPAR γ / RXR α heterodimers on a DR1 element has been determined using two distinct methods. PPAR γ and mutant PPAR α and RXR α containing the P-box of glucocorticoid receptor (GR), giving both PPAR α -P-GR and RXR-P-GR the binding specificity of GR were tested for binding to a DR1 containing a GR half-site in either the 5' or 3' position. (Direnzo, J. *et al* 1997, Ijpenberg, A. *et al* 1997 and Osada, S. *et al* 1997) PPAR α -P-GR / RXR α heterodimers were shown to bind to the DR-1 elements in which the 5' half site contained a GR half site. PPAR γ / RXR-P-GR binding was only observed for the GR half-site in the 3' position. Photo cross-linking of PPAR γ / RXR α heterodimers to an acyl-CoA oxidase PPRE found that PPAR γ occupies the 5' half-site and RXR α the 3' half-site (Direnzo, J. *et al* 1997). Thus the polarity of PPAR binding is conserved between both the α and γ isoforms. Vitamin D receptor (VDR) / thyroid hormone receptor (TR) heterodimer polarity directs the ligand sensitivity of transactivation. On the Vitamin D response element (VDRE) of rat 9k calbindin gene promoter the polarity is 5'-TR/VDR-3', but on the mouse 28k calbindin VDRE the polarity is 5'-VDR/TR-3'. The ligand for the downstream receptor controls the transcriptional activity of the heterodimeric complex (Schrader, M. *et al* 1994). RAR / RXR heterodimers bind to both DR1 and DR5 elements. On a DR1 RAR binds to the 5' half-site, but on a DR5 it binds to the 3' half-site. RAR has ligand induced transcriptional activation only on DR5 sites. Mutations that reverse the polarity of RAR / RXR heterodimers on DR5 elements reverse the ligand activated transcriptional response (Kurokawa, R. *et al* 1993 and 1994).

Section 1.3.2 Nuclear receptor cross talk regulates transcription.

PPAR α receptor signaling occurs through heterodimerisation with RXR α , and subsequent binding to DNA response elements. Proteins which can influence this signaling by competing

for binding to PPAR α or RXR α or to the DNA response element are described to “cross-talk” with the signaling pathway. The affinity of binding of other nuclear steroid hormone receptors with either PPAR α or RXR α will vary. Therefore the concentration of each type of receptor will be critical in deciding how the signaling pathway is influenced. An excess of a particular type of receptor may titrate out available PPAR α or RXR α , preventing PPAR α /RXR α heterodimers from forming. Examples of this type of cross-talk have been identified for PPAR α /RXR α mediated signaling. Jow, L. and Mukherjee, R. 1995 demonstrated that PPAR β (hNUC1) could repress peroxisome proliferator signaling mediated by hPPAR α /RXR α heterodimers. Increasing amounts of PPAR β titrated out RXR α , and formed PPAR β /RXR α heterodimer complexes bound to a PPRE. Miyamoto, T. *et al* 1997 demonstrated that high levels of thyroid hormone receptor (TR) could repress PPAR α /RXR α mediated signaling. The inhibitory action of TR was lost when a mutation was introduced into the DNA binding domain of TR, indicating that competition for DNA binding was involved. RXR α /TR heterodimers were shown to bind PPRES in electromobility shift assays. Thus it was concluded that RXR α /TR competition for binding to PPRES was the mechanism of inhibitory cross-talk by TR. The α isoform of TR (TR α) has been shown to bind to PPAR α in solution without the presence of DNA. TR α /PPAR α heterodimers did not bind to a DR4 thyroid hormone response element (TRE). TR β a different isoform of TR was found to form heterodimeric complexes on a DR2 TRE with PPAR α , and that TR β /PPAR α could induce the transcription of a reporter gene under the control of a DR2 TRE (Bogazzi, F. *et al* 1994). Thus PPAR α can cross-talk with thyroid hormone receptor signaling in either a positive manner or negative manner depending on the type of TR isoform expressed. COUP-TFII is another nuclear steroid hormone receptor shown to repress induction of gene expression mediated by peroxisome proliferators and PPAR α /RXR α heterodimers (Baes, M. *et al* 1995 and Marcus, S.L. *et al* 1996). PPAR α /RXR α heterodimers have been shown to bind to estrogen receptor response elements (EREs),

and upregulate gene expression of a reporter gene under the control of the vitellogenin A2-ERE (Nunez, S.B. *et al* 1997). The orphan nuclear steroid hormone receptor LXR α can cross-talk with PPAR α signaling. LXR α can bind to either PPAR α or RXR α in solution, but not as a heterodimer bound to a PPRE. The expression of LXR α in mammalian cell blocked peroxisome proliferator signaling mediated by PPAR α /RXR α heterodimers (Miyata, K.S. *et al* 1996).

Section 1.3.3 Phosphorylation regulates nuclear steroid hormone receptor function

Immunoprecipitation of endogenous PPAR α from primary rat adipocytes pre-labelled with [32 P]-orthophosphate and treated with vanadate and okadaic acid demonstrated that PPAR α is a phosphoprotein. Insulin was shown to produce a time dependent increase in phosphorylation of PPAR α . The change in phosphorylation was paralleled by an enhancement of transcriptional activation by PPAR α (Shalev, A. *et al* 1996). *In vivo* [32 P]-orthophosphate labelling experiments have demonstrated that PPAR γ is also a phosphoprotein. PPAR γ can undergo epidermal growth factor (EGF) -stimulated MEK/mitogen activated protein (MAP) kinase dependent phosphorylation. Mutation of the Ser82 phosphorylation site in PPAR γ to Ala82 inhibited phosphorylation of PPAR γ and inhibited growth factor mediated transcriptional repression (Camp, H.S. and Tafuri, S.R. 1997). Phosphorylation of human thyroid receptor β (TR β) enhances the formation of TR β /RXR β heterodimers on thyroid hormone response elements (TRE). Dephosphorylation led to the loss of ability to form heterodimers. Okadaic acid inhibition of phosphatases 1A and 2A increased *in vivo* phosphorylation of TR β and increased reporter gene expression under the control of a TRE (Bhat, M.K. *et al* 1994).

Section 1.3.4 DNA binding domains define specific DNA interactions

The nuclear steroid hormone receptor superfamily is a well conserved group of receptors (Laudet, V. *et al* 1992 and Motojima, K. 1993). The tertiary structures of glucocorticoid receptor (GR), estrogen receptor (ER) and retinoid X receptor (RXR) have been solved by

crystallography (Luisi, B.F. *et al* 1991 and Schwabe, J.W. *et al* 1993) and by NMR studies (Schwabe, J.W.R. *et al* 1990, Lee, M.S. *et al* 1993 and 1994). The DNA binding domain (DBD) of this group of nuclear receptors contains two zinc finger structures making them distinct from other groups of DNA binding proteins. The Zn^{2+} ions are tetrahedrally co-ordinated by four cysteines stabilising two peptide loops. This type of DBD differs from other eukaryotic zinc finger containing receptors such as TFIIA, ADR-1 and Xfin. Zn^{2+} ions in these receptors are co-ordinated by two histidines and two cysteines (Freedman, L.P. and Luisi, B.F. 1993). The Zn^{2+} co-ordination site of the yeast transcription factor GAL-4 is different as it has two Zn^{2+} ions sharing a cluster of six cysteines (Marmomstein, R. *et al* 1992). These structurally distinct zinc finger containing domains share the general feature that Zn^{2+} fingers stabilize and orientate an α -helix for interaction with the major groove of the DNA response element (Freedman, L.P. and Luisi, B.F. 1993). Analysis of the tertiary structures of the GR and ER DBDs complexed with their cognate response elements indicate that the P-box in the first zinc finger functions as the recognition helix that is inserted into the major groove (Luisi, B.F. *et al* 1991 and Schwabe, J.W.R. *et al* 1990). A feature of PPARs that makes them a distinct sub-family from other steroid hormone receptors is the size of the D-box in the second zinc finger. PPARs have three amino acids, whereas all other receptors have 5 (Laudet, V. *et al* 1992 and Motojima, K. 1993). The function of the D-box in PPARs has not been defined. The cloning and expression of PPAR α DBD would facilitate the possibility of detailed structural and functional analysis of PPAR α DBD. X-ray crystallographic studies, NMR studies and electromobility shift assays could be performed on PPAR α DBD to determine the structural and sequence specific features of PPAR α that make them distinct from other nuclear steroid hormone receptors. This information will advance our understanding of the mechanism by which PPAR α is controlled and how specific gene regulation is mediated. It has been an aim of my work to clone, express and purify soluble mPPAR α -DBD protein and to determine if as a single domain it can retain its DNA binding function.

Section 1.3.5 DNA binding domains contain important dimerisation sequences

Structural features of Retinoid X Receptor (RXR), Retinoic Acid Receptor (RAR), Thyroid Hormone Receptor (TR), Hepatic Nuclear Factor-4 (HNF-4) and Vitamin-D Receptor (VDR) which regulate their function have been characterised. Wild type and mutant forms of the DBD of RXR, RAR, TR and HNF-4 have been produced as stable proteins and have been assayed in DNA binding experiments. Both binding specificity to DNA response elements and heterodimerisation function have been located in the DBD of these receptors (Mader, S *et al* 1993 and Zechel, C. *et al* 1994). The D-box of the C-terminal CII zinc finger of RXR forms a surface specifically required for the formation of the heterodimerisation interface on direct repeat-4 (DR4) and DR5 elements. RAR / RXR heterodimerisation on DR5 elements requires the tip of the RAR CI zinc finger. TR / RXR heterodimers need a seven amino acid sequence encompassing the pre-finger region in the TR partner (Zechel, C. *et al* 1994). The HNF-4 receptor like RXR has an important dimerisation region in the DBD called the T-box (Jiang, G. *et al* 1997 and Wilson, T.E. *et al* 1992). The T-box of RXR forms an α -helix immediately after the conserved Gly-Met boundary that signals the end of the zinc finger region. The T-box helix mediates both protein-protein and protein-DNA interactions required for co-operative, dimeric binding of RXR-DBD to DNA (Lee, M.S. *et al* 1994). The T-box is conserved between HNF-4 and RXR but not PPARs. HNF-4 has an A-box region next to the T-box which makes important protein-DNA contacts with nucleotides flanking the core recognition sequence of the response element (Jiang, G. *et al* 1997).

Section 1.3.6 Ligand binding domains contain important dimerisation sequences

The ligand binding domains (LBDs) of RXR and TR contain important dimerisation sequences. Mader, S. *et al* 1993 found that dimerisation function in the LBD stabilises but does not change the receptors DNA binding specificity. Qi, J-S. *et al* 1995 used GAL-4.DBD-RXR.LBD and GAL-4.DBD-TR.LBD fusion proteins to demonstrate that functional dimerisation could take

place in the absence of DBDs in RXR or TR. Gal-4:DBD-RXR:LBD coexpression in a cell line with full length PPAR γ could induce transcriptional activation of a GAL-4 response element containing reporter gene construct in the presence of Wy-14,643. This result shows that there is sufficient heterodimerisation interface in the LBD of RXR to allow functional interactions with PPAR to take place (Qi, J-S. *et al* 1995). The crystal structure of RXR LBD homodimers found that approximately 11% of each monomer solvent accessible surface contributes to the dimerisation interface, typical of specific protein-protein interactions (Bourguet, W. *et al* 1995).

Section 1.3.7 LBDs interact with basal transcription machinery

RXR-LBD makes specific and direct contacts with a conserved region of TATA-binding protein, a protein of the cells basal transcription machinery. Mutations that reduced ligand dependent transcription by RXR also reduced RXR-TATA binding protein interactions (Schulman, I.G. *et al* 1995). Using a yeast two hybrid protein interaction assay MacDonald, P.N. *et al* 1995 found that the LBD of TR forms specific protein contacts with the basal transcription factor TFIIB. This interaction was also demonstrated in an *in vitro* binding assay. Similar regions in RXR or RAR did not bind TFIIB.

Section 1.3.8 Nuclear steroid hormone receptors contain two transcriptional activation domains

Regions involved in transcriptional activation (Activation Functions , AFs) have been mapped in PPAR γ , RXR α , RXR β and RAR α . An N-terminal ligand independent transcriptional activation domain corresponding to amino acids 31-99 in PPAR γ has been characterised (Werman, A. *et al* 1997). The AF domain of PPAR γ 2 exhibits 6-fold greater activity than the AF domain of PPAR γ 1 isoform. Leng, X. *et al* 1995 demonstrated a separable AF domain within the E-region, 21 amino acids long at the extreme C-terminal end of RXR β . Deletion of this AF domain resulted in a constitutive transcriptional silencer receptor. RXR and RAR contain an AF1 domain in the N-terminal A region, and an AF2 domain in the LBD. AF1 fused to a

GAL-4 DBD functioned as a transcription activator in the absence of ligand, whereas AF2 functioned as a transcriptional activator only in the presence of ligand (Folkers, G.E. *et al* 1996). The activity of AF1 displayed strong cell type specificity, with AF2 cell type specificity to a lesser degree. These results implied cell specific co-activator molecules were required for maximal transcriptional activity.

Section 1.3.9 Nuclear receptors interact with co-activator proteins

Folkers, G.E. *et al* 1996 found that in some cell lines, the additional expression of adenoviral E1A protein, a transcriptional co-activator, synergistically activated transcription of RAR and RXR. *In vitro* transcription experiments by Conaway, R.C *et al* 1993 had already demonstrated that for activated transcription by AF domains protein co-factors were required. Ligand dependent transcription by RAR on DR5 elements requires the removal of nuclear receptor co-repressor (N-CoR), and recruitment of co-activators P140 and P160. N-CoR associates with RAR/RXR heterodimers on DR1 and DR5 response elements. RAR or RXR ligand causes the dissociation of N-CoR from RAR/RXR heterodimers, but only on DR5 elements (Kurukawa, S. *et al* 1995). N-CoR was shown to interact within the hinge region of RAR. This stretch of amino acids was defined as the CoR-box. The AF2 domain of ER interacts with P140 and P160 in an estrogen dependent manner (Halachmi, S. *et al* 1994). BRL49653, a PPAR γ agonist stimulates the binding of P160 to PPAR γ . P140 and P160 interact with RXR α homodimers and RXR α / PPAR γ heterodimers in the presence of RXR ligand LG69 (Direnzo, J. *et al* 1997). Cloning of the cDNA of P160 (Hong, H. *et al* 1996) revealed that it was an extended form of co-activator SRC-1, originally cloned by Onate, S.A. *et al* 1995. SRC-1 is a protein that interacts with multiple nuclear receptors in a ligand dependent manner, and functions as a co-activator of transcription. The coactivator SRC-1 has been shown to bind PPAR α in a ligand specific dependent manner (Krey, G. *et al* 1997). A newly identified coactivator protein PPAR γ -binding protein (PBP) has been shown to bind to PPAR α also in a ligand dependent manner (Zhu, Y.

et al 1997). However, neither SRC-1 nor PBP have been tested to see if they can augment peroxisome proliferator induced transcription mediated by PPAR α . It is possible that the species differences in response to peroxisome proliferators is due to differing expression of coactivator proteins or differences in interactions of coactivator proteins with PPAR α . The cloning of coactivator proteins from responsive and non-responsive species and the characterisation of their interaction and activity with PPAR α needs to be determined. LG69 and BRL49653 can both induce the interaction of SRC-1 with PPAR γ / RXR α heterodimers on an acyl-CoA oxidase PPRE. Over expression of SRC-1 enhanced PPAR γ ligand induced activation of a luciferase reporter containing a PPRE. PPAR γ LBD was fused to a GAL-4 DBD and tested for ligand induced activation of a GAL-4 response element containing reporter, in the presence and absence of SRC-1. The presence of SRC-1 markedly increased ligand induced reporter activity (Direnzo, J. *et al* 1997). These experiments indicate that SRC-1 is a co-activator of PPAR γ . Direnzo, J. *et al* 1997 also examined N-CoR interactions with PPAR γ . Using a GST-PPAR γ pull down assay no interaction of N-CoR with PPAR γ was found. Human transcriptional intermediary factor 2 (TIF-2) a 160 kDa protein with partial sequence homology to SRC-1 interacts *in vitro* with RXR, TR, ER, and RAR in an agonist dependent manner. TIF-2 enhanced AF2 and ligand dependent PR, ER and androgen receptor (AR) transcriptional activation in Cos-1 cells, but no significant enhancement of ligand induced transcriptional activation was seen for RAR (Voegel, J.J. *et al* 1996). TIF-2 is therefore described as a transcriptional co-activator for some nuclear steroid hormone receptors. Other co-activator proteins like hTAFII30, RIP140, mSUG1 and TIF1 have been shown to interact with various nuclear steroid hormone receptors in an agonist and AF2 domain dependent manner (Jacq, X. *et al* 1994, Cavailles, V. *et al* 1995 and vom Buar, E. *et al* 1996).

Section 1.3.10 Differential promoter usage and alternative splicing

PPAR γ is expressed in adipose tissue in two distinct isoforms γ 1 and γ 2. Mouse PPAR γ 1 and

PPAR γ 2 mRNAs result from transcription of different promoters within the PPAR γ gene and alternative splicing of the PPAR γ transcript (Zhu, Y. *et al* 1995). mPPAR γ 2 has an additional 30 N-terminal amino acids and hPPAR γ 2 an additional 28 N-terminal amino acids (Zhu, Y. *et al* 1995 and Elbrecht, A. *et al* 1996). Both isoforms of human PPAR γ bind thiazolidenedione ligands with the same affinity and both were equal in their ability to transactivate a reporter gene under the control of an AP2 gene regulatory response element (Elbrecht, A. *et al* 1996 and Mukherjee, R. *et al* 1997). Though PPAR γ 1 and PPAR γ 2 are functionally similar, their expression can be differentially modulated by nutritional control. In fasting mice the expression of PPAR γ 2 is reduced to a much greater extent than PPAR γ 1 (Vidal Puig, A. *et al* 1996). This may reflect distinct roles for each subtype of PPAR γ receptor *in vivo*. The retinoic acid receptor (RAR) family has three isoforms, α , β and γ , with each isoform having multiple subtypes. This diversity is generated from differential promoter usage and alternative splicing. The resultant receptors have differing domain structures and recognise different DNA response elements (Blumberg, B. *et al* 1992, Kastner, P. *et al* 1990, Giguere, V. *et al* 1990, Zelent, A *et al* 1991, Leroy, P *et al* 1991 and Nagpal, S *et al* 1992). The human glucocorticoid receptor (hGR) has two isoforms α and β , produced as a result of alternative splicing of the last two exons (Hollenberg, S.M. *et al* 1985 and Encio, I.J. *et al* 1991). hGR β is unable to bind glucocorticoid hormones or transactivate transcription (Hurley, D.M. *et al* 1991, Chrousos, G.P. *et al* 1993 and Karl, M. *et al* 1993). hGR β has been shown to inhibit the effects of hormone hGR α on a glucocorticoid-responsive reporter gene in a concentration dependent manner. hGR α and hGR β have similar patterns of tissue expression, therefore the ratio expression of these receptors will be critical in regulating a target cells responsiveness to glucocorticoid hormones (Bamberger, C.M. *et al* 1995 and Oakley, R.H. *et al* 1997). A novel vitamin D receptor VDR1 has been cloned from rat. The difference between VDR1 and VDR is generated during splicing of VDR mRNA. An intron is retained within the mRNA producing a distinct receptor. VDR1 does not exhibit ligand binding

of vitamin D but does exhibit DNA binding as a homodimer or heterodimer with VDR on vitamin D response elements. VDR1 can act as a dominant negative repressor of VDR transactivation, thus the levels of expression of VDR1 will be important for vitamin D signaling. The expression levels of VDR1 were determined to be at least 15-fold less than VDR, indicating that VDR1 activity in rat may not be significant (Ebihara, K. *et al* 1996). The Thyroid hormone receptor α (TR α) isoform has three subtypes α 1, α 2 and α 3, generated by alternative splicing of TR α mRNA. The alternative splicing is believed to disrupt a putative dimerisation domain. In DNA binding studies it was found that TR α 1 could bind to a thyroid hormone response element (TRE) as a monomer or homodimer. TR α 2 and TR α 3 could not bind to a TRE as a monomer or homodimer but could form a heterodimeric complex with RXR α on a TRE. Thus as a result of alternative splicing a complex pattern of response element binding by TR can be achieved (Nagaya, T. *et al* 1996). Differential splicing of the estrogen receptor (ER) mRNA results in the formation of many types of ER receptor being expressed. Alternative splicing resulting in deletion of exons 3 and 7 has been found for ER in many breast tumours (Zhang, Q-X. *et al* 1996). The role of these splice variants in tumour development and resistance to drug therapies targeted at the ER receptor is not known. A mutant ER receptor resulting from genomic DNA rearrangement of exons has been identified in a human breast cancer cell line (Pink, J.J. *et al* 1996).

There has not been any evidence found to suggest that PPAR α subtypes can be produced from differential promoter usage or alternative splicing, as is found for PPAR γ receptors. It is possible that PPAR α subtypes could exist in non-responsive species and that these subtypes could exert a dominant negative effect over PPAR α , resulting in the non-responsive phenotype to peroxisome proliferators.

Section 1.4 Summary

Peroxisome proliferating chemicals cause peroxisome proliferation and hepatocellular carcinogenesis to varying degrees in rodent species. The peroxisome proliferation response has been characterised in responsive species such as rats and mice. A member of the nuclear steroid hormone receptor superfamily, peroxisome proliferator activated receptor α (PPAR α) has been shown to mediate the action of peroxisome proliferators. This transcription factor is highly expressed in the liver of responsive species and regulates gene expression through specific DNA response elements called peroxisome proliferator response elements (PPREs).

Humans which are believed to be non-responsive to peroxisome proliferators also have a functional PPAR α gene expressed in the liver, which can mediate peroxisome proliferator induced transcriptional control of genes containing a PPRE. Humans therefore have some of the molecular characteristics of the mechanism of peroxisome proliferation that is observed in responsive species. This knowledge is insufficient though for determining the risk of humans getting peroxisome proliferation or hepatocellular carcinogenesis. It would be advantageous to be able to model the human response to peroxisome proliferation in an appropriate non-responsive species. Our current knowledge suggests that the guinea pig would be an appropriate laboratory animal model for peroxisome proliferation in humans. But it is not known if guinea pigs have similar characteristics to humans, such as an expressed functional PPAR α receptor. It is therefore very important for the validation of the guinea pig as a model species, that it be determined if they have an expressed functional PPAR α receptor. It is also important to understand the detailed molecular functioning of the PPAR α receptor. This can be achieved by cloning and expressing functional PPAR α receptor and PPAR α receptor domains. This will then allow experiments to be carried out which will determine what it is within the PPAR α receptor that defines and controls its regulation of gene expression.

Section 1.5 Experimental objectives

- 1) Examine the expression of mouse liver PPAR α receptor, relating functional receptor and protein levels to the PPAR α mediated physiological responses induced by peroxisome proliferators.

- 2) Investigate the molecular basis of the inability of the guinea pig to respond to peroxisome proliferators by cloning and characterising the guinea pig PPAR α receptor.

- 3) Clone and express the DNA binding domain of mPPAR α , allowing functional and structural studies of this domain.

Chapter 2 Methods

Section 2.1 Laboratory animals

Adult male Wistar Rats, adult (8-10 week) male C57 Bl/6 mice and Dukin-Hartley guinea pigs (400g) were obtained from Harlan-Olac and fed standard laboratory chow *ad lib*. Animals were kept in a standard 12 hour dark /light cycle. Mice were dosed i.p. with 100µl of 2mg/ml Methyclofenopate in corn oil (10 mg /kg body weight), or 100µl corn oil for 3 days. Animals were sacrificed by terminal exsanguination under anaesthesia. Livers were collected and weighed before processing. For diurnal studies animals were sacrificed at 6.00 am, 12.00 noon, 6.00 pm and 12.00 midnight.

Section 2.2 General Molecular Biology Techniques.

Section 2.2.1 Bacterial growth media

Luria-Bertani Broth (LB); 10g Bactotryptone, 5g Bacto yeast extract, 10g NaCl, made up to 1 litre with Ultra High Pure (UHP) water and autoclaved. LB-Agar plates; 15g agar added to 1litre of LB and then autoclaved. Media was melted, antibiotics added and poured into 10 cm petri dishes. Antibiotics were used at the following final concentrations. Tetracycline at 50µg/ ml, Ampicillin at 12.5µg / ml , Kanamycin at 12.5µg/ ml and Chloramphenicol at 34 µg/ ml. For blue white selection 40 µl of a 20 mg / ml IPTG solution and 40µl of 20 mg / ml 5-bromo-4-chloro-3-indolyl-b-D-galactoside (X-gal) solution was added and spread evenly per plate.

Section 2.2.2 Preparation of CaCl₂ competent XL1 Blue *E.coli* and BL21 (DE3) pLys S *E.coli*

Components used:

LB-Tet / Amp

LB- Chl / Amp

0.1M CaCl₂ (0.22µM filtered)

0.1M CaCl₂, 10% glycerol (0.22μM filtered)

Single colonies of XL1 Blue and BL21 (DE3)pLysS *E.coli* were inoculated in 10ml of LB-Tet/ Amp and LB-Chl / Amp media respectively. Cultures were grown in a shaking incubator overnight at 37 C. 5 ml of each culture was used to seed 500 ml of LB- Tet / Amp and 500 ml LB- Chl / Amp media. Large cultures were grown in a shaking incubator at 37 C until an OD_{600nm} = 0.6–0.8 was reached. The cultures were placed on ice for 10mins, then centrifuged in a JA14 rotor at 7000rpm for 15minutes at 4 C. 10 ml of ice cold 0.1M CaCl₂ was used to resuspend cell pellets, 10 ml per 100 ml of spun culture was used. Cells were pelleted again by a centrifugation at 7000 rpm in a JA14 rotor. Cells were resuspended in 2 ml of ice cold 0.1M CaCl₂, 10% glycerol per 50ml of original culture pelleted. Cells were put into 200 μl aliquots and stored at -80 C.

Section 2.2.3 Transformation of DNA into CaCl₂ competent *E.coli*

Cells were aliquoted into 50 μl volumes and kept on ice. 25 ng of plasmid DNA or 5 μl of a ligation reaction was added to the cells and allowed to incubate on ice for 10mins. The cells were then heat shocked at 42 C for 90 seconds and then immediately placed on ice for 2 minutes. 1ml of LB-glucose media (20 mM glucose) was added to the cells which were then cultured at 37 C for 1 hour. 100 μl of cell was added per agar plate. Plates wer incubated overnight at 37 C.

Section 2.2.4 Preparation of electro-competent *E.coli*

Components used:

LB-Tet / Amp

LB- Chl / Amp

sterile UHP water

Single colonies of XL1 Blue and BL21 (DE3) pLysS *E.coli* were inoculated in 10ml of LB-Tet/Amp and LB-Chl / Amp media respectively. Cultures were grown in a shaking incubator overnight at 37 C. 5 ml of each culture was used to seed 500 ml of LB- Tet / Amp and 500 ml LB- Chl / Amp media. Large cultures were grown with shaking at 37 C until an OD_{600nm} = 0.6-0.8 was reached. The cultures were placed on ice for 10mins, then centrifuged in a JA14 rotor at 7000rpm. 10 ml of ice cold sterile UHP water was used to resuspend the cell pellets, 10ml was used per 100ml of spun bacterial culture. Cells were pelleted by centrifugation at 7000 rpm in a JA14 rotor at 4 C for 15 minutes. Cell resuspension and pelleting was repeated a further five times with sterile UHP water. Cells were finally resuspended in 2ml of sterile UHP water , 10% glycerol per 50 ml of original culture pelleted. Cells were put into 200µl aliquots and stored at -80 C.

Section 2.2.5 Transformation of electro- competent *E.coli*

Electroporation cuvettes and cuvette holder were put on ice to cool. Frozen aliquots of cells were thawed quickly using hand warmth and then immediately put onto ice. 50µl of cells was added to 25ng of plasmid DNA . Ligation reaction DNA was first ethanol / sodium acetate precipitated and resuspended in 10 µl of UHP water. 5 µl of ligation DNA was added to 50µl of cells and put on ice. Cells were electroporated at 1.8kV using a bio-rad electroporator. 1ml of LB-glucose was immediately added and the cells allowed to recover at 37 C for 1 hour. 100µl of transformed cells were spread per agar plate.

Section 2.2.6 Phenol:Chloroform treatment of nucleic acids.

Components used:

phenol:chloroform (1v:1v)

2 volumes of phenol:chloroform was added to the sample of nucleic acid, and then vortexed thoroughly. Organic and aqueous phases are separated by centrifugation at 15000 rpm for 5

minutes in a benchtop mini-centrifuge. Contaminant proteins partition at the interface between the organic and aqueous phases. The aqueous phase is carefully removed and kept as it contains the nucleic acid.

Section 2.2.7 Precipitation of nucleic acids using the ethanol / sodium acetate protocol.

Components used:

100 % Ethanol

70 % Ethanol (v/v)

3 M sodium acetate (pH=5.2), 0.22 μ M filtered

1/10th volume of sodium acetate was added to the nucleic acid sample. 2 volumes of ethanol are added to this solution, mixed and placed on ice or at -20 C to precipitate the nucleic acid. Nucleic acid pellets were washed in a minimum of 200 μ l of 70% Ethanol. The pellet was spun to the bottom of the tube and the ethanol extracted by careful pippeting. Nucleic acid pellets were air dried to remove traces of ethanol. DNA pellets were resolubilised in UHP water and RNA pellets were resolubilised in DEPC treated water.

Section 2.2.8 Plasmid DNA purification by Alkaline lysis method

Components used:

Solution 1: 10 μ g / ml RNase A in 25 mM Tris (pH=8.0), 10 mM EDTA

Solution 2: 0.4 M NaOH, 1% SDS

Solution 3: 3M K-Acetate, 11.5% glacial acetic acid

phenol:chloroform (1v/1v)

3M Na-Acetate (pH=5.2)

100 % ethanol

70% ethanol

UHP water

1.5ml of bacterial culture was pelleted by centrifugation at 15000 rpm for 5 mins, and the supernatant discarded. A further 1.5ml of culture was pelleted in the same tube and the supernatant discarded. 100 µl of solution 1 was used to resuspend the pellet. 200µl of solution 2 was added and mixed by pipetting. The tubes were stood at room temperature for 5 mins. 150 µl of ice cold solution 3 was added and mixed by inverting the tube. The tube was put on ice for 10 mins to precipitate proteins. Precipitate was pelleted by centrifugation at 15000 rpm for 10 mins.

The supernatant was transferred to fresh tubes and 900 µl of phenol:chloroform added. The tube was vortexed thoroughly and then centrifuged at 15000 rpm for 5 minutes. The aqueous phase was transferred to new tubes and 45µl of 3M Na-Acetate added. 1 ml of 100 % ethanol was then added and the tube put on ice for 30 minutes. DNA was pelleted by centrifugation at 15000 rpm for 30 mins. The DNA pellet was washed in 200 µl of 70% ethanol. The ethanol was pipetted off and the pellets allowed to air dry. 20 µl of UHP water was used to resuspend the DNA pellet. Purified plasmid DNA was stored at -20 C until required.

Section 2.2.9 Purification of plasmid DNA on Qiagen Mini-prep and Maxi-prep columns

Components used:

Buffer P1: 50 mM Tris-Cl (pH=8.0), 10 mM EDTA, 100 µg / ml RNase A

Buffer P2: 200 mM NaOH, 1% SDS

Buffer P3: 3.0M Kac (pH=5.5)

Buffer QBT: 750 mM NaCl, 50 mM MOPS (pH=7.0), 15% v/v isopropanol, 0.15% v/v Triton X-100

Buffer QC: 1 M NaCl, 50 mM MOPS (pH=7.0), 15% v/v isopropanol

Buffer QF: 1.25 M NaCl, 50 mM Tris-Cl (pH=8.5), 15 % v/v isopropanol

70% v/v Ethanol

Autoclaved UHP water

Qiagen tip columns contain diethylaminoethanol (DEAE) anion exchange resin. The negative charge on the phosphate backbone of DNA causes the DNA to bind to this resin, and is only eluted from it at high salt concentrations. Impurities such as RNA, protein, carbohydrates and small metabolites are washed from the resin in medium salt buffers.

Section 2.2.9.1 Mini-prep method

3ml of an 10 ml overnight culture was pelleted by centrifugation at 15000 rpm. The bacterial pellet was resuspended in 0.3ml of buffer P1. 0.3 ml of buffer P2 was added and mixed thoroughly, and incubated at room temperature for 5 minutes. 0.3 ml of chilled buffer P3 was added and mixed by inversion of the sample tube. The sample was incubated on ice for 10 minutes. The sample was centrifuged at 15000 rpm for 15 minutes, then the supernatant was promptly removed and stored on ice. A Qiagen-tip 20 was equilibrated with 1 ml of buffer QBT. The supernatant was applied to the column and allowed to drain through, using gravity to pull the solution through. The column was washed four times with 1 ml of buffer QC. DNA was

eluted with 0.8 ml of buffer QF. DNA was precipitated by the addition of 0.56 ml of isopropanol. The solution was centrifuged at 15000 rpm for 30 minutes. The DNA pellet was washed with 1 ml of 70 % ethanol. 20 µl of autoclaved UHP water was used to resolubilise the DNA. The concentration of DNA was determined by measuring the $A_{260\text{nm}}$ of a diluted sample. DNA samples were stored at -20 C.

Section 2.2.9.2 Maxi-prep method

500 ml LB + antibiotics was seeded with 5ml of a 10 ml overnight culture. The 500 ml culture was then grown overnight with shaking at 37 C. The 500 ml of culture was pelleted by centrifugation at 15000 rpm. The bacterial pellet was resuspended in 10 ml of buffer P1. 10 ml of buffer P2 was added and mixed thoroughly, and incubated at room temperature for 5 minutes. 10 ml of chilled buffer P3 was added and mixed by inversion of the sample tube. The sample was incubated on ice for 20 minutes. The sample was centrifuged at 15000 rpm for 15 minutes, then the supernatant was promptly removed and stored on ice. A Qiagen -tip 500 was equilibrated with 1 ml of buffer QBT. The supernatant was applied to the column and allowed to drain through, using gravity to pull the solution through. The column was washed twice with 30 ml buffer QC. DNA was eluted with 10.5 ml of buffer QF. DNA was precipitated by the addition of 15 ml of isopropanol. The solution was centrifuged at 15000 rpm for 30 minutes. The DNA pellet was washed with 5 ml of 70 % ethanol. 300 µl of autoclaved UHP water was used to resolubilise the DNA. The concentration of DNA was determined by measuring the $A_{260\text{nm}}$ of a diluted sample. DNA samples were stored at -20 C.

Section 2.2.10 Purification of PCR products

Components used:

PB buffer

PE wash buffer

Qiaquick columns

Autoclaved UHP water

250 μ l of PB buffer was added to each PCR reaction. The sample was placed in a qiaquick spin column and centrifuged in a bench-top microcentrifuge at 14000 rpm for 60 seconds. The flow through was discarded. 750 μ l of PE buffer was added to the spin column, and then centrifuged at 14000rpm for 60 seconds. The flow trough was discarded and the column centrifuged again at 14000 rpm for 60 seconds to remove traces of residual PE wash buffer. 50 μ l of water added to the column, and centrifuged at 14000 rpm for 60 seconds to elute the bound DNA.

Section 2.2.11 Restriction endonuclease digests of DNA samples

Components used:

NBL buffer 6: 50 mM Tris-HCl (pH=7.8), 100 mM NaCl, 10 mM MgCl₂, 1 mM DTT

NBL buffer 4: 10 mM Tris-HCl (pH=8.3), 100 mM NaCl, 5 mM MgCl₂, 1 mM 2-Mercaptoethanol

Boehringer Mannheim buffer A: 33 mM Tris-Ac (pH=7.9), 10 mM MgOAc, 66 mM KOAc, 0.5 mM DTT

Boehringer Mannheim buffer B: 10 mM Tris-HCl (pH=8.0), 5 mM MgCl₂, 100 mM NaCl, 1 mM 2-Mercaptoethanol

Boehringer Mannheim buffer H: 50 mM Tris-HCl (pH=7.5), 10 mM MgCl₂, 100 mM NaCl, 1 mM Dithioerythritol

Stratagene Universal Buffer: 25 mM Tris-Ac (pH=7.6), 100 mM KOAc, 10 mM MgOAc, 0.5 mM 2-Mercaptoethanol, 10 μ g/ ml BSA

The above restriction digest buffers were used with the appropriate manufacturers restriction enzyme. Concentrations given are final assay concentrations. Assay volumes and amount of DNA digested varied according to the purpose of the assay. Analytical digests were incubated at 37 C for 1 hour. Restriction digests used for the purpose of cloning were carried out at 37 C for up to 3 hours.

Section 2.2.12 Shrimp Alkaline Phosphatase (SAP) treatment of vectors.

Components used:

10★ SAP buffer: 200 mM Tris-HCl (pH=8.0), 100 mM MgCl₂. (United States Biochemical-USB)

Shrimp Alkaline Phosphatase Enzyme (SAP). (USB)

UHP water

Restriction enzyme cut plasmid vector was gelpurified first using GeneClean II kit. Purified DNA was added to SAP buffer (assay concentration = 1★) and SAP and made up to either 30µl or 50 µl final volume. The assay reaction was incubated at 37 C for 30 minutes and then heat inactivated by incubation at 65 C for 15 minutes. DNA treated with SAP was then extracted with 2 volumes of phenol:chloroform (1v:1v) and then ethanol / sodium acetate precipitated. Pelleted DNA was resolubilised in 5-10µl of UHP water.

Section 2.2.13 Purification of DNA excised from an agarose gel,

Components used:

1★ TAE Agarose gel

NaI solution

Glassmilk silica matrix in UHP water

New Wash Buffer

UHP water

DNA was first separated and resolved on a 1★ TAE agarose gel. The gel is kept in its perspex casting tray and is visualised on a UV transilluminator to minimise UV damage to the DNA. Bands of interest were excised using a scalpel and were weighed. Three gel slice volumes of NaI was added to the gel slice. The gel slices were dissolved by heating the tube to 55 C. 5µl of glassmilk was added to the DNA solution and vortexed thoroughly. The DNA binds to the glassmilk by incubation at room temperature for a minimum of 5 minutes. The glassmilk was pelleted by centrifugation at 15000 rpm for 5 seconds. The supernatant was extracted and discarded. The glassmilk pellet was washed three times with 400 µl of ice cold New Wash Buffer. The Glassmilk was pelleted again and then resuspended in 5-10µl of UHP water to elute the DNA. The tube was heated to 55 C for 2 minutes and then centrifuged. The supernatant containing the purified DNA was carefully extracted and stored at -20 C. A second DNA elution was done by repeating the above elution step.

Section 2.2.14 Non denaturing electrophoresis in agarose gels.

Components used:

Agarose

0.5★ TBE: 5.4g / l Tris, 2.75g /l Boric Acid, 2ml / l 0.5M EDTA (pH= 8.0)

1★ TAE: 4.84g / l Tris, 1.142ml /l Glacial acetic acid, 2ml / l 0.5M EDTA (pH=8.0)

Ethidium Bromide: 10 mg / ml in UHP water

10 ★ Load Buffer: 0.25% Bromophenol Blue, 0.25% Xylene Cyanol FF, 30% Glycerol

1 kb marker ladder: 75 bp -12kbp, 0.5 µg / mm width of lane (Gibco BRL)

Electrophoresis tank, casting gel, comb and electrophoresis power supply.

UV light transilluminator

Photographic equipment

For minigels 60 ml of 0.5★ TBE or 1★ TAE buffer was placed in a duran bottle. Agarose solid was added to this solution to give a final percentage between 0.7-1.5% w/v. The solution was heated in a microwave at full power in 20 second bursts until all the agarose was dissolved. The agarose solution was allowed to cool to a hand hot temperature. The agarose was poured into a cast, containing a comb and was allowed to set. The gel was placed in the electrophoresis tank and covered with the same buffer as used to make the gel. DNA samples between 10 and 30 µl volume were prepared in a 1 ★ load buffer solution. After loading of samples the gel was run at constant voltage , 7-18v per cm gel. The gel was run for period of time that gave the desired resolution. DNA bands were visualised by illumination with UV light and photographed.

Section 2.2.15 DNA sequencing method

DNA sequencing was carried out by John Keyte in the Biomolecular Synthesis and Analysis unit, Queens Medical Centre, Nottingham. Briefly the ABI prism dye terminator cycle sequencing ready reaction kit (Perkin Elmer) was used for the PCR stage of the sequencing protocol. Only qiagen purified DNA template was used for DNA sequencing. PCR sequencing reactions were analysed on a 373A DNA sequencer (Perkin Elmer). Raw DNA sequence were inspected and edited using GCG sequence analysis software. The software programs used were, TED, SEQED, BESTFIT, GENASSEMBLE and MAP (Wisconsin Package Version 9.0). Protein sequence

alignments and phylogenetic analysis was done using GCG, CLUSTALW 1.6 (Thompson, J.D. et al 1994), SAGA (Notredame, C. and Higgins, D.G. 1996), Puzzle 4 (Strimmer, K. and von Haeseler, A. 1996), Genedoc (Nicholas, K.B. and Nicholas J.B. 1997), and Treeview computer programs.

Section 2.2.16 Purification of total RNA

Components used:

Lysis Buffer: 5M Guanidine thiocyanate, 10mM EDTA, 50 mM Tris-HCl and 8% (v/v)

2-mercaptoethanol

Precipitation Buffers: 4M LiCl and 3M LiCl

SDS-TE buffer: 0.1% SDS (w/v), 1 mM EDTA, 10mM Tris-HCl

Diethyl Pyrocarbonate (DEPC) treated water (0.1%)

RNA was extracted from liver tissue using the method of Cathala, G *et al* 1983. 1g of liver was homogenised for 30 seconds in an RNase free vial containing 5ml of lysis buffer, using a Silverston Homogeniser. 35 mL of ice cold precipitation buffer was added and mixed by tube inversion. Precipitation was carried out at 4 C overnight. The sample was centrifuged at 11000g for 90 minutes at 4 C in a JA20 rotor. The supernatant was discarded and the pellet resolubilised in 5ml of ice cold 3M LiCl. This solution was centrifuged at 11000g for 60 minutes at 4 C in a JA20 rotor. The supernatant was discarded and the pellet resolubilised in 5ml of SDS-TE. 5 mL of phenol:chloroform (1v:1v) was added. The sample was put on ice, with 20sec long vortexing every 5 minutes. The sample was then frozen at -80 C for 30 minutes. The sample was thawed on ice and then centrifuged at 10000g for 15 minutes at 4 C in a JA20 rotor. The aqueous phase was extracted and treated with phenol:chloroform as described above. The aqueous phase was

then ethanol/ sodium acetate precipitated at -20°C overnight. RNA was pelleted by centrifugation at 10000g for 15 minutes at 4°C in a JA20 rotor. The pellet was first washed in 90% ethanol in DEPC water, and then resuspended in 1 ml DEPC treated water.

Quantification of amount of RNA produced was done by measuring the $A_{260\text{ nm}}$ of a diluted sample of the RNA. The quality and integrity of the RNA was visualised by analysis of 2 μl and 4 μl of RNA in a 0.8% agarose gel made with 1 \times TBE, 0.1% SDS run at 90v for 1 hour. The gel was prestained with ethidium bromide.

Section 2.2.17 Purification of polyA⁺ RNA

Components used:

5 \times Bind buffer: 2.5M NaCl , 50 mM Tris-HCl (pH=7.5) , 0.5% (v/v) Sarkosyl , 5 mM EDTA (pH=8.0)

DEPC treated water

0.1M NaOH

Note: 1 \times Bind buffer was filtered through a 0.22 μm filter.

0.08g of Oligo -dT resin (Pharmacia) was preswollen at 4°C for 1hour by the addition of 5ml of DEPC treated water. Swollen resin was poured into a syringe barrel stuffed with glasswool at the base, and allowed to settle. The packed bed volume was approximately 0.5ml. The resin was washed first with 20 volumes of 0.1M NaOH , and then 30 volumes of DEPC treated water. The resin was then washed with 10 volumes of 1 \times Bind buffer.

1.25 mg of guinea pig total RNA was ethanol/ sodium acetate precipitated, then resuspended in 2.5ml of 1 \times Bind buffer to give a final RNA concentration of 0.5 mg/ml. The RNA sample

was heated to 65 C and loaded onto the column. The eluate was collected, heated to 65 C and loaded onto the column again. This step was repeated once more. The column was washed with 5ml of 1* Bind buffer to remove unbound RNA. Ten 0.5ml DEPC treated water samples were preheated to 65 C. Each 0.5 ml was loaded onto the column with individual 0.5ml eluate fractions being collected. RNA in each eluate fraction was precipitated using the ethanol / sodium acetate method, then resolubilised in 10ul of DEPC treated water. 2µl of each RNA fraction was analysed on a 0.8% agarose gel , made with 1*TBE / 0.1% SDS. Fractions containing intact poly A+ RNA were pooled. The amount of polyA+ RNA was quantitated by measuring the A_{260nm} of a diluted sample.

Section 2.2.18 Incorporation of [^{32}P]-labelled nucleotides

Components used:

0.5 M $Na_2 HPO_4$

DE 81 filters (whatmann)

100 % ethanol

UHP water

Hi-Safe liquid scintillant

The synthesised probe was first diluted 10 fold using UHP water (or DEPC treated water if an RNA probe was being assayed). Six 1µl aliquots of diluted probe were spotted onto six DE 81 filters and allowed to dry. Three filters were then placed in a radiation shielded container. These filters were labelled with a T to represent total counts. The other three filters were washed four times in 10 ml of 0.5M Na_2HPO_4 . Residual Na_2HPO_4 was removed by washing the filters in two 10ml UHP water washes. Filters were then rinsed in 100% ethanol and allowed to air dry.

3ml of liquid scintillant was put into a scintillation vial. Each dry filter was then put in its own scintillation tube and counted on a [^{32}P] program for 1 minute in a Packard 1900 TR liquid scintillation analyser. The amount of incorporation was calculated as follows:

mean washed filter counts / mean total filter counts \star 100 = % incorporated

Section 2.3 Protein methodologies

Section 2.3.1 Purification of liver nuclear proteins.

Components used:

Homogenisation buffer: 10 mM Hepes (pH=7.6), 25 mM KCl, 0.5 mM Spermine, 1 mM EDTA 2M Sucrose, 10% Glycerol (v/v)

Protein extraction buffer 10 mM Hepes (pH=7.6) 100 mM KCl, 3 mM MgCl_2 , 0.1 mM EDTA, 1 mM DTT, 1 mM PMSF, 10 % Glycerol (v/v)

Dialysis buffer: 25 mM Hepes (pH=7.6), 40 mM KCl, 0.1 mM EDTA, 1 mM DTT

10 % Glycerol (v/v)

Fresh liver tissue was homogenised in 8ml ice cold Homogenisation Buffer (HB). Ten mini-ultracentrifuge tubes were prepared with 400 μl cushions of ice cold HB. 550 μl of homogenate was layered onto each cushion. Tubes were centrifuged in a TLA 120.2 rotor at 120000 rpm for 8 min, at 4 C. Supernatant was discarded and new HB cushions poured over the pelleted nuclei. Remaining homogenate was layered over the cushions and the centrifugation step repeated. The nuclei pellets were resuspended in 2ml of HB. This was layered over six 500 μl cushions and centrifuged at 120000rpm for 8 min at 4 C. Nuclei pellets were resuspended in 4ml of protein extraction buffer and were incubated on ice for 30 min. 1/10th volume of 4M $(\text{NH}_4)_2\text{SO}_4$ was added and gently mixed. The solution was incubated on ice for 30 min. The solution was divided

between four mini-ultracentrifuge tubes and was centrifuged at 120000rpm for 23min at 4 C. The supernatant was collected , solid $(\text{NH}_4)_2\text{SO}_4$ was added to a final concentration of 0.3g/ml and dissolved slowly on ice. After 30min the solution was centrifuged at 120000 rpm for 23min at 4 C to pellet precipitated proteins. The protein pellet was resuspended in 800 μl of dialysis buffer and was dialysed for approximately for 18 hours against 2 litre of dialysis buffer. After dialysis the protein solution was centrifuged in eppendorf tubes at 15000 rpm for 10 min. Supernatant was collected , aliquoted out and stored at -20 C. Protein concentration was determined by Bradford assay. The integrity of the protein in the samples was analysed using SDS-polyacrylamide gel electrophoresis (SDS-PAGE).

Section 2.3.2 Bradford (Coomassie Blue) Protein Assay

Components used:

Bradford reagent: 100 mg Serva blue G dissolved in 100 ml of 85% phosphoric acid and 50 ml of 95% ethanol. This solution is made up to 1 litre and filtered through whatman paper.

1 M NaOH

Bovine Serum Albumin: 2 mg / ml in UHP water

UHP water

30 μl of protein sample was added to 50 μl of 1 M NaOH. To this 950 μl of Bradford reagent is added. The assay solution was vortexed thoroughly. The assay solution was put into a cuvette and the absorbance at 590nm was measured. BSA protein standard assays are done between the range 0-40 μg / ml. All assays are done in triplicate and the mean result determined. A plot of BSA concentration against A590nm measurements produces a linear plot. Linear regression was carried out on the data to produce the equation:

Absorbance = Slope ([] protein sample) + constant

Data from plots where $R^2 > 0.95$ were used. Unknown concentration of protein samples was calculated from the above formula.

Section 2.3.3 Polyacrylamide gel electrophoresis of proteins (PAGE)

Components used:

5★ SDS load buffer: 250 mM Tris-HCl (pH=6.8), 0.5M DTT, 10% SDS (w / v), 0.5% bromophenol blue, 50% glycerol (v / v)

Denaturing running buffer: 25 mM Tris-HCl (pH=8.3), 250 mM glycine, 0.1% SDS (w / v)

Denaturing stacking gel acrylamide solution: 4% acrylamide/bis acrylamide (30%), 125 mM Tris-HCl (pH=6.8), 0.1% SDS, 0.001% TEMED, 0.005% Ammonium persulphate (APS)

Denaturing separation gel acrylamide solution: 20% -6% acrylamide / bis acrylamide (30%), 375 mM Tris-HCl (pH=8.8), 0.1% SDS, 0.001% TEMED, 0.005% APS

Native running buffer: 0.25★TBE

Native separation gel acrylamide solution: 20% -6% acrylamide / bis acrylamide (30%), 375 mM Tris-HCl (pH=8.8), 0.001% TEMED, 0.005% APS

Protein markers: Low Molecular Weight Range, Sigma M3913 High Molecular Weight Range, Sigma SDS-7B.

Coomassie Blue stain: 0.25g coomassie brilliant blue R250 in 90 ml methanol:water (1v/1v) + 10 ml glacial acetic acid.

Destain solution: 30% Methanol (v/v), 10% glacial acetic acid.

UHP water

For denaturing polyacrylamide gel electrophoresis (SDS-PAGE) protein samples were made up to between 30 and 60 μ l volumes with 5 \times SDS load buffer (final [] = 1 \times) and UHP water and then boiled for three minutes. SDS-PAGE polyacrylamide gels for separating proteins were made at a final percentage of between 6 and 20%, depending on the size resolution required. A mini-protean gel system (Bio-Rad) was used to run the gels. After electrophoresis, the gels were stained in coomassie blue stain for 30 minutes, and then destained to remove unbound dye with several washes with destain solution. Gels were dried onto Whatman 3MM chromatography paper using a heated flatbed dryer under vacuum. For native polyacrylamide gel electrophoresis separation gels were made with native PAGE solutions, and did not have a stacking gel. Reactions run on native gels such as electromobility shift assays were not boiled in denaturing load buffer. Gels were dried onto whatman 3MM chromatography paper using a heated flatbed dryer under vacuum

Section 2.3.4 Immunoblotting analysis of liver nuclear protein extracts

Components used:

SDS-PAGE: see denaturing polyacrylamide gel electrophoresis section

Transfer buffer: 25 mM Tris-HCl, 192 mM glycine, 20% methanol (v/v), 0.1% SDS (w / v)

Methanol

PVDF membrane (Millipore Immobilon-P 0.45 μ M pore size)

Whatman Paper

1 \times TBS: 20mM Tris-HCl (pH=7.6), 500 mM NaCl

1★ TTBS: 20mM Tris-HCl (pH=7.6), 500 mM NaCl,

0.1% Tween 20 (polyoxyethylenesorbitan monolaurate)

Marvel dried milk powder

Primary antibody: Rabbit Anti-mouse PPAR α polyclonal antibody

Secondary antibody: Goat Anti-rabbit IgG (H+L) horseradish peroxidase conjugate antibody (Bio-Rad)

ECL western blotting detection kit (Amersham Life Science)

Hyperfilm (Amersham Life Science)

1★ Developer solution (Ilford)

1★ Fixing solution (Ilford)

UHP water

20 μ g of liver nuclear protein was separated using denaturing SDS-page on 7.5% or 10% gels. After electrophoresis the gel was soaked in transfer buffer for 10 minutes. A square of PVDF membrane, large enough to cover the whole of the gel was presoaked in methanol for 2 minutes and then soaked in transfer buffer for 10 minutes. The gel was placed onto two sheets of whatman paper pre-wetted with transfer buffer. All air bubbles between the gel and paper were carefully removed. The soaked PVDF membrane was overlaid on to the gel , carefully removing air bubbles. Two more sheets of pre-wetted whatman paper were overlaid onto the PVDF membrane. The sandwich gel was placed into a electro-transfer cassette , with the gel side nearest to the cathode and membrane side nearest the anode electrode. Proteins were transferred to the

PVDF membrane by electro-transfer in transfer buffer at 4 C, and at a constant 75mA. After transfer, the membrane was blocked in 1*TBST, 10% Marvel skimmed milk overnight. The blot was then incubated in 20 ml of 1*TTBS containing rabbit anti-mouse PPAR α antibody at a 1:10000 dilution for 1 hour with rocking. The blot was then washed with four 100 ml 1*TTBS washes. The blot was then incubated in 20ml of 1*TTBS containing goat anti-rabbit IgG-HRP antibody at a 1:40000 dilution for 1 hour with rocking. The blot was then washed with four 100 ml 1*TTBS washes and developed using the ECL kit according to the manufacturers instructions. Blots were then exposed to hyperfilm for 1 hour. Films were soaked in 1* developer for 2 mins, washed in water for 2 mins, fixed in 1* fixing solution for 2 mins and then allowed to air dry.

Section 2.4 cDNA cloning methodologies

Section 2.4.1 Synthesis of 1st strand cDNA by reverse transcription

Components used:

Superscript II RNase H- Reverse Transcriptase, 200u / μ l (Gibco BRL, Life Technologies)

5* First strand Buffer: 250 mM Tris-HCl (pH=8.3), 375 mM KCl, 15 mM MgCl₂, 0.1 M Dithiothreitol (DTT)

Section 2.4.1.1 1st strand cDNA synthesised using total RNA as a template.

5, 2.5 and 1 μ g of total RNA was each added to 500ng of Oligo -dT (12-18) primer and the total volume made up to 11 μ l with DEPC treated water. Each reaction was heated to 70 C for 10 minutes and then chilled on ice immediately, then centrifuge. To each tube the following were added. 4 μ l of 5* 1st strand buffer, 2 μ l 0.1M DTT, 1 μ l 10mM dATP, dGTP, dCTP and dTTP mix. To one tube 1 μ l of [³H] dCTP (50 μ M stock) was added. 1 μ l of DEPC treated water was added to the other two tubes. All three tubes were heated to 42 C for 2 minutes, then 1 μ l of Superscript II enzyme was added to each tube and mixed thoroughly. The tubes were incubated

at 42 C for a further 50 minutes, then at 70 C for 15 minutes. The tubes were cooled on ice, and 2µl of Rnase H added to each. These were then incubated at 37 C for 20 minutes. A DE81 assay was carried out on the reaction containing [³H]dCTP. This verified that 1st cDNA had been made.

Section 2.4.1.2 1st strand cDNA synthesised using poly A+ RNA.

The method that was used to generate 1st strand cDNA from total RNA was used, except that 600ng and 300ng of poly A+RNA was used as template material.

Section 2.4.2 PCR Amplification of guinea pig cDNA's.

PCR primers were designed from regions of DNA sequence identity of mouse , human and xenopus PPARa's. Two sets of primers were used to generate 436bp and 1056bp DNA fragments from reverse transcribed guinea pig total and poly A+ RNA. Guinea pig primer (GPIGP) 2 and GPIGP3 were used to generate the 436bp fragment. GPIGP4 and GPIGP3 were used to generate the 1056bp fragment.

Components used:

Primer name and DNA sequence

GPIGP2 5' -GATGAACAAAGACGGGATGCTG-3'

GPIGP3 5' -CTCAGTACATGTCCCTGTAGAT-3'

GPIGP4 5' TACGGAGTTCACGCATGTGAAGGCTGCAAGGGCTTCTT-3'

10 * KlenTaq PCR reaction buffer: 400 mM Tricine-KOH (pH 9.2 at 25 C), 150 mM KOAc, 35 mM Mg(OAc)₂, 750 µg/ml Bovine Serum Albumine.

Klen Taq Polymerase Mix: Taq start antibody: Antibody dilution buffer: DNA polymerase in the ratio 1:4:1 volumes

dNTP mix : 10 mM dATP, dGTP, dCTP, dTTP (Pharmacia)

Autoclaved UHP water

The general PCR reaction contained 5 µl 10× Klen Taq PCR reaction buffer, 2µl 5'-Primer (~70 pmol), 2µl 3'-Primer (~70 pmol), 1µl dNTP mix, 2µl cDNA or 25ng positive control plasmid, 1µl Klen Taq polymerase mix and water to a final volume of 50 µl. 2 drops of mineral oil was overlayed onto each reaction to prevent evaporation. A three step cycle was used for each PCR reaction. A denaturation temperature of 94 °C and extension temperature of 72 °C were used. The annealing temperature was dependant upon the sequence of the primers used. The following formula was used to calculate appropriate annealing temperatures.

$$81.5 + 16.6(-\log [\text{salt} +]) + 0.41 (\% \text{ GC}) - (675 / \text{number of nucleotides in primer})$$

5µl of each PCR reactions was analysed on appropriate percentage agarose gels, made with 0.5× TBE, prestained with ethidium bromide (final [] = 0.166 µg/ml) and run at 100v for 1 hour.

Section 2.4.3 Ligation of amplified putative guinea pig PPAR α cDNA fragments.

Components used:

pGEM -T vector (50 ng / µl): pGEM-5Zf(+) digested with EcoRV and 3' terminal thymidines added (Promega)

10 × T4 DNA ligase buffer: 300mM Tris-HCl (pH=7.8), 100 mM MgCl₂, 100 mM DTT, 5 mM ATP (Promega)

T4 DNA ligase in 10 mM Tris-HCl (pH=7.4), 50 mM KCl, 1 mM DTT, 0.1 mM EDTA, 50% Glycerol (Promega)

Autoclaved UHP water

The following ligation reactions were assembled. 1µl 10[×] T4 DNA ligase buffer, 1µl pGEM-T vector, 1µl T4 DNA ligase, 1 or 5 µl Qiaquick spin purified PCR product, and water to a final reaction volume of 10µl. The reactions were incubated at 4 C overnight. 5µl of each ligation reaction was transformed into 50µl of CaCl₂ competent XL1 Blue *E.Coli*. Blue/ white selection was used to select for plasmids containing an insert 10 white colonies to 2 blues colonies were cultured in 5ml of TET/AMP Lbroth. DNA was miniprepped from each culture using the alkaline lysis method. 1µl of uncut DNA from each miniprep was analysed on 1% agarose gel. Plasmid DNA without an insert has a lower molecular weight and migrates through the gel faster than plasmid DNA with an insert. Therefore plasmids containing an insert are easily distinguishable. Three plasmids positive for both cDNA inserts were purified using Qiagen miniprep columns and DNA sequenced. The following primers were used for sequencing.

pUC/M13 forward primer 5' -GTTTTCCTCCAGTCACGAC-3'

pUC/M13 reverse primer 5' -GGAAACAGCTATGACATG-3'

GPIGP8 primer 5' -GCGGATCTACGAGGCCTACCTG-3'

GPIGP9 primer 5' -CCGCAAACCCTTCTGCGACATG-3'

GPIGP10 primer 5' -GCCGGGCCGATCTCCGCAGCA-3'

GPIGP11 primer 5' -CCACCGACACACACTGGCAGC-3'

GPIGP12 primer 5' -CTGTCCCGGTCACAGGTGAGG-3'

Section 2.5 Amplification of 5'-cDNA ends using RACE

Components used:

GPIGP6 primer: 5' -GCCCTTTGCAGCCTTCACATGCGTGAAGTCC-3' (35 pmol / µl)

GPIGP7 primer 5' -GATCTTGCAGCTGCGGTCACATTTGTCG-3' (35 pmol / μ l)

5' RACE system for rapid amplification of cDNA ENDS (version 2, Gibco BRL.)

5' RACE abridged anchor primer:

5' -GGCCACGCGTCGACTAGTACGGGIIGGGIIGGGIIG-3'

Universal amplification primer:

5' -CUACUACUACUAGGCCACGCGTCGACTAGTAC-3'

Guinea pig total RNA

Guinea pig polyA+ RNA

DEPC treated water

Synthesis of cDNA

Two reactions were setup as follows. 3.5 pmol of GPIGP7 primer was added to 1 μ g of polyA+ RNA and 1 μ g of total RNA in separate tubes. DEPC water was added to a final volume of 15.5 μ l. The tubes were heated to 70 C for 10 mins to denature secondary RNA structures. The tubes were then chilled on ice and then centrifuged briefly. 2.5 μ l of 10 \times PCR buffer, 2.5 μ l of 25mM MgCl₂, 1 μ l of 10mM dNTP mix and 2.5 μ l of 0.1 mM DTT were added to each tube. The tubes were incubated at 42 C for 1 minute and then 1 μ l of Superscript II reverse transcriptase was added to each. The reactions were incubated for a further 50 mins at 42 C. Final composition of the reaction was 20mM Tris-HCl (pH=8.4), 50 mM KCl, 2.5 mM MgCl₂, 10 mM DTT, ~ 1.4 ng GPIGP7 primer, 400 μ M dATP,dCTP,dTTP,dGTP, 40ng/ μ l RNA and 200 units of reverse transcriptase. Reverse transcription was terminated by incubating the tubes

at 70 C for 15 mins. The tubes were centrifuged and then 1µl of RNase mix was added to each tube. The reactions were incubated at 37 C for 30 mins.

Section 2.5.1 Purification of cDNA

cDNA's were purified using Glassmax DNA isolation spin cartridges. Briefly, 120µl of 6M NaI was added to each tube of cDNA. The solution containing the cDNA's was transferred to a spin cartridge, which was then centrifuged for 20 seconds at maximum g. Four 350µl aliquots of wash buffer and two aliquots of 70% ethanol was used to wash the bound cDNA. cDNA was eluted from the spin cartridge by the addition of 50µl of water (pre-heated to 65 C) and centrifugation for 20 seconds.

Section 2.5.2 Homopolymeric tailing of cDNA

Purified cDNA was treated with Terminal deoxynucleotidyl transferase (TdT) to add a homopolymeric tail of dCTP's. The following reaction was setup for cDNA made from both polyA+ RNA and total RNA. 6.5 µl of DEPC treated water, 5 µl of 5★ tailing buffer, 2.5µl of 2mM dCTP was added to 10µl of cDNA. The tubes were incubated at 94 C for 2 minutes, and then chilled on ice immediately , and then centrifuged. 1µl of TdT enzyme was added to each tube and the reactions were incubated at 37 C for 10 mins. TdT was heat inactivated by incubation at 65 C for 10 mins.

Section 2.5.3 PCR amplification of dC-tailed cDNA

cDNA produced from both polyA+ RNA and total RNA was amplified with (a) 5'RACE kit reagents (reactions 1 and 2) and (b) Pharmacia Taq DNA polymerase reagents (reactions 3 and 4). The general reaction was as follows:

10★ PCR Buffer 5µl

25 mM MgCl₂ (omitted from (b) reactions) 3µl

GPIGP6 primer 1 μ l

5' RACE primer 2 μ l

10 mM dNTP mix 1 μ l

dC-tailed cDNA 5 μ l

Water (made up to a volume of 47 μ l)

Taq DNA polymerase mix 3 μ l

The reactions were amplified using the conditions [94 C ,1 min; 61 C, 1 min; 72 C ,1 min 30 secs] for 35 cycles. 5 μ l of each reaction was analysed on a 1% agarose gel (0.5 * TBE). A negative control reaction was done for each set of reagents. These reactions did not contain any cDNA template. PCR products were identified on a 1% agarose gel. 1 μ l of each reaction was reamplified, using GPIGP6 and universal anchor primers, using the above conditions for 20 cycles. The products of reactions 3 and 4 were diluted 20-fold and 100-fold respectively and were reamplified using GPIGP6 and universal anchor primers. The products of the reamplification step were analysed on a 1% agarose gel. DNA fragments were produced from reactions 1, 3 and 4. These fragments were purified using Qiagen QIAquick PCR purification spin columns (see general molecular biology methods section). Purified PCR product was resuspended in 30 μ l of ultra high pure water.

Section 2.5.4 Cloning and sequencing of 5' cDNA ends.

Components used:

pGEM -T vector (50 ng / μ l): pGEM-5Zf(+) digested with EcoRV and 3' terminal thymidines added (Promega)

10 ★ T4 DNA ligase buffer: 300mM Tris-HCl (pH=7.8), 100 mM MgCl₂, 100 mM DTT, 5 mM ATP (Promega)

T4 DNA ligase in 10 mM Tris-HCl (pH=7.4), 50 mM KCl, 1 mM DTT, 0.1 mM EDTA, 50% Glycerol (Promega)

Autoclaved UHP water

The following ligation reactions were assembled. 1µl 10★ T4 DNA ligase buffer, 1µl pGEM-T vector, 1µl T4 DNA ligase, 5 µl Qiaquick spin purified PCR product, and water to a final reaction volume of 10µl. The reactions were incubated at 4 C overnight. 5µl of each ligation reaction was transformed into 50µl of CaCl₂ competent XL1 Blue *E.Coli*. Blue/ white selection was used to select for plasmids containing an insert. 10 white colonies and 2 blue colonies were cultured in 5ml of TET/AMP LB-broth. DNA was minipreped from each culture using the alkaline lysis method. 1µl of uncut DNA from each miniprep was analysed on 1% agarose gel. Clones for all of the purified PCR products were obtained. Five plasmid clones were purified using qiagen mini prep columns and were sequenced with the following primers. The clones were termed GP11, GP12, GP13, GP14 and GP15.

pUC/M13 forward primer 5' -GTTTTCCTCCAGTCACGAC-3'

pUC/M13 reverse primer 5' -GGAAACAGCTATGACATG-3'

GPIGP14 primer 5' -CTTGGAGGCCGAGGACCTGGAG-3'

GPIGP15 primer 5' -TCCAGGTCCTCGGCCTCCAAGG-3'

Section 2.6 Overlapping PCR method

The strategy used to generate full length cDNA involved PCR amplification of two overlapping

PCR products. A 394 bp 5' product was made by PCR amplification of 5'cDNA end clone GP11 with GPIGP16 (5' -GGACTGGCTCCTCCCCGCGGACATGGTGG-3') and GPIGP6 (5' -GCCCTTTGCAGCCTTCACATGCGTGAAGTCC-3') primers. A 1056 bp was generated by PCR amplification of clone GP1, using GPIGP4 and GPIGP3 primers. The general PCR reaction was as follows.

2µl each primer

5µl 10★ Taq polymerase buffer

1µl 10 mM dNTP's

0.5 µl Template DNA (25 ng)

3.3µl Taq Polymerase Mix

36.2µl UHP water

The reaction was amplified under the following conditions, [94 C, 1 min; 56 C, 1 min; 72 C, 2 min] for 25 cycles. The 394bp product and 1056bp product were used in a two stage amplification was used to generate the full length cDNA:

Reaction (A)

5µl 10★ Taq Polymerase buffer

1 µl 10 mM dNTP's

1µl 394bp product

1µl 1056bp product

41.5 µl UHP water

The reaction was assembled and overlayed with 3 drops of mineral oil, then heated to 94 C for 1 min. 0.5µl of Taq polymerase was added to the reaction. DNA was then amplified under the following conditions [94 C, 1 min; 57 C, 1 min; 72 C, 2 min] for 10 cycles.

Reaction (B):

5µl 10★ Taq Polymerase Buffer

1µl 10 mM dNTP's

2µl GPIGP16 primer

2µl GPIGP3 primer

1µl 10-fold diluted reaction (A)

38.5µl UHP water

The reaction was assembled and overlayed with 3 drops of mineral oil, then heated to 94 C for 1 min. 0.5µl of Taq polymerase was added to the reaction. DNA was then amplified under the following conditions [94 C, 1 min; 57 C, 1 min; 72 C, 2 min 30s] for 25 cycles. 5µl of reaction (B) was analysed on a 1% agarose gel. PCR produced was purified using a Qiagen QIAquick PCR purification spin column (see general molecular biology methods section). A 1.4kb product was produced and ligated into pGEM-T vector, and then transformed into XL1 Blue *E.coli* cells. Putative clones termed α1-full-pGEM-T were mapped with the restriction enzymes Pst I, Sac II, Not I and Eco 52I for verification of correct insert DNA.

Section 2.6.1 Cloning of 1.4kb cDNA into pBK-CMV

1.4kb cDNA was cloned into a mammalian expression vector, pBK-CMV. The 1.4kb cDNA could not be cloned directly into pBK-CMV, and so was first cloned into pBluescript SK(+). $\alpha 1$ -full-pGEM-T and pBluescript SK (+) was cut with Sac II and Not I restriction enzymes. Each restriction digest was run on a 0.8% agarose gel made with 1 \times TAE buffer. The 1.4kb insert and linearised pBluescript SK(+) vector were gel excised and purified using the GeneClean II kit (see general molecular biology techniques section) .The 1.4 kb insert and linearised pBluescript SK(+) DNAs were ligated together and were transformed into XL1 Blue *E.coli* cells. Putative $\alpha 1$ -full-pBluescript clones were isolated. A Sac I / Not I double restriction enzyme digest was performed to verify the presence of the the 1.4kb insert. $\alpha 1$ -full-pBluscript DNA was then purified using a Qiagen mini prep column.

$\alpha 1$ -full-pBluescript and pBK-CMV DNAs were digested with Sac I and Not I restriction enzymes. Each restriction digest was run on a 0.8% agarose gel made with 1 \times TAE buffer. The 1.4kb insert and linearised pBK-CMV were gel excised and purified using GeneClean II kit. The 1.4kb insert and linearised pBK-CMV were ligated together and were transformed into XL1 Blue *E.coli* cells. Putative clones of full length cDNA-pBK-CMV (gpig α -pBK-CMV) were screened for the presence of an insert by restriction digest with a Sac I / Not I double digest. gpig α -pBK-CMV DNA was purified using a quiagen mini-prep column. The 1.4kb insert in gpig α -pBK-CMV was mapped with the following enzymes Xho I, Nar I, Eco 52I, Pst I, and Bgl II for verification that the insert was was the correct product. gpig α -pBK-CMV DNA was sequenced with the following primers in order to verify that the overlap between the 394bp and 1056 bp product had formed correctly and to also verify that the insert was correct.

GPIGP9: 5'-CCGCAAACCCTTCTGCGACATG-3'

GPIGP12: 5'-CTGTCCCGGTCACAGGTGAGG-3'

GPIGP16: 5' -GCCCTTTGCAGCCTTCACATGCGTGAAGTCC-3'

gpig α -PBK-CMV plasmid DNA was maxi-prepped using a Qiagen maxi prep column (see general molecular biology techniques section). The concentration of DNA was determined by measuring the absorbance at 260 nm.

Section 2.7 *In vitro* transcription and translation

Promegas TNT Coupled Rabbit Reticulocyte Lysate System was used to produce PPAR α and RXR α receptors *in vitro*. The manufacturers protocol was followed.

DEPC treated water 6 μ l

TNT reaction buffer 2 μ l

RNase Inhibitor (Pharmacia) 1 μ l

Plasmid DNA (1 μ g) 1 μ l

RNA polymerase 1 μ l

Amino acid mixture (- Met) 1 μ l

TNT Rabbit Reticulocyte Lysate 25 μ l

[³⁵S]-L-Methionine [1458Ci / mmol, 12.25Ci / ml] 3 μ l

Each reaction was incubated at 30 C for two hours, and then placed at 4 C until use. T3 RNA polymerase and T7 RNA polymerase were used. gpig α -pBK-CMV, hPPAR α -pBK-CMV and pGEM-RXR α plasmid DNAs were all purified on Qiagen DNA purification columns before use. 10 μ l of each transcription / translation reaction was analysed on a 10 % SDS-PAGE gel. The gels were dried and autoradiographed either on hyperfilm, or by using a BioRad G250 Phosphor

Imaging system.

Section 2.8 RNA protection assays

Section 2.8.1 Synthesis of RNA probes for RNA protection assay

General reaction:

5µl 5★ TCS buffer

1 µg Linearised template plasmid DNA

1µl 10 mM ATP, GTP, UTP

1µl 0.75 mM DTT

3 µl 12.5 µM [α -³²P] CTP , specific activity 600 Ci/mmol

3µl 10µM CTP

1µl Sp6 or T7 RNA polymerase

DEPC treated water to a final volume 25µl

Components used:

DNase I

Phenol:chloroform (1v/1v)

3M sodium acetate (pH=5.2)

100% Ethanol

Formamide solution

The transcription assay was setup as listed above and incubated at 37 C for 1 hour. 1 µl of the assay was diluted 10-fold with DEPC treated water. The diluted assay sample subjected to a DE81 assay to measure incorporation of labelled nucleotide into synthesised RNA. (see DE81 assay method) If incorporation of radiolabel greater than 10% was achieved 1 µl of DNase I was added to the synthesis reaction to degrade template DNA. RNA probe was incubated with DNase I for 30 minutes at 37 C. The reaction was cleaned up by extraction with phenol:chloroform and by precipitation by the sodium acetate/ethanol protocol. RNA was resolubilised in 20 µl of formamide solution. RNA probe was stored for a maximum of 6 hours at -20 C until use in an RNA protection assay.

Section 2.8.2 Synthesis of [α - 32 P]dCTP labelled 100 bp DNA ladder

Components used:

5ml 5* Labelling buffer: 50 mM Tris-HCl (pH=7.5), 250 mM NaCl, 50 mM MgCl₂

5 µl 10mM dATP, dTTP, dGTP mix (Pharmacia)

5 µl 100 bp DNA ladder [] = 1 µg / µl

5 µl [α - 32 P] dCTP (3.3 µM) (Dupont ICN)

2 µl Klenow (fragment of *E.coli* DNA polymerase) DNA polymerase, 5U/µl (Nbl)

3 µl UHP water

The above reaction was setup and incubated at room temperature for 2 hours. Incorporation of radiolabelled nucleotide was measured by DE 81 assay.

Section 2.8.3 Determination of gene expression levels using an RNA protection assay

Components used:

Guinea pig total RNA

Yeast tRNA: 7 µg/ ul in DEPC water

³²P-labelled RNA probe

Solution I: 80% formamide (v/v), 40 mM pipes (pH=6.7), 0.4 M NaCl, 1 mM EDTA

Solution II: 10 mM Tris-HCl (pH= 7.5), 0.35 M NaCl, 5 mM EDTA, 10 µg/ ml RNase A

100µg/ml Proteinase K

10% SDS (w/v)

Phenol:chlorofom (1v/1v)

3M sodium acetate (pH=5.2)

Denaturing load buffer: 80 % formamide (v/v), 10 mM EDTA (pH=8.0), 1 mg/ ml

Xylenecyanol FF, 1 mg/ ml bromophenol blue

1★ TBE

6% denaturing urea-acrylamide gel:

Fixing solution

Hyperfilm

A bio-rad protean gel system was used. Sequagel concentrate and diluent was used to make 50ml gels. The following formulae were used to determine the appropriate amounts of concentrate and diluent to be used in order to make a certain fixed percentage gel.

$$[(\% \text{ acrylamide gel need}) \star (\text{ volume of gel})] / 25 = \text{ volume of concentrate needed}$$

$$\text{volume of gel} - (1/10\text{th volume of gel} + \text{ volume of concentrate}) = \text{ volume of diluent}$$

For a 6% gel 5ml of 10★ TBE, 12 ml of concentrate and 33ml of diluent was mixed. 30µl of TEMED and 500µl of 10% APS was added and mixed. The gel solution was pipetted in the gel cast without introducing air bubbles. The comb was inserted into the gel and the gel was allowed to set. After setting the gel was placed in the gel tank and 1★ TBE was used to fill the anode and cathode compartments. Unpolymerised acrylamide was washed out of each well using a syringe. The gel was then heated to 55 C and pre-run at 50v for 1hour.

Section 2.8.4 RNase protection assay

30 µg of total RNA was precipitated by the ethanol / sodium acetate protocol. Two 30µg aliquots of tRNA were also precipitated. Pellets were stored at -20 C until use. ³²P labelled RNA probe was diluted 100 fold in solution I. 30µl of solution I was used to resolubilise each RNA pellet. After resolubilisation of RNA tubes were heated to 85C for 3 minutes to denature RNA secondary structure. Tubes were then switched to a 45 C waterbath and incubated overnight to allow probe hybridisation. 350 µl of solution II , minus RNase A was added to one tube containing tRNA and probe. To the remaining tubes, 350 µl of solution II plus RNase A was added. All tubes were incubated at 37 C for one hour. During this step all single strand RNA is degraded. Duplex RNA is protected from degradation. 4µl of proteinase K and 20 µl of 10% SDS was added to each tube, which were then incubated at 50 C for 45 minutes. Each protection reaction was treated with 800 µl of phenol:chloroform. The aqueous phase was extracted and ethanol / sodium acetate precipitated. Pellets were dissolved in 10µl of load buffer, heated to 85 C for 3 mins and then centrifuged. The sample was reheated to 85 C , centrifuged and then loaded onto a 6% denaturing UREA- polyacrylamide gel. 1★ TBE running buffer was stirred throughout the electrophoresis. RNA samples were electrophoresed at 250v until the Xylene

cyanol FF dye front had travelled at least 75% through the gel. The gel was fixed for 30 minutes in fixing solution and then dried under vacuum. Dried gels were exposed to hyperfilm at -70 C for between 1 and 3 days. Hyper film was developed according to the manufacturers instructions.

Section 2.9 Tissue culture procedures

Section 2.9.1 Growth and Passage of Human Embryonic Kidney 293 cells

293 cells are human embryonic kidney cells transformed with sheared human Ad5 DNA . A frozen (-80 C) ampule of 293 cells was obtained from the European collection of animal cell cultures.

Components used:

DFPS medium: 90% v/v DMEM-glutamax I (-sodium pyruvate, + pyridoxine, + L-alanyl-L glutamine), 10% foetal calf serum, 26µg / ml penicillin G, 8.2 µg / ml streptomycin.(0.22µM filtered), pre-warmed to 37 C before use.

1★ PBS: 0.21g/l KH_2PO_4 , 9g/l NaCl, 0.726 g/l $\text{Na}_2\text{HPO}_4 \cdot 7\text{H}_2\text{O}$ (pH= 7.2)

25cm² Falcon flasks

trypan blue dye

37 C incubator with 5% CO₂ and humidification

Section 2.9.2 Resurrection of frozen 293 cells

Cells were thawed at room temperature for 1 minute, then warmed to 37 C until fully thawed.

10 ml DFPS media was added to the cells, which were then pelleted by centrifugation at 100 g for 5 minutes. The supernatant was extracted and the cells resuspended in 5 ml of DFPS media, and then put into a single culture flask and incubated for 1 week. At the 1st passage the culture media was removed from the flask and the confluent cell layer was detached by washing with 5

ml of 1*PBS. Cells were pelleted by centrifugation at 100g for 5 mins. The supernatant was discarded and the cells were resuspended in 5 ml of DFPS medium. 0.5ml of cells was seeded into 4.5ml of DFPS medium in new culture flasks and incubated for 1 week. Flasks with confluent cell layers were chosen for further passage and experimentation.

Section 2.9.3 Passage of 293 cells

Medium from flasks containing confluent cell layers was removed and the cells detached by washing with 5 mL 1* PBS + 0.5mM EDTA for 5 mins at 37 C. 293 cells were pelleted by centrifugation at 100g for 5 minutes and then resuspended in 1 ml of DFPS medium. Total cell number and cell viability were determined by the following procedure. 100µl of resuspended cells were added to 20 µl of trypan blue dye. 20 µl of these cells were placed onto a haemocytometer. The total number of cells per square and the total number of blue cells per square were counted for five squares. Viable cells do not take up the blue dye as their membrane is still intact. The percentage of viable cells was calculated from the following equation:

$$[(\text{total number of cells counted} - \text{total number of blue cells}) / 100] * 100$$

The total number of cells resuspended is calculated from the following equation:

$$\text{mean number of cells per square} * 400000 (\text{number of squares in 1 ml}) * 0.83 (\text{dilution factor of dye assay})$$

The total number of viable cells can be got from multiplying the percent of viable cells by the total number of cell in 1 ml. $0.5 * 10^6$ viable cells were seeded into DFPS medium (total volume = 5 ml) for cell propagation flasks and for transfection experiments. All flasks were incubated at 37 C, with humidification.

Section 2.9.4 Synthesis of cationic liposome transfection reagent

Components used:

Dope: 10 mg / mL L- α -phosphatidylethanolamine, dioleoyl (C18:1, [cis]-9), dissolved in 1ml chloroform.(Sigma)

Dotma: 10 mg (N-[I-(2,3-dioleyloxy)propyl]-N,N,N-triethylammonium) (generous gift from C.Elcombe , Zeneca CTL)

Nitrogen Gas

Sterile UHP water

10 mg Dotma was dissolved in 1 mL of Dope, and dried at room temperature under nitrogen gas and in the dark. The dried dotma/dope mix was dissolved in 2ml of sterile UHP water and then sonicated in a 50-60Hz, 80watts Polaron Sonibath for 5 minutes. An opaque particulate solution was formed and stored at 4 C. Final concentration of dotma / dope mix was 5 μ g / μ l.

Section 2.9.5 Synthesis of (ACO-PPRE)₂.pGL3-Luc reporter vector

Components used:

pGL3-Luc promoter vector (Promega)

Long (ACO-PPRE)₂ primer A: 5' -CCCGAACGTGACCTTTGTCCTGGTC

CCCTCCGAACGTGACCTTTGTCCTGGTCCCCTTA-3'

Long (ACO-PPRE)₂ primer B: 5' -GATCTAAGGGGACCAGGACAAAGGTCA

CGTTTCGGAAGGGGACCAGGACAAAGGTCACGTTTCGGGAGCT-3'

1 μ g pGL3-Luc promoter vector was cut with Sac I and Bgl II restriction enzymes. The linearised

plasmid was run on a 0.7% agarose gel run in 1× TAE. The cut plasmid was gel excised and purified by Gene Clean II kit. The cut pGL3-Luc vector was resolubilised in 12 µl of UHP water. The following ligation reaction was setup and incubated at 4 °C overnight.

1 µl 10× T4 DNA ligase buffer: 300mM Tris-HCl (pH=7.8), 100 mM MgCl₂, 100 mM DTT, 5 mM ATP

1 µl Sac I / Bgl II cut pGL3-Luc vector

3 µl Long (ACO-PPRE)₂ primer A

3 µl Long (ACO-PPRE)₂ primer B

1 µl T4 DNA ligase in 10 mM Tris-HCl (pH=7.4), 50 mM KCl, 1 mM DTT, 0.1 mM EDTA, 50% Glycerol

1 µl UHP water

5 µl of ligation reaction was transformed into CaCl₂ competent XL1 blue *E.coli*. Putative (ACO-PPRE)₂.pGL3-Luc clones were screened for the loss of the Mlu I polylinker restriction site. Positive clones which had lost the Mlu I site were sequenced with RV3 primer (5'-CTAGCAAATAGGCTGTCCC-3'). (ACO-PPRE)₂.pGL3-Luc vector was Qiagen Maxi-prepped.

Section 2.9.6 293 cell transfection protocol

Components used:

Dotma / Dope cationic liposome mixture

DMEM medium

Qiagen pure plasmid DNA (maxiprep DNA)

Solution A: (5-12 µg DNA + 300 ul DMEM) ★ number of flasks to be transformed

Solution B: (5µl dotma / dope mix + 300 ul DMEM) ★ number of flasks to transformed

Solution A and B were made up in the class II cabinet and left to stand at room temperature for 40 mins. A and B were then mixed and left to stand for a minimum of 15 mins to form solution C. Whilst A and B were being incubated together, medium from the flasks to be transformed was removed. The attached cells were washed with no agitation in 1★ PBS for 20 seconds. The PBS was removed and 2.4 ml of DMEM added to each flask. When solution C had completed its minimum incubation period, 600 µl of this solution was added to each flask. The flasks were incubated at 37 C with 5% CO₂ and humidification for 4 hours. After 4 hours the transfection medium was removed and replaced with 5 ml of DMEM medium. Flasks were then cultured for 2 days .

Section 2.9.7 β-galactosidase histochemistry (Sanes, J.R. et al 1986)

Components used:

1★ PBS: 150 mM NaCl, 15 mM Na₂H₂PO₄ (pH=7.3)

Fixing solution: 2% Formaldehyde (v/v), 0.2% glutaraldehyde (v/v) in 1★ PBS

Developing reagent: 5 mM Ferricyanide, 5 mM Ferrocyanide, 2 mM MgCl₂ in 1★ PBS (stored in the dark at 4 C.)

5-bromo-4-chloro-3-indolyl-β-D-galactoside (X-Gal): 40 mg/ml in DMSO (stored at 20 C)

Culture media from transfected flasks was removed. 3ml of fixing solution was added to each flask, which were then incubated at 4 C for 5 minutes. The fixing solution was removed and flasks

were washed with 3ml of 1★ PBS. 3ml developer reagent was added to each flask , along with 75 µl of X-gal. Flasks were incubated at 37 C overnight. Transformed cells develop a blue cytoplasm and can be easily distinguished from non-transformed cells.

Section 2.9.8 Cell extract harvesting for reporter assays

Components used:

1★ PBS : 150 mM NaCl, 15 mM Na₂H₂PO₄ (pH=7.3)

1★ Reporter lysis buffer (Promega)

1★ Passive lysis buffer (Promega)

Medium from transfected flasks was removed and the cell layer was washed without agitation with 5 ml 1★ PBS. For extracts for CAT and Firefly luciferase assays the 1★ PBS was removed and 900 µl of 1★ reporter lysis buffer was added to each flask. Flasks were rocked for 5 mins and then scraped with a tissue culture cell scraper. Cell extract was pipetted into a microfuge tube. Extracts to be assayed for CAT activity and Firefly luciferase activity were snap frozen in liquid nitrogen, and then immediately thawed at room temperature, vortexed and then centrifuged at 15000 rpm for 15 seconds. The supernatant was transferred to fresh tubes and stored at -70 C until required for assaying. For extracts for dual luciferase assays, the 1★ PBS was removed from each flask and 900µl of 1★ passive lysis buffer was added. Flasks were rocked for 5 mins and then scraped with a tissue culture cell scraper. Cell extract was pipetted into a microfuge tube and placed on ice until use.

Section 2.9.9 Chloramphenicol acetyltransferase assay

Components used:

[D-threo-[dichloroacetyl-1-¹⁴C] Chloramphenicol, 54 mCi / mmol (Amersham)

1M Tris (pH =8.0)

25 mM n-butyryl-Coenzyme A

1.208 mg /ml Chloramphenicol in 2% Ethanol

UHP water

Transfected cell extract

5 ml Polystyrene tubes (Sarstedt cat. no. 55-476)

Xylene:2,6,10,14-Tetramethyl-pentadecane (1v:2v)

Hi-Safe Scintillation liquid

20 µl of cell extract was mixed with 30 µl of UHP water and was incubated at 65 C for 15 minutes. The tube was spun and then 10 ml Tris (pH= 8.0), 10 µl n-butyryl-CoA, 5ml [¹⁴C]-Chloramphenicol and 25µl of Chloramphenicol were added. Reactions were incubated overnight at 37 C. 200µl of Xylene:TMPD was added to each reaction, which were then vortexed thoroughly, and then centrifuged for 5 min in a benchtop centrifuge at maximum rpm. The xylene phase was pipetted into 3ml of scintillation fluid. Reactions were counted for 1 minute on a ¹⁴C program in a Packard 1900 TR Liquid scintillation analyser.

Section 2.9.10 Firefly luciferase assay

Components used:

Luciferase assay system (Promega)

Cell extract

Cell extracts were prepared using 1[×] reporter lysis buffer. 20 μ l of cell extract was mixed with 100 μ l of Luciferase assay reagent (Promega) in a tube, and placed in a Packard (PICO-LITE) luminometer analyser. Luminescence was measured for ten, 10 s periods. The average luminescence over this period was used as the final measurement.

Section 2.9.11 Dual luciferase assay

Components used:

Luciferase assay reagent II (Promega)

Stop & Glo reagent (Promega)

Cell extracts were prepared using 1[×] passive lysis buffer. 20 μ l of cell extract was added to 100 μ l luciferase assay reagent II. The luminescence of the Firefly luciferase reaction was taken over four 10s intervals in a Packard (PICO-LITE) luminomter. 100 μ l of Stop & Glo reagent was then added to the tube and the luminescence of the Renilla luciferase reaction was taken over four 10s intervals. The average luminescence for each luciferase assay was used as the final measurement.

Section 2.10 Cloning of PPAR α DNA binding domain

A 335bp cDNA fragment corresponding to amino acids 95G -198S of mPPAR α DNA binding domain was amplified by PCR from the full length mPPAR α cDNA. Two mismatch oligonucleotide primers were designed, such that a Pst I restriction endonuclease site was engineered at the 5' end of the PCR fragment , and that a translation stop codon was engineered at the 3' end of the PCR fragment. The DBD DNA fragment was subcloned into pRSETA, a prokaryotic expression vector that contains an in-frame N-terminal His⁶ tag and enterokinase cleavage site. The pRSETA-mPPAR α -DBD vector was transformed into the BL21 (DE3) pLys S strain of *E.coli*, specially designed for high level protein expression. Fusion protein expression is driven by the addition of IPTG to the culture media. BL21 (DE3) cells contain bacteriophage

DE3, a lambda derivative that carries a DNA fragment containing the lacI gene, lacUV5 promoter, the beginning of the lacZ gene and the gene for T7 RNA polymerase. T7 RNA polymerase transcription is inducible by IPTG. The T7 RNA polymerase can then transcribe the mPPAR α -DBD fusion protein from the T7 promoter present in the pRSETA vector. BL21 (DE3) pLys S cells carry a plasmid which expresses low levels of T7 lysozyme, an inhibitor of T7 RNA polymerase. The low level expression of T7 lysozyme inhibits any basal expression of fusion protein which may be cytotoxic to the cell. The low level of T7 lysozyme does not interfere with induced expression as large amounts of T7 RNA polymerase are produced. It may however cause a lag in the production of target protein.. The presence of pLys S has a secondary advantage. T7 is a bifunctional protein and also has the ability to cut specific bonds within the peptidoglycan layer of the *E.coli* cell wall. This aids lysis of the cells after a freeze thaw cycle (Mierendorf, R. et al 1994 and Tabor, S. 1990).

Components used:

1 μ l Taq DNA polymerase (in 50 % glycerol, 50 mM Tris-HCl (pH=8.0), 100 mM NaCl, 0.1 mM EDTA, 5 mM DTT, 1% Triton X-100. Promega)

5 μ l 10 * Polymerase buffer: 500 mM KCl, 100 mM Tris-HCl (pH=9.0), 1% Triton X-100

0.5 μ l 20 mM dATP, dGTP, dCTP, dTTP mix

2.5 μ l 25 mM MgCl₂

0.5 μ l upstream primer : 5' -GAGTCCCCCTGCAGTGCCCTG-3' (35 pmol / μ l)

0.5 μ l downstream primer : 5' -GAGGTCTGCAGTTTACGAATC-3' (35 pmol / μ l)

2 μ l pGEM-7 -mPPAR α plasmid (1.3 μ g / ml)

40 μ l UHP water

1.5% Agarose (1 \times TBE) gel

The above PCR reaction was assembled minus the Taq DNA polymerase, along with a negative control reaction lacking template DNA and minus polymerase. Two drops of mineral oil were overlaid onto each reaction. Reactions were heated to 94 C and then the Taq DNA polymerase added. The following cycle conditions were used, [94 C 1min, 50 C 1min, 72 C 1min] for 15 cycles. 5 μ l of each reaction were analysed on a 1.5% agarose gel. The 335bp fragment was gel purified with GeneClean II kit and restriction digested with Pst I. The bacterial vector pRSET A was restricted with Pst I and then treated with Shrimp Alkaline Phosphatase I. The digested mPPAR α -DBD fragment and pRSET A were ligated and transformed into electrocompetent XL1 Blue *E.coli* cells. Cells were plated on Tet/Amp plates and grown for 24 hour. Individual colonies were cultured and DNA purified by the alkaline lysis method. DNA preps with putative inserts were digested with Kpn I enzyme. Plasmids containing an insert in the correct orientation produced a 274 bp fragment. pRSETA-mPPAR α -DBD positives were purified with Qiagen Plasmid purification kit. pRSETA-mPPAR α -DBD DNA was transformed into BL21(DE3)pLysS *E.coli* cells using a CaCl₂ protocol and plated onto Chl / Amp plates.

Section 2.11 Cloning of thioredoxin-mPPAR α fusion

Pst I cut pThio-His.A was run on a 1% TAE gel at a constant 100v for 1hour 30 min. The linearised plasmid band was gel excised and purified using GeneClean II Kit (see general molecular biology techniques section). Purified Pst I cut pThio-His.A was ligated with Pst I cut mPPAR α -DBD PCR fragment at 4 C for 2 days. The ligation mix was transformed into CaCl₂ competent XL-1 blue *E.coli*. 12 colonies were picked and grown overnight in 5ml cultures. DNA was purified by the alkaline lysis method, and then digested with Pst I and Bgl II restriction enzymes for verification of the presence and orientation of the DNA insert. pThio-His.A-

mPPAR α -DBD DNA was transformed into BL21 (DE3) pLys S *E.coli*.

Section 2.12 Expression of DBD fusion proteins in *E.coli*

Section 2.12.1 Small scale cultures

Components used:

pRSETA-mPPAR α -DBD BL21 (DE3) pLys S *E.coli*

LB-Chl / Amp media

IPTG

15% SDS-PAGE gel

Several colonies of pRSETA-mPPAR α -DBD BL21 (DE3) pLys S *E.coli* were cultured at 37 C with shaking in 10 ml of LB-Chl / Amp media. Cultures were grown until on OD_{600nm} of 0.6–0.8 had been reached. 2ml of uninduced culture was saved and put onto ice. IPTG was added to each culture at a final concentration of 0.5 mM. A control culture of BL21 (DE3) pLys cells was grown and induced with IPTG as well. After three hours induction at 37 C with shaking, 2 ml of each culture was centrifuged to pellet the cells. 100 μ l of 2*SDS-load buffer was used to resuspend the cells, which were then boiled for 5 minutes. 10 μ l from each boiled sample was analysed on a 15% SDS-page gel.

Section 2.12.2 Large scale culture

Components used:

pRSETA-mPPAR α -DBD BL21 (DE3) pLys S *E.coli* or pThio-His.A-mPPAR α -DBD BL21 (DE3) pLys S *E.coli*

LB-Chl / Amp media

IPTG

Talon bind buffer: 50 mM NaH_2PO_4 , 10 mM Tris-HCl (pH=8.0), 100 mM NaCl, 200 μM ZnSO_4 , 5% Glycerol

Denaturing Talon bind buffer: 50mM NaH_2PO_4 , 10 mM Tris-HCL (pH=8.0), 6M Guanidinium HCl, 100 mM NaCl, 5% Glycerol

Invitrogen ProBond Binding Buffer: 20mM Sodium Phosphate, 500 mM NaCl, pH=7.8

15% & 20% SDS-PAGE gels

A colony of pRSETA-mPPAR α -DBD BL21 (DE3) pLys S *E.coli* or pThio-His.A-mPPAR α -DBD BL21 (DE3) pLys S *E.coli* was cultured at 37 C with shaking in 10 ml of LB-Chl / Amp media. Four 2.5ml aliquots of this culture was used to seed four 500ml aliquots of LB-Chl / Amp media. Each 500 ml culture was grown at 37 C with shaking to an $\text{OD}_{600\text{nm}} = 0.6-0.8$ and then induced to express mPPAR α -DBD fusion protein by the addition of IPTG to a final concentration of 0.5mM. Culturing was continued for a further 3 hours. Cells were harvested by centrifugation in a JA14 rotor at 7000rpm, 4 C for 15mins. Cell pellets were resuspended in Talon bind buffer or ProBond Binding buffer, 2ml per 25ml of centrifuged culture. Cells were freeze thawed once and then sonicated in six, 15 second bursts to lyse the cells. Soluble and insoluble material was separated by ultra-centrifugation in a TLX optima centrifuge and TLA120.2 rotor at 100000 rpm for 8 minutes at 4 C. Soluble proteins were stored at -20 C until required. Insoluble material was solubilised in 20 ml of denaturing talon buffer, and stored at -20 C until needed. The protein concentration of the soluble and insoluble fractions was determined by bradford assay. 12.5 μg of each protein sample was analysed on a 15% SDS-PAGE gel.

Section 2.13 Purification of DBD fusion proteins

Section 2.13.1 Clontech Talon affinity resin

Components used:

Talon Metal Affinity resin

Wash buffer: 50 mM NaH_2PO_4 , 10 mM Tris-HCl (pH=8.0), 100 mM NaCl, 5% Glycerol

Elution buffer: 50 mM NaH_2PO_4 , 10 mM Tris-HCl (pH=6.2), 100 mM NaCl, 5% Glycerol

Denaturing Talon wash buffer: 50mM NaH_2PO_4 , 10 mM Tris-HCL (pH=8.0), 6M Guanidinium HCl, 100 mM NaCl, 5% Glycerol

Denaturing Talon elution buffer: 50mM NaH_2PO_4 , 10 mM Tris-HCL (pH=6.2), 6M Guanidinium HCl, 100 mM NaCl, 5% Glycerol

Dialysis buffer: 25 mM Hepes (pH=7.6), 100mM NaCl, 400 μ M ZnSO_4

Native and denatured protein samples were incubated with talon affinity resin to purify His*6 tagged proteins. 3ml of Talon affinity resin (packed volume) was aliquoted into a 50ml falcon tube. The tube was spun at 700g for 5mins then the supernatant was extracted and discarded. The resin was resuspended in 15ml talon bind buffer, and centrifuged again at 700g for 5mins. The supernatant was discarded. This wash step was repeated one more time, then 10ml of the native protein sample was applied to the resin. The protein solution and resin was mixed slowly at room temperature for 20mins, and then centrifuged at 700g for 5mins. The supernatant was collected and stored at -20 C. 30 ml of Talon wash buffer was used to resuspend the resin. The tube was agitated gently for 5mins at room temperature. The resin was pelleted by centrifugation at 700g for 5mins. The wash solution was discarded. The resin was washed twice more by the same procedure. 3ml of elution buffer was used to resuspend the talon resin

pellet. The elution buffer and resin were mixed at room temperature for five minutes, and then centrifuged at 700g for 5mins. The supernatant was collected and stored at -20 °C. Two more elution steps were carried out. The native protein sample, unbound protein sample and each elution sample were analysed on a 15% SDS-PAGE gel. Talon resin was recycled as instructed by the manufacturer. His⁶ tagged proteins were purified from the denatured protein sample using the same method as used for native proteins, except that denaturing buffers were used. Elutions 1 and 2 were dialysed against 5 × 600ml of dialysis buffer over a 2 hour period at room temperature. Dialysed protein samples were analysed on a 20 % SDS-PAGE gel.

Section 2.13.2 Invitrogen ProBond Resin

Components used:

Invitrogen prepacked ProBond resin column

Binding buffer: 20mM Sodium Phosphate, 500 mM NaCl, pH=7.8

Wash buffer: 20mM Sodium Phosphate, 500 mM NaCl, pH=6.0

Imidazole elution buffers: 20mM Sodium Phosphate, 500 mM NaCl, pH=6.0 plus 50, 200, 350 or 500 mM imidazole.

ProBond resin was equilibrated with binding buffer prior to addition of soluble protein extract, according to the instruction manual. The resin in the pre-equilibrated ProBond column was resuspended in 5 ml of soluble protein extract (see large scale culturing of fusion proteins). The column was capped and gently rocked for 10 minutes. The resin was pelleted by low speed centrifugation (< 800g), the supernatant removed, and then stored on ice. A further 5 ml of soluble protein extract was bound to the resin using the same procedure. The column resin was washed twice with three 4 ml aliquots of wash buffer, by resuspending the resin and rocking for

two minutes, and then centrifugation at low speed to pellet the resin. The supernatant was removed from each wash and stored on ice. Proteins were eluted from the resin by sequential addition of 5 ml of each imidazole elution buffer. The resin was incubated in each elution buffer for 5 minutes with gentle rocking, then pelleted by centrifugation. The supernatant from each elution was collected and analysed for proteins by SDS-PAGE. The ProBond resin was recharged according to instructions in the ProBond resin manual.

Section 2.14 *In vitro* coupled transcription/translation

Components used:

6µl DEPC treated water

2µl TNT reaction buffer (Promega)

1µl RNase Inhibitor (Pharmacia)

1µl Plasmid DNA (1µg)

1µl RNA polymerase (Promega)

1µl Amino acid mixture (- Met) (Promega)

25µl TNT Rabbit Reticulocyte Lysate (Promega)

3µl [³⁵S]-L-Methionine [1458Ci / mmol, 12.25Ci / ml] (Dupont ICN)

Each reaction was incubated at 30 C for two hours, and then placed at 4 C until use. T3 RNA polymerase and T7 RNA polymerase were used. Qiagen purified pRSETA-mPPAR α -DBD, pGEM-mRXR α and pT7-7.mPPAR α DNAs were used. 10µl of each transcription / translation reaction was analysed on a 15 % SDS-PAGE gel. The gels were dried and

autoradiographed on hyperfilm.

Section 2.15 Electromobility shift assay methodologies

Synthesis of [α -³²P] dCTP labelled con-4A6z-PPRE probes

Components used:

3ml 5★ Labelling buffer: 50 mM Tris-HCl (pH=7.5), 250 mM NaCl, 50 mM MgCl₂

5μl 10mM dATP, dTTP, dGTP mix (Pharmacia)

2μl PPRE primer oligonucleotide (35 pmol / μl) 5' -CCCTGACC-3'

1μl PPRE oligonucleotide (35 pmol / μl) 5' -CAAACTAGGTCAAAGGTCAGGG-3'

5μl [α -³²P] dCTP (3.3 μM)

1μl Klenow DNA polymerase (fragment of *E.coli* DNA polymerase), 5U/μl (NBL)

5μl UHP water

The labelling assay was setup with the appropriate PPRE primers and oligonucleotides and was incubated at room temperature after the addition of Klenow polymerase for 2 hours. Synthesis of labelled probe was measured by DE 81 assay. Single mutant and double mutant ACO-PPRE probes were synthesised by the same method, using appropriate mutant oligonucleotides

Section 2.15.1 Electromobility shift assays

Components used:

Native polyacrylamide gels

0.25★ TBE

Liver nuclear protein extracts

In vitro translated proteins

³²P-labelled PPRE probes

p(dI-dC.dI-dC) (Pharmacia)

1★ Hepes EMSA buffer: 10mM Hepes (pH=7.9), 125 mM NaCl, 0.1mM EDTA, 7% v/v BSA, 1 mM DTT, 150μM PMSF

Incubation reactions of liver nuclear proteins or in vitro translated proteins with PPRE probes were setup, in the presence or absence of non-specific competitor DNA. The incubation reactions were either carried out at room temperature or on ice, then electrophoresed on an appropriate percentage native polyacrylamide gel in 0.25★ TBE running buffer. Gels were dried and autoradiographed either on hyperfilm or by phosphoimaging on a Bio-Rad GS250 Molecular imager.

Chapter 3

Results

Section 3.1 Rat liver nuclear protein binds specifically to a PPRE

It has previously been shown that rat liver nuclear proteins (rLNP) bind to the rat acyl-CoA oxidase gene PPRE (Osumi, T. et al 1993). To investigate PPAR α binding to its cognate response element, nuclear receptors were isolated from liver tissue samples, allowing functionally active PPAR α receptors to be assayed. Using *in vivo* protein samples, the effects of dosing rodents with peroxisome proliferators, on the levels of PPAR α can be investigated. rLNP were isolated and tested for binding to peroxisome proliferator response elements using electromobility shift assays. The acyl-CoA oxidase PPRE was synthesised as an oligonucleotide containing the sequence 5' -TGACCT T TGTCT-3', and labelled with [α - 32 P] dCTP, by using Klenow DNA polymerase. Incorporation of labelled nucleotide ranged from 45% to 90%. Non- 32 P labelled probes were made using unlabelled dCTP and [3 H] dCTP, for use in competition binding assays, to demonstrate that binding to the 32 P labelled probe to LNP samples was saturable. Figure 3.1 shows that the binding of rat LNP to ACO-PPRE was not competed out by an excess of non-specific competitor DNA. Figure 3.2 demonstrates that an excess of

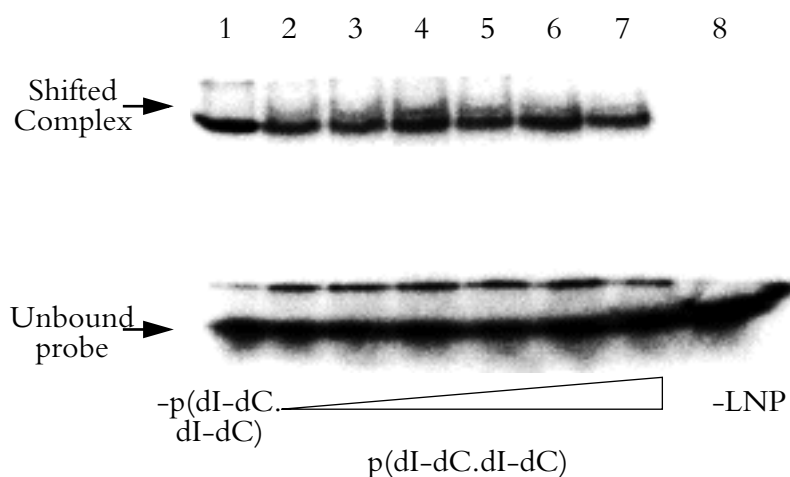


Figure 3.1 Rat liver nuclear protein binds specifically to an acyl-CoA oxidase gene PPRE. 0.165 pmol [32 P]-labelled ACO-PPRE probe was incubated with 11 μ g rat LNP at room temperature for 30 min in 1*Hepes EMSA buffer (10mM Hepes (pH=7.9), 125 mM NaCl, 1mM EDTA, 7% v/v BSA, 1 mM DTT, 150 μ M PMSF). Protein-DNA complexes were resolved on a 10% native polyacrylamide gel in 0.25*TBE, at 4 C. Lane 1 has no non-specific competitor DNA, lanes 2 to 7 have increasing amounts of poly (dI-dC.dI-dC) competitor DNA, 64ng, 128ng, 384ng, 800ng, and 1440ng respectively. Lane 8 contains no LNP. Radioactivity was visualised by phosphor-imaging on a Bio-Rad GS250 Molecular imager.

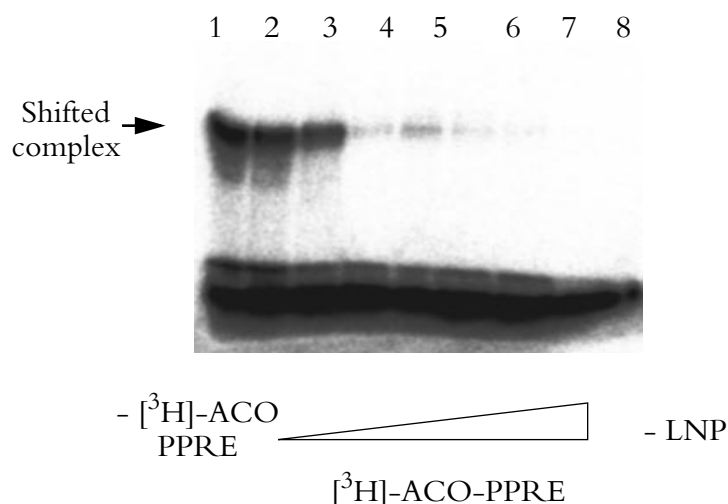


Figure 3.2 Rat LNP binding to ACO-PPRE is saturable. 41 fmol [32 P]-labelled ACO-PPRE probe was incubated with 11 μ g rat LNP and 625 ng p(dI-dC.dI-dC) at room temperature for 30 min in 1*Hepes EMSA buffer (10mM Hepes (pH=7.9), 125 mM NaCl, 1mM EDTA, 7% v/v BSA, 1 mM DTT, 150 μ M PMSF). Protein-DNA complexes were resolved on a 10% native polyacrylamide gel in 0.25*TBE, at 4 C. Binding was assayed with increasing amounts of [3 H] ACO-PPRE, lanes 2 (1.6 pmol), 3(3.3 pmol),4(5 pmol),5 (13.2 pmol), 6 (33.2 pmol) and 7 (66.4 pmol), the absence of [3 H] ACO-PPRE lane 1 and in the absence of LNP, lane 8. Radioactivity was visualised using a Bio-Rad GS250 Molecular Imager.

unlabelled ACO-PPRE can specifically compete out rLNP binding to [32 P] labelled ACO-PPRE. These two results demonstrate that the shifted complex formed between rLNP and ACO-PPRE is specific and is saturable. The binding of the receptors to DNA probes in an in vitro assay may be less stable at room temperature. Experiments were carried out to see if this was occurring. Figure 3.3, lanes denoted B shows that rLNP and ACO-PPRE can form a specific complex at both room temperature and on ice. There was no observable difference in the amount, or pattern of receptor binding when the incubation step was carried out at room temperature or on ice.

The non-specific competitor DNA used in the EMSA assays was a synthetic DNA molecule containing nucleotide, deoxyinosine, not found in cellular DNA. It is possible that this synthetic DNA is inappropriate for demonstrating that the binding of nuclear receptors to the PPRE is sequence specific. Therefore the binding of rLNP was assayed with PPRES containing a single nucleotide change. If an excess of these mutant PPRES could compete for binding to rLNP it would show that the observed shifted complex was formed from a non-specific binding

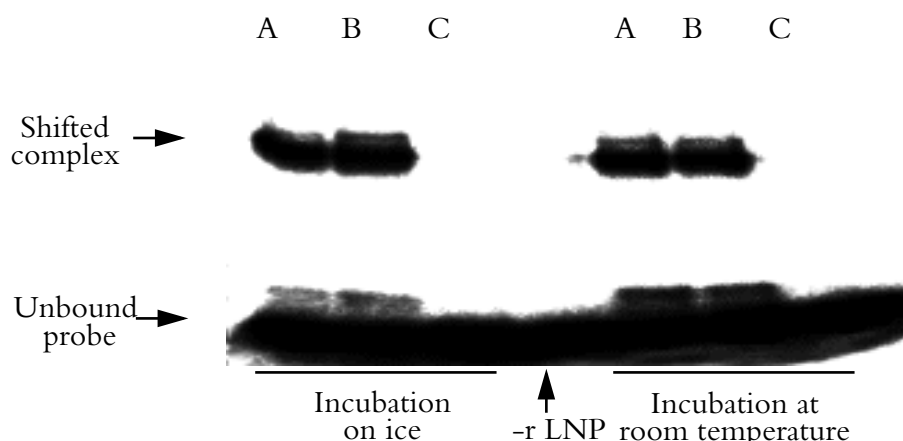


Figure 3.3 Effect of incubation temperature on ACO-PPRE EMSA. 0.165 pmol [32 P]-labelled ACO-PPRE probe was incubated with 11 μ g rat LNP and with either A-no p(dI-dC.dI-dC), B- 625ng p(dI-dC.dI-dC) or C- an excess of unlabelled ACO-PPRE(33.2 pmol) for 30 min at the indicated temperature in 1*Hepes EMSA buffer (10mM Hepes (pH=7.9), 125 mM NaCl, 1mM EDTA, 7% v/v BSA, 1 mM DTT, 150 μ M PMSF). Protein-DNA complexes were resolved on a 7.5% native polyacrylamide gel in 0.25*TBE, at 4 C. Radioactivity was visualised using a Bio-Rad GS250 Molecular Imager.

interaction. [32 P]dCTP and [3 H]dCTP labelled ACO-PPRE probe containing a single mutation at position 3 in the PPRE (5' -TGGCCT T TGTCT-3') was synthesised. The single mutant ACO-PPRE (mACO-PPRE) was a very poor competitor substrate in binding assays containing rLNP and ACO-PPRE. Figure 3.4A, lane 3 shows that [3 H]-mACO-PPRE failed to completely compete out the binding of rLNP to ACO-PPRE at greater than 10000 fold molar excess. When [32 P] labelled mACO-PPRE is used as a binding substrate with an excess of non-

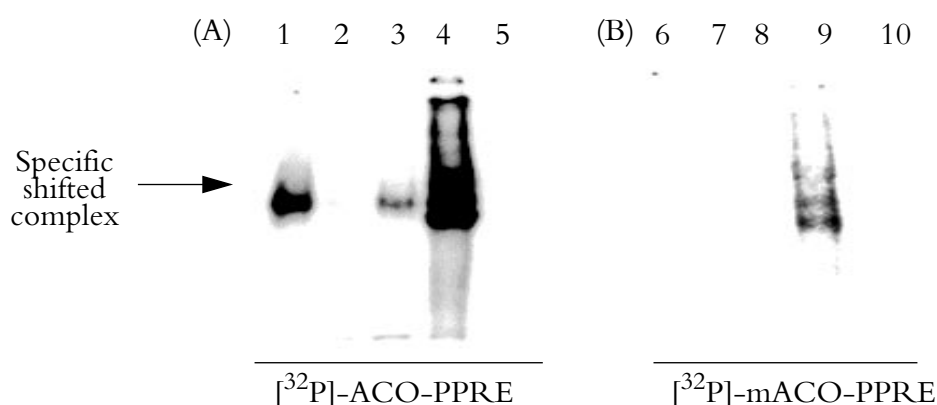


Figure 3.4 Rat LNP does not bind efficiently to a mutant ACO-PPRE. 1.8 fmol [32 P]-labelled ACO-PPRE probe (A) or 4.7 fmol [32 P]-labelled mACO-PPRE probe (B) was incubated with 11 μ g rat LNP (lanes 1-4 and 6-9)at room temperature for 30 min in 1*Hepes EMSA buffer (10mM Hepes (pH=7.9), 125 mM NaCl, 1mM EDTA, 7% v/v BSA, 1 mM DTT, 150 μ M PMSF). Lanes 1 and 6 had the addition of 1 μ g p(dI-dC.dI-dC), lanes 2 and 7 had the addition of 13.2 pmol [3 H]-ACO-PPRE, plus 1 μ g p(dI-dC.dI-dC), lanes 3 and 8 had the addition of 20 pmol [3 H]-mACO-PPRE plus 1 μ g p(dI-dC.dI-dC), lanes 4 and 9 no p(dI-dC.dI-dC) and lanes 5 and 10 no LNP was added. Protein-DNA complexes were resolved on a 7.5% native polyacrylamide gel in 0.25*TBE, at 4 C. Free probe was run off the gel. Radiation was visualised by phosphor-imaging on a Bio-Rad GS250 Molecular Imager.

specific competitor DNA no specific shifted complex is observed, see figure 3.4B. These results demonstrate that rLNP binding to ACO-PPRE is highly sequence specific.

A double mutant ACO-PPRE (dmACO-PPRE) containing two mutations at position 2 and 3 in the PPRE (5'-TTGCCT T TGTCCT-3') was synthesised and labelled with [32 P] dCTP. This dmACO-PPRE was assessed for binding to rLNP in an electromobility shift assay. Figure 3.5, lane 2 demonstrates that rLNP does not bind to dmACO-PPRE in the presence of an excess of non-specific competitor DNA.

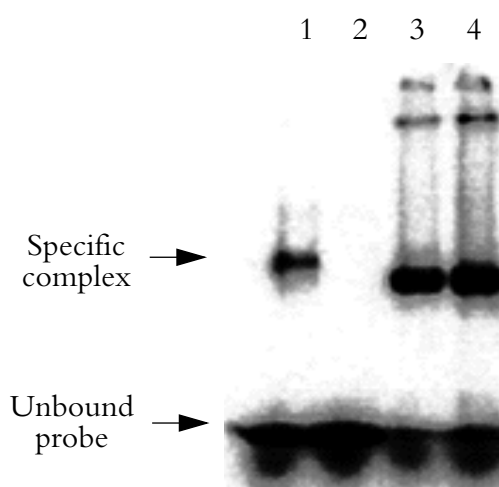


Figure 3.5 rLNP does not bind to a double mutant ACO-PPRE. 0.113 pmol [32 P]-labelled ACO-PPRE probe was incubated with 11µg rat LNP at room temperature for 30 min in 1*Hepes EMSA buffer (10mM Hepes (pH=7.9), 125 mM NaCl, 1mM EDTA, 7% v/v BSA, 1 mM DTT, 150µM PMSF), in the presence (lane 1) and absence (lane 3) of 1µg p(dI-dC.dI-dC). 0.13 pmol [32 P]-labelled double mutant ACO-PPRE probe was incubated with 11µg rat LNP at room temperature for 30 min in 1*Hepes EMSA buffer (10mM Hepes (pH=7.9), 125 mM NaCl, 1mM EDTA, 7% v/v BSA, 1 mM DTT, 150µM PMSF), in the presence (lane 2) and absence (lane 4) of 1µg p(dI-dC.dI-dC). Protein-DNA complexes were resolved on a 7.5% native polyacrylamide gel in 0.25*TBE, at 4 C. Radioactivity was visualised by phosphor-imaging on a Bio-Rad GS250 Molecular Imager.

Section 3.1.1 Mouse liver nuclear proteins bind specifically to a PPRE

Purified mouse liver nuclear proteins (mLNP) were assessed for binding to rat acyl-CoA oxidase PPRE using an electromobility shift assay. Figure 3.6 demonstrates that a specific protein-DNA complex is formed between mLNP an ACO-PPRE containing the sequence 5' -TGACCT T TGTCCT-3'. An excess of non-specific competitor DNA did not abolish mLNP-ACO-PPRE complex formation. Increasing amounts of mLNP incubated with ACO-PPRE results in an

increasing amount of shifted complex formed.

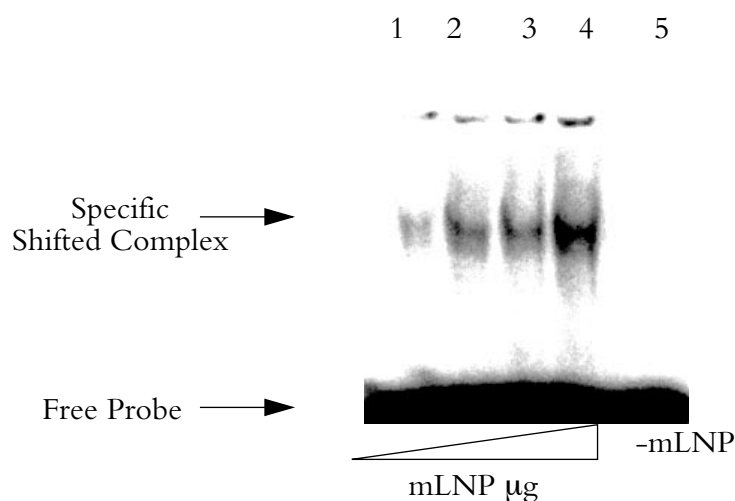


Figure 3.6 Binding of mouse LNP to rat acyl-CoA oxidase PPRE probe. 0.011pmol [32 P]-ACO-PPRE was incubated with increasing amounts of mLNP (lane 1, 5.1 μ g; lane 2, 10.2 μ g; lane 3, 15.3 μ g; lane 4, 25.5 μ g and lane 5 no mLNP) at room temperature in 1* Hepes EMSA buffer (10 mM Hepes, 1 mM EDTA, 7% v/v Glycerol, 5 μ g/ μ l BSA, 1 mM DTT, 150 μ M PMSF and 100 mM NaCl), in the presence of 0.75 μ g p(dI-dC.dI-dC). Protein-DNA complexes were resolved on a 7.5% native acrylamide gel run at 200 v for 1hour in 0.25* TBE. Shifted complexes were visualised by phosphor-imaging on a Bio-Rad GS250 Molecular Imager.

C57 Bl/6 mice were intraperitoneally injected with 100ml of either 10mg/Kg of methylclofenapate in corn oil or corn oil alone at 9.00 am for three consecutive days. The animals were sacrificed at 9.00 AM on day four of the experiment.. The livers of corn oil treated (control) or methylclofenapate (MCP) treated mice were weighed before being processed for liver nuclear

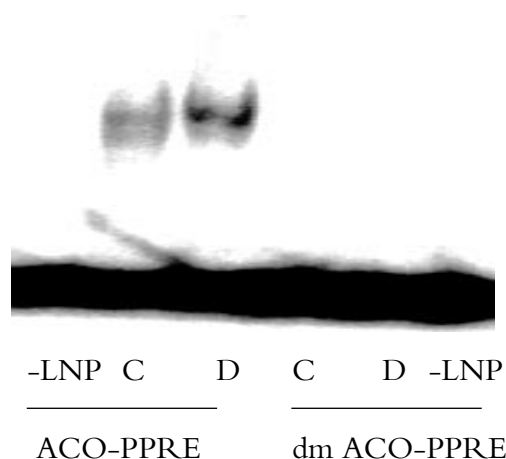


Figure 3.7 mLNP from mice dosed with MCP does not bind a double mutant PPRE. 0.011pmol [32 P] ACO-PPRE or 0.013 pmol [32 P] dm ACO-PPRE was incubated with 20 μ g Control mLNP (C) or 20 μ g dosed mLNP (D) at room temperature in 1* Hepes EMSA buffer (10 mM Hepes, 1 mM EDTA, 7% v/v Glycerol, 5 μ g/ μ l BSA, 1 mM DTT, 150 μ M PMSF and 100 mM NaCl), in the presence of 0.75 μ g p(dI-dC.dI-dC). Protein-DNA complexes were resolved on a 7.5% native acrylamide gel run at 200 v for 1hour in 0.25* TBE. Radioactivity was visualised by phosphor-imaging on a Bio-Rad GS250 Molecular Imager

proteins. The liver:body weight ratio of MCP treated mice was 35% larger ($p < 0.001$) compared to the liver:body weight ratio of control mice (Table 3.1). This shows that the livers of MCP treated mice had peroxisome proliferator induced hepatomegaly.

Control mice liver weight (g)	Control mice body weight (g)	Liver:Body weight ratio	MCP treated mice liver weight (g)	MCP treated mice body weight (g)	Liver:Body weight ratio
1.15	23.2	0.0496	1.54	23.4	0.0658
1.24	23.1	0.0537	1.44	22.9	0.0629
1.09	21.9	0.0498	1.61	23.9	0.0674
1.21	24.5	0.0494	1.77	24.0	0.0738

Table 3.1 **Methylclofenapate induced liver enlargement in C57 Bl / 6 mice.** Male ten-week old mice were dosed *i.p.* with 10mg of MCP per kg per day for three days, or corn oil vehicle. Animals were killed and liver and body weights determined for each of 4 mice per group.

mLNP purified from mice dosed with (MCP) and mLNP from control mice dosed were assayed for binding to ACO-PPRE and dm ACO-PPRE. Figure 3.7 demonstrates that mLNP from control mice and from MCP treated mice do not bind to dmACO-PPRE DNA.

Section 3.1.2 Binding of mLNP from MCP-treated mice to a PPRE

The total amount of mLNP-DNA complex formed from control and dosed mLNP binding to an excess of ACO-PPRE was determined. Figure 3.8 shows triplicate EMSA assays for each of two independently isolated batches of mLNP from control treated mice and two independently isolated batches of mLNP from MCP dosed mice. The mean total amount of control mLNP-PPRE complex formed, as measured by phospho-imaging was not significantly different to the mean total amount of dosed mLNP-PPRE complex formed. Statistical calculations were performed using students T-Test.

Section 3.1.3 Isolation of liver nuclear proteins

Rat, mouse and guinea pig liver nuclear proteins (LNP) were purified using a modified version of protocol by Gorski, K. *et al* 1986. For diurnal studies mouse and guinea pig livers were isolated

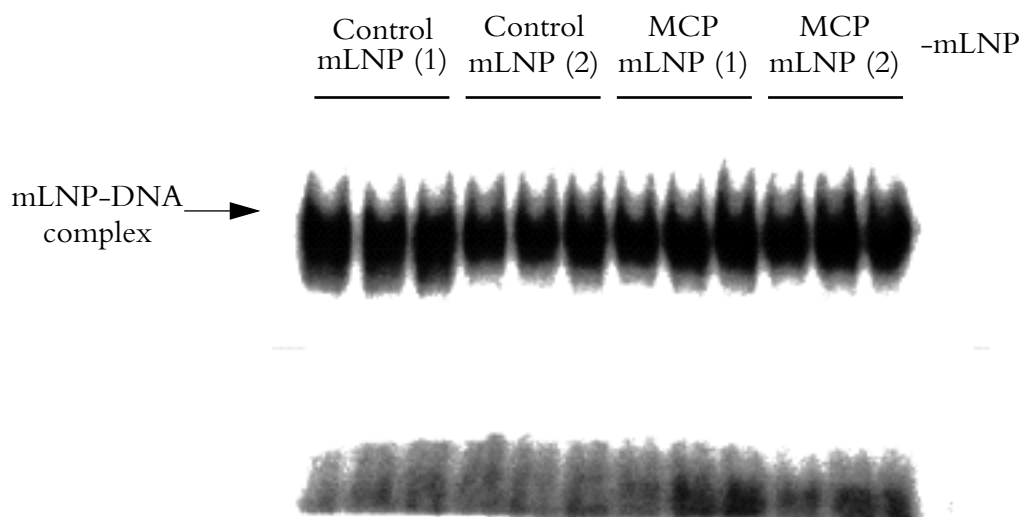


Figure 3.8 ACO-PPRE EMSA with mLNP from control and MCP treated mice. 0.005 pmol [32 P] ACO-PPRE was incubated with 10 μ g of mLNP at room temperature in 1* Hepes EMSA buffer (10 mM Hepes, 1 mM EDTA, 7% v/v Glycerol, 5 μ g/ μ l BSA, 1 mM DTT, 150 μ M PMSF and 100 mM NaCl), in the presence of 0.75 μ g p(dI-dC.dI-dC). mLNP(1) and mLNP(2) refer to two independent batch purifications of liver nuclear proteins. Protein-DNA complexes were resolved on a 7.5% native acrylamide gel run at 200 v for 1hour in 0.25* TBE. Radioactivity was visualised by phosphor-imaging on a Bio-Rad GS250 Molecular Imager. Free probe was run off the gel.

at 6.00 AM, 12.00 Noon, 6.00 PM and 12.00 Midnight. Figure 3.9 shows that mouse LNP proteins isolated from livers taken at each time point are similar and are intact. There are small differences in the banding patterns between some of the samples isolated from livers taken at each time point. The banding pattern and amount of high molecular weight protein in region A of

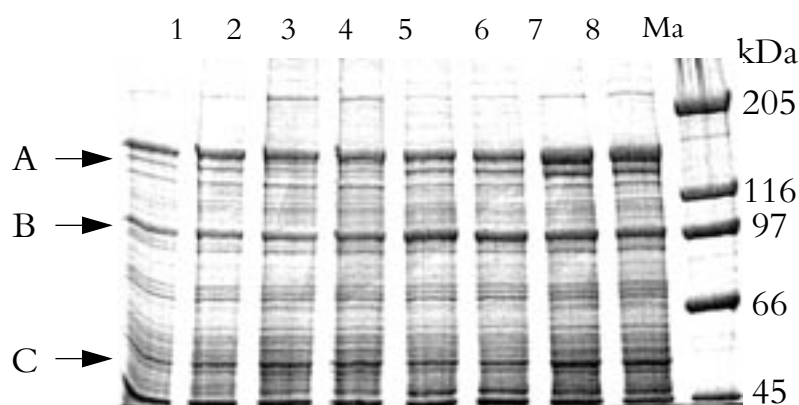


Figure 3.9 SDS-Page analysis of mouse liver nuclear proteins . 20 μ g of mouse liver nuclear protein (mLNP) was run in each lane on a 7.5% SDS-polyacrylamide gel. Lanes 1 and 2 shows mLNP isolated from livers taken at 6.00 AM, 3 and 4 mLNP from livers taken at 12.00 Noon, 5 and 6 mLNP from livers isolated at 6.00 PM and 7 and 8 mLNP from 12.00 Midnight. Lane denoted Ma contains marker proteins. Proteins were visualised by Coomassie blue staining. A, B and C denotes regions containing differences in banding patterns.

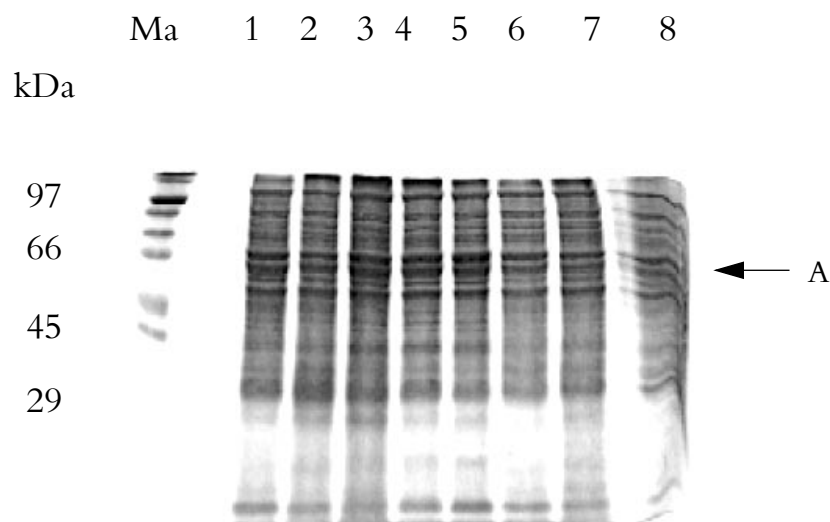


Figure 3.10 SDS-Page analysis of guinea pig liver nuclear proteins. 20 μ g of guinea pig liver nuclear proteins (LNP) were analysed on a 10 % SDS-polyacrylamide gel. Each lane shows a sample of LNP purified from livers taken at 12 midnight (lane 1 & 2), 6.00 AM (lane 3 & 4), 12 Noon (lane 5 & 6) and 6.00 PM (lane 7 & 8). Lane denoted Ma contains marker proteins. The region marked by arrow A shows variation in the banding pattern of a proteins, approximately 50 kDa in size. Protein was visualised by Coomassie blue staining.

LNP isolated from livers taken at 6.00 PM (lanes 5 and 6) and 12 Midnight (lanes 7 and 8) are different to LNP samples from livers taken at 6.00 AM (lanes 1 and 2) and 12 Noon (lanes 3 and 4). At region B a protein of approximate molecular weight 97 kDa increases in amount, from 6.00 AM to 12 Midnight. At region C proteins of approximate molecular weight 50 kDa are higher in amount at 12.00 Noon and 12 Midnight. Figure 3.10 shows guinea pig nuclear proteins analysed by SDS-PAGE. An individual sample of nuclear extract isolated at each time point is shown. There are small differences in the banding patterns between some of the samples isolated from livers taken at each time point. The banding pattern and amount of proteins of approximate molecular weight 50 kDa in region A of LNP isolated from livers taken at 6.00 AM (lanes 3 and 4) and 12.00 Noon (lanes 5 and 6) are different from LNP samples isolated from livers taken at 12.00 Midnight (lanes 1 and 2) and 6.00 PM (lanes 7 and 8).

Section 3.1.4 Immunoblotting analysis of mouse LNP

Sera containing anti-mouse PPAR α antibody were previously prepared in our laboratory and demonstrated to be specific for the mPPAR α isoform (Savory, R. 1997. PhD thesis). Specifically no cross reactivity was observed with PPAR β and PPAR γ isoforms (Savory, R. 1997. PhD

thesis). Figure 3.11 shows that anti-mouse PPAR α antibody detected levels of immunoblotted recombinant mPPAR α protein ranging from 20ng antigen to 140 ng antigen.

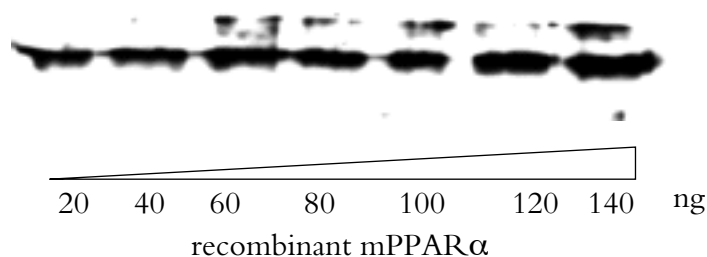


Figure 3.11 Western blot analysis of purified recombinant mouse PPAR α protein. Increasing amounts of purified mPPAR α protein were run on a 10% SDS-polyacrylamide gel. Protein was transferred by electroblotting onto PVDF membrane as described in the methods. PPAR α protein was detected by incubation of the blot in anti-mPPAR α (1:10000 dilution) for 1 hour, then with goat anti-rabbit-IgG-Horseradish Peroxidase antibody (1:40000) for 1 hour. PPAR α bands were visualised using ECL chemiluminescence kit and exposure to hyperfilm.

Anti-mPPAR α antibody was used to detect the expression of mPPAR α protein in protein extracts of mouse liver nuclear proteins (mLNP) by immunoblotting. Figure 3.12 demonstrates that a protein of approximate molecular weight 52 kDa is detected in equivalent amounts in mouse liver nuclear protein samples purified from livers isolated at 6.00 AM, 12.00 Noon, 6.00 PM and 12.00 Midnight. The protein detected by anti-mPPAR α antibody in mLNP co-migrates with purified recombinant mPPAR α protein. This strongly suggests that the protein

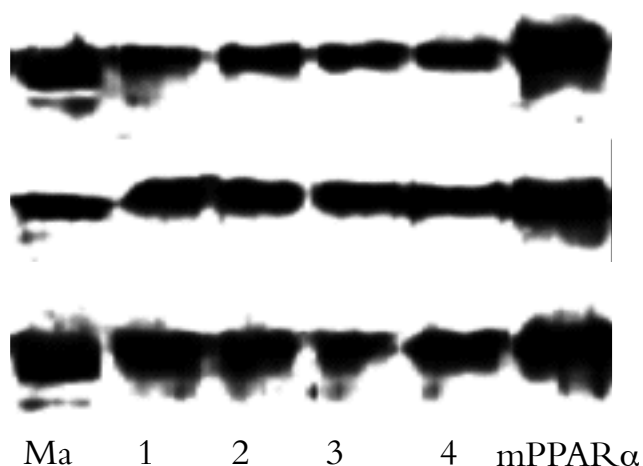


Figure 3.12 Western blot analysis of mLNP with anti-mPPAR α antibody. 10 μ g mouse liver nuclear protein (LNP) and 40 ng purified recombinant mPPAR α protein were run on a 10 % SDS-polyacrylamide gel and blotted on to PVDF membrane. Detection of PPAR α was as described in the methods. The band detected in the lane denoted Ma is Fumarase, a 48.5 kDa protein marker. The secondary antibody alone was found to detect this pre-stained marker protein. Four livers were pooled and homogenised to produce mLNP samples. Lanes 1-4 contain mLNP samples purified from livers of animals killed at 6.00 AM, 12 Noon, 6.00 PM and 12 Midnight respectively. The lane containing purified recombinant mPPAR α is denoted mPPAR α . The results of three separate western blot experiments are shown.

detected in mLNP samples was mPPAR α protein. The results in figure 3.12 show that mPPAR α protein expression does not vary in a diurnal manner in C57 Bl / 6 mice.

Section 3.1.5 Expression of mPPAR α protein in guinea and mouse

Nuclear protein extracts were isolated from the livers of mice sacrificed at 12.00 Midnight and from liver of guinea pigs sacrificed at 06.00 AM. Western blotting of these nuclear protein extracts with anti-mPPAR α antibody revealed the presence of a band of ~52 kDa in mouse liver, and also revealed the presence of a band of similar mobility in guinea pig liver which was less intense (Figure 3.13). The mobility of the detected mPPAR α in liver nuclear extracts and putative guinea pig PPAR α was the same as purified recombinant mPPAR α .

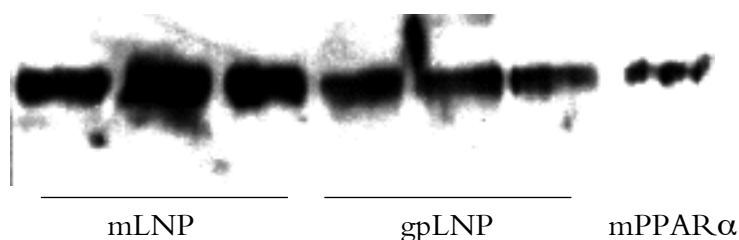


Figure 3.13 Western blot analysis of mouse and guinea pig liver nuclear proteins. 20 ng of recombinant mPPAR α protein, and 10 μ g of mouse (mLNP) and guinea pig liver nuclear protein (gpLNP) purified from each liver isolated at 12.00 midnight and 06.00 AM respectively were run in triplicate on a 10% SDS-polyacrylamide gel, and then probed by western blotting with rabbit anti-mPPAR α antibody (1:10000 dilution) and anti-rabbit-IgG-HRP antibody (1:40000) as described in the methods section. Development of the blot was carried out using ECL detection kit.

Section 3.1.6 Expression of PPAR α immuno-reactive protein in guinea pig LNP

Guinea pig liver nuclear protein samples (gpLNP) were analysed by immunoblotting with the

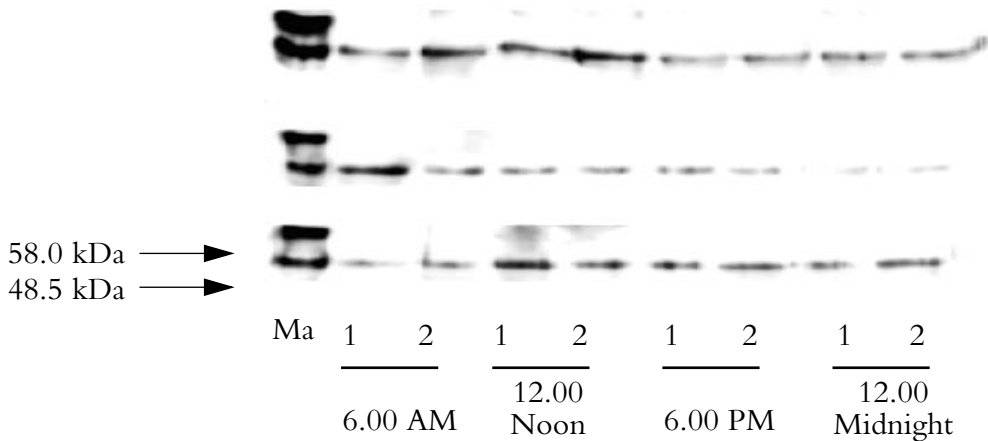


Figure 3.14 Western blot analysis of guinea pig liver nuclear protein. gpLNP was isolated from individual livers of two guinea pigs sacrificed at each time point. Both gpLNP samples from each timepoint were analysed in three separate western blot experiments. 20 μ g of gpLNP was run on a 10% SDS-polyacrylamide gel, and then probed by western blotting with rabbit anti-mPPAR α antibody (1:10000 dilution) and anti-rabbit-IgG-HRP antibody (1:40000) as described in the methods section. Development of the blot was carried out using ECL detection kit. Protein markers (Ma) Pyruvate Kinase and Fumarase were detected by the secondary antibody.

same rabbit anti-mPPAR α antibody that was used to probe mLNP samples. Figure 3.14 demonstrates a protein of approximate molecular weight 52 kDa was detected in gpLNP samples purified from livers isolated at 6.00 AM, 12.00 Noon, 6.00 PM and 12.00 Midnight. These results provide strong evidence to suggest that guinea pigs have a PPAR α receptor, and that it is expressed in a similar manner to mPPAR α . There was no significant difference in the expression of this 52 kDa protein accross a 24 hour period.

Section 3.2 Cloning of guinea pig PPAR α cDNA

Section 3.2.1 Purification of guinea pig RNA

Total RNA was purified from guinea pig liver using the method of Cathala et al . Figure 3.15 shows total RNA analysed by electrophoresis in an agarose gel. The approximate yield of total RNA was 0.5 mg per 2 g of liver tissue processed.

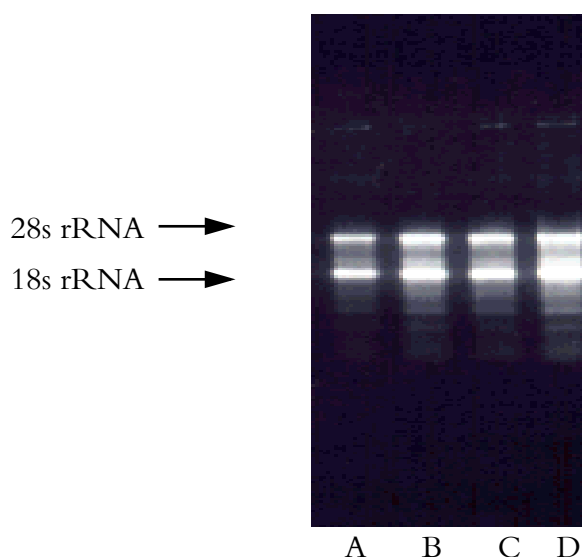


Figure 3.15 Analysis of guinea pig liver RNA by agarose gel electrophoresis. RNA samples were analysed on a 0.8 % agarose gel (1×TBE, 0.1% SDS) run at a constant 90v for 1 hour. Lanes A and B contain 4 and 8 µg of RNA from liver RNA prep 1, and lanes C and D contain 6.6 and 13.2 µg of RNA from liver prep 2.

Section 3.2.2 PCR amplification of guinea pig 1st strand cDNA

Primers GPIGP2, GPIGP3 and GPIGP4 were designed from the DNA sequences of three regions of identity in human, mouse and xenopus PPAR α . Figure 3.16 shows the amino acid alignment of the regions of the PPAR α receptor used to design the PCR primers. GPIGP2 corresponds to 325-MNKDGML-331, GPIGP3 corresponds to 463-IYRDMY-468-XX (X= 3'non-coding triplet) and GPIGP4 corresponds to 114-YGVHACEGCKGFF-126. 1st strand cDNA was synthesised from total and poly A+ purified guinea pig liver RNA. Figure 3.17, lanes 1 to 3 demonstrates that a 436 bp fragment was amplified from guinea pig liver cDNA using GPIGP2 and GPIGP3 primers. Lanes 6 and 7 contain a 436 bp amplified fragment from pSG5-mPPAR α and hPPAR α -pBK-CMV plasmid DNAs. The PCR product of lane 4 was reamplified using the same primers and was then purified by qiagen PCR Qiaspin-quick columns. The purified DNA was cloned into pGEM-T vector. Three independent clones containing the 436 bp insert were purified and sequenced. Each 436bp clone was sequenced only once on each strand. Double stranded sequence was analysed for homology to known PPAR α cDNA sequences. DNA sequence analysis of the cloned 436 bp guinea pig PCR products

(A)



(B)



(C)

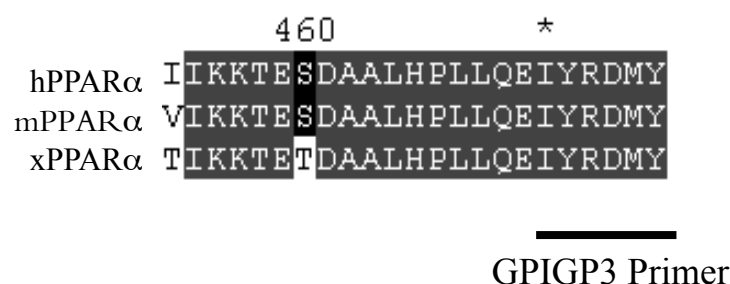


Figure 3.16 Alignment of human, mouse and xenopus PPAR α amino acid sequences. The amino acid sequences of hPPAR α (y07619), mPPAR α (x57638) and xPPAR α (m84161) were aligned using the pileup tool within GCG sequence analysis program, and displayed using GeneDoc program. The numbers above the sequence alignment correspond to the position of the amino acid in the xenopus receptor. Identical amino acids in all three PPAR sequences are shaded in grey. Amino acids identical in two of the three sequences are shaded in black. (A) shows the amino acid alignment in the DNA binding domain, (B) the ligand binding domain, and (C) the C-terminal end of the PPAR α receptors. The regions of amino acid identity used to design PCR primers GPIGP2, GPIGP3 and GPIGP4 are underlined.

demonstrated that they showed sequence similarity, but not identity to mouse, human, rat and xenopus PPAR α cDNA sequences. GPIGP3 and GPIGP2 primers amplified a partial guinea pig PPAR α cDNA fragment. Figure 3.18, lanes 1 to 3 demonstrates that a 1056 bp fragment was amplified from guinea pig liver cDNA using GPIGP3 and GPIGP4 primers. Lanes 10 and 11 contain a 1056 bp amplified fragment from pSG5-mPPAR α and pBK-CMV-hPPAR α plasmid DNAs. The PCR products of lanes 1-4 were reamplified using the same primers. The products of these reactions are shown in figure 3.18, lanes 5-8. The PCR product of lane 7 was purified

by qiagen PCR Qiaspin-quick columns, and was cloned into pGEM-T vector. Three independent clones containing the 1056bp insert were purified and sequenced in full on both strands of DNA. DNA sequence analysis of the cloned 1056 bp guinea pig PCR products demonstrated that they showed sequence similarity, but not identity to mouse , human, rat and xenopus PPAR α cDNA sequences.

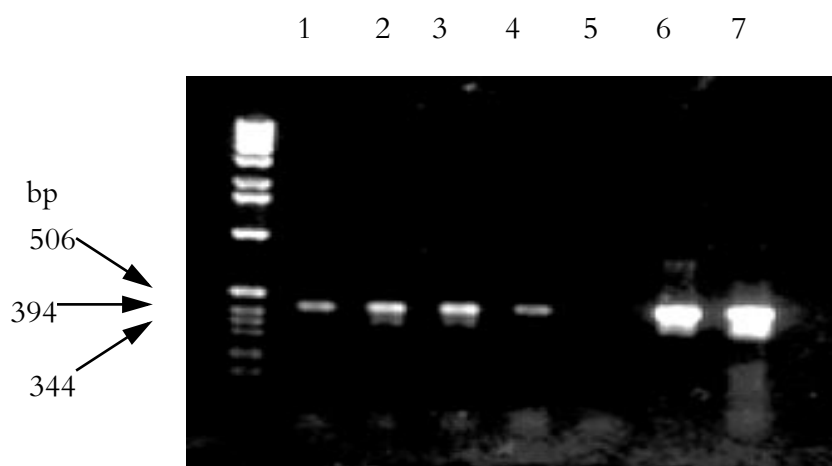


Figure 3.17 Amplification of guinea pig cDNA with GPIGP2 and GPIGP3 primers. 5 μ l of each PCR reaction was analysed on a 1.5 % agarose gel (1* TAE) run at a constant 100v for 1hour. Lanes 1-3 contains PCR products from the amplification of 1st strand cDNA produced from total RNA. Lane 4 contains products from the amplification of 1 st strand cDNA produced from poly A+ RNA. Lane 5 is a negative control in which no template DNA was added. Lanes 6 and 7 contain the products of amplification of pSG5-mPPAR α plasmid DNA and pBK-CMV-hPPAR α plasmid DNA respectively. Primers GPIGP2 and GPIGP3 were used in all PCR reactions

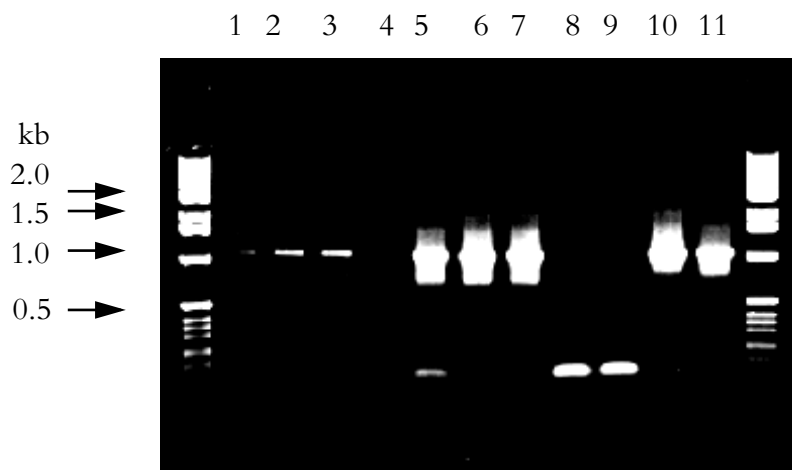


Figure 3.18 Analysis of the PCR amplification of guinea pig liver cDNA. 5 μ l of each PCR reaction was analysed on a 1 % agarose gel (1* TAE) run at a constant 100v for 1hour. Lanes 1-3 contains PCR products from the amplification of 1st strand cDNA produced from total RNA. Lane 4 contains products from the amplification of 1 st strand cDNA produced from poly A+ RNA. Lanes 5-8 contains products of the reamplification of reactions 1-4. Lane 9 is a negative control in which no template DNA was added. Lanes 10 and 11 contain the products of amplification of pSG5-mPPAR α plasmid DNA and pBK-CMV-hPPAR α plasmid DNA respectively. Primers GPIGP3 and GPIGP4 were used in all PCR reactions.

Section 3.2.3 5'RACE of guinea pig RNA

A 5'- rapid amplification of cDNA ends' (RACE) kit (Gibco BRL) was used to clone the remainder of the gPPAR α CDNA containing the N-terminal coding region. Using the completed DNA sequence of the 1056 bp clones two primer GPIGP6 and GPIGP7 were designed and used for cloning the 5' gPPAR α cDNA end. GPIGP7 corresponds to amino acids DKCDRSCKI of the 1056 bp gPPAR α clone and was used to synthesise 1st strand cDNA from

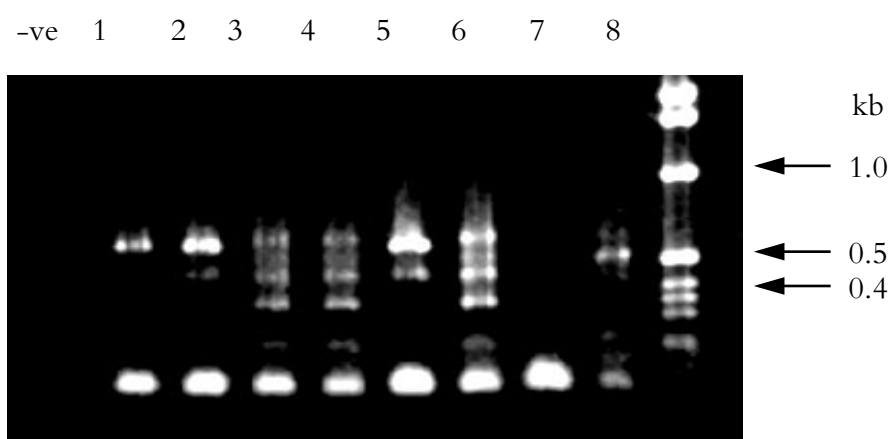


Figure 3.19 5'RACE of gPPAR α cDNA ends. 5 μ l of each 5'RACE PCR reaction was analysed on a 1% agarose gel (0.5* TBE) run at a constant 100 v for 1hour. Lanes 1, 3, 5 and 6 contain PCR products from the reamplification of cDNA ends produced from 1st strand cDNA derived from poly A+ RNA. Lanes 2, 4, 7 and 8 contains PCR products from the reamplification of cDNA ends produced from 1st strand cDNA derived from total guinea pig liver RNA. 5' RACE kit DNA polymerase reagents were used for reactions in lanes 1 and 2. Pharmacia Taq DNA polymerase reagents were used for all other reactions. Lane denoted -ve refers to the control amplification of no template DNA. GPIGP6 and Universal Amplification Primer were used in all reactions.

purified poly A⁺ RNA and total RNA. This 1st cDNA was dC-tailed using Terminal deoxynucleotidyl transferase and then purified. Putative gPPAR α 5' cDNA clones were amplified using GPIGP6 primer (corresponding to amino acids GVHACEGCKG of the 1056 bp gPPAR α clone) and 5'RACE anchor primer. Analysis of the amplified 5'cDNA found that very low levels of product were produced from amplification of 1st strand cDNA derived from poly A⁺ and total RNA. The products of the first round of amplification were reamplified using GPIGP6 and Universal Amplification Primer. Figure 3.19 shows putative amplified gPPAR α 5'cDNA products. The PCR products of reactions 1 and 3 were purified by Qiagen Qiaspin quick columns, and cloned into pGEM-T vector. Seven independent clones were purified and sequenced. Five clones of the PCR products from reactions 1 and 3 showed high identity to PPAR α , and were termed GP11, GP12, GP13, GP14 and GP15. The sequence of the last 10 amino acids of the 3' end of the 5' cDNA clones was derived from the consensus GPIGP4 primer, not from actual guinea pig cDNA sequence. To obtain the cDNA sequence of these 10 amino acids, PCR cloning of a fragment which overlaps the 1056bp and 5' cDNA end clones was underway, but not completed. Clones GP11 to GP15 were sequenced in full on both strands of DNA. GP13, GP14 and GP15 contained cDNA fragments of length 302 bp. GP12 contained an insert of size 582 bp and GP11, an insert of 467 bp in size.

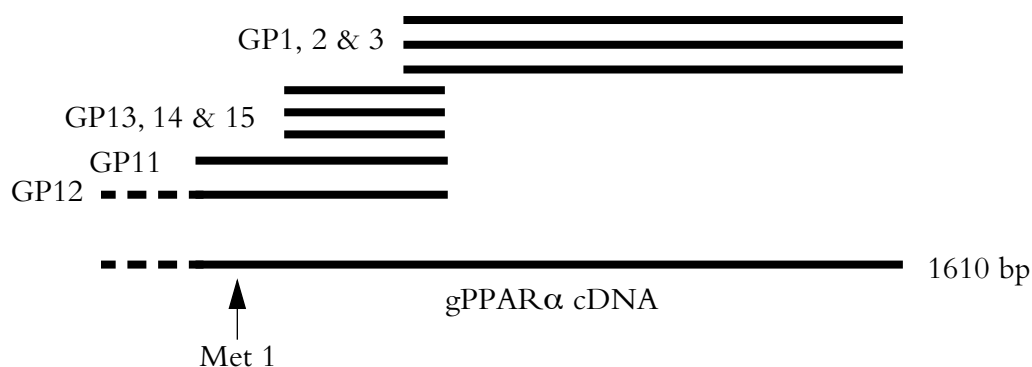


Figure 3.20 Diagram showing assembly of guinea pig cDNA clones. cDNA clones GP1, 2, 3, 11, 12, 13, 14 and 15 was aligned using GELMERGE and GELASSEMBLE tools within the GCG sequence analysis program. Solid black lines denote over lapping identical sequence. Hashed lines indicate sequence derived from a single cDNA clone. The first translational methionine start site is indicated as Met 1.

Section 3.2.4 Sequence analysis of guinea pig cDNAs

Guinea pig cDNA clone DNA sequences were analysed using the TED, BESTFIT, SEQED, and TRANSLATE sequence tools within GCG sequence analysis program. Guinea pig cDNA clones were assembled into a contiguous single cDNA sequence using GELMERGE and GELASSEMBLE tools within GCG sequence analysis program. All double strand gPPAR α cDNA sequences were aligned and assembled into a single contiguous DNA sequence 1610 bp long, see figure 3.20. The DNA sequence of the assembled cDNA is shown in figure 3.21.

```

1      TGCAATTTGA TTCTCCCCTA AAACCTCGCT GGCCGATGGC CCCACCGAGG
51     GTCAGCACCA GCAGCCTGAA AGGGCTGGAT GGGCACGCGG GGCACGTGTG
101    CCCTCAGCCT GCCGGATGGG GCCGTGACCT GTGCGCAGGG CTGGAAGGCG
151    TCTCCTTCAG CATTTCCAAG GTCACAGCTC AGTGGCAGGA CTGGCTCCTC
201    CCCGCCGACA TGGTGGACAT GGAGAGCCCC CTGTGTCCGC TGTCCCCCTT
251    GGAGGCCGAG GACCTGGAGA GCCCACTGTC CGAGTACTTC CTCCAGGAAA
301    TGGGGACCAT CCAGGACATC TCGAGGTCCC TCGGTGAAGA CAGCTCCGGG
351    AGCTTCGGCT TCCCTGAGTA CCAGTATCTG GGCAGCGGCC CCGGCTCGGA
401    CGGATCGGTC ATCACAGATA CCCTGTCCCC GGCTTCCAGC CCCTCCTCCG
451    TCAGCTACCC CGAGGTCCCC TGTGGCGTGG ATGAGCCGCC CAGCAGCGCC
501    CTGAACATCG AGTGCAGGAT CTGCGGGGAC AAGGCCTCAG GCTACCACTA
551    CGGAGTTCAC GCATGTGAAG GCTGCAAGGG CTTCTTCCGA AGGACCATCC
601    GGCTGAAGCT GGTGTACGAC AAATGTGACC GCAGCTGCAA GATCCAGAAA
651    AAGAACCGCA ACAAGTGCCA GTACTGCCGC TTCCACAAGT GCCTGTCAGT
701    CGGGATGTCC CACAACGCCA TTCGCTTCGG ACGGATGCCG AGGTCTGAGA
751    AAGCAAACT AAAAGCCGAA GTCCTCACCT GTGACCGGGA CAGCGAGGGC
801    GCCGAGACCG CCGACCTCAA GTCCCTGGCC AAGCGGATCT ACGAGGCCTA
851    CCTGAAGAAC TTCCACATGA AACAAGGTCA GGCCCGCATC ATCCTGGCCG
901    GGAAGACCAG CAGCCATCCG CTTTTCGTCA TCCACGACAT GGAGACGCTG
951    TGCACGGCCG AGAAGACGCT GATGGCCAAG GTGGTGTCCG ACGGCATCCG
1001   CGACAAGGAG GCCGAGGTCC GCATCTTCCA CTGCTGCCAG TGTGTGTCGG
1051   TGGAGACCGT CACCAACCTC ACGGAGTTCG CCAAGGCCAT CCCGGGTTTC
1101   GCCAGCCTGG ACCTGAACGA CCAGGTCACC CTGCTGAAGT ACGGCGTGTA
1151   CGAAGCCATC TTCACCATGC TGTCTCCAC CATGAACAAG GACGGGATGC
1201   TGGTGGCCTA CGGACACGGC TTCATCACCC GCGAGTTCCT CAAAAACCTC
1251   CGCAAACCTT TCTGCGACAT GATGGAACCC AAGTTCAATT TTGCCATGAA
1301   GTTCAACGCC CTGGAGCTGG ACGACAGCGA CATCTCGCTG TTCGTGGCCG
1351   CCATCATTTG CTGCGGAGAT CGGCCCCGCC TCCTAAATAT CGACCACATC
1401   GAGAAAATGC AGGAGGCTAT CGTGCACGTG CTCAAACCTC ACCTGCAAAG
1451   CAACCACCCC GACGACACCT TCCTCTTCCC CAAACTGCTC CAGAAGCTGG
1501   CGGACCTGCG GCAGCTGGTG ACGGAGCATG CCCAGCTCGT GCAGGTCATC
1551   AAGACGGAGT CAGACGCCGC GCTGCACCCG CTGCTGCAGG AGATCTACAG
1601   GGACATGTAC

```

Figure 3.21 cDNA sequence of gPPAR α . cDNA clones GP1, 2, 3, 11, 12, 13, 14 and 15 were aligned and assemble into a single cDNA sequence using GELMERGE and GELASSEMBLE tools within the GCG sequence analysis program. The open reading frame from the putative methionine start site Met 1 is highlighted in bold. This open reading frame encodes for a 467 amino acid protein.

Analysis of the contiguous guinea pig cDNA sequence identified a putative methionine start site in an open reading frame encoding a 467 amino acid protein of predicted molecular weight 52 290 Da. Comparison of the predicted protein sequence of the cloned guinea pig cDNA with known PPAR α receptors demonstrated that the cDNA encodes a PPAR α protein. The amino acid sequence of the putative guinea pig PPAR α (gPPAR α) is shown in figure 3.22. The gPPAR α protein sequence is 1 amino acid shorter than the known mammalian PPAR α 's. A deletion of a Lysine (K) residue at position 447 has occurred. The coding region of gPPAR α cDNA is 1401 bp long. The open reading frame contains two putative methionine start sites, Met 1 closely followed by Met 2, highlighted in bold on figure 3.22. The DNA sequence of Met 1 shows the highest conservation (4 nucleotides out of 6) to the Kozak Methionine start sequence motif (Kozak, M. 1994 and 1995). A third methionine start site (Met 3) is present in the 200 bp of cDNA 5' to Met 1. Met 3 has poor similarity to the consensus Kozak sequence, only 2 out of six nucleotides are conserved.

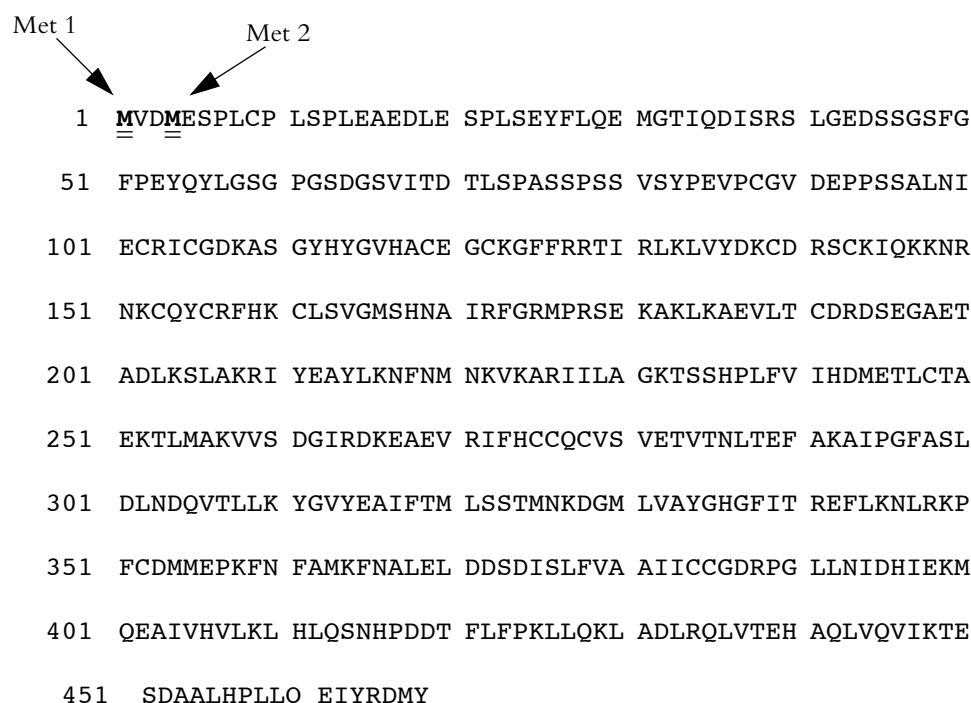


Figure 3.22 Amino acid sequence of gPPAR α . The guinea pig cDNA sequence was translated using the TRANSLATE tool within GCG sequence analysis program. An open reading frame of 467 amino acids from Methionine translational start site 1 (Met 1) is shown. The predicted amino acid sequence was compared to known PPAR α amino acid sequences and was found to have high similarity, indicating that it encodes a PPAR α receptor. A second putative methionine translational start site (Met 2) is indicated.

Section 3.2.5 Multiple sequence analysis of PPAR α amino acid sequences.

A comparison between the amino acid sequence of gPPAR α and other known PPAR α 's was done using the BESTFIT tool within GCG sequence analysis program. Guinea pig PPAR α has 88% amino acid identity to human, mouse and rat PPAR α s, but only 71% and 72% amino acid identity to mPPAR γ and rPPAR δ . Table 3.2 gives a breakdown of the percent amino acid identity between individual protein domains of gPPAR α and other known PPAR isoforms. The DNA binding domain of gPPAR α is identical to mouse and human PPAR α . The ligand binding domain shows highest identity to the PPAR α isoform. The largest amount of variation between sequences occurs in the putative A/B transactivation domain and putative hinge region.

Domain (aa region)	A/B (1-101)	DBD (102-166)	Hinge (167-280)	LBD (281-467)
hPPAR α	85	100	81	91
mPPAR α	78	100	80	93
rPPAR α	79	98	80	93
xPPAR α	51	87	78	87
rPPAR δ	44(30)	86	52	70
mPPAR γ	60(10)	83	46	66

Table 3.2 Amino acid sequence identity between gPPAR α and other PPARs. The amino acid sequences of guinea pig, human (y07619), mouse (x57638), rat (m88582) and xenopus (m84161) PPAR α s, and rat PPAR δ (u40064) and mouse PPAR γ (u01664) have been compared using the BESTFIT tool within GCG sequence analysis program. The amino acid (aa) position of the domains of PPAR α are given in brackets below the domain name. A/B denotes putative transactivation domain, DBD denotes DNA binding domain and LBD denotes the ligand binding domain. The figures in brackets next to the percent identities are the length of amino acid stretch over which the identity was matched. The 10 amino acids derived from the consensus primer were included in the DBD BESTFIT analyses.

The amino acid sequences of gPPAR α , hPPAR α (y07619), mPPAR α (x57638), rPPAR α (m88582) and xPPAR α (m84161) have been aligned for comparison using the PILEUP tool within GCG sequence analysis package. Figure 3.23 shows the differences in the amino acid sequence of gPPAR α to the aligned sequences. There are 22 amino acid positions which are identical in rPPAR α and mPPAR α but are different in gPPAR α and hPPAR α . Of these 22 changes, 14 are conserved between gPPAR α and hPPAR α , with the remaining eight being

		*		20	*		40	*		
gppar	:	~~~~MVDME SPLC P LSPLEA DLESPLSEYFLQEMGTIQDISRSLG EDSS	:	46						
hppar	:	-----T..... GE..... N .. E ..Q.. I	:	46						
mppar	:	-----T.. I DE..... N .. E ..Q.. I .. E	:	46						
rppar	:	-----T.. I DE..... N .. E ..Q.. E	:	46						
xppar	:	MSTI...TN. E .. I .T.. DEDGE...DIVD....TQT H . D . G .	:	50						
		60	*		80	*		100		
gppar	:	GSFGFPEYQYL GS GP SGDSV ---ITDTLSPASSPSSVSYP EV PCGVDEP	:	93						
hppar	:T..... C-----T.. V .. GS .. S	:	93						
mppar	:AD..... C .. E-----R..... C .VI.AST.. S	:	93						
rppar	:S.AD..... C .. E----- C .A.. TST .. S	:	93						
xppar	:	TP.. AS .H.FF.NS...I...STDL.....A.ITF.AAS GS AEDA	:	100						
		*		120	*		140	*		
gppar	:	PSSALNIECRIC CGDKASGYHYGV HACEGCKGF FRTIR LKL VYDKCD RSC	:	143						
hppar	:	..G.....-.....-.....-.....-.....-.....-.....-.....	:	143						
mppar	:	..G.....-.....-.....-.....-.....-.....-.....-.....	:	143						
rppar	:	..GN.....-.....-.....-.....-.....-.....-.....-.....	:	143						
xppar	:	ACKS...L...V.S...F.....-.....-.....-.....R.E.M.	:	150						
		160	*		180	*		200		
gppar	:	KIQKKNRNKCQYCRFH KCLSVGM SHNAIRFGRM PSEKA KLKA EVLTCD R	:	193						
hppar	:-.....-.....-.....-.....-.....-.....-..... I .. EH	:	193						
mppar	:-.....-.....-.....-.....-.....-.....-..... I .. EH	:	193						
rppar	:-.....-.....-.....-.....-.....-.....-..... I .. EH	:	193						
xppar	:-.....E.. N-.....-.....-.....M.. Q	:	200						
		*		220	*		240	*		
gppar	:	DSEGAE TADLR SLAKRI VEAY LKNFNMMNKVKARIL AGKTSSH PLF VIHD	:	243						
hppar	:	..I.DS.....-.....-.....-.....-.....W.. S .. A .. NN .. P	:	243						
mppar	:	..LKDS.....-.....G.. H-.....W.. S .. A .. NN .. P	:	243						
rppar	:	..LKDS.....-.....H.....-.....W.. S .. A .. NN .. P	:	243						
xppar	:	..VKDSQM...L...RL.. D-.....A.. T .. A .. -N .. P	:	249						

		260	*	280	*	300	
gppar	:	METLCTAEKTLMAKVVSDG	TRDK	EA	EVRI	IFHCCQCQVSVETVTNLT	TEFAKA
hppar	:M.....V..L..AN..	QM..	V.....T.....E.....			
mppar	:M.....V..M..AN..	VE..	F.....M.....E.....			
rppar	:M.....V..M..AN..	VE..	F.....M.....E.....			
xppar	:M.....V..L..AN..	QM..T.....E.....S			
		*	320	*	340	*	
gppar	:	IPGFASLDLNDQVTL	LKYGVYEA	IFT	MLSS	TMNRD	GMLW
hppar	:	..A..M.....A..V.....N.....			
mppar	:M.....L.....	I..N.....			
rppar	:M.....L.....	I..N.....			
xppar	:	...TE.....	M..A..A..V.....N.....			
		360	*	380	*	400	
gppar	:	LKMLRKPFCD	MMEPKFNFAMKFN	ALELDDSD	ISLFVAA	ICCGDRPGL	LN
hppar	:	..S.....I.....D.....					
mppar	:I.....D.....					
rppar	:I.....D.....					
xppar	:	..S.....IG.....E.....		L.....L.....V.....			
		*	420	*	440	*	
gppar	:	IDHIERMQE	AIHVHLKLHL	QSNHPDD	TFLFPKLL	QKL	DLRQLVTEHAQL
hppar	:	VG.....G.....R.....	I.....M.....				
mppar	:	..CY..L..C.....				MV.....	
rppar	:	..CY..L..C.....				MV.....	
xppar	:	..PS.....S.....		S.....M.....			
		460	*				
gppar	:	VQWI-KTES	DAALHPLLQEIYRDMY				
hppar	:	..I..K.....					
mppar	:K.....					
rppar	:K.....					
xppar	:	..T..K...T.....					

Figure 3.23 Amino acid sequence alignment of mammalian and *Xenopus* PPAR α 's. The amino acid sequences of gPPAR α , hPPAR α (y07619), mPPAR α (x57638), rPPAR α (m88582) and xPPAR α (m84161) have been aligned for comparison using the PILEUP tool within GCG sequence analysis package. The dots (.) denote identical amino acids and hyphens (-) indicate absent amino acids. 80% conservation of amino acids in all five sequences are highlighted with grey shading and 60% conservation of amino acids between all five sequences are shaded in black. The alignments were visualised with the GENEDOC program.

histidine residue in mPPAR α and rPPAR α . At position 264 in gPPAR α , an arginine residue (positively charged), and 264 in hPPAR α , a glutamine residue (polar uncharged) is changed to a glutamate (negatively charged) residue in rat and mouse PPAR α 's.

Section 3.2.6 Phylogenetic analysis of PPAR α genes

The tree shown in figure 3.24 is a typical output from Puzzle 4 with a Jones, Taylor and Thornton (JTT) amino acid substitution matrix (Jones, D.T. et al 1992), with all branches strongly supported ($P > 0.89$). The length of the gPPAR α branch compared to human, mouse and rat is much longer, indicating that the gPPAR α gene is evolving more rapidly than the PPAR α gene in these other species. The most likely tree places the guinea pig between the human and rodent orders, with a bootstrap probability of approximately 0.93. The most likely remaining trees with a combined bootstrap probability of approximately 0.07 excluded a monophyletic association of guinea pig with mouse and rat.

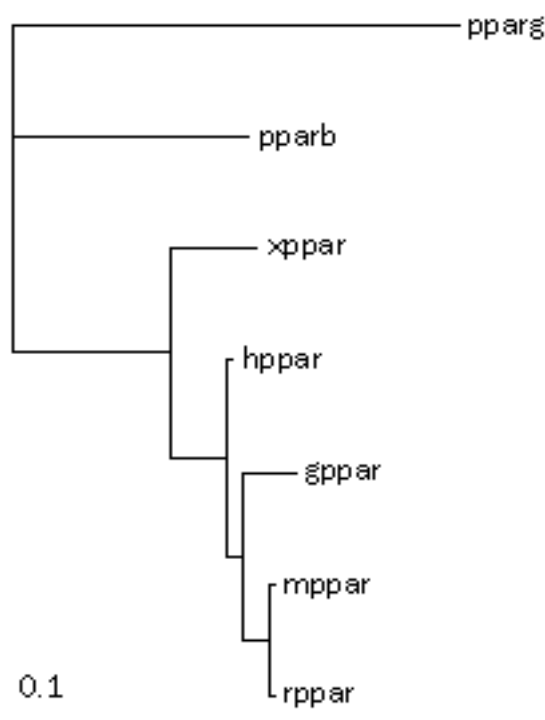


Figure 3.24 Phylogenetic analysis of PPAR α genes. The deduced protein sequence of guinea pig PPAR α was initially aligned with the mouse (x57638), rat (m88592), human (s74349) and xenopus (m84161) PPAR α protein sequences, and the mouse PPAR β (u10375) and mouse PPAR γ (u10374) with CLUSTALW 1.6, then refined with SAGA. The mouse PPAR β and γ sequences are added as outgroups to the analysis. Maximum likelihood analysis of the aligned peptide sequences utilised ProtML and Puzzle 4, compiled to run on OS/2 using the gnu C compiler. The branch lengths are proportional to the evolutionary rate of the gene. The tree output was visualised with treeview. The branches are defined as gppar = guinea pig PPAR α , mppar = mouse PPAR α , hppar = human PPAR α , rppar = rat PPAR α , xppar = xenopus PPAR α , pparb = mouse PPAR β and pparγ = mouse PPAR γ . The scale indicates a Ks = 0.1

Section 3.2.7 gPPAR α cDNA contains an extended 5' ORF

Initial DNA sequence analysis indicated a stop codon upstream of Met 1 ATG start site. Final

detailed analysis of the assembled 5' cDNA sequence of clones, GP11 and GP12 demonstrated that a continuous open reading frame 5' to the putative methionine start site Met 1 was present. The extended open reading frame contains a putative methionine translational start site, indicated by Met 3 in figure 3.25. Translation of gPPAR α mRNA from Met 3 would add an additional 58 amino acids to the gPPAR α protein. The gPPAR α protein sequence containing the N-terminal extended open reading frame was compared with sequences in the databank Genembl. This sequence similarity search revealed that a gPPAR α sequence (accession number AJ000222) had been submitted to the databank. A comparison of the N-terminal ends of each gPPAR α is shown in figure 3.25. Figure 3.25 demonstrates that the amino acid sequences are identical over a 13 amino acid stretch immediately N-terminal to Met 1, with the remaining N-terminal sequence being different.

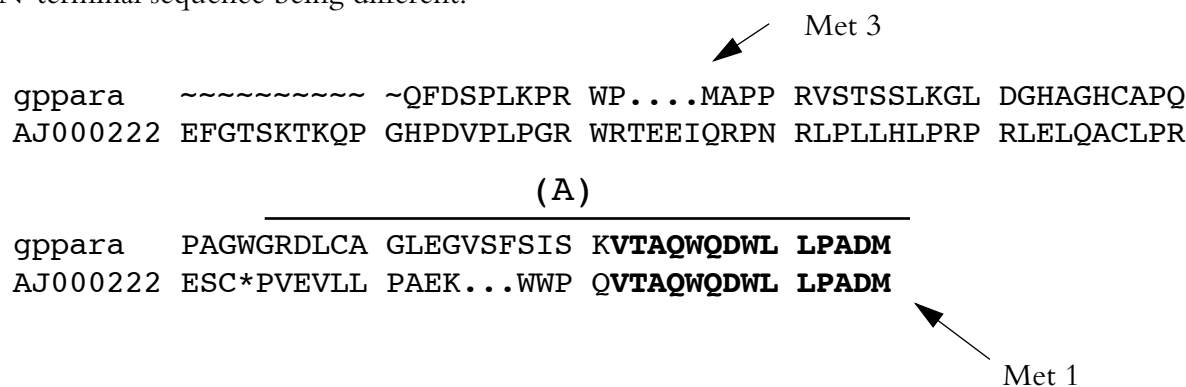
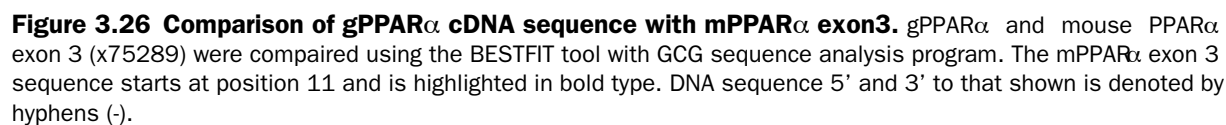


Figure 3.25 Alignment of cloned gPPAR α protein with AJ000222. Alignment of gPPAR α amino acid sequence with the amino acid translation of AJ000222 cDNA using BESTFIT tool of GCG sequence analysis program. Identical sequence between gPPAR α cDNA and AJ000222 cDNA, N-terminal of the Met 1 translational start site is given in bold type. A putative methionine translational start site Met 3 is indicated in the upstream reading frame of gPPAR α . The gPPAR α cDNA sequence region highlighted as (A) was derived from clones GP11 and GP12 and were identical over this stretch. All gPPAR α cDNA sequence upstream of region A was derived from one 5' cDNA clone, GP12.

The 5' nucleotide sequence of gPPAR α cDNA was compared to the exon DNA sequences encoding the N-terminal region of mPPAR α . The cDNA sequence of the N-terminal end of gPPAR α shown in bold in figure 3.26, aligns with start of mouse exon 3 (x75289) DNA sequence (figure 3.26). The region of N-terminal identity between gPPAR α and AJ000222 also starts at this 5' intron-exon junction. The difference in the N-terminal sequence of gPPAR α and AJ000222 could result from alternative splicing of gPPAR α mRNA.



2 ATGAACAAAGACGGGATGCTGGTGGCCCTACGGACACGGGCTTCATCACCCG 51
||||| |||||||||
973 ATGAACAAGGACGGGATGCTGGTGGCCCTACGGACACGGCTTCATCACCCG 1022

52 CGAGTTCCTCAAAAACCTCCGCAAACCTTCTGCGACATGATGGAACCCA 101
||||| |||||||||
1023 CGAGTTCCTCAAAAACCTCCGCAAACCTTCTGCGACATGATGGAACCCA 1072

10 AGTTCAATTTTGCCATGAAGTTCAACGCCCTGGAGCTGGACGACAGCGAC 151
||||| |||||||||
1073 AGTTCAATTTTGCCATGAAGTTCAACGCCCTGGAGCTGGACGACAGCGAC 1122

152 ATCTCGCTGTTCGTGGCCGCCATCATTTGCTGCGGAGGACAGATCGGCCC 201
||||| |||||||||
1123 ATCTCGCTGTTCGTGGCCGCCATCATTTGCTGCGG.....AGATCGGCCC 1167

202 GGCTCCTTAAATATCGACCACATCGAGAAAATGCAGGAGGCTATCGTGCA 251
||||| |||||||||
1168 GGCTCCTTAAATATCGACCACATCGAGAAAATGCAGGAGGCTATCGTGCA 1217

252 CGTGCTCAAAC TCCACCTGCAAAGCAACCACCCGACGACACCTTCTCT 301
||||| |||||||||
1218 CGTGCTCAAAC TCCACCTGCAAAGCAACCACCCGACGACACCTTCTCT 1267

302 TCCCCAAACTGCTCCAGAAGCTGGCGGGACCTGCGGCAGCTGGTGACGGA 351
||||| |||||||||
1268 TCCCCAAACTGCTCCAGAAGCTGGC.GGACCTGCGGCAGCTGGTGACGGA 1316

352 GCATGCCCAGCTCGTGCAGGTCATCAAGACGGAGTCAGACGCCGCGCTGC 401
||||| |||||||||
1317 GCATGCCCAGCTCGTGCAGGTCATCAAGACGGAGTCAGACGCCGCGCTGC 1366

402 AcCCGCTGCTGCAGGAGATCTACAGGGACATGTA 435
||||| |||||||||
1367 ACCCGCTGCTGCAGGAGATCTACAGGGACATGTA 1400

Page 130

Sequence analysis of gPPAR α GP4 clone revealed that this gPPAR α clone contained a 5 nucleotide insert in the ligand binding domain region. This 5 nucleotide insert can be seen in figure 3.27. The 5 nucleotide insert causes a frame shift in the open reading frame, leading to incorrect sequence and a premature stop codon. Figure 3.27 shows the DNA sequence alignment of the the GP4 clone and gPPAR α cDNA . The regions shown were compared to the DNA sequences of mouse PPAR α exons 7 and 8. The 5 nucleotide insert aligns at the position of the junction between exons 7 and 8. The donor GT- site of the intron between exon 7 and 8 forms a lariat structure with an AG- acceptor site at the end of the intron. In the mRNA that the GP4 cDNA was derived the donor site of the intron between exons 7 and 8 has differentially spliced with another AG- acceptor site four nucleotides 5' to the correct AG- acceptor site. This results in intron sequence being left in the normal coding region. Figure 3.28 shows a cartoon of the mechanism of differential splicing that would give rise to a 5 nucleotide insert.

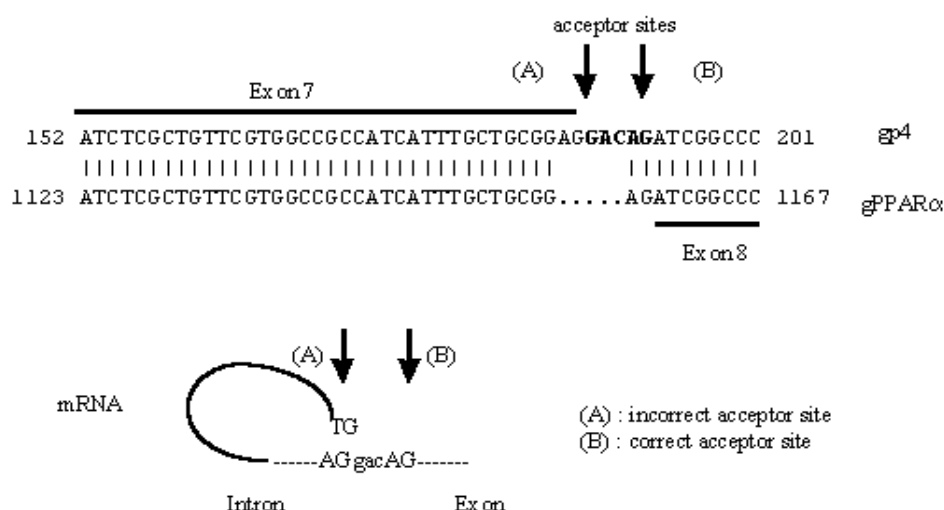


Figure 3.28 gPPAR α GP4 clone contains differentially spliced exons. The DNA sequence of the GP4 cDNA clone was compared to the DNA sequence of gPPAR α cDNA and to mPPAR α exons 7 (x75293) and 8 (x75294) using BESTFIT tool within GCG sequence analysis program. The regions of high similarity between GP4 cDNA and mPPAR α exons 7 and 8 are highlighted by bold lines. The five nucleotide insert lies between the regions of similarity to exons 7 and 8. A cartoon of the mRNA lariat formation on the incorrect acceptor site is shown below the sequence alignment.

Section 3.3 Cloning of full length gPPAR α cDNA

Full length gPPAR α cDNA was generated by an overlapping PCR strategy. The cDNA inserts of clones GP1 and GP11 were amplified using GPIGP6 and GPIGP16 for GP11, and GPIGP4 and GPIGP3 for GP1. These amplifications gave rise to a 414 bp fragment encoding

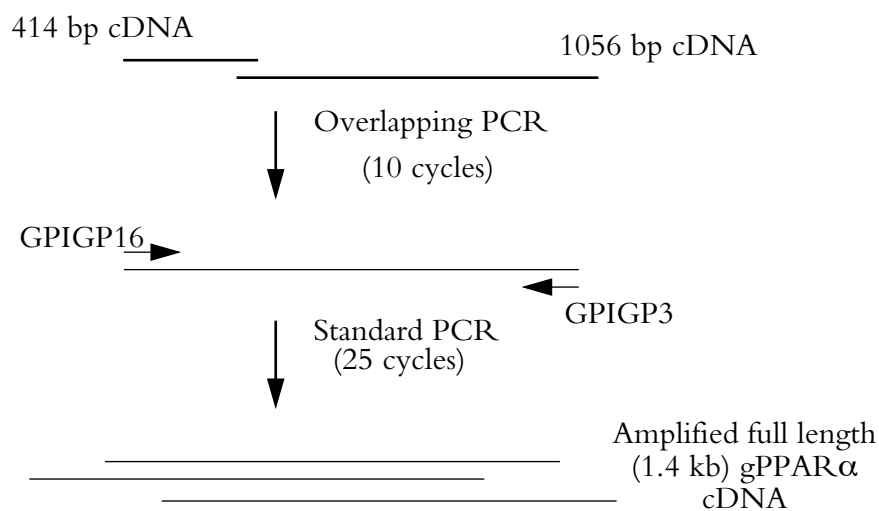


Figure 3.29 Cartoon of two stage overlapping PCR strategy.

DWLLPADMVD to GVHACEGCKG and a 1056 bp fragment encoding YHYGVHACEGCKGFF to IYRDMY. These overlapping fragments were amplified for 10 cycles using the annealed overlap region as primer sites. This PCR reaction was then amplified

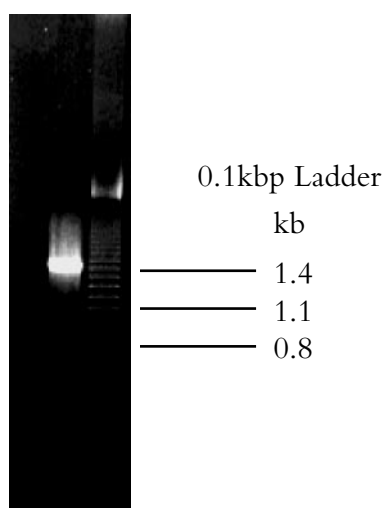


Figure 3.30 PCR amplification of full length gPPAR α cDNA. 5 μ l of PCR reaction was analysed on a 1% agarose gel (0.5*TBE) run at a constant 100v for 1.5 hours. The 414bp and 1056 bp DNA fragments were amplified for 10 cycles in the following conditions [94 C, 1 min; 57 C, 1 min; 72 C, 2.5 min]. 0.1 μ l of the overlapping PCR reaction was amplified with GPIGP16 and GPIGP3 for 25 cycles in the following conditions [94 C, 1 min; 57 C, 1 min, 72 C, 2.5 min]. The PCR product was sized using a 100 bp DNA ladder.

using GPIGP16 and GPIGP3 to generate a 1423 bp gPPAR α cDNA. Figure 3.29 shows a cartoon of the strategy used to produce the amplified 1.4 kb gPPAR α cDNA, and figure 3.30 shows the final product of the PCR strategy analysed by gel electrophoresis.

The 1.4kb gPPAR α cDNA was purified and cloned into pGEM-T vector, producing the clone α 1-fullpGEM-T. The 1.4 kb insert was cut out of α 1-fullpGEM-T using Sac II and Not I restriction enzymes and cloned into Sac II / Not I cut pBluescript SK (+) vector, to produce α 1-full-pBluescript. The 1.4 kb insert was then cut out of α 1-full-pBluescript using Sac I and Not I restriction enzymes and cloned into Sac I / Not I cut pBK-CMV vector. A cartoon of the cloning strategy is given in figure 3.31. gPPAR α -pBK-CMV vector was verified by DNA sequencing using primers GPIGP9, GPIGP12 and GPIGP16. The DNA sequence of gPPAR α -pBK-CMV verified that the overlapping PCR strategy worked correctly. gPPAR α -pBK-CMV was mapped using the Xho I, Nar I, Eco 52I, Pst I and Bgl II restriction enzymes. The results of these digests also confirmed that full length gPPAR α cDNA had been produced and cloned correctly.

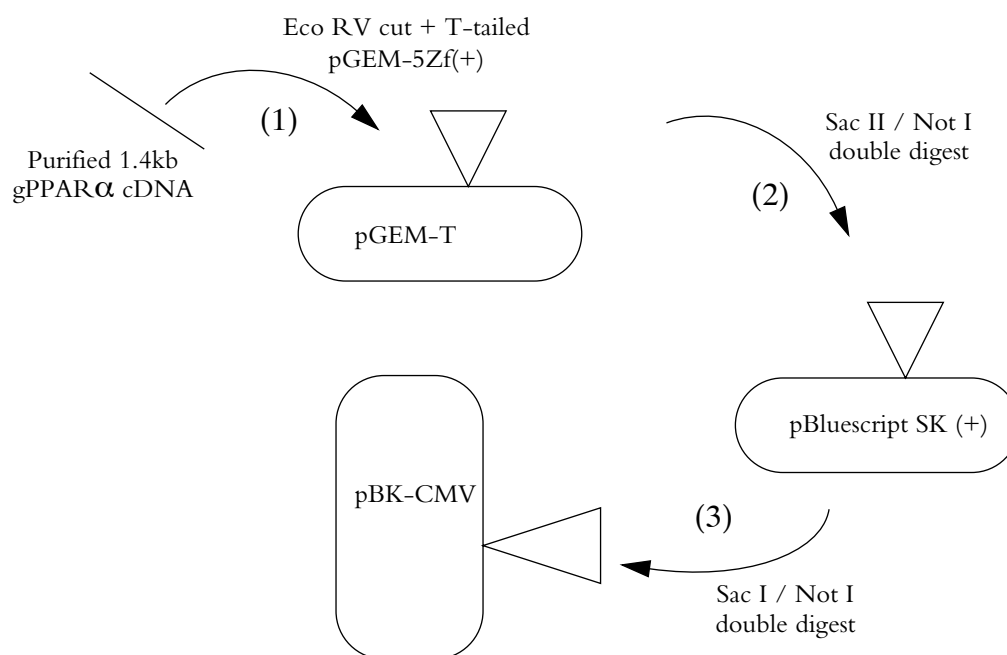


Figure 3.31 Cartoon of the cloning of full length gPPAR α cDNA .

Section 3.3.1 *In vitro* synthesis of gPPAR α protein

gPPAR α -pBK-CMV plasmid was transcribed and translated *in vitro*, producing gPPAR α protein. Promega's TNT rabbit reticulocyte lysate system was used to produce [35 S] labelled gPPAR α , hPPAR α and mRXR α proteins. Figure 3.32 shows SDS-PAGE analysis of *in vitro* translated proteins produce using this system. *In vitro* transcription and translation of gPPAR α -pBK-CMV vector yielded a protein of approximate molecular weight 52 kDa. This result confirms that a full length open reading frame of gPPAR α was cloned and that the protein produced from this open reading frame corresponded to the predicted molecular weight.

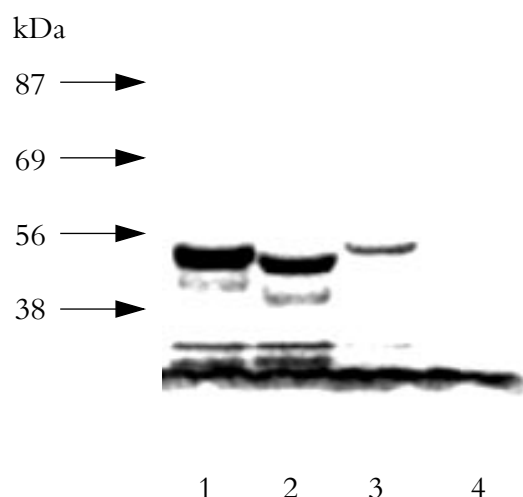


Figure 3.32 SDS-PAGE analysis of *in vitro* translated gPPAR α , hPPAR α and mRXR α . SDS-PAGE analysis of proteins produced by *in vitro* transcription and translation of gPPAR α -pBK-CMV vector (lane 1), hPPAR α -pBK-CMV (lane 2), mRXR α -pGEM5 (lane 3) and control, no vector DNA (lane 4). 10 μ l of each transcription/ translation reaction was analysed on a 10 % SDS-PAGE gel run in 1 \times Laemmli buffer. The gel was fixed and dried and exposed for 4.5 hours on a high intensity [35 S] screen. [35 S] labelled protein bands were visualized using a Bio-Rad Molecular Imager.

Section 3.4 Functional characterisation of gPPAR α

Section 3.4.1 Optimisation of transfection.

Human embryonic kidney 293 cells were cultured in 25 cm² falcon flasks. Briefly confluent monolayers of 293 cells were separated into individual unattached cells by incubation in 1 \times PBS, 0.5 mM EDTA for 5 minutes at 37 C. Cells were pelleted by centrifugation at approximately 100g for 5 minutes. 293 cell pellets were resuspended in culture medium and assessed for viability

by Trypan Blue Dye exclusion assay. Cell preparations which had a viability of 70–90% were used for propagation of the cell line. 0.5×10^6 viable cells were seeded in 5 ml of culture medium and allowed to attach over 3 days of incubation. Flasks with attached cells were either used for continued propagation of the cell or used in transfection experiments.

A protocol for transfecting primary cultures of rat hepatocytes was established in our laboratory. This protocol was used as the starting point for optimisation of transfection of 293 cells with plasmid DNA. pRSV- β GAL vector, a eukaryotic expression vector for β -galactosidase was used as the test plasmid for optimisation. The amount of transfected plasmid and amount of L- α -phosphatidylethanolamine, dioleoyl (C18:1,[cis]-9) / N-[I-(2,3-dioleoyloxy)propyl]-N,N,N-triethylammonium (Dotma/Dope 1:1 mix) cationic liposome transfection reagent (Felgner, D.L. et al 1987) was varied to elucidate optimal transfection conditions. Transfection efficiency was measured as the percentage of 293 cells per flask that stained a positive blue after X-gal chromogenic assay (Sanes, J.R. et al 1986). Tables 3.3 and 3.4 show the results of optimising the amounts of DNA and Dotma / Dope (DD) cationic liposome transfection reagent. The optimal conditions for transfection of 293 cells were found to be 8–12 μ g of DNA and 5 μ g of DD reagent. Under these conditions 1–3% of cells were transfected successfully with DNA. Transfections using amounts of DD higher than 5 μ g led to cytotoxic effects, as measured by the amount of cell detachment.

Amount of DNA μ g per flask	4	8	12
% of cells transfected	1%	1–3%	2–3%

Table 3.3 Effect of amount of plasmid DNA on transfection efficiency . The amount of Dotma / Dope transfection reagent was kept constant at 5 μ g per flask of 293 cells. The % of cells transfected was determined by counting the number of cell stained blue by the X-gal chromogenic assay in at least six microscope fields and by representing this number as a fraction of the total number of cells in the fields observed. (see methods)

Amount of DD μ g per flask	5	10	15	20
% of cells transfected	1-3%	< 1%	cytotoxic	cytotoxic

Table 3.4 Effect of amount of Dotma/Dope (DD) on transfection efficiency. The amount of DNA transfected into each flask was kept constant at 8 μ g per flask of 293 cells. The % of cells transfected was determined by counting the number of cell stained blue by the X-gal chromogenic assay in at least six microscope fields and by representing this number as a fraction of the total number of cells in the fields observed.(see methods). Cytotoxicity was characterised by detachment of cells

Section 3.4.2 Construction of (ACO-PPRE) reporter plasmid.

The rat acyl-CoA oxidase gene PPRE were cloned into promega's pGL3-Luc promoter vector as a tandem repeat. Two complementary long oligonucleotides containing two tandem copies of the PPRE were annealed to give Sac I and Bgl II overhangs. pGL3 -Luc vector was cut with Sac I and Bgl II restriction enzymes and ligated to the PPRE DNA fragment. Positives for the insert were screened by Mlu I digestion of positive clones. The Sac I/ Bgl II digest of pGL3-Luc removed the polylinker Mlu I site. Clones positive for a PPRE did not cut with Mlu I enzyme. A (ACO-PPRE)₂-pGL3-Luc positive was sequenced accross the insert site to DNA confirm the presence and sequence of the tandem PPREs.

Section 3.4.3 Optimistation of transfection normalisation

Initial transfection assay conditions used 2 μ g pCAT-control transfection normalisation vector with 3 μ g hPPAR α -pBK-CMV vector and 6 μ g (ACO-PPRE)₂-pGL3-Luc vector, transfected into 293 cells. Cells were dosed with peroxisome proliferator or vehicle and incubated for 48 hours. Cell extracts were harvested according to the instructions given in promega's firefly luciferase assay kit. The luciferase activity of each cell extract was done according to the manufacturers instructions. Transfection of pCAT-control into mammalian cells results in strong expression of CAT enzyme. Detection of CAT enzyme activity was performed by using [¹⁴C] labelled chloramphenicol and n-butyryl co-enzyme A as substrates. CAT transfers the n-butyryl

moiety of the co-factor to chloramphenicol. n-butyryl-[^{14}C]-chloramphenicol products can be isolated from unreacted [^{14}C]-chloramphenicol using a xylene extraction process (Seed, B and Sheen, J.Y. 1988). The amount of [^{14}C]-chloramphenicol turned over was measured by liquid scintillation counting and was directly proportional to the amount of CAT enzyme produced in transfected cells.

hPPAR α -pBK-CMV, (ACO-PPRE) $_2$ pGL3-Luc and pCAT-control vectors were transfected into 293 cells in varying ratios. Extracts from flasks transfected with all three vectors together were assayed for Firefly luciferase activity and CAT activity. Table 3.5 summarises the detection of each type of reporter gene activity at various ratios of transfected plasmid.

Amount of vector of hPPAR α : Luciferase: CAT (μg / flask)	Firefly luciferase activity	CAT activity
3 : 6 : 2	100-7000 fold above background	None detected
3 : 3 : 6	100-7000 fold above background	None detected
0 : 0 : 6	Not assayed	4-fold above background
0 : 0 : 12	Not assayed	12-fold above background

Table 3.5 Summary of CAT and Luc reporter gene activity.

CAT activity was measured in cell extracts to normalise the transfection efficiency of the Luciferase reporter vector. The CAT activity measured for each cell extract was not above background levels, except for cell extracts derived from flasks that had been only transfected with pCAT-control vector. The presence of hPPAR α -pBK-CMV and (ACO-PPRE) $_2$ pGL3-Luc vectors caused CAT expression from pCAT-control to be suppressed completely. 293 cell extracts from cells only transfected with 6 μg or 12 μg of pCAT-control gave CAT activity values 4-fold and 12-fold above control respectively. Firefly luciferase activity measured in different

extracts from flasks transfected with (ACO-PPRE)₂-pGL3-Luc varied between 100-fold to 7000-fold above background Luciferase activity.

It is possible that these results are due to interaction of the CMV promoter based plasmids with the pCAT-control transfection normalisation plasmid, or due to toxicity resulting from high levels of CMV promoter based plasmids. Therefore the transfection normalisation vector was changed to pRL-CMV and the amounts of CMV promoter based plasmids was reduced. The plasmid pRL-CMV (promega) contains the Renilla Luciferase gene (Sea Pansy luciferase gene) under the control of cytomegalovirus (CMV) enhancer and immediate promoter. 293 cells co-transfected with pRL-CMV and hPPAR α -pBK-CMV (or gPPAR α -pBK-CMV) and (ACO-PPRE)₂-pGL3-Luc produced extracts which when assayed for Renilla luciferase activity gave measurements 20-7000 fold above background values. 293 cells transfected with between 0.1 - 6 μ g of (ACO-PPRE)₂-pGL3-Luc vector produced cell extracts which when assayed for firefly luciferase activity gave measurements between 60 and 7000-fold above background measurements.

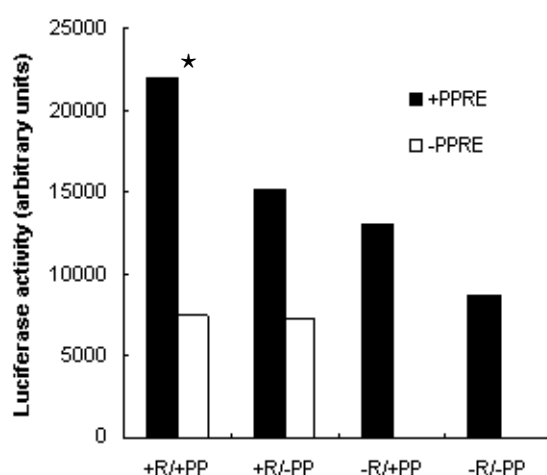


Figure 3.33 Induction of luciferase requires a PPRE. 293 cells were transfected with 0.3 μ g of hPPAR α -pBK-CMV expression vector, 1 μ g pRL-CMV, 1 μ g of either (ACO-PPRE)₂-pGL3-Luc or 1 μ g pGL3-Luc.pRSET-B was added to each flask make the final DNA amount per flask 5 μ g. Flasks were either dosed with 100 mM Wy-14,643 or DMSO vehicle control and incubated for 48 hours. Cell extracts were harvested and assayed for Firefly luciferase activity and Renilla luciferase activity. Firefly luciferase activity was normalised with Renilla luciferase activity. The mean of duplicate assays is plotted. R denotes PPAR α receptor and PP denotes the peroxisome proliferator Wy-14,643. *- Reporter activity in the presence of PPRE is significantly higher than in the absence of PPRE ($p = 0.05$, $df=2$). Data points were analysed by Student's T-test

Section 3.4.4 Induction of luciferase by PPAR α and peroxisome proliferators

The induction of firefly luciferase reporter gene in (ACO-PPRE)₂-pGL3-Luc by hPPAR α and the peroxisome proliferator Wy-14,643 was dependent on the presence of the PPRE. pGL3-Luc control vector which does not contain either regulatory response elements or enhancer elements was not induced by the expression of PPAR α and presence of peroxisome proliferator in 293 cells, see figure 3.33. (ACO-PPRE)₂-pGL3-Luc was not induced in the absence of both hPPAR α and peroxisome proliferator.

The amount of (ACO-PPRE)₂-pGL3-Luc vector was increased to 6 μ g per flask to see if a larger peroxisome proliferator induced response could be obtained. The amount of hPPAR α -pBK-CMV vector per flask was varied from 0 to 0.3 μ g per flask in the presence of high amounts of ACO-PPRE reporter vector. Figure 3.34 demonstrates that as the amount of hPPAR α expression vector is increases the total amount of normalised firefly luciferase activity decreases.

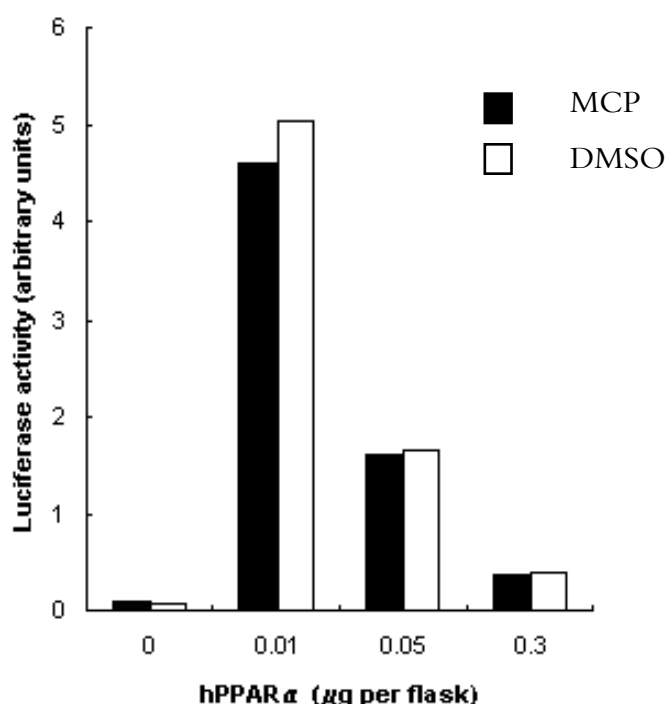


Figure 3.34 Effect of plasmid quantity on luciferase expression. 293 cells were transfected with 0, 0.01, 0.05 and 0.3 μ g of hPPAR α -pBK-CMV expression vector, with equivalent amounts of pRL-CMV (except for flasks with 0 μ g of PPAR α which had 0.3 μ g of pRL-CMV co-transfected), 6 μ g of either (2*ACO-PPRE)pGL3-Luc. pRSET-B was added to each flask make the final DNA amount per flask 9 μ g. Triplicate flasks were either dosed with 50 μ M methylclofenopate (MCP) or DMSO and incubated for 48 hours. Cell extracts were harvested and assayed for Firefly luciferase activity and Renilla luciferase activity. Firefly reporter gene activity was normalised with Renilla luciferase activity. The mean of triplicate assays is plotted.

Under these assay conditions 50 μM MCP was not able to augment reporter gene activity in the presence of PPAR α receptor. Substantial peroxisome proliferator independent activation of reporter gene activity was observed, but in the absence of PPAR α receptor activation of the PPRE containing reporter vector was not observed.

A comparison of peroxisome proliferator induced activation of (ACO-PPRE)₂-pGL3-Luc reporter vector was tested at moderate (1 μg) and low (0.1 μg) levels of PPRE containing reporter vector per flask. These two levels of (ACO-PPRE)₂-pGL3-Luc vector were assayed at 0, 0.05 and 0.1 μg of gPPAR α -pBK-CMV per flask in the presence or absence of 100 μM Wy-14,643. Figure 3.35 shows that reducing the amount of PPRE containing reporter gene 10-fold, causes a 10-fold reduction in reporter gene activity at all levels of gPPAR α expression vector tested, and in a peroxisome proliferator independent manner. Figure 3.35 also shows that Wy-14,643

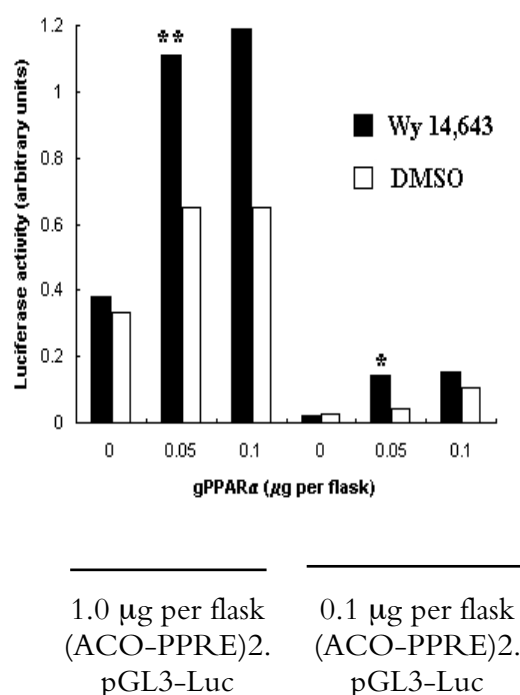


Figure 3.35 Optimisation of quantity of transfected DNAs. 293 cells were transfected with 0, 0.01, and 0.05 μg of gPPAR α -pBK-CMV expression vector, 0.01 μg pRL-CMV, and 1 μg of either (ACO-PPRE)₂-pGL3-Luc. pRSET-B was added to each flask to make the final DNA amount per flask 5 μg . Duplicate flasks were either dosed with 100 μM Wy-14,643 or DMSO and incubated for 48 hours. Cell extracts were harvested and assayed for Firefly luciferase activity and Renilla luciferase activity. Firefly reporter gene activity was normalised with Renilla luciferase activity. * Wy-14,643 induced transcriptional activation of reporter gene 3.4 fold (df=2, p=0.02) over DMSO control and ** Wy-14,643 induced transcriptional activation of reporter gene 1.7 fold (df=2, p=0.05) over DMSO control. The mean of duplicate assays is plotted. Data points were analysed by Student's T-test.

could activate a PPRE containing reporter gene construct 3.4 fold ($p=0.05$, $df=2$) in flasks containing 0.1 μg of (ACO-PPRE)2-pGL3-Luc and 0.05 μg of gPPAR α -pBK-CMV vectors. A smaller, 1.7-fold ($p=0.02$, $df=2$) induction of reporter gene activity was observed in flasks containing 1 μg of (ACO-PPRE)2-pGL3-Luc and 0.05 μg gPPAR α -pBK-CMV, dosed with 100 μM Wy14,643. The degrees of freedom used to calculate the statistical significance of these results was low due to the low number of replicate flasks. Therefore the experimental conditions which gave rise to a 3.4-fold induction of reporter gene activity were examined using more flasks to give a higher degree of statistical accuracy. Figure 3.36 demonstrates that Wy-14,634 induced (ACO-PPRE)2-pGL3-Luc reporter vector 2.3-fold ($p=0.001$, $df=6$) in the presence of exogenously expressed gPPAR α receptor.

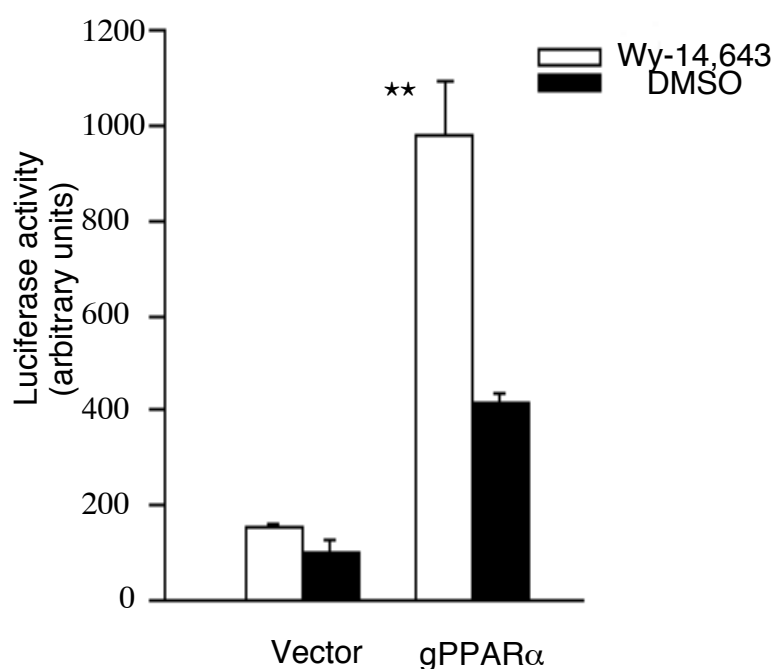


Figure 3.36 Wy-14,643 induces gPPAR α transcriptional activation. 293 cells were transfected with 0.05 μg of gPPAR α -pBK-CMV expression vector or 0.05 μg pBK-CMV vector, 10 ng pRL-CMV, 0.1 μg of (ACO-PPRE)2-pGL3-Luc. pRSET- β plasmid DNA was added to each flask make the final DNA amount per flask 5 μg . Flasks were dosed with either 100 μM Wy-14,643 or DMSO and incubated for 24 hours. Cell extracts were harvested and assayed for Firefly luciferase activity and Renilla luciferase activity. Firefly reporter gene activity was normalised with Renilla luciferase activity. The mean of quadruplicate assays is plotted. **-. Reporter activity in the presence of Wy-14,643 is significantly higher than in the presence of DMSO ($p= 0.001$, $df=6$). The error bars shown represent the standard deviation from the mean. Data points were analysed by Student's T-test

Section 3.5 Expression of gPPAR α and mPPAR α mRNA

RNAse protection assays were used to examine the expression of mPPAR α and gPPAR α mRNA in liver. Anti-sense ribo-probes corresponding to the C-terminal end of the coding sequence were generated and hybridised to purified total liver RNA. Hybridisation of ribo-probe to PPAR α mRNA results in an RNA duplex structure which is resistant to digestion with Ribonuclease A. The protected RNA fragments are run on a denaturing acrylamide gel and can be visualised by autoradiography. Figure 3.37 (A) demonstrates that mPPAR α is highly expressed

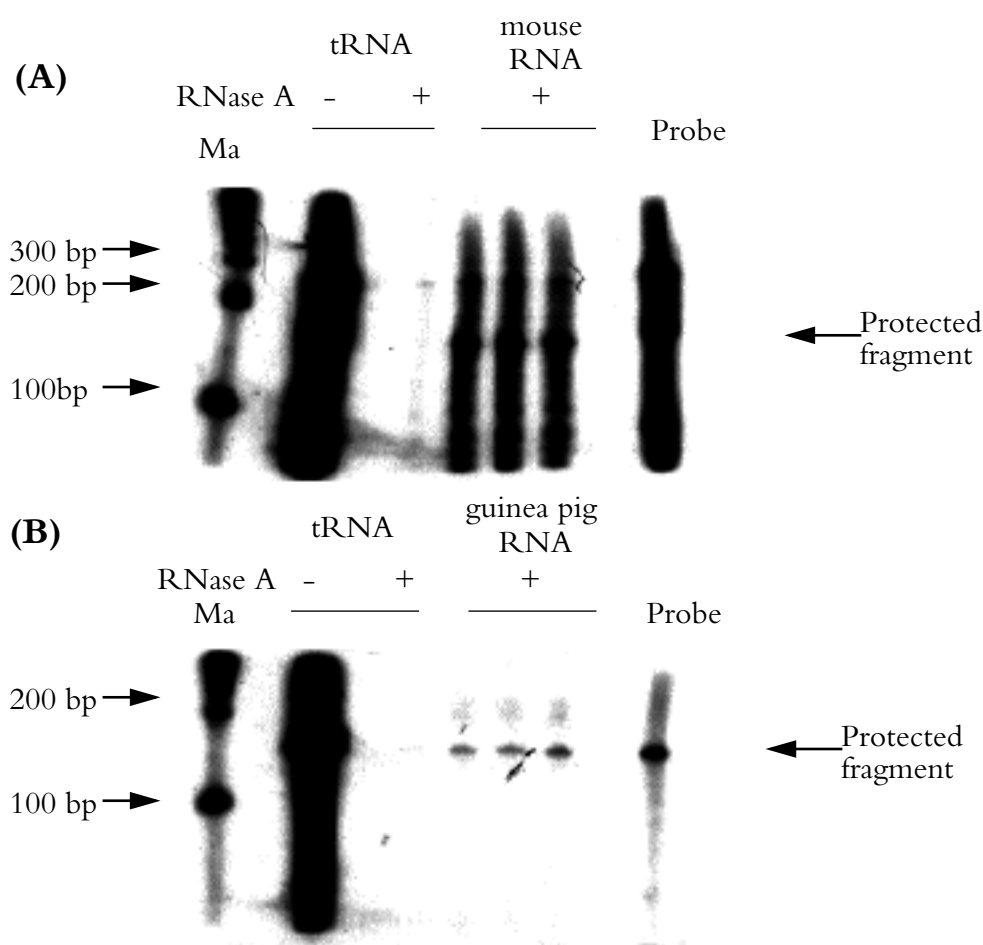


Figure 3.37 Expression of gPPAR α and mPPAR α mRNA in liver. Determination of expression of mouse PPAR α (A) mRNA and guinea pig PPAR α mRNA (B) by RNase protection assay. 30 μ g of RNA was hybridised with each ribo-probe. Anti-sense mPPAR α probe was made by transcribing Ase I cut pT7-7-anti sense mPPAR α plasmid with T7 RNA polymerase. Full length mPPAR α probe was 282 bp and protected fragment length was 193 bp long. 30 μ g tRNA hybridised with mPPAR α probe was treated with and without RNase A to determine if non-specific mRNA species were being protected. RNase protection assays were run on a 6% denaturing acrylamide gel in 1* TBE at 300 v. Anti-sense gPPAR α probe was made by transcribing Pvu II cut gPPAR α -pBK-CMV plasmid with T7 RNA polymerase. Full length gPPAR α probe was 170bp. RNase protection assays were run on a 8% denaturing acrylamide gel run in 1* TBE at 300 v. Gels were fixed, dried and exposed to the same piece of hyperfilm at -70 C for 2 days.

in the liver, and figure 3.37 (B) demonstrates that gPPAR α is also expressed in the liver. The negative control (marked tRNA -) shows that the riboprobe synthesised is full length and in excess of the protected fragments. The addition of RNase A to yeast tRNA (figure 3.37 (A) tRNA +) results in near complete digestion of probe: therefore the protected fragments observed in the guinea pig and mouse liver result from specific hybridisation. The mPPAR α and gPPAR α anti-sense probes were synthesised in tandem using the same reagents, and thus had the same specific activity. The protected mPPAR α fragment was 193 bp long and the gPPAR α signal was 170 bp long. Thus equimolar amounts of the mPPAR α and gPPAR α fragments in figure 3.37 would produce a signal ratio of 1.14: 1. Figure 3.37 shows that the amount of mouse PPAR α RNA is much greater than the amount of guinea pig PPAR α RNA: however, this data is an autoradiogram, and is not suitable for quantitative analysis. Subsequent analysis of these RNA samples by phosphor imaging showed that mPPAR α mRNA expression was at least 10-fold greater than gPPAR α mRNA expression (D. Brady, personal communication). The

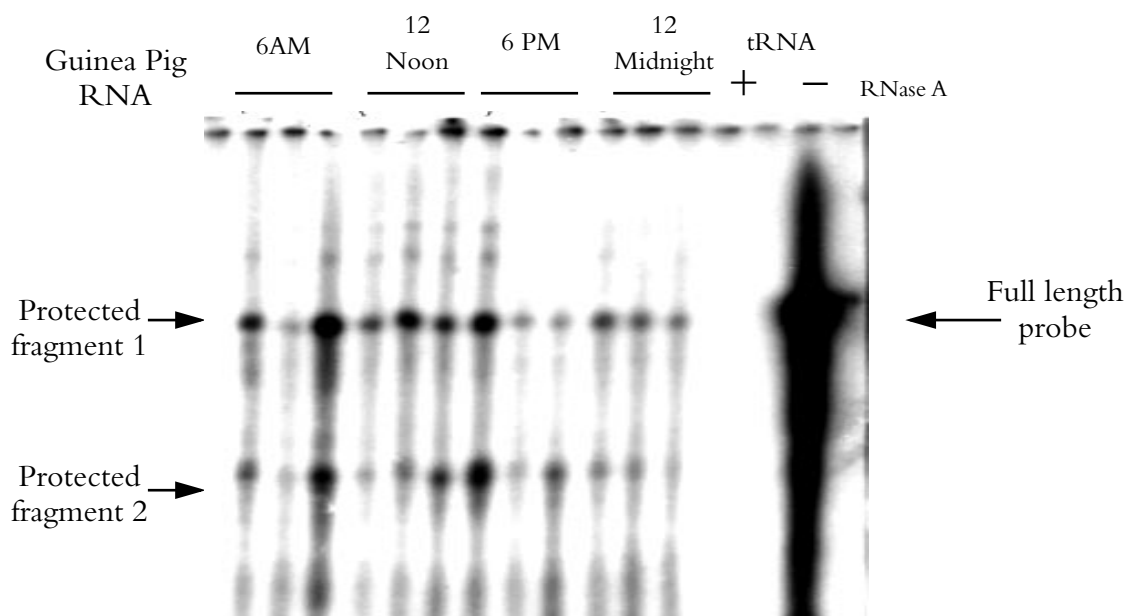


Figure 3.38 Expression of gPPAR α mRNA across a 24 hour period. Anti-sense gPPAR α probe was made by transcribing Pvu II cut gPPAR α -pBK-CMV plasmid with T7 RNA polymerase. Full length gPPAR α probe was 170bp and protected fragment length was 97 bp. The size of the protected fragment in 1 was the same as the full length probe due to lack of RNase A digestion of the single strand RNA over hang in the probe / mRNA hybrid duplex. Protected fragment 2 is the probe / mRNA hybrid that has had single strand over hang (corresponding to transcribed vector DNA) completely digested by RNase A, leaving only protected gPPAR α mRNA. RNase protection assays were run on a 8% denaturing acrylamide gel run in 1* TBE at 300 v. Gels were fixed, dried and exposed to hyperfilm at -70 C for 2 days.

expression of gPPAR α mRNA was determined in liver of animals killed at 6.00 AM, 12.00 Noon, 6.00 PM and 12.00 Midnight. Figure 3.38 shows that gPPAR α mRNA expression in liver does not vary across a 24 hour period.

Section 3.6 Expression of mPPAR α DNA binding domain

A 336 bp DNA fragment spanning the mPPAR α DNA binding domain (mPPAR α -DBD) was amplified from pSG5-mPPAR α DNA using primers mPPAR α -P1 and mPPAR α -P2. A Pst I site was engineered into the 5' end of the fragment by using a single nucleotide mismatch in mPPAR α -P1. The nucleotide change results in a Glycine to Cysteine amino acid transition. A 3' translational stop codon was engineered by a nucleotide mismatch in primer mPPAR α -P2. The translational stop site occurs at position 199. The 336 bp amplified fragment spans from amino acids 92 E to 203 L. Figure 3.39 shows an amplified DNA fragment corresponding to the predicted size.

mPPAR α -DBD DNA was purified using Qiagen Qiaquick spin columns and was cloned into pRSET-A prokaryotic expression vector. The mPPAR α -DBD was cloned inframe to an N-

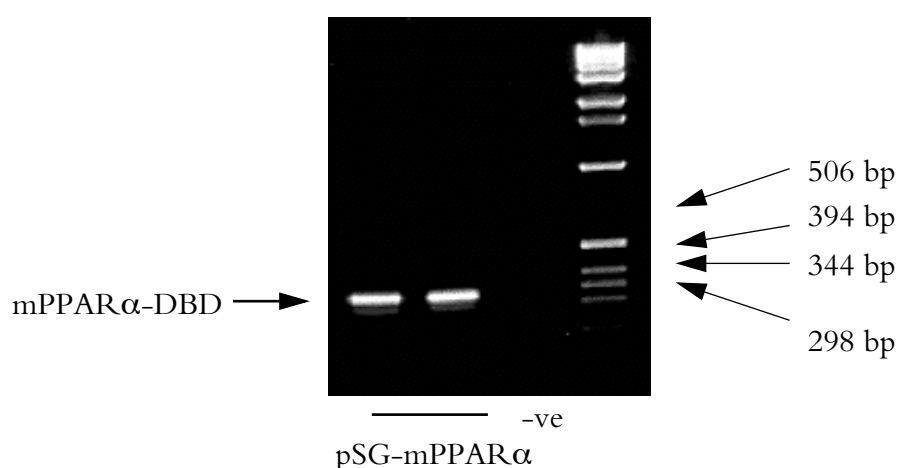


Figure 3.39 PCR amplification of mPPAR α -DBD DNA. 5 μ l of PCR reaction was analysed on a 1.5% agarose gel, run in 0.5* TBE at 100v for 2 hours . DNA bands were visualised by ethidium bromide staining. mPPAR α -DBD DNA was amplified using pSG5-mPPAR α template DNA and primers mPPAR α -P1 and mPPAR α -P2. The lane marked negative contains products from a PCR with no template DNA. PCR reactions were amplified for 25 cycles at [94 C, 1 min; 50 C, 1min; 72 C, 1 min].

terminal 41 amino acid tag. The N-terminal peptide contains a six histidine (His*6) tag that allows purification on Ni^{2+} containing resins or other metal affinity resins such as Talon Metal Affinity Resin . The N-terminal peptide provided by the pRSET-A vector also contains a protease cleavage site for the protease enzyme Enterokinase. The cloning strategy used for cloning mPPAR α -DBD was not directional, therefore clones positive for an insert were screened for correct orientation using a Kpn I digest. Figure 3.40 two shows DNA digests of two pRSET-A-mPPAR α -DBD positive clones. The Pst I digest releases the mPPAR α -DBD DNA, producing a 317 bp fragment. The Kpn I digest of pRSET-A-mPPAR α -DBD DNA will yield two DNA fragments. If the insert is in the correct orientation a 274 bp and a 2962 bp fragment will be produced, but if the insert is in the wrong orientation a 64bp fragment and a 3172 bp fragment will be released. The two pRSET-A-mPPAR α -DBD clones in figure 3.40 are in the correct orientation. The Kpn I digest has released 274 bp and 2962 bp DNA fragments.

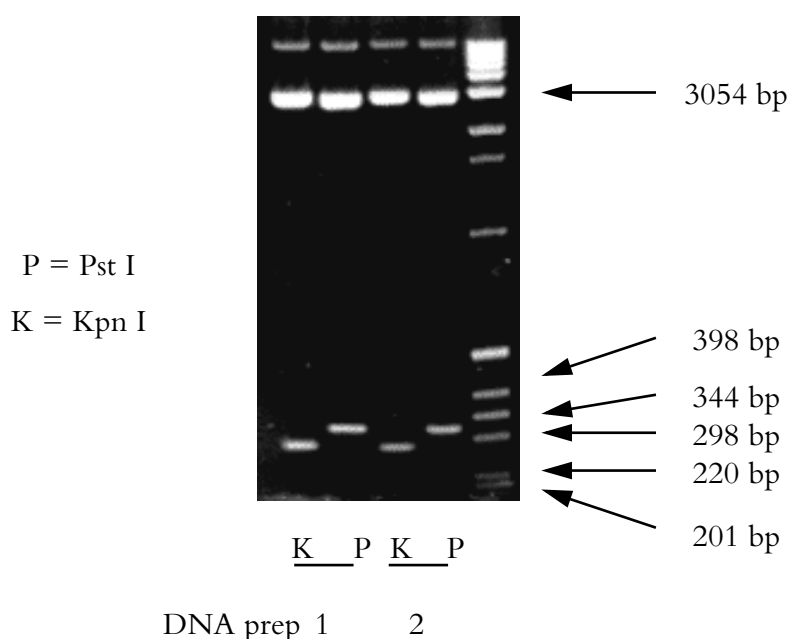


Figure 3.40 Cloning of mPPAR α -DBD into pRSET-A vector. pRSET-A-mPPAR α -DBD clones were digested with Pst I and Kpn I restriction enzymes. The products of each restriction digest were analysed on a 2% agarose gel run in 0.5* TBE at 100v for 2 hours. DNA bands were visualised by ethidium bromide staining. DNA fragments were sized using a 1kb DNA marker ladder.

Section 3.6.1 Prokaryotic expression of mPPAR α -DBD

pRSET-A-mPPAR α -DBD plasmid DNA was transformed into BL21 (DE3)pLys S *E.coli* cells.

Small scale (10 ml) cultures of BL21 (DE3)pLysS-pRSET-A-mPPAR α -DBD were grown in LB-broth in a shaking incubator. Cultures of OD_{600nm} = 0.6-0.8 were induced for expression of His*6 tagged mPPAR α -DBD protein by the addition of IPTG to the culture medium. Total cell extracts from induced and uninduced BL21 (DE3) pLysS and BL21 (DE3)pLysS-pRSET-A-mPPAR α -DBD were analysed by SDS-PAGE. Figure 3.41 shows the analysis of such cell extracts. The predicted molecular weight of the tagged mPPAR α protein is 16.6 kDa. An induced band of molecular weight < 20 kDa is observed in BL21 (DE3)pLysS-pRSET-A-mPPAR α -DBD cultures but not BL21(DE3)pLysS control cultures.

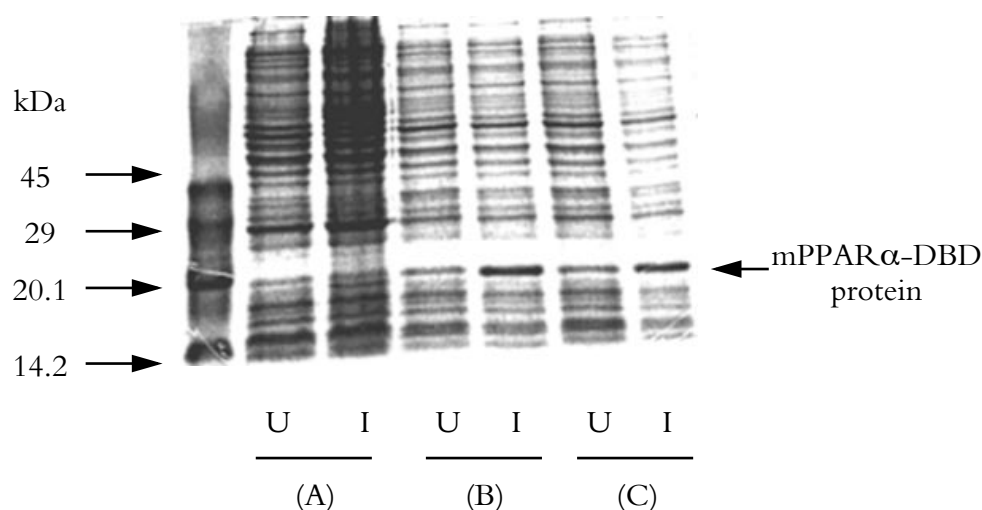


Figure 3.41 Induction of mPPAR α -DBD protein. SDS-PAGE analysis of total cell extracts of induced and un-induced BL21 (DE3) pLysS (A) and BL21 (DE3)pLysS-pRSET-A-mPPAR α -DBD (B and C). 0.5 mM IPTG (final concentration) was used for induced cultures. Proteins were run on a 15% SDS-polyacrylamide gel, in 1* laemmli buffer at a constant 70 mA for 1 hour. Proteins were visualised by Coomassie Blue staining.

Two litres of BL21 (DE3)pLysS-pRSET-A-mPPAR α -DBD culture was grown to an optical OD_{600nm} = 0.6. mPPAR α -DBD protein expression was induced by the addition of IPTG to a final concentration of 0.5 mM. Cells were harvested by centrifugation. The cell pellet was resuspended in 1* Talon Binding Buffer, freeze-thawed once, and then sonicated to disrupt the cell membrane. Soluble and insoluble material was clarified by ultra-centrifugation. Proteins from the soluble and insoluble fractions were analysed by SDS-PAGE. Figure 3.42 demonstrates

that the induced mPPAR α -DBD protein segregates into the insoluble fraction.

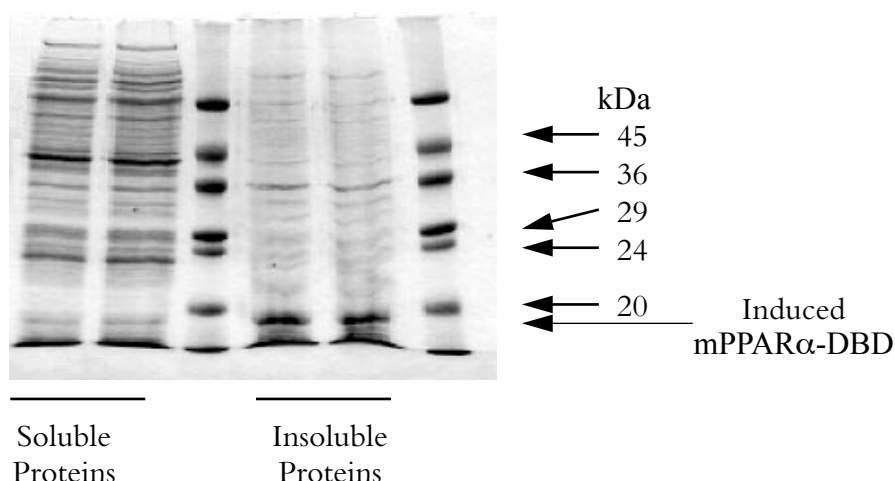


Figure 3.42 SDS-PAGE of purified proteins from induced cultures. Approximately 12.5 μ g of soluble and insoluble protein extract, isolated from an induced BL21 (DE3) pLysS-pRSET-A-mPPAR α -DBD culture were run on a 15% SDS-polyacrylamide gel, in 1 \times Laemmli buffer at 70 mA for 1 hour. Proteins were visualised by Coomassie Blue Staining.

Section 3.6.2 Effect of lower temperature on protein solubility

BL21 (DE3)pLysS-pRSET-A-mPPAR α -DBD cultures were grown at 30 C and 37 C and were induced for the expression of mPPAR α -DBD protein by the addition of IPTG to a final concentration of 0.5 mM. Figure 3.43 demonstrates that mPPAR α -DBD protein induced at 30 C did not segregate into the insoluble or soluble fraction differently than mPPAR α -DBD

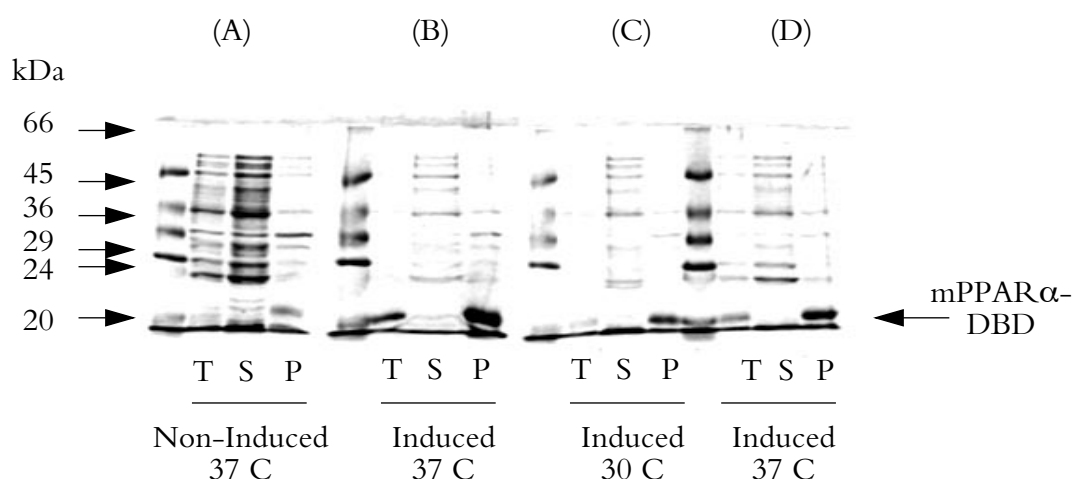


Figure 3.43 Induction of mPPAR α -DBD at 37 C and 30 C. SDS-PAGE analysis of total cell extracts (T), soluble cell extracts (S) and insoluble cell extracts (P) of uninduced (gel A) and induced (gel B) BL21 (DE3)pLysS-pRSET-A-mPPAR α -DBD cultures grown at 37 C. Cultures analysed in A and B were grown in a shaking incubator. SDS-PAGE analysis of total cell extracts (T), soluble cell extracts (S) and insoluble cell extracts (P) of induced BL21 (DE3)pLysS-pRSET-A-mPPAR α -DBD cultures grown at 30 C (gel C) and 37 C (gel D). Cultures analysed in C and D were grown in waterbaths, without mechanical shaking. 0.5 mM IPTG (final concentration) was used for induced cultures. Proteins were run on a 15% SDS-polyacrylamide gel, in 1 \times Laemmli buffer at a constant 70 mA for 1 hour. Proteins were visualised by Coomassie Blue staining.

protein induced at 37 C. Induction at a 30 C did not alter the solubility of over-expressed mPPAR α -DBD protein.

Section 3.6.3 Affinity purification of mPPAR α -DBD protein

The soluble fraction of proteins produced from a 37 C, IPTG induced culture of BL21 (DE3)pLysS-pRSET-A-mPPAR α -DBD was passed through Talon Metal Affinity Resin. No trace levels or low levels of soluble His*6 tagged mPPAR α -DBD bound to the affinity resin. Figure 3.44 shows that no proteins from the soluble fraction bound to the affinity resin. This result demonstrates that all mPPAR α -DBD protein produced segregated into the insoluble fraction. Insoluble proteins were solubilised in 1* Talon Binding Buffer containing 6M Guanidine. His*6 tagged mPPAR α -DBD protein was purified from the resolubilised protein fraction using Talon metal affinity resin. Elution fractions 1 and 2 were dialysed against a 25 mM Hepes, 100 mM NaCl, 0.4 mM ZnSO₄ solution, pH=7.6 using a “Slide-a-lyzer” dialysis cassette with molecular weight cut off of 10 000 Da. Renatured His*6 tagged mPPAR α -DBD was analysed for purity by SDS-PAGE. Figure 3.45 shows highly purified His*6 tagged mPPAR α -DBD protein. The total amount of protein in elution fractions 1 and 2 was 432 μ g and 516 μ g

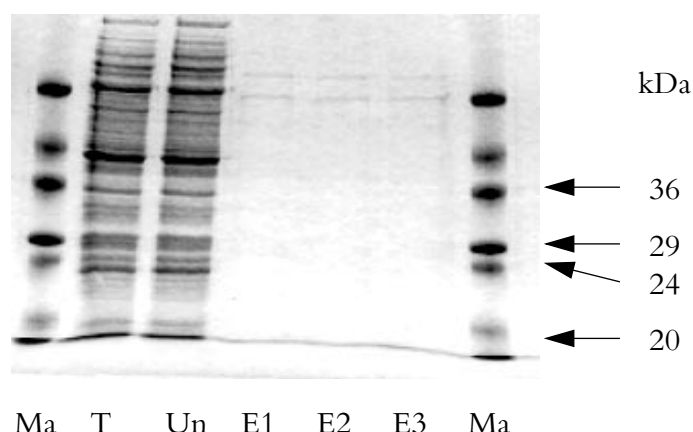


Figure 3.44 Purification of protein using Talon resin. SDS-PAGE analysis of soluble proteins from a 37 C, IPTG induced culture of BL21 (DE3)pLysS-pRSET-A-mPPAR α -DBD , purified on Talon metal affinity resin. Total soluble proteins (T), unbound soluble proteins (Un) , eluted proteins (fractions E1, E2 and E3) and marker proteins (Ma) were run on a 20 % SDS-polyacrylamide gel, in 1* laemmli buffer at a constant 35 mA for 1 hour. Proteins were visulised by Coomassie Blue staining.

respectively.

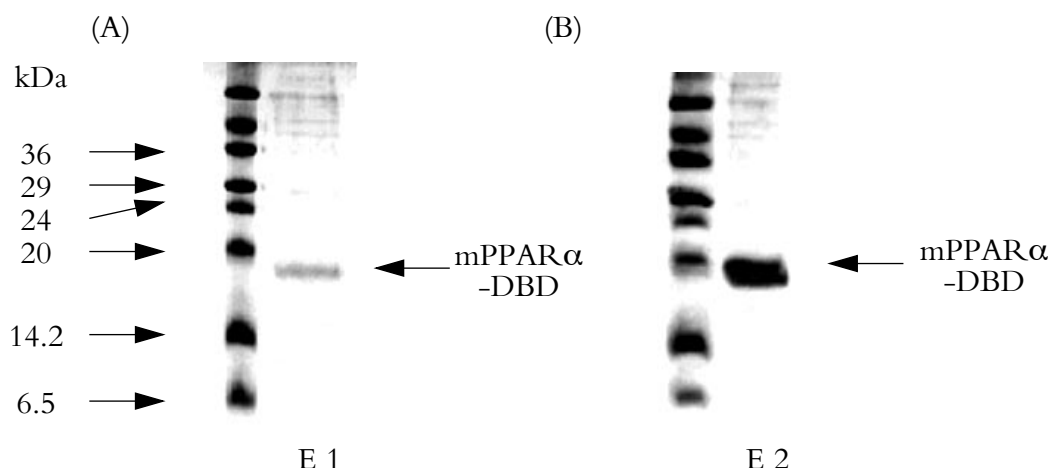


Figure 3.45 Purification of mPPAR α -DBD from resolubilised proteins. SDS-PAGE analysis of His*6 tagged mPPAR α -DBD proteins purified from the isolated insoluble protein fraction of a 37 C, IPTG induced culture of BL21 (DE3)pLysS-pRSET-A-mPPAR α -DBD. Talon metal affinity resin was used to purify resolubilised His*6 tagged protein. Eluted fractions E1 and E2 were dialysed against dialysis buffer: 25 mM Hepes (pH=7.6), 100mM NaCl, 40 μ M ZnSO₄ to remove denaturing agent. 50 μ l of each dialysed fraction was run on a 20 % SDS-polyacrylamide gel, in 1* laemmli buffer at a constant 35 mA for 1 hour. Proteins were visualised by Coomassie Blue staining.

Section 3.6.4 Removal of His*6 Tag from mPPAR α -DBD

Enterokinase protease enzyme was used to cleave off the His*6 tag from the His*6 tagged mPPAR α -DBD fusion protein. 88 μ g of DBD protein was treated with enterokinase. Analysis of the cleavage of the fusion protein was done by sampling small aliquots of the protease digestion reaction at 1 hour intervals. Figure 3.46 demonstrates that cleavage of a significant proportion of the fusion protein occurred within one hour of protease treatment. A proportion of fusion protein

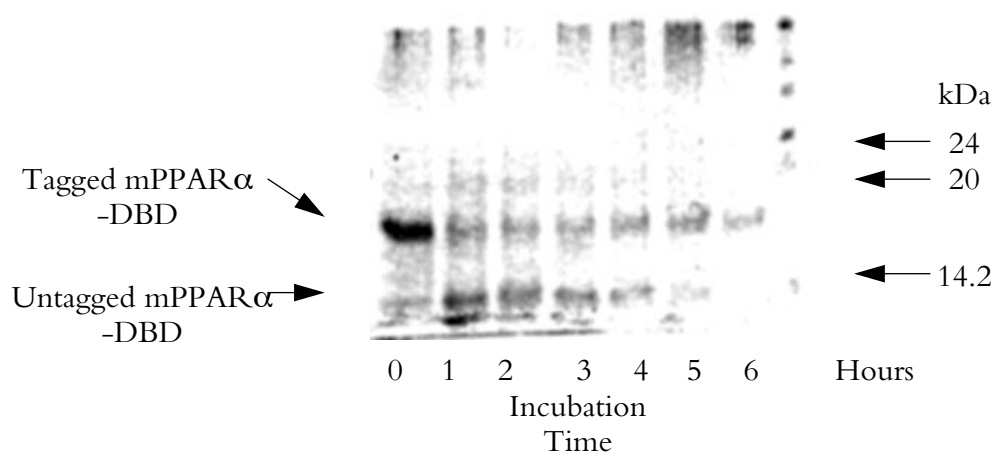


Figure 3.46 Cleavage of His*6 tag from mPPAR α -DBD. 88 μ g of His*6 tagged mPPAR α -DBD in buffer (25 mM Hepes pH=7.6, 100 mM NaCl, 0.4 mM ZnSO₄), protein was treated with 1.8 μ g of Enterokinase protease in a final volume of 1 ml. 40 μ l of this reaction was collected at 1 hour intervals. Protein samples were run on a 20% SDS-polyacrylamide gel in 1* laemmli buffer at 35 mA for 1 hour. Proteins were visualised by Coomassie blue staining.

remained resitant to protease treatment over the six hour incubation period.

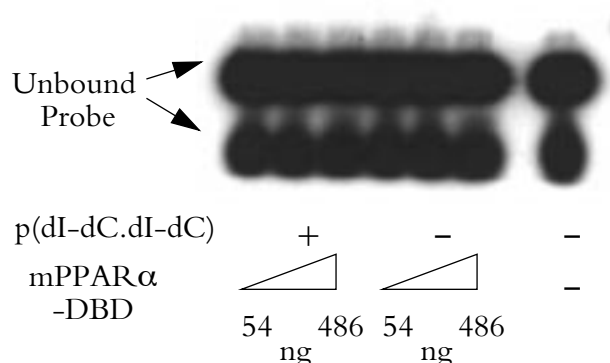


Figure 3.47 Binding of His*6 tagged mPPAR α -DBD to con-4A6z PPRE. 0.41 pmol [32 P]-con-4A6-PPRE was incubated with between 54 and 486 ng of purified His*6 tagged mPPAR α -DBD protein in 1* Tris EMSA buffer (10 mM Tris-HCl pH=8.0, 5% Glycerol (v/v), 0.1 mM EDTA, 0.4 mM DTT, 100 μ M PMSF, 50 mM KCl) in the presence or absence of 0.1 μ g p(dI-dC.dI-dC). Gel was fixed and dried and exposed to hyperfilm overnight.

Section 3.6.5 Electromobility shift assay of mPPAR α -DBD

An oligonucleotide containing the cytochrome P450 4A6 gene z element PPRE with consensus 5' flanking sequence (5' -CAAACTAGGTCAAAGGTCAGGG-3') was used to make a [32 P] labelled PPRE probe. This probe termed con-4A6-PPRE was tested for binding to purified His*6 tagged mPPAR α -DBD and untagged mPPAR α -DBD protein in an electromobility shift assay. Figure 3.47 demonstrates that His*6 tagged mPPAR α -DBD protein did not bind to the con-4A6-PPRE probe, even in the absence of non-specific competitor DNA. Figure 3.48 shows that untagged mPPAR α -DBD protein does not bind to the con-4A6-PPRE. The con-4A6-PPRE was tested for binding to mouse liver nuclear proteins and was found to a suitable DNA substrate for electromobility shift assays (data not shown).

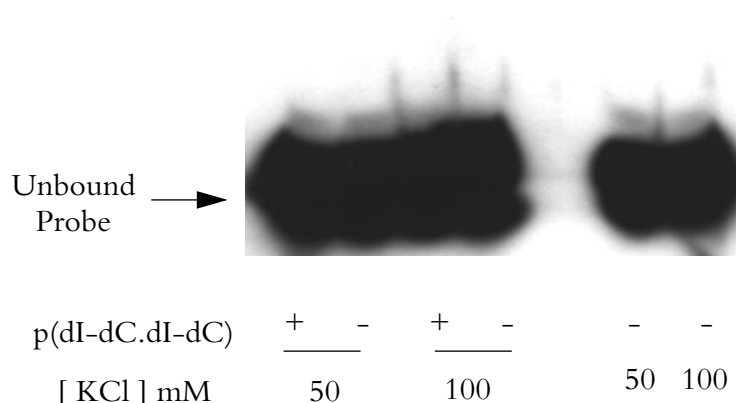


Figure 3.48 Binding of untagged mPPAR α -DBD to con-4A6z PPRE. 0.41 pmol [32 P]-con-4A6-PPRE was incubated with between 54 and 486 ng of purified His*6 tagged mPPAR α -DBD protein in 1* Tris EMSA buffer (10 mM Tris-HCl pH=8.0, 5% Glycerol (v/v), 0.1 mM EDTA, 0.4 mM DTT, 100 μ M PMSF, 50 mM or 100 mM KCl) in the presence or absence of 0.1 μ g p(dI-dC.dI-dC). Gel was fixed and dried and exposed to hyperfilm overnight.

Section 3.6.6 Cloning of thioredoxin-mPPAR α -DBD

mPPAR α -DBD DNA was cloned into pThio-His.A prokaryotic expression vector. pThio-His.A contains the coding sequence for an in frame fusion of *E.coli* thioredoxin protein. The resultant thioredoxin-mPPAR α -DBD fusion protein has a predicted molecular weight of 27

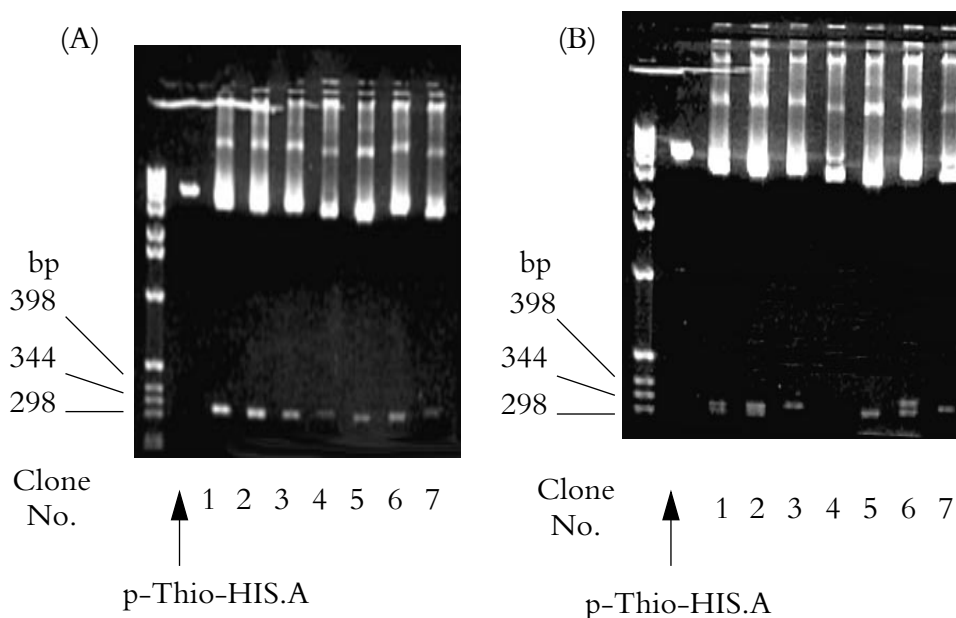


Figure 3.49 DNA digests of putative pThio-His.A-mPPAR α -DBD clones. Putative pThio-His.A-mPPAR α -DBD clones were screened for the presence of an insert DNA by Pst I restriction digestion (gel A). The same clones (numbers 1-7) were restriction digested with Bgl II restriction enzyme to determine the orientation of the inserts (gel B). pThio-HIS.A vector was cut with Pst I and Bgl II as an internal control. Products of each restriction digest were run on a 1.5 % agarose gel run in 0.5* TBE at 100v for 1.5 hours. DNA bands were visualised by ethidium bromide staining. DNA fragments were sized using a 1kb marker ladder.

kDa. The thioredoxin domain has been modified at E31 and Q63. These two residues have been changed to Histidine residues, which in the native folded protein forms a “His-patch” which can bind to metal affinity resins (Invitrogen pThio-His.A manual). The cloning of mPPAR α -DBD DNA into pThio-His.A was non-directional. Therefore putative clones had to be screened for the presence and orientation of the insert. Figure 3.49 (A) shows Pst I digests of seven putative pThio-His.A-mPPAR α -DBD clones. All seven are positive for a DNA insert. A Bgl II digest was carried out on these seven clones. An insert in the correct orientation will yield a 288 bp fragment and a 4448 bp fragment. An insert in the wrong orientation will yield a 112 bp fragment and a 4624 bp fragment. Figure 3.49 (B) shows that only clone 5 is positive for an insert in the right orientation. Clone 4 contains a single insert in the wrong orientation, and all other clones have 2 or more concatenated inserts in various orientations. Clone 5 was used for thioredoxin-mPPAR α -DBD fusion protein expression studies.

Section 3.6.7 Expression of thioredoxin-mPPAR α -DBD protein

pThio-His.A-mPPAR α -DBD expression vector was transformed into BL21 (DE3)pLysS *E.coli*. Fusion protein expression was induced by the addition of IPTG to the culture medium. Small scale cultures of BL21 (DE3)pLysS pThio-His.A-mPPAR α -DBD were induced to express fusion protein at a final IPTG concentration of 1.5 mM. Cells from induced cultures were pelleted and

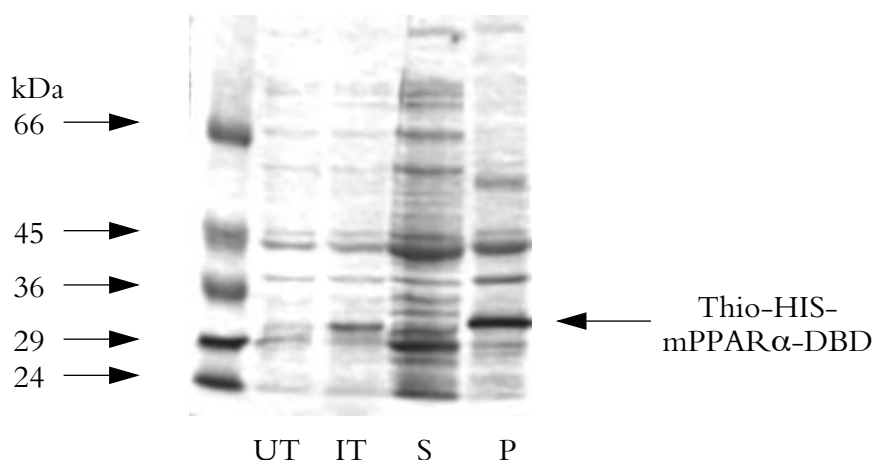


Figure 3.50 Induction of thioredoxin-mPPAR α -DBD protein in *E.coli*. Proteins from total cell extract of uninduced cultures (UT) and induced cultures (IT), and soluble (S) and insoluble (P) proteins from induced cultures c BL21(DE3)pLysS-pThio-His.A-mPPAR α -DBD were analysed on a 12% SDS-polyacrylamide gel. The running condition: were 1* laemmli buffer, constant 50 mA for 1 hour. Proteins were visualised by Coomassie blue staining.

sonicated to disrupt the cell wall. Soluble and insoluble proteins were clarified by ultracentrifugation, and then analysed by SDS-PAGE. Figure 3.50 shows that an induced protein of approximate molecular weight 30 kDa was present in abundance in the insoluble fraction. Expression of fusion protein cannot be seen in the soluble fraction. The molecular weight of the induced band is approximately 3 kDa greater in size from the theoretically calculated molecular weight of the thioredoxin-mPPAR α -DBD fusion protein.

The possibility that low levels of soluble thioredoxin-mPPAR α -DBD fusion protein were not produced could not be eliminated by the SDS-PAGE analysis of soluble and insoluble fractions. The presence of soluble thioredoxin-mPPAR α -DBD protein was tested by binding soluble protein extracts to two types of metal affinity resin. Invitrogens nickel-charged sepharose resin and Clontechs Talon metal affinity resin were used. Figure 3.51 shows the unbound and bound soluble proteins that were eluted from the nickel-charged affinity resin at different concentrations of imidazole. The eluted fractions demonstrate that the nickel-charged sepharose resin bound most soluble proteins in a non-specific manner. This resin was unable to specifically bind any

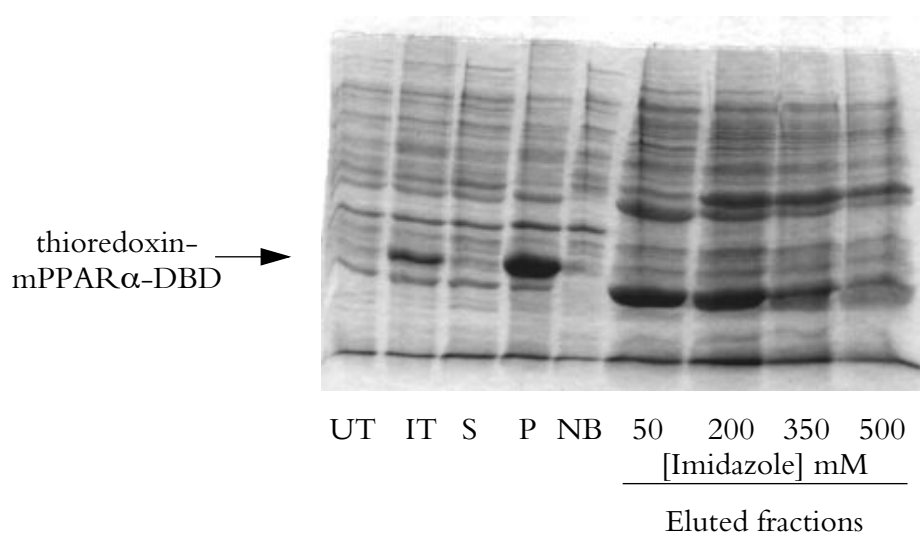


Figure 3.51 Purification of soluble thioredoxin-mPPAR α protein. ProBond nickel charged sepharose resin was used to purify fusion protein from the soluble protein fraction as described in the methods section. Proteins were analysed on a 12% SDS-PAGE gel, run in 1 \times laemmli buffer at 35mA for 1 hour. Proteins were visualised by Coomassie Blue staining. Lanes marked UT and IT are uninduced total cell extract and IPTG induced total cell extract. Lanes marked S and P are soluble (S) and insoluble (P) protein fractions clarified from induced total cell extract. Lane marked NB are soluble proteins which did not bind to the ProBond resin. The proteins eluted from the ProBond resin at specific imidazole concentrations are indicated.

soluble thioredoxin-mPPAR α -DBD protein that may have been present. Figure 3.52 demonstrates that no soluble thioredoxin-mPPAR α -DBD protein bound to Talon metal affinity resin. Comparison of the lanes marked S for soluble proteins and NB, non-bound proteins shows that few soluble proteins bound to Talon metal affinity resin in a non-specific manner. The eluted fractions E1 and E2 contained very little protein. These two purification experiments indicate that the induced thioredoxin-mPPAR α -DBD protein exclusively segregated into the insoluble protein fraction. The presence of the thioredoxin protein in the fusion protein did not increase the solubility of the mPPAR α -DBD protein.

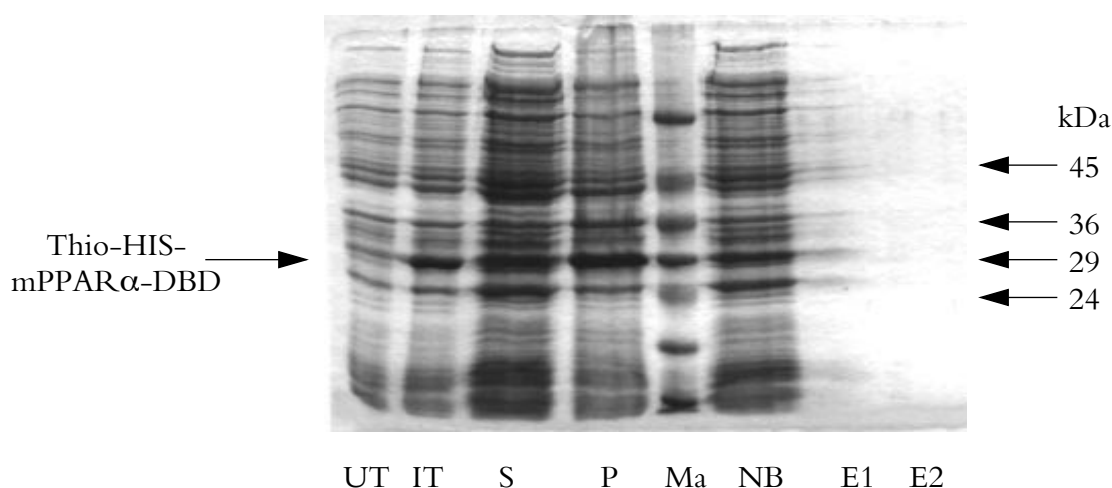


Figure 3.52 Purification of soluble thioredoxin-mPPAR α -DBD protein using Talon resin. Talon metal affinity resin was used to purify fusion protein from the soluble protein fraction as described in the methods section. Proteins were analysed on a 12% SDS-PAGE gel, run in 1* laemmli buffer at 35mA for 1 hour. Proteins were visualised by Coomassie Blue staining. Lanes marked UT and IT are uninduced total cell extract and IPTG induced total cell extract. Lanes marked S and P are soluble (S) and insoluble (P) protein fractions clarified from induced total cell extract. Lane marked NB are soluble proteins which did not bind to the Talon resin. The proteins eluted from the Talon resin at a lower pH buffer are indicated by E1 and E2.

Section 3.6.8 *In vitro* synthesis of mPPAR α -DBD protein

A third strategy was used to make soluble mPPAR α -DBD protein. The expression vector pRSET-A-mPPAR α -DBD contains a T7 RNA polymerase binding site which can be utilised in *in vitro* transcription / translation experiments. Rabbit reticulocyte lysate extracts were used with T7 RNA polymerase to produce mPPAR α -DBD protein from pRSET-A-mPPAR α -DBD expression vector. Full length mPPAR α and mRXR α were also produced. Figure 3.53

shows SDS-PAGE analysis of *in vitro* translated mPPAR α -DBD, mPPAR α and mRXR α .

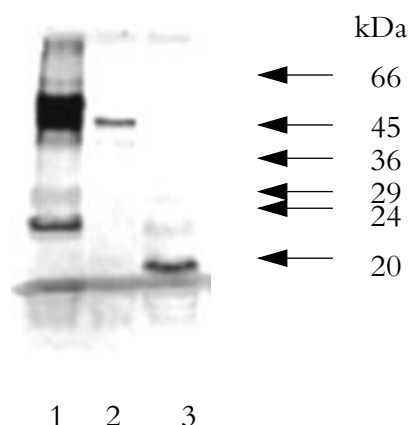


Figure 3.53 In vitro expression of mPPAR α , mRXR α and mPPAR α -DBD proteins. *In vitro* translated [35 S] Methionine labelled mPPAR α (lane 1), mRXR α (lane 2) and His*6 tagged mPPAR α -DBD (lane 3) were produced from pT7-mPPAR α , pGEM5-mRXR α and pRSET-A-mPPAR α -DBD expression vectors using rabbit reticulocyte lysate extract. T7 RNA polymerase was used for the transcriptional component of the synthesis reaction. 5 μ l of each transcription / translation reaction was analysed on a 12% SDS-PAGE gel run in 1 \times laemmli buffer at 50 mA for 1 hour. The gel was dried and exposed to hyperfilm at -70 C for 2 days.

These *in vitro* translated proteins were tested for their capacity to bind to PPRE probes in electromobility shift assays. No specific protein-DNA complexes were observed for mPPAR α -DBD, mPPAR α -DBD/mRXR α heterodimers, mPPAR α , mRXR α , and mPPAR α /

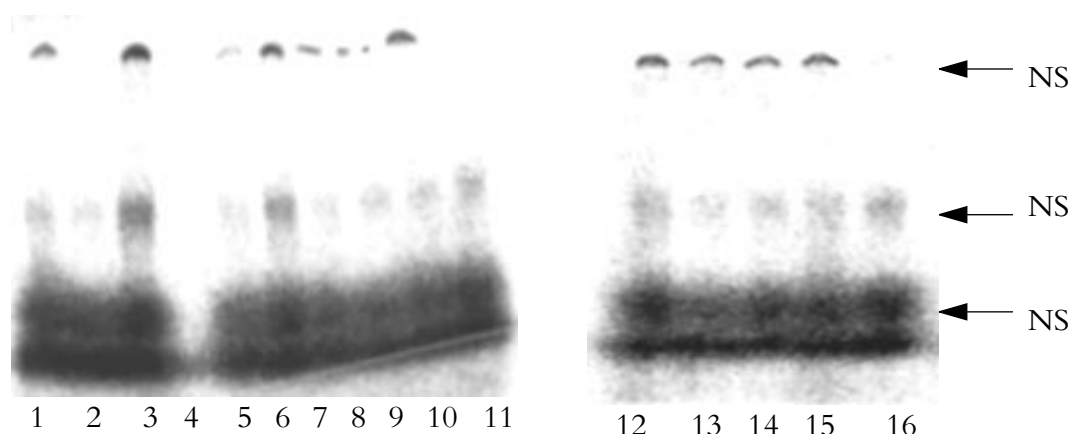


Figure 3.54 Binding of *in vitro* translated proteins to con-4A6-PPRE. *In vitro* translated mPPAR α -DBD, mPPAR α and mRXR α proteins were assayed for binding to 0.41 pmol [32 P]-con4A6-PPRE 1 \times Hepes EMSA buffer (10mM Hepes (pH=7.9), 125 mM NaCl, 1mM EDTA, 7% v/v BSA, 1 mM DTT, 150 μ M PMSF). A total of 2.5 μ l of translation reaction extract was used per assay. No non-specific competitor DNA was added. Protein-DNA complexes were resolved on a 7% native acrylamide gel run in 0.25 \times TBE at a constant 100v. Lane 1 contains mRXR α , lane 2 mPPAR α (preparation 2), lane 3 mPPAR α (preparation 1), lane 4 no *in vitro* translation reaction proteins, lane 5 mPPAR α (2)/mRXR α , lane 6 mPPAR α (1)/mRXR α , lane 7 mPPAR α -DBD (1), lane 8 mPPAR α -DBD(2), lane 9 mPPAR α -DBD (3), lane 10 control reticulocyte lysate extract, lane 12 mRXR α , lane 13 mRXR α /mPPAR α -DBD(1), lane 14 mRXR α /mPPAR α -DBD(2), lane 15 mRXR α /mPPAR α -DBD(3) and lane 16 control reticulocyte lysate extract. NS are non-specific shifted protein-DNA complexes. Radioactivity was detected by phosphor-imaging.

mRXR α heterodimers with con4A6-PPRE probe, see figure 3.54. Independent batches of *in vitro* translated proteins were assayed to show reproducibility. Wild type and mutant rat acyl-CoA oxidase probes and mutant con4A6-PPRE probes were also assayed. No specific protein-DNA complexes were observed under any of the conditions tested (data not shown).

His*6 tagged mPPAR α -DBD and thioredoxin-mPPAR α fusion proteins were successfully produced in BL21 (DE3)pLys S *E.coli* cultures. However the induced fusion proteins segregated into the insoluble inclusion body particles in these *E.coli*. No readily soluble mPPAR α -DBD was produced that could be purified using Metal ion affinity resins. Attempts to denature and renature insoluble mPPAR α -DBD fusion protein did not yield a protein which could bind to a PPRE in electromobility shift assays. Therefore synthesis of a functional soluble mPPAR α -DBD was done using a rabbit reticulocyte *in vitro* coupled transcription / translation kit. The *in vitro* synthesised mPPAR α -DBD also did not bind to a PPRE in an electromobility shift assay.

Chapter 4 Discussion

Section 4.1 The molecular mechanism of peroxisome proliferation

During the past seven years a large amount of knowledge about the molecular aspects of peroxisome proliferation have been elucidated. The effects of peroxisome proliferators are mediated by a transcription factor called peroxisome proliferator activated receptor α (PPAR α) (Issemann, I. and Green, S. 1990 and Lee, S. S-T. *et al* 1995). PPAR α is part of a large family of transcription factors known as the nuclear steroid hormone receptor superfamily. PPAR α is highly expressed in the liver (Jones, P. *et al* 1995) and works by interacting with specific DNA response elements (Tugwood, J.D. *et al* 1992), present in genes that are modulated by peroxisome proliferators (Osumi, T. *et al* 1991, Zhang, B. *et al* 1992, Muerhoff, A.S. *et al* 1992).

At the onset of the work presented here, peroxisome proliferators were considered to be activators of PPAR α , as evidence for a direct interaction with peroxisome proliferators had not been found, and no endogenous ligand had been determined. An aim of my work was to investigate any changes in the interaction of nuclear proteins from animals dosed with a peroxisome proliferator with a DNA response element for the PPAR α receptor.

Section 4.1.1 EMSA of LNP binding to DNA response elements

The rat acyl-CoA oxidase gene PPRE (ACO-PPRE) was characterised by Osumi, T. *et al* 1993 using liver nuclear protein extracts in both DNase I footprinting assays and electromobility shift assays (EMSA's). The EMSA assay is a suitable assay for examining the effects of peroxisome proliferators on the expression of liver nuclear proteins which bind to DNA response elements. If peroxisome proliferators were to increase the expression of PPAR α , as has been suggested by certain research groups (Gebel, T. *et al* 1992 and McNae, F. *et al* 1994) the assay would detect the formation of more DNA-PPAR α /RXR α complexes in assays using LNP extracts from peroxisome proliferator treated animals. The assay could also detect if the effect of peroxisome

proliferators caused a pre-existing population of receptors to have enhanced DNA binding capabilities, caused possibly by post-translational modification such as phosphorylation (Shalev, A. *et al* 1996). EMSA assays though would not be able to discriminate between these two possibilities.

Section 4.1.2 Sequence-specific protein binding to an acyl-CoA oxidase PPRE

Purified rat liver nuclear protein extracts (rLNP) were assayed for binding to a DNA probe containing the A region (-578 to -553) of the rat acyl-CoA oxidase gene (ACO-PPRE). Specific controls were carried out first using rat liver nuclear extracts to demonstrate that the EMSA results obtained by Osumi, T. *et al* 1993 could be repeated. Figure 3.1 demonstrates that a shifted complex between rLNP and ACO-PPRE probe is formed. The binding of rLNP to ACO-PPRE was specific as a >500 fold excess of non-specific competitor DNA did not abolish the formation of the shifted complex. Osumi, T *et al* 1993 observed a similar single shifted complex when using the A region as an EMSA probe. Figure 3.2 shows that a molar excess of unlabelled ACO-PPRE can abolish the shifted complex observed in the EMSA assay, demonstrating that rLNP binding to PPRE is saturable. The effect of temperature on the formation of shifted complex was assayed by carrying out rLNP / ACO-PPRE incubations at room temperature (~20 C) and on ice (< 4 C). Figure 3.3 shows that no change in the amount of protein-DNA complex or pattern of protein-DNA complexes was observed by altering the incubation temperature to < 4 C. The specificity of binding of rLNP to PPRE was demonstrated using PPRES that contained either a single mutation in the 5' half site (mACO-PPRE) or a double mutation in the 5' half site (dmACO-PPRE). Figure 3.4 (A), lanes 2 and 3 shows that an excess of [³H] labelled mACO-PPRE is a poor competitor DNA compared to [³H] labelled ACO-PPRE, indicating that mACO-PPRE has a much reduced affinity for rLNP. Figure 3.4 (B) demonstrates that rLNP-PPRE complex does not form when [³²P]-mACO-PPRE is used as a substrate in the presence of an excess of non-specific competitor DNA. Figure 3.5 confirms that the binding of

rLNP to PPRE is specific to the sequence of the DNA, as rLNP shows no binding to a [³²P]-dmACO-PPRE (lane 2, figure 3.5).

Evidence to confirm the importance of the sequence specificity of the PPAR α / RXR α -PPRE interaction has come from two sources. Issemann, I. *et al* 1993 demonstrated that mutation of a PPRE in a reporter gene construct abolished PPAR and peroxisome proliferator dependent induction of the reporter gene in transfected Hepa1c1c7 cells. Further to this, the binding of bacterially produced PPAR α and RXR α receptors in EMSA assays can be abolished by mutation of three nucleotides within the CYP 4A6 PPRE (Palmer, C.N.A. *et al* 1995). The binding of *in vitro* translated PPAR α and RXR α receptors to the Apolipoprotein AI PPRE is abolished by mutation of a nucleotide in each half-site of the PPRE (Vu-Dac, N. *et al* 1994). None of these experiments however show the importance of sequence specificity of the PPRE to the binding of endogenous *in vivo* receptors. The results in figures 3.4 and 3.5 demonstrate that the electromobility shift assay can be used to demonstrate that specific binding of liver nuclear proteins to a PPRE is dependent on the DNA sequence of the response element.

It is assumed that the complex observed in the EMSA assays of rLNP with ACO-PPRE is comprised of PPAR α and RXR α . The possibility that the shifted complex is made up of other DNA binding proteins cannot be excluded. To test whether or not the shifted complex contained either receptor, supershift assays could be performed using specific antibodies raised against each receptor. This limitation in interpreting the results does not alter the usefulness of the assay for detecting differences in LNP binding to response elements from control and peroxisome proliferator treated animals.

Section 4.1.3 Peroxisome proliferators do not affect LNP binding to a PPRE

It has been reported that peroxisome proliferators induce the expression of hepatic PPAR α (Gebel, T. *et al* 1992 and McNae, F. *et al* 1994). Other researchers such as Jones, P. *et al* 1995

and Miller, R. *et al* 1996 found no such evidence for the induction of PPAR α expression by peroxisome proliferators. Measuring an induction in the amount of mRNA transcribed from a gene or the amount of translated product from this RNA by western blotting does not show if an increase in functional protein has occurred. It was decided to examine this discrepancy between the literature using a technique that examines the amount of functional receptor in a protein extract. Electromobility shift assays were used to examine whether or not a potent peroxisome proliferator, methylofenapate (Bell, D.R. *et al* 1991) induced the amount of functional PPAR α receptor in C57 Bl / 6 mice liver, as measured by enhanced DNA binding of liver nuclear proteins in an *in vitro* EMSA assay. Mouse liver nuclear proteins (mLNP) were tested for binding to ACO-PPRE in the presence of an excess of non-specific competitor DNA. Figure 3.6 demonstrates that mLNP forms a similar shifted complex to rLNP when assayed under the same conditions. Lanes 1 to 4, figure 3.6 show that as the amount of mLNP increases per assay, the amount of shifted complex increases. This demonstrates that the experimental conditions under which LNP binding was tested produced a linear binding response. mLNP was purified from mice dosed with methylofenapate (10mg / kg body weight) for 3 days, and tested for binding to wild type ACO-PPRE and a double mutant ACO-PPRE. Figure 3.7 demonstrates that the same pattern of specific shifted complexes was observed for control mLNP binding to wild type ACO-PPRE as for dosed mLNP binding to wild type ACO-PPRE. No shifted complex was observed for mLNP from control and MCP treated mice binding to a [32 P]-dmACO-PPRE (see figure 3.8). This result shows that peroxisome proliferator treatment of mice does not relax the sequence specific binding properties of liver nuclear proteins to PPREs. Figure 3.8 demonstrates that the amount of binding of control and MCP treated mice LNP samples to a wild type ACO-PPRE does not differ. The amount of shifted complex formed by each type of mLNP was measured by phosphor-imaging. The total amount of mLNP-PPRE from control and treated animals was compared using a students t-test and was found to be not

significantly different. This result is important as it supports the findings of Jones, P. *et al* 1995 and Miller, R. *et al* 1996. It strongly supports the theory that peroxisome proliferators act through a pre-existing pool of PPAR α receptor to cause peroxisome proliferation. There is however a limitation to the interpretation of the findings of the electromobility shift assay studies presented here. It is possible that peroxisome proliferators induce phosphorylation modification of the PPAR α receptor and that this modification is required for enhanced binding of the receptor to a PPRE. The protein purification protocol did not contain any phosphatase inhibitors and thus during purification dephosphorylation of activated PPAR α may occur. Therefore any difference in the pool of activated PPAR α receptor from control and treated animals would disappear. The resulting mLNP samples when assayed would exhibit no difference in the total amount of binding to PPRE.

Using an *in vitro* electromobility shift assay rodent liver nuclear proteins have been shown to bind to DNA response elements in a sequence specific manner and that LNP samples from peroxisome proliferator treated mice do not have enhanced binding to a PPRE. These results suggest that in methylclofenapate treated mice, PPAR α levels with functional DNA binding do not increase. In studies showing peroxisome proliferator induction of PPAR α expression, it is possible that the observed induction is a result of stress caused by the dose of that particular peroxisome proliferator. Lemberger, T. *et al* 1996 demonstrated that stress was able to induce the expression of PPAR α .

Section 4.1.4 Mouse PPAR α protein levels do not change across a 24 hour (diurnal) period

It has been demonstrated that methylclofenapate does not induce PPAR α protein levels in C57 Bl / 6 mice liver. Peroxisome proliferation must occur as a result of the interaction of peroxisome proliferator with endogenous levels of PPAR α . It was discovered that PPAR α receptor levels in rat liver were upregulated in response to glucocorticoid dosing (Lemberger, T *et al* 1994 and

Steineger, H.H. *et al* 1994). This finding led to the hypothesis that endogenous corticosteroid hormones may regulate the expression of PPAR α receptor. Glucocorticoid, a corticoid steroid hormone, is regulated in rats in a diurnal manner, with peak levels occurring around the light to dark switch in the evening. Lemberger, T. *et al* 1996 measured in rat liver, a peak of expression of rat PPAR α protein at 5.30 PM, approximately coinciding with the peak of corticoid steroid hormone. It could be hypothesised that the higher levels of PPAR α in the early evening in rat are critical for the peroxisome proliferation response. The PPAR α protein levels may have to reach a threshold level in order to facilitate the peroxisome proliferation response, and that this threshold level occurs in the evening as a result of diurnal variation in expression. Lemberger, T *et al* 1996 only examined the diurnal expression of PPAR α receptor in one strain of rat (Fischer 344) and at time points across a nine hour period, not a full 24 hour period. With this limited amount of data it is not possible to conclude that diurnal regulation of PPAR α is general phenomenon that occurs in all rodent species, or to what role any differences in expression of PPAR α across a 24 hour period would have on species responsiveness to peroxisome proliferators

The expression of mouse PPAR α in liver, across a 24 hour period was examined to see if this receptor's expression was diurnally regulated. Mouse liver nuclear proteins (mLNP) were purified from mouse liver tissue isolated at 6.00 AM, 12.00 Noon, 6.00 PM and 12.00 Midnight. Livers from 4 male C57 Bl / 6 mice sacrificed at each time point were pooled and processed together to eliminate individual variance in expression of PPAR α proteins. mLNP extracts were analysed by SDS-PAGE to see if there was observable diurnal differences in the proteins expressed at each time point. Figure 3.9 demonstrates that there is a difference in the protein banding patterns of high molecular weight (> 116 kDa) proteins, indicated by arrow A. A protein of approximate molecular weight 97 kDa (marked by arrow B) increases in expression at 6.00 PM and at 12.00 Midnight. There is also a difference in the banding pattern of 50 kDa proteins

in the region marked by arrow C across the diurnal period. These results clearly demonstrate that some mouse liver nuclear proteins are regulated in a diurnal manner.

PPAR α protein levels in mouse liver were examined by immunoblotting to see if diurnal variation in expression of PPAR α protein occurred in rodent species highly responsive to peroxisome proliferators. Figure 3.11 demonstrates that the anti-mPPAR α antibody used was sensitive enough to detect as little as 20 ng PPAR α receptor on a western blot.

No observable difference was found in the expression of mPPAR α protein in liver across a diurnal period, see figure 3.12. It is possible that corticosteroid hormone levels in the C57 Bl/ 6 mice do not exhibit diurnal variation, leading to a lack of diurnal variation in PPAR α expression. The circulating blood levels of corticosteroid hormone in this mouse strain would need to be determined, to validate this hypothesis. It could also be possible that the glucocorticoid regulation of PPAR α in C57 Bl / 6 mice is impaired. Thus any rise and fall in circulating blood corticosteroid hormone levels would not cause any change in PPAR α expression. The dosing of C57 Bl / 6 mice with glucocorticoid hormone, followed by determination of PPAR α expression levels should be done to test this hypothesis. C57 Bl /6 mice have been shown to be highly responsive to peroxisome proliferators (Permadi, H. *et al* 1992 and Budroe, J.D. *et al* 1992), and thus the response to peroxisome proliferators in this strain of mouse will be mediated by steady state levels of expression of PPAR α protein.

The expression of a rat liver transcription factor, D-site binding protein (DBP) follows a circadian rhythm, with levels rising in the afternoon and peaking at 8.00 PM (Wuarin, J. and Schibler, U. 1990). However, the regulation of liver DBP by glucocorticoids differs from glucocorticoid regulation of rPPAR α , by having its expression suppressed by high levels of this hormone. The

diurnal expression of rat PPAR α has only been examined in the Fisher 344 (F344) strain of rat. Dhabhar, F.S *et al* 1993 examined corticosteroid levels in three strains of rat, Sprague-Dawley, Fischer 344 and Lewis rats, and found differences in the diurnal levels of corticosteroid hormone in these strains. F344 rats exhibited the largest evening peak levels of corticosteroid hormone, whereas Lewis rats failed to show the expected evening rise in corticosteroid hormone levels. As some strains of rat do not exhibit diurnal corticosteroid regulation, the diurnal regulation of PPAR α by corticosteroid cannot be a ubiquitous phenomenon.

There are physiological and environmental factors which can influence the circulating blood levels of corticosteroid hormones. Female Wistar rats in the estrous cycle have higher levels of corticosteroid hormone, but do not have an altered diurnal rhythmicity, compared to non estrous female, or male rats (Atkinson, H.C. and Waddell, B.J. 1997). Food restriction in rats (a parameter which could induce stress) causes corticosteroid levels to rise in Han-Wistar rats (Holmes, M.C. *et al* 1997). It is therefore important when interpreting the results of receptor expression across a diurnal period in relation to the physiological function of that receptor, that diet, stress, sex and reproductive state (in females) are considered as influencing factors.

Section 4.1.5 Anti-mPPAR α antibody detects a protein in guinea pig liver

Guinea pigs and humans are considered to be non-responsive to peroxisome proliferators (Cornu, M.C. *et al* 1992, Reo, N.V. *et al* 1994, De La Inglesia, F.A *et al* 1982 and Blumcke, S. *et al* 1983). The lack of peroxisome proliferator responsiveness in both species could be due to a lack of expression of a functional PPAR α gene. In humans, a PPAR α gene has been cloned and shown to be functional in reporter gene assays (Sher, T. *et al* 1993), and that recombinantly expressed hPPAR α can bind to PPREs in *in vitro* assays (Jow, L. and Mukherjee, R. 1995). However, it is not known if guinea pigs have a functional, expressed PPAR α receptor. To examine the possibility that guinea pigs have a PPAR α protein expressed in liver, guinea pig liver

nuclear proteins were isolated and tested to see if an immunoreactive protein corresponding to the size of known PPAR α proteins, was present.

Guinea pig LNP (gpLNP) samples were purified from livers isolated at 6.00 AM, 12 Noon, 6.00 PM and 12.00 Midnight. The expression of a putative guinea pig PPAR α protein is demonstrated in figure 3.14. The anti-mPPAR α antibody detects an immunoreactive protein in gpLNP samples that has the same electrophoretic mobility as purified recombinant mPPAR α and mPPAR α in mLNP samples. The anti-PPAR α antibody used was known to be specific for the α isoform, versus the β and γ isoforms (Savory, R. Ph.D thesis), and so it is likely that the immunoreactive band is an α - variant of PPAR. However, immunoreactivity against an antibody raised against mPPAR α is itself not sufficient proof to demonstrate the presence of a guinea pig PPAR α , as cross reactivity with an unrelated protein is still a possibility.

gpLNP extract from liver tissue isolated at each time point was analysed for variation in protein expression across a diurnal period by SDS-PAGE. Figure 3.10 demonstrates that a protein of approximate molecular weight 50 kDa (marked by arrow A) increases in expression at 6.00 AM and 12.00 Noon. This result indicates that some guinea pig liver nuclear proteins are regulated in a diurnal manner. Anti-mouse PPAR α antibody was then used to probe immunoblots of guinea pig liver nuclear proteins for expression of a the PPAR α protein. Figure 3.13 shows that a protein of approximate molecular weight 52 kDa was detected by anti-mPPAR α antibody. The expression of this 52 kDa protein did not vary in guinea pig nuclear protein extracts isolated from livers taken at 6.00 AM, 12.00 Noon, 6.00 PM and 12.00 Midnight. The results in figure 3.13 and 3.14 strongly suggest that guinea pigs have a PPAR α receptor expressed in the liver. However, in order to prove the existence of a guinea pig PPAR α receptor it was necessary to clone a cDNA corresponding to guinea pig PPAR α . If a cDNA corresponding to guinea pig PPAR α cannot be isolated, it would suggest that the putative gPPAR α detected by western

blotting was an artifact generated by fortuitous cross reactivity of the anti-mPPAR α antibody with a guinea pig protein.

Section 4.2 Cloning of guinea pig PPAR α cDNA

Section 4.2.1 Design of guinea pig PPAR α PCR primers

Human, mouse and xenopus PPAR α protein sequences were aligned and examined for regions of identity between all three PPAR α sequences. Regions of exact identity between an amphibian PPAR α protein, a rodent PPAR α protein and a primate PPAR α protein are likely to be important functionally and therefore likely to be conserved in a putative guinea pig PPAR α protein. A total of 13 regions comprising of a stretch of seven or more amino acids was identified to be identical in all three PPAR α 's. The DNA coding sequence of these regions was then examined to see which were the most conserved at the DNA level. One region in the DNA binding domain was selected, one in the ligand binding domain region and the DNA sequence encoding the stretch of amino acids at the C-terminal end were found to be highly conserved (see figure 3.16). Where there was a difference in the DNA sequence between the PPARs the most common nucleotide was chosen. From the aligned cDNA sequences of human, mouse and xenopus PPAR α 's, consensus PCR primers were designed and used for amplifying putative guinea pig PPAR α cDNAs.

Section 4.2.2 Amplification of guinea pig cDNAs

cDNA pools produced from total and poly A⁺ mRNA template were investigated for the presence of a cDNA encoding a guinea pig PPAR α (gPPAR α) receptor. Primers GPIGP3 and GPIGP4 were expected to amplify a cDNA fragment 1056 bp long if guinea pigs have a PPAR α receptor the same length as other species. Figure 3.18, lanes 1 to 4 shows that a guinea pig cDNA fragment approximately 1 kb long was amplified from cDNAs derived from both total and poly A⁺ RNA. A 436 bp putative gPPAR α cDNA fragment was amplified by PCR using the same C-terminal end primer (GPIGP3) as used for the 1kb product amplification, and a primer

(GPIGP2) designed from a region of amino acid identity in the ligand binding domain (figure 3.17). Analysis of the complete double strand DNA sequence of the 1kb putative gPPAR α cDNA confirmed that a partial gPPAR α cDNA had been cloned. Where double stranded sequence of the 436bp putative gPPAR α cDNA clones was obtained it was found that two of the clones were identical to the 1 kb clone. The clone termed GP4 was a gPPAR α partial cDNA fragment, but was different as it contained a 5 nucleotide insert in the middle of the fragment.

A 5' Rapid Amplification of cDNA Ends system (5'RACE) was used to clone 5' cDNA of gPPAR α . Figure 3.19 shows that several 5' cDNA fragments were amplified by primers GPIGP6 and Universal Amplification Primer. Seven 5' cDNA clones, varying in size from 302 bp to 582 bp were obtained and sequenced. Five of the cDNA clones corresponded to the 5' end of gPPAR α . The remaining two 5' RACE clones showed high sequence identity with the expressed sequence tags, accession numbers MMAA25380 and AA668556 deposited in the geneml databank.

Section 4.3 Sequence analysis of the cloned guinea pig cDNAs

The open reading frame of gPPAR α contains two putative methionine translational start sites separated by 3 amino acids (figure 3.22). To determine which methionine start site is the most probable initiator of translation, the DNA sequence around each Met (ATG) start codon was analysed for similarity to the Kozak consensus translational start sequence (Kozak, M. 1994 and 1995). Met 1 has 4 nucleotides out of 6 conserved and Met 2 has 3 nucleotides out of 6 conserved, therefore Met 1 is considered to be the translational start site. Initiation of translation of the guinea pig mRNA at Met 1 would result in a 467 amino acid protein being produced. The predicted molecular weight of this 467 amino acid gPPAR α was determined to be 52 290 Da.

The gPPAR α predicted protein sequence was compared to known PPAR protein sequences and

was found to have amino acid identity of 88% to human, mouse and rat PPAR α 's. The identity of gPPAR α with rPPAR δ and mPPAR γ was lower, being 71% and 72% respectively. A detailed protein sequence comparison was done between the domains of gPPAR α and domains of other PPAR receptors to verify that the cloned cDNA was a PPAR α isoform. Table 3.1 shows the results of these sequence comparisons.

The DNA binding domain (DBD) of gPPAR α is identical to human and mouse PPAR α DBD. The sequence comparison of the gPPAR α DBD includes the 10 amino acids derived from the consensus primer GPIGP4. Amino acid sequence identity with the DBD of a δ and γ PPAR isoforms was much lower. This evidence proves that the cloned guinea pig cDNA is a member of the PPAR family of steroid hormone nuclear receptors and indicates that it is most likely to be a PPAR α isoform. The DNA binding domain of PPAR receptors contain a feature which make the PPAR family a distinct sub-family from other steroid hormone receptors. PPAR's only have three amino acids in the D-box of the second zinc finger of the DNA binding domain, other steroid hormone receptors have five amino acids in the D-box (Laudet, V. et al 1992 and Motojima, K. 1993). The complete identity of gPPAR α DBD with hPPAR α and mPPAR α DBD's would suggest that the gPPAR α will have the ability to bind to DNA. A change in a single amino within the DNA binding domain can result in a loss of DNA binding activity. This has been shown for the Hepatic Nuclear Factor-4 receptor (Taylor, D.G. *et al* 1996).

Strong evidence to confirm that it is a PPAR α isoform comes from analysis of the ligand binding domain (LBD). The deduced gPPAR protein sequence shows the highest identity (93%) to rat and mouse PPAR α LBDs. rPPAR δ and mPPAR γ show much lower identity, 70% and 66% respectively in this region. This LBD sequence identity evidence firmly suggests the cloned guinea pig cDNA is an α isoform.

The greatest amount of variation in the gPPAR α sequence and the other PPAR α 's occurs in the

A/B domain and the hinge domain. The putative transcriptional activation domain (A/B domain) of the guinea pig PPAR α has a greater identity with hPPAR α than with either mPPAR α or rPPAR α . The non-responsive nature of human and guinea pigs could be due to their PPAR α 's containing a less functional transactivation domain compared to rat and mPPAR α 's *in vivo*.

gPPAR α protein is 1 amino acid shorter than other mammalian PPAR α 's due to a deletion of a lysine (K) residue at position 447. The loss of this amino acid in the ligand binding domain is only observed in the guinea pig. Peroxisome proliferators at physiological pH would have their carboxylate anion, ionized to form a COO⁻ moiety (Lewis, D. and Lake, B. 1993). This COO⁻ moiety could form electrostatic interactions with a positively charged amino group (NH₃⁺) of a lysine residue. It is therefore possible that peroxisome proliferators exhibit a weaker interaction with guinea pig PPAR α and thus are less responsive. Dowell, P. *et al* 1997 modelled the C-terminal end of mPPAR α with the solved crystal structure of human RXR α (Bourguet, W. *et al* 1995). The deletion of K447 in guinea pig PPAR α would lie in helix 11 of the modelled structure. Helix 11 in human RXR α forms part of the ligand dependent transcriptional activation function (AF 2) domain (Bourguet, W. *et al* 1995). If PPAR's have a similar AF2 domain, then a deletion of an amino acid in this domain could have a deleterious effect on its function.

Analysis of the heterodimerisation and DNA binding properties of truncated mutants of mPPAR α by Dowell, P. *et al* 1997, demonstrated that the last 20 C-terminal amino acids of mPPAR α are not necessary for heterodimerisation with RXR α but add stability of the heterodimeric complex when bound to DNA. The deletion of lysine 447 in gPPAR α may result in a less stable heterodimer of gPPAR α / RXR α being formed.

Detailed analysis of the differences in amino acid sequences of the PPAR α 's from responsive and

non-responsive species identified 22 amino acid residues which are conserved between rat and mouse PPAR α but are different in guinea pig and human PPAR α (Figure 3.23). Of these changes 14 are conserved between guinea pig and human PPAR α . The amino acid at position 83 in gPPAR α and hPPAR α is a tyrosine residue, compared to a cysteine residue in rPPAR α and mPPAR α . This change could have implications for the functioning of the PPAR α receptor *in vivo* in guinea pig and humans. The loss of a cysteine residue could result in the loss of an important disulphide bridge, changing the tertiary structure of the receptor. A change in the charge properties of a particular residue may also impact on the functioning of a receptor. Again alterations in tertiary structure are possible, changes in the stability of ligand binding or altered protein-protein interactions could result from a change in the charge property of an amino acid residue. At position 196, the gPPAR α and hPPAR α contains a glutamate residue (negatively charged), compared to a lysine residue (positively charged) in mPPAR α and rPPAR α . At position 211 a positively charged histidine residue in mPPAR α and rPPAR α is changed for a bulky, aromatic tyrosine residue in gPPAR α and hPPAR α , and at position 264 in gPPAR α , a positive arginine residue is present, in hPPAR α a glutamine residue (polar uncharged) is present, but in mPPAR α and rPPAR α a negatively charged glutamate residue is present. These differences between the receptors of non-responsive and responsive species may be important in determining the *in vivo* response to peroxisome proliferators.

The presence of endogenous activators of wild type PPAR α in cell culture causes transcriptional activation of PPARE reporter gene constructs *in vitro*. A mutant mPPAR α cDNA was cloned in which the glutamate 282 residue is changed for a glycine residue, has demonstrated how a loss of a charged residue in a PPAR α receptor can alter its functional properties. This mutant mPPAR α termed PPAR-G does not exhibit peroxisome proliferator independent transcriptional activation of a reporter gene *in vitro* (Muerhoff, A.S *et al* 1992). The PPAR-G mutant may have much lower affinity for endogenous activators, and is therefore unable to

transcriptionally activate reporter gene expression in the absence of peroxisome proliferators.

Recently a mutant human cDNA has been cloned, which contains four different amino acids compared to wild type hPPAR α (Tugwood, J.D. *et al* 1996). In this mutant hPPAR α , termed hPPAR α 6/29 threonine 71 is changed to a methionine, lysine 123 to a methionine, valines 268 and 444 to alanine residues. hPPAR α 6/29 has been shown to bind to PPREs in *in vitro* DNA binding assays, but has been shown to be unactivatable by peroxisome proliferators. Restoration of methionine 123 and alanine 444 in hPPAR α 6/29 to the wild type amino acids restored peroxisome proliferator induced transcriptional activation (Myers, K.A. *et al* 1997). The gPPAR α receptor does not contain any of these described mutations. However, there are still several amino acid differences between gPPAR α and hPPAR α , mPPAR α and rPPAR α which could render the gPPAR α receptor non-responsive to peroxisome proliferators.

Section 4.4 Phylogenetic analysis of mammalian PPAR α genes

The relationship of the PPAR α genes from mouse, rat, guinea pig and human were examined using phylogenetic analysis. The technique used was the maximum likelihood method, a method which is robust enough to include genes evolving at different rates. Felsenstein, J. 1978 demonstrated that the maximum-parsimony method can produce misleading results when genes evolving at different rates are used. Alignment of the mammalian PPAR α protein sequences was done in tandem with xenopus PPAR α , an evolutionary distant PPAR α , and PPAR β and PPAR γ genes as well. In order to examine the relationship between the mammalian PPAR α genes we need to be able to include in the analysis, genes which are related to PPAR α but which are known to have evolved before the divergence of the genes being examined. The inclusion of genes which have evolved before the evolution of the mammalian PPAR α genes adds perspective to the analysis. The PPAR β and PPAR γ genes have been found in the xenopus species, an amphibian species. It can be concluded that these two PPAR genes must have

diverged from the PPAR α gene before the evolutionary separation of amphibians and mammals. PPAR β and PPAR γ genes are therefore ideal as outgroups to root the analysis and to give phylogenetic perspective to the analysis.

Figure 3.24 shows that the guinea pig PPAR α gene is evolving more rapidly, nearly 14 fold faster than either the human, mouse or rat PPAR α genes. The guinea pig hepatic lipoprotein lipase gene has also been shown to have a higher rate of evolution compared to mouse and human hepatic lipoprotein lipase genes (Semenkovich, C.F. *et al* 1989). The phylogenetic tree in figure 3.24 positions the guinea pig PPAR α gene between the human and mouse, rat genes, with a bootstrap probability of ~ 0.93 . There is insufficient resolution in the phylogenetic analysis to place the exact evolutionary position of the guinea pig species in relation to the mouse and rat species. This is due to the number of rodent species analysed being too small a sample and that only a single gene has been examined. But it is interesting to note that $\sim 7\%$ of the remaining phylogenetic PPAR α trees produced excluded the monophyletic relationship of the guinea pig with the mouse and rat order (Myomorph order).

Section 4.4.1 Is the guinea pig a rodent?

If the guinea pig is more closely related genetically to humans than to mouse or rat, it would lend support for the use of the guinea pig as a more appropriate experimental model species for modelling the human response to peroxisome proliferators. Currently there is much debate about the evolution of the guinea pig species and its relationship to other rodents, lagomorphs and primates. Morphological, biochemical and genetic analyses have all been used to address this problem.

Guinea pigs cannot synthesise L-ascorbic acid (Burns, J.J. 1957), have an insulin which shows very low biological activity (Blundell, T.L. and Wood, S.P. 1975) and an alanine:glyoxylate amino transferase with limited substrate specificity (Nogochi, T *et al* 1994), making them

biochemically distinct from other rodent species. Based on biochemical comparisons between rodents Noguchi, T. *et al* 1994 concluded that guinea pigs are distinct from other rodents. Their conclusion contradicts the traditional view of rodent monophyly, based on comparative morphology (Luckett, W.L. and Hartenberger, J.-L. 1985). Several groups have examined the evolutionary relationship of the guinea pig within the rodent order using various molecular evolution analysis methods, but the relationship of the guinea pig species within the myomorph rodent order remains a subject of controversy. Graur, D. *et al* 1991 using maximum parsimony methods concluded that the rodent order was polyphyletic, with the guinea pigs having a separate evolutionary origin to rodents such as rat or mouse. Goto, K. *et al* 1994 and Nakatani, T *et al* 1995 analysed the phylogeny of α -1-Antiproteinase gene from several rodent species and concluded that the guinea pig was more closely related to the rabbit (lagomorph) order, forming a distinct clade. The analyses of α -1-Antiproteinase gene failed to calculate any bootstrap statistical significance to their phylogenetic trees, and admitted to the limited nature of analysing a single gene in order to place the evolutionary position of a species. Bulow, H.E. *et al* 1996 examined the genetic phylogeny of cytochrome P450 11B-hydroxylase gene by maximum parsimony and neighbour joining method. The results from each method were contradictory, with the neighbour-joining method supporting monophyly and the maximum parsimony method supporting polyphyly leading to the conclusion that a definitive branching order could not be established from the data. Work by Cao, Y. *et al* 1994 and 1997, Kuma, K. and Miyata, T. 1994 and Frye, M.S. and Blair-Hedges, S. 1995 have all demonstrated weaknesses in the analysis by Graur, D. *et al* 1991, concluding that the rodent monophyly hypothesis cannot yet be excluded. D'Erchia, A.M. *et al* 1996 examined the phylogeny problem of the guinea pigs by examining mitochondrial gene evolution. They used all three methods, the maximum-parsimony method, the maximum-likelihood and the neighbour joining method and found that the phylogenetic trees produced with the highest bootstrap probability separated the rodents into

polyphyly.

The evolutionary position of the guinea pigs is still unresolved, but from the analysis of the PPAR α genes presented here we know that the speed of evolution of individual genes from the different rodent species can differ dramatically. Further work on the phylogenetic analysis of genes from many rodent species needs to be carried out before we can confidently position the guinea pig species in the evolution of rodents.

Section 4.5 Evidence for alternative splicing of gPPAR α mRNA

The assembled 5' cDNA sequence of gPPAR α , derived from DNA sequence of clones GP11 and GP12 was analysed against the cDNA sequence AJ000222 (a putative gPPAR α) which became available in the geneml DNA sequence database, when this thesis was in preparation. The sequences were identical for 39 nucleotides 5' to the ATG (Met 1) translational start site, whereas DNA sequence 5' to these 39 nucleotides are different. The translated gPPAR α and AJ000222 cDNA sequences are aligned and shown in figure 3.25. The amino acid sequence of gPPAR α in the region marked (A) is derived from double strand DNA sequence of two independently cloned cDNAs that were identical over this stretch, but amino acid sequence N-terminal to region (A) was derived from a single cDNA clone. This sequence is less robust, as it was not possible to eliminate the possibility of PCR amplification artifacts or DNA sequencing artifacts. The difference in the 5' cDNA sequence of the cloned gPPAR α and AJ000222 sequences could be due to differential splicing of gPPAR α mRNA, giving rise to two distinct transcripts.

The viability of the differential splicing theory was investigated by aligning the DNA sequence of exon 3 of mouse PPAR α (x75289) with the 5' gPPAR α cDNA sequence. It was found that the region of N-terminal identity between gPPAR α and AJ000222 sequence exhibited high identity with the 5' end of mouse PPAR α exon 3 (Figure 3.26). The 5' end of the identical N-

terminal amino acid sequence of gPPAR α and AJ000222 aligns with the site of an intron / exon boundary found in mPPAR α mRNA. Therefore the differences between the cloned gPPAR α and AJ000222 sequence is probably due to differential splicing. It is important that the more 5' gPPAR α cDNA cloning is done in order to verify the possibility that guinea pigs have a novel PPAR α subtype.

Preliminary DNA sequence data indicated the presence of a translation stop codon N-terminal to Met 1, so cloning work of the 467 amino acid open reading frame was started. Complete detailed DNA sequence analysis revealed that there was no translation stop codon found in the amino acid sequence upstream of Met 1.

If the 5' DNA sequence beyond region (A) is correct, the identified 467 amino acid open reading frame from Met 1 is extended a further 58 amino acids to another putative methionine translational start site. This would make this receptor a novel PPAR α subtype, possibly with altered functionality. A N-terminal transactivation domain has not been defined for PPAR α receptors, but has for PPAR γ receptors (Werman, A. *et al* 1997). The PPAR γ receptor in mouse and humans is produced as two distinct isoforms, PPAR γ 1 and PPAR γ 2 (Zhu, Y. *et al* 1995 and Elbrecht, A. *et al* 1996), produced from alternative use of promoters within the PPAR γ gene. mPPAR γ 2 has 30 additional N-terminal amino acids to the Met translational start in mPPAR γ 1. The transcriptional activity of PPAR γ 1 and γ 2 N-terminal domains has been characterised, with the activation function of PPAR γ 2 being 6-fold greater than PPAR γ 1 (Werman, A. *et al* 1997). Thus the extra 30 N-terminal amino acids in PPAR γ 2 are involved in the enhanced activation function activity. The amino acid sequence identity between gPPAR α and mPPAR γ N-terminal A/B domains is very low, therefore extrapolation of activation function activity in PPAR α using amino acid sequence comparisons is not possible.

Section 4.5.1 GP4 gPPAR α cDNA clone contains differential splicing

DNA sequence alignment of the 436 bp GP4 gPPAR α cDNA clone with the assembled gPPAR α cDNA sequence revealed the presence of a 5 nucleotide insert in the ligand binding domain region (see figure 3.27). The 5 nucleotide insert causes a frame shift in the open reading frame, leading to a change in the last seven translatable amino acids and a premature stop codon, resulting in the loss of 74 amino acids. The truncation of 74 amino acids in the ligand binding domain would almost certainly affect the binding of peroxisome proliferators and heterodimerisation properties of the receptor. Significant expression of this mutant gPPAR α could explain the non-responsive phenotype observed in guinea pigs.

The GP4 cDNA could arise from alternative splicing of gPPAR α mRNA. The possibility of differential splicing was investigated by comparing the GP4 cDNA sequence with mPPAR α exons 7 and 8 DNA sequence. Figure 3.28 shows that from alignment of gPPAR α cDNA with exons 7 and 8 that the 5 nucleotide insert occurs at the end of mPPAR α exon 7 and beginning of mPPAR α exon 8. It is possible that the donor GT site of the intron between exons 7 and 8 has differentially spliced with another AG acceptor site 4 nucleotides of the correct AG acceptor site. The resultant alternatively spliced mRNA contains intron sequence being left within the normal coding region. Figure 3.28 shows a cartoon of the proposed mechanism of differential splicing that gave rise to the mRNA that was PCR amplified to give clone GP4. Three 1.056 kb gPPAR α and two 436 bp gPPAR α cDNA clones were obtained that did not contain the five nucleotide insert. Therefore it is most probable that the mRNA species from which the GP4 cDNA clone was derived is a rare gPPAR α mRNA species, arising from differential splicing.

Ebihara, K. *et al* 1996 identified and characterised a novel vitamin D receptor (VDR1) in rat which is produced from differential splicing of VDR mRNA. VDR1 is translated from a mRNA

in which intron 8 is retained within the final spliced mRNA species. A premature stop codon causes truncation of the receptor by 86 amino acids at the C-terminal end. VDR1 receptor can bind to vitamin D response elements but is unable to bind ligand. Expression of VDR1 in cell culture demonstrated that this receptor can act in a dominant negative manner over VDR. Expression of VDR1 was found to 1/15th of the expression of VDR in adult rat, therefore it is possible that the VDR1 isoform functions physiologically to negatively modulate vitamin D signalling pathways. Differential splicing of the human glucocorticoid receptor (hGR) mRNA produces two distinct transcripts, which when translated yields two receptors hGR α and hGR β . The hGR α isoform binds glucocorticoids and mediates glucocorticoid signalling, whereas hGR β does not bind glucocorticoid ligand and acts as a dominant negative suppressors of hGR α . The difference between the two proteins occurs at the C-terminal end. The last 50 amino acids in hGR α are changed for 15 different amino acids in hGR β (Bamberger, C.M *et al* 1995, Oakley, R.H. *et al* 1997). These two examples demonstrate the effect of differential splicing for normal receptor functionality. It is interesting to speculate if in guinea pigs a truncated PPAR α receptor is expressed, and if so does this receptor impinge on PPAR α mediated signalling pathways.

Section 4.6 Cloning of full length gPPAR α cDNA

A 1.4 kb gPPAR α cDNA encompassing the coding region from Met 1 was generated by overlapping PCR, and was cloned into a eukaryotic protein expression vector pBK-CMV. The gPPAR α -pBK-CMV construct contains T3 and T7 RNA polymerase promoter sites which can be utilised in *in vitro* coupled transcription / translation reactions. To verify that the cDNA sequence of gPPAR α from Met 1 encoded a full length open reading frame of 467 amino acids, gPPAR α protein was produced from gPPAR α -pBK-CMV in an *in vitro* coupled transcription / translation reaction. [³⁵S]-Methionine labelled gPPAR α was produced in such a reaction and was analysed by SDS-PAGE. Figure 3.32, lane 1 shows that a protein of approximate molecular weight 52 kDa was synthesised, demonstrating that the 1.4kb gPPAR α cDNA encoded a

polypeptide of the same molecular weight as known mammalian PPAR α proteins. After demonstrating that the gPPAR α cDNA encoded a full length polypeptide, experiments to determine if gPPAR α was functional were carried out.

Section 4.7 Functional testing of gPPAR α in a mammalian cell based reporter system

It was reasoned that guinea pigs may not respond to peroxisome proliferators in the same way as rats and mice because guinea pigs did not express a PPAR α receptor or that if a PPAR α was expressed it did not have the capacity to bind and be activated by peroxisome proliferators. The data already presented here shows that guinea pigs have a PPAR α gene expressed and that gPPAR α protein can be detected in guinea pig liver. However a functional characterisation of the cloned gPPAR α needed to be done to either support or reject the hypothesis of a disfunctional PPAR α receptor being the cause of non-responsiveness to peroxisome proliferators. gPPAR α was tested for peroxisome proliferator induced transcriptional activation of gene expression through a PPRE. Demonstration of activation of a PPRE containing reporter construct by gPPAR α and peroxisome proliferators would show that gPPAR α had similar functional capabilities to other mammalian PPAR α 's which have been assayed in a similar manner (Isseman, I. et al 1993, Marcus, S.L. et al 1993 and Mukherjee, R. et al 1994).

A luciferase reporter gene system was used in human embryonic kidney 293 cells (293 cells). This cell line is derived from kidney cells which have been transformed with sheared human adenovirus (Ad5) DNA, and is suitable for transfection studies. 293 cells have been used for functional studies of thyroid hormone receptor (TR), a member of the nuclear steroid hormone receptor superfamily. Bigler, J. and Eisenman, R.N. 1995 analysed novel TR response elements in the presence of exogenously expressed TR. TR signalling through a TR response element was observed in the absence of co-expression of retinoid X receptor (RXR). Van der Leede, B-J. M. *et al* 1993 demonstrated that RXR α is expressed in 293 cells. The levels of RXR α in 293

cells are sufficient for TR signalling of a TR response element containing reporter gene. RXR α is an essential component of PPAR α signalling through a PPRE, and sufficient endogenous levels of RXR would be required for gPPAR α functionality studies. It was concluded that 293 cells would be a suitable host cell line for gPPAR α functionality studies

A tandem repeat of two copies of the rat acyl-CoA oxidase gene PPRE (Osumi, T. *et al* 1991) was inserted into the polylinker of pGL3-Luc vector, producing the construct (ACO-PPRE)₂.pGL3-Luc. Multiple copies of a PPRE have been demonstrated to give a high response when testing peroxisome proliferator induced gene transcription through a PPAR α and PPRE. Gearing, K.L. *et al* 1993 and Marcus, S.L. *et al* 1993 successfully used a reporter gene containing two copies of an ACO-PPRE, and Kliewer, S.A. *et al* 1994 have used and tested a reporter gene containing three copies of an ACO-PPRE.

Section 4.7.1 Induction of luciferase by PPAR α and peroxisome proliferators

Firefly reporter gene expression was determined for cells transfected with PPAR α alone, cells dosed with Wy-14,643 alone, or in cells transfected with PPAR α and dosed with Wy-14,643. Figure 3.33 shows that the presence of both PPAR α receptor and peroxisome proliferator, induced firefly reporter gene expression greater than when either was present alone. Firefly reporter gene expression from (ACO-PPRE)₂.pGL3-Luc in the absence of PPAR α or peroxisome proliferator was the same as reporter gene expression measured for pGL3-Luc vector containing no PPRE in the presence of PPAR α and presence or absence of peroxisome proliferator. These results demonstrate the requirement of the PPRE in (ACO-PPRE)₂.pGL3-Luc for PPAR α and peroxisome proliferator mediated induction of reporter gene expression.

The amount of transfected plasmid containing CMV based promoters was lowered to see if the induction of reporter gene in (ACO-PPRE)₂.pGL3-Luc could be augmented to give a greater response to peroxisome proliferator and PPAR α . Equivalent amounts of hPPAR α -pBK-CMV

vector and pRL-CMV vector from 0 to 0.3 μg were transfected per flask. Figure 3.34 shows that increasing amounts of these two vectors caused a reduction in the amount of normalised firefly reporter gene expressed. The peroxisome proliferator methylclofenapate (MCP) was tested at a final concentration of 50 μM to see if could activate hPPAR α and induce reporter gene expression. No induction over DMSO vehicle control was seen, but substantial peroxisome proliferator independent induction of firefly reporter gene expression was observed.

Section 4.7.2 Guinea pig PPAR α is activated by a peroxisome proliferator

293 cells were transfected with gPPAR α -pBK-CMV plasmid DNA in increasing amounts from 0 μg to 0.1 μg . (ACO-PPRE)2.pGL3-Luc was co-transfected with these amounts of gPPAR α expression vector at 1 μg and 0.1 μg levels per flask. Induction of Firefly reporter gene was assayed in the presence and absence of the peroxisome proliferator Wy-14,643. Figure 3.35 demonstrates that reducing the amount of PPRE containing reporter vector 10-fold, reduces reporter gene expression 10-fold at all levels of gPPAR α expression vector tested. Peroxisome proliferator induced expression of reporter gene does not occur in the absence of exogenous expression of gPPAR α receptor, indicating that 293 cells have very low levels of endogenous PPAR α receptor. Flasks transfected with 0.05 μg of gPPAR α -pBK-CMV plasmid DNA exhibited significant peroxisome proliferator induced expression of reporter gene expression. 100 μM Wy-14,643 induced reporter activity 3.4 fold ($p=0.02$, $df=2$) in flasks transfected with 0.05 μg of gPPAR α -pBK-CMV and 0.1 μg of (ACO-PPRE)2.pGL3-Luc. The degrees of freedom used to determine the statistical significance of the data was low due to the low number of replicate flasks used. Therefore the experimental conditions which showed a 3.4-fold rise in reporter gene activity were repeated using more flasks in order to give a higher degree of statistical accuracy. Figure 3.36 shows the results of the repeated experiment using more culture flasks. 100 μM Wy-14,643 induced (ACO-PPRE)2.pGL3-Luc reporter vector 2.3-fold ($P=0.001$, $df=6$) in the presence of exogenous expression of gPPAR α receptor.

It has been demonstrated that the cloned guinea pig PPAR α receptor can be activated to induce transcription of a gene under the control of a PPRE by a potent peroxisome proliferator. The size of induction of reporter gene was not large, but was statistically significant. A full characterisation of several peroxisome proliferators, at a wide range of concentrations will need to be done for the gPPAR α receptor. This will allow the identification of possible structural differences between gPPAR α and other mammalian PPAR α 's which cause functional differences to be observed.

Both gPPAR α and hPPAR α exhibited substantial peroxisome proliferator independent transcriptional activation of reporter gene activity in the reporter gene system used. Other researchers have observed a similar a phenomenon for mPPAR α and rPPAR α (Muerhoff, A.S. *et al* 1992, Bardot, O. *et al* 1993, Marcus, S.L. *et al* 1993 and Aldridge, T.C. *et al* 1995). Table 5 summarises experimental work which has tested peroxisome proliferator activated transcription of a reporter gene, mediated by a PPAR α receptor and PPRE. The magnitude of the observed inductions by peroxisome proliferator over control drug delivery vehicle are generally low, with inductions less than 2-fold being reported (McNae, F. *et al* 1994). Results by Kliewer, S.A. *et al* 1994 are exceptions to this as they observed very large induction in reporter gene activity by different peroxisome proliferators. The species type of PPAR α receptor used, type of reporter gene construct used, and type of cell line transfected varies considerably. Marcus, S.L 1993 *et al* did compare mPPAR α and rPPAR α in the same cell line, using two types of peroxisome proliferator and two types of PPRE containing reporter gene construct. rPPAR α was shown to be slightly more responsive to peroxisome proliferators than mPPAR α . It is not clear whether this difference in activation observed in an artificial system would make a biological significance *in vivo* to the way each species responds to peroxisome proliferators. Mukherjee, R. *et al* 1994 compared the dose response of clofibric acid, Wy-14,643 and 5,8,11,14-eicosatetraynoic acid (ETYA) activation of transcription mediated by both rPPAR α and hPPAR α in CV-1 cell,

HepG2 cells and H4IIEC3 cells. In CV-1 cells (a monkey Kidney cell line) and HepG2 cells (a human hepatoma cell line) Wy-14,643 was a more potent activator of rPPAR α than hPPAR α . Each PPAR α receptor demonstrated a similar dose response to clofibric acid in HepG2 cells, but in these cells ETYA was a more potent activator of hPPAR α compared to rPPAR α . In H4IIEC3 cells (a rat hepatoma cell line) only rPPAR α exhibited a dose dependent response to Wy14,643. These results show that different PPAR α receptors respond differently to various peroxisome proliferators, depending on the type of cell line used. These differences in responsiveness could be due to differences in the affinities of peroxisome proliferator binding to the PPAR α 's, or different metabolic processing of the peroxisome proliferator, or due to the requirement of cell type specific co-activators. Recent studies by Keller, H. *et al* 1997 have shown that *in vitro* species differences in response to peroxisome proliferators are mediated primarily by the ligand binding domain. The amino acid residues I272 and T279 are crucial in hPPAR α for mediating its higher sensitivity to ETYA, than Wy-14,643, when compared to mPPAR α . In guinea pig PPAR α position 272 is also an isoleucine, but position 279 is a valine, different to that found in both hPPAR α and mPPAR α . It is not possible to tell by sequence identity, whether or not guinea pig PPAR α will exhibit ligand sensitivity more similar to human or mouse PPAR α .

Receptor	Cell line	Reporter Construct	Drug	Fold Induction over vehicle	Reference
mPPAR α	Hepa 1	pACO(-1273/-471).G-CAT	10 μ M Wy14,643 10 μ M Nafenopin 10 μ M Ciprofibrate 10 μ M methylclofenapate	14 11 6 4.5	Issemann, I. <i>et al</i> 1993

Table 4.1 Overview of PPAR α mediated induction of reporter genes.

Receptor	Cell line	Reporter Construct	Drug	Fold Induction over vehicle	Reference
mPPAR α	Cos 1	pHD-PPRE(*3)Luc pACO-PPRE(*2)Luc	100 μ M Wy14,643 500 μ M Ciprofibrate 100 μ M Wy14,643 500 μ M Ciprofibrate	2 < 0.5 2.5 2	Marcus, S.L. <i>et al</i> 1993
mPPAR α	H4IIE C3	pACO(-1273/-470)CAT	10 μ M Wy14,643	<2	McNae, F. <i>et al</i> 1994
mPPAR α	CV-1	pACO-PPRE(*3)-tk-Luc	5 μ M Wy14,643	>10 0	Kliwer, S.A. <i>et al</i> 1994
rPPAR α	Cos 1	pHD-PPRE(*3)Luc pACO-PPRE(*2)Luc	100 μ M Wy14,643 500 μ M Ciprofibrate 100 μ M Wy14,643 500 μ M Ciprofibrate	3.3 4.5 4 2.5	Marcus, S.L. <i>et al</i> 1993
hPPAR α	CV-1	pACO-PPRE(*3)-tk-Luc	1 mM Clofibric Acid	9	Mukherjee, R. <i>et al</i> 1994
hPPAR α	Hepa 1	pACO(-640/-472)-tk-CAT pCYP4A6z-PPRE(*3) -tk-CAT	300 μ M Clofibric Acid 300 μ M Clofibric Acid	4.9 3.7	Pineau, T. <i>et al</i> 1996
xPPAR α	HeLa	pACO-PPRE-tk-luc pHD-PPRE-tk-Luc pCyp4A6z-PPRE-tk-Luc	100 μ M Wy14,643 100 μ M Wy14,643 100 μ M Wy14,643	3 6.4 4.7	Krey, G. <i>et al</i> 1993

Table 4.1 Overview of PPAR α mediated induction of reporter genes.

Section 4.8 Guinea pig PPAR α is expressed in liver tissue

The fact that gPPAR α receptor gene was cloned from cDNA derived from liver tissue mRNA demonstrates that the gPPAR α gene is expressed. PCR is a sensitive technique which can

amplify DNA from very low levels of template DNA. Thus the fact that a guinea pig PPAR α cDNA was amplified does not give any indication as to the extent of expression of the gene. Therefore RNase protection assays, a sensitive technique used for determining the level of gene expression was used to determine the levels of expression of gPPAR α in liver tissue. The expression of mPPAR α gene in mouse liver was also determined, so that a direct comparison of the expression of each gene could be made from a peroxisome proliferator responsive species and non-responsive species. mPPAR α and gPPAR α anti-sense ribo-probes were synthesised, with the mouse probe being twice the length of the guinea pig probe, but each with the same specific activity. Therefore to generate the equivalent signal two guinea pig ribo-probes need to be protected to every one mPPAR α ribo-probe. An excess of each probe was hybridised with liver RNA samples so that all PPAR α mRNA species would anneal to their respective probes. Figure 3.37 (A) demonstrates that mPPAR α is highly expressed in mouse liver, and figure 3.37 (B) shows that guinea pig PPAR α is expressed in guinea pig liver. Each gel was exposed for the same amount of time on hyperfilm and are directly comparable as the probes had the same specific activity. It is clear by comparing panel (A) with panel (B) that the amount of mPPAR α ribo-probe protected is much greater than twice the amount of gPPAR α ribo-probe protected. Therefore mPPAR α gene expression is much greater than gPPAR α gene expression in the liver of each respective species. The species difference in responsiveness to peroxisome proliferators could be due to the differences in expression levels of PPAR α .

The expression of gPPAR α gene was determined in liver tissue isolated at 6.00 AM, 12.00 Noon, 6.00 PM and 12.00 Midnight using an RNase protection assay. Figure 3.38 shows that gPPAR α mRNA expression does not vary greatly across a 24 hour period. These results support the results of gPPAR α protein expression determined by immunoblot analysis shown in figure 3.14. The pattern of expression of the 52kDa protein detected by anti-mPPAR α antibody in guinea pig liver nuclear extracts is the same as the pattern of gPPAR α mRNA expression as

determined by RNase protection analysis.

Section 4.9 Evidence for a functional PPAR α in guinea pig *in vivo*

Further evidence to support that guinea pigs respond to peroxisome proliferators in the same manner as humans has been demonstrated in experiments in which guinea pigs were dosed with two peroxisome proliferator hypolipidaemic drugs Wy-14,643 and methylclofenapate. Both drugs were shown to lower serum triglyceride levels significantly (Bell, A.R. *et al* 1998, in press). It is known that Wy-14,643 and methylclofenapate are selective activators of PPAR α , as opposed to β and γ (Kliewer, S.A. *et al* 1994 and 1997, Forman, B.M. *et al* 1997), and it is therefore likely that the peroxisome proliferator induced hypolipidaemia is mediated through gPPAR α .

Section 4.10 Guinea pigs model the non-responsiveness phenotype in humans

The molecular basis whereby rat and mouse undergo peroxisome proliferation in response to peroxisome proliferators, but humans and guinea pigs do not, is of critical importance to the hazard assessment of peroxisome proliferators to humans. A suitable laboratory model system is required so that the molecular differences between responsive and non-responsive species can be elucidated. Guinea pigs are proposed to model the human response to peroxisome proliferators, but it is not known if guinea pigs have the same molecular characteristics of the mechanism of peroxisome proliferation that has been determined in humans.

It has been demonstrated that the guinea pig has a functional PPAR α which is expressed in the liver. The gPPAR α mediates transcriptional activation through the PPRE of the rat acyl-CoA oxidase gene enhancer. Transcriptional activation of gPPAR α was observed in the absence of exogenous peroxisome proliferator, but addition of the potent peroxisome proliferator led to a significant induction of transcriptional activation. This demonstrates that the guinea pig PPAR α

is capable of responding to peroxisome proliferators. The non-responsive phenotype observed in guinea pigs is not due to an absence of gPPAR α expression, as it was found that gPPAR α is expressed both at RNA and protein levels in guinea pig liver.

The guinea pig models the human response to peroxisome proliferators, both in the observed peroxisome proliferation phenotype and in the peroxisome proliferator induced hypolipidaemic response. The guinea pig has a functional PPAR α gene expressed in the liver, the same as is observed for humans. Therefore the guinea pig offers a model system for understanding peroxisome proliferator induced hypolipidaemia and peroxisome proliferator responsiveness in humans.

Section 4.11 Steroid hormone DNA binding domains

Human Retinoid X Receptor α (hRXR α) DNA binding domain (DBD), amino acids 130F – 223T has been cloned, expressed and purified as a soluble DNA binding protein. Detailed NMR studies have been performed with this protein, elucidating the tertiary structure of hRXR α DBD (Lee, M.S. *et al* 1993 and 1994). Zechel, C. *et al* 1994 and Mader, S. *et al* 1993 cloned and expressed in bacteria the DNA binding domains of Retinoid X Receptor α (135–237), Retinoic Acid Receptor α 1 (83–187) and Thyroid hormone receptor α (46–150). Both Zechel, C. *et al* 1994 and Mader, S. *et al* 1993 demonstrated that these receptor DBD's were soluble in crude bacterial extracts and could bind to DNA in electromobility shift assays. PPAR α DNA binding domain (PPAR α -DBD) is highly similar to other nuclear steroid hormone binding domains. NMR, x-ray crystallographic and DNA binding studies have not been performed on PPAR α DNA binding domain. Structural analysis of PPAR α -DBD should reveal detailed molecular information about the PPAR α receptor, which hopefully can be related to the functioning of this receptor in molecular signalling and control of gene expression. An example of where structural studies by NMR or x-ray crystallography on PPAR α is needed, is to elucidate the function of the D-box of PPAR α receptors. The PPAR D-box in the DBD is two amino acids shorter than the D-boxes found in other types of steroid hormone receptor (Laudet, V. *et al* 1992 and Motojima, K. 1993), and the significance of this has yet to be determined. Thus the cloning and expression of soluble functioning mouse PPAR α -DBD was attempted.

Section 4.11.1 Cloning of mPPAR α -DBD

The DNA binding domain of mPPAR α has only been defined by homology to other steroid hormone receptors. Issemann, I. and Green, S. 1990 defined the DBD starting from amino acid 102 to 166 in mPPAR α . A structural characterisation of mPPAR α has not been done, so the exact boundaries of the DBD in mPPAR α are not known. A region of mPPAR α cDNA encompassing the DNA binding domain, residues 95 G to 198 S was amplified and cloned into

prokaryotic expression vectors. The cloned fragment contains extra residues both N- and C-terminal to the defined mPPAR α -DBD (amino acids 102 to 166). The G at position 95 is mutated to a cysteine residue by the mPPAR α -P1 mismatch primer, so that a Pst I restriction site was engineered in the amplified PCR product.

pRSET A prokaryotic expression vector (Invitrogen) contains a multiple cloning site 3' to a protein leader sequence that contains a tract of six histidine residues (His*6 motif) and an enterokinase protease cleavage site. mPPAR α -DBD DNA was cloned in frame with this leader sequence, producing a mPPAR α -DBD fusion protein expression plasmid. An extra N-terminal 41 amino acids are added to the mPPAR α -DBD protein. The His*6 motif functions as a useful tool for purification of expressed protein, as it forms a metal binding domain in the translated protein that can bind to metal affinity resins. The expressed protein can be purified by one step affinity chromatography on Ni²⁺ containing resins or other metal ion based affinity resins such as Clontech's Talon Metal Affinity Resin. The enterokinase protease cleavage site allows the removal of the N-terminal protein leader sequence by digestion of the expressed protein with enterokinase protease enzyme.

Section 4.11.2 Expression of mPPAR α -DBD in BL21 (DE3)pLysS *E.coli*

Figure 3.41 demonstrates that an induced protein of molecular weight < 20 kDa was expressed in cultures treated with IPTG. Cultures grown without the addition of IPTG did not exhibit any induced protein expression. Cultures of BL21 (DE3)pLys S cells treated with IPTG did not have any low molecular weight proteins induced. Figure 3.42 demonstrates that induced mPPAR α -DBD separated into the insoluble protein fraction.

It has been found that expression of recombinant interferon proteins in *E.coli* cultured at 30 C produces significantly higher yields of soluble protein (Schein, C.H. 1989). Similar results have been obtained for P22 tailspike protein, diphtheria toxin, basic fibroblast growth factor and pro-

subtilisin proteins (Haase-Pettingwell, C.A. and King, J. 1988, Bishai, W.R. *et al* 1987, Squires, C.H. *et al* 1988 and Takagi, H. *et al* 1988). The effect of culturing BL21(DE3)pLys S-pRSET-A-mPPAR α -DBD *E.coli* at 30 C on the solubility of expressed mPPAR α -DBD protein was investigated. Figure 3.43 demonstrates that mPPAR α -DBD protein expression induced at 30 C did not segregate into the insoluble or soluble protein fraction differently than mPPAR α -DBD protein expression induced at 37 C. Induction at 30 C did not increase the solubility of overexpressed mPPAR α -DBD protein. Low level expression of soluble mPPAR α -DBD in BL21(DE3)pLys S-pRSET-A-mPPAR α -DBD *E.coli* induced at 37 C was not detected by SDS-PAGE, using Coomassie Blue staining. It was possible that low levels of soluble mPPAR α -DBD were produced, therefore the soluble protein fraction was subjected to metal affinity chromatography to purify any soluble His*6 tagged mPPAR α -DBD present. Figure 3.44 shows that no proteins from the soluble protein fraction bound to Talon Metal Affinity Resin.

Section 4.11.3 Purification of denatured mPPAR α -DBD

mPPAR α -DBD present in the insoluble protein fraction was purified by denaturing metal affinity chromatography, using the denaturing agent 6M guanidine and Talon Metal Affinity Resin. Proteins specifically eluted from the Talon resin were dialysed against a low salt buffer, containing Zn²⁺ ions, to remove the denaturing agent, and potentially refold proteins into a functional conformation. The dialysed eluted proteins were analysed by SDS-PAGE. Figure 3.45 (A) and (B) shows highly purified mPPAR α -DBD protein was obtained after dialysis of eluted denatured proteins. The total amount of renatured mPPAR α -DBD purified was 848 μ g. A sample of His*6 tagged mPPAR α -DBD protein was treated with enterokinase protease enzyme to remove the His*6 tag. Progression of the cleavage was determined by sampling aliquots of the reaction at hourly intervals and analysing these samples by SDS-PAGE. Figure 3.46 demonstrates that cleavage of the His*6 tag from a significant proportion of mPPAR α -DBD occurred within 1 hour. A proportion of the purified mPPAR α -DBD remained resistant to protease digestion

after six hours. The protein band marked un-tagged mPPAR α -DBD diminishes in intensity after 1 hour, indicating that degradation of untagged mPPAR α -DBD protein by enterokinase increased with time.

Section 4.11.4 Electromobility shift assays of mPPAR α -DBD

The binding of tagged and untagged mPPAR α -DBD to a PPRE was tested by electromobility shift assays. A suitable DNA substrate had to be chosen so that binding of a monomer or dimer could be accommodated. It has been shown for receptors such as Rev-ErbA α , NGFI-B and ROR, which bind to DNA response elements as a monomer that DNA sequence immediately 5' to the core binding site is important for receptor binding (Harding, H.P. and Lazar, M.A. 1993, Wilson, T.E. *et al* 1993 and Giguere, V. *et al* 1994). Palmer, C.N.A *et al* 1995 demonstrated that the seven nucleotides immediately 5' to the core PPRE in the Cyp4A6z element are important for binding of PPAR α /RXR α heterodimers. A PPRE containing a consensus 5' flanking region designed from genes containing PPREs and the Cyp4A6z element core PPRE was shown to be more effective at binding PPAR α /RXR α heterodimers than native PPREs (Palmer, C.N.A. *et al* 1995). This consensus Cyp4A6z PPRE was chosen as a substrate for EMSA assays of mPPAR α -DBD as it contains extended 5' flanking sequence. Figures 3.47 and 3.48 show that neither tagged or untagged mPPAR α -DBD bind to the con-4A6z PPRE DNA, even in the absence of non-specific competitor DNA. The lack of even non-specific DNA binding by purified mPPAR α -DBD protein suggests that the purified protein did not refold into a conformation that could bind DNA. The removal of the His*6 tag did alter the conformation of mPPAR α -DBD into a protein which could bind DNA.

Section 4.11.5 Recovery of functional DNA binding domain proteins

Reducing agents such as β -mercaptoethanol or dithiothreitol were not added at the solubilisation stage due to incompatibilities with the metal affinity resins. Therefore if the mPPAR α -DBD had formed insoluble aggregates due to disulphide bond formation between mPPAR α -DBD

monomers, or formed aggregates of incorrectly folded monomers caused by incorrect intra-molecular disulphide bridges, the solubilisation process would not break these disulphide bonds. The denatured mPPAR α -DBD was refolded by removal of the 6M Guanidinium HCl by dialysis into a Hepes-Zinc based buffer containing no denaturant, or reducing agents. The cysteine residues in the zinc finger regions do not form disulphide bridges in the native protein, but are tetrahedrally co-ordinated to a Zn²⁺ ion (Freedman, L.P and Luisi, B.F. 1993). If these cysteine residues have formed disulphide bridges, they will need to be broken first by reduction, then allowed to coordinately bind to a zinc ion. It is a possibility that the extra cysteine engineered in by the mismatch primer was causing incorrect disulphide bridge formation during expression of the protein. The purification process used to isolate, denature and renature mPPAR α -DBD contained no reducing agents, and therefore would not be able break erroneous disulphide bond formation. Denaturation of the insoluble mPPAR α -DBD in the presence of reducing agents, then dialysis into a zinc containing buffer (devoid of denaturant and reducing agent) should be attempted to refold mPPAR α -DBD, before purification this particular His⁶ tagged mPPAR α -DBD on a metal affinity resin. The production of soluble mPPAR α -DBD during the initial culturing or a successful renaturation strategy will be important for obtaining a functional DNA binding protein.

Section 4.11.6 Cloning and expression of thioredoxin-mPPAR α -DBD fusion protein

To increase the solubility of mPPAR α -DBD protein expressed in *E.coli* it was decided to make a fusion protein of *E.coli* thioredoxin (*trxA*) and mPPAR α -DBD using the commercial expression vector pThioHis (Invitrogen). Thioredoxin is a small (11.7 kDa) highly soluble protein which when N-terminally attached to a heterologous protein confers increased solubility to the heterologous protein when over expressed in *E.coli* (LaVallie, E.R. *et al* 1993). Proteins can be isolated from inclusion bodies by denaturation, but the resolubilised proteins then require to be correctly refolded, often a very difficult process to achieve (Schein, C.H 1989). The

expression of eukaryotic proteins fused to thioredoxin has been found to circumvent the problem of inclusion body formation (LaVallie, E.R. 1993). Human interferon gamma receptor α chain, T cell receptor chains α and β , and human fatty acid synthase, three very different eukaryotic proteins have all been expressed as highly soluble thioredoxin fusion proteins (Williams, G. *et al* 1995, Schodin, B.A. *et al* 1996 and Jayakumar, A. *et al* 1996).

DNA was amplified from mPPAR α cDNA by PCR, corresponding to the DNA binding domain of mPPAR α (95G-198S), and was cloned into the Pst I site of pThioHis A vector. The 5' Pst I site in the DBD PCR fragment was generated by a mismatch primer and resulted in 95 G being mutated to 95 C. A translational stop codon was also engineered into the 3' mPPAR α -DBD PCR primer. Putative pThioHis.A-mPPAR α -DBD clones were screened for the orientation of the DBD insert by digestion with Bgl II restriction enzyme, see figure 3.49 (B). Clone 5 was chosen for thioredoxin-mPPAR α -DBD fusion protein expression studies.

Section 4.11.7 Prokaryotic expression of thioredoxin-mPPAR α -DBD fusion protein

Large scale cultures (500 ml) of BL21(De3)pLysS-pThioHis.A-mPPAR α -DBD were grown until the growth of cells had reached an $OD_{600nm} = 0.6$. IPTG was added to the culture medium to induce expression of thioredoxin-mPPAR α fusion protein. Cells were pelleted and sonicated in 1 \times Talon Bind buffer. Soluble and insoluble proteins were separated by ultracentrifugation, and then analysed by SDS-PAGE. Figure 3.50 shows that an induced protein of approximate molecular weight 30 kDa was present in abundance in the insoluble protein fraction. The presence of fusion protein cannot be seen in the soluble protein fraction, but this does not excluded the possibility of low levels of fusion protein being present in the soluble fraction. The presence of thioredoxin-mPPAR α -DBD in the soluble protein fraction was tested by binding soluble protein extracts to two types of metal affinity resin. Invitrogens nickel charged sepharose resin (ProBond Resin) and Clontech's Talon Metal Affinity resin were used. Figure 3.51 shows

SDS-PAGE analysis of uninduced and induced total cell extracts, insoluble and soluble protein fractions, and unbound and eluted soluble proteins from the ProBond resin. Bound proteins were eluted from the resin in buffers containing increasing amounts of imidazole. The gel demonstrates that most soluble proteins bound to the ProBond resin in a non-specific manner, and that this resin was unable to specifically purify any thioredoxin-mPPAR α -DBD fusion protein. Figure 3.52 demonstrates that Talon metal affinity resin did not bind any soluble thioredoxin-mPPAR α -DBD fusion protein. The lane marked NB for non-bound soluble proteins shows that Talon metal affinity resin does not bind soluble proteins non-specifically to the same extent as ProBond Resin. The results of the experiments shown in figure 3.51 and 3.52 demonstrate that the induced thioredoxin-mPPAR α -DBD protein exclusively segregated into the insoluble protein fraction. The fusion of thioredoxin to the mPPAR α -DBD did not increase its solubility, when over expressed in *E.coli*.

The insolubility of the thioredoxin-mPPAR α -DBD fusion protein could have been caused by the 95G to 95 C mutation. This cysteine residue is not native to mPPAR α and could be causing erroneous disulphide bridge formation, leading to aggregation of the expressed protein. Creating a similar mPPAR α -DBD fusion protein with the 95 C residue changed to a small unreactive amino acid should be done in order to verify if it is the 95 C residue that is causing the solubility problems. Other future experiments could attempt to produce soluble fusion protein by culturing the IPTG induced *E.coli* cultures at a temperature lower than 30 C, possibly at 25 C. Another strategy which could be investigated in order to produce soluble His*6 tagged mPPAR α -DBD or thioredoxin-mPPAR α -DBD is that of adding sorbitol and glycyl betaine to the *E.coli* growth medium. Blackwell, J.R. and Horgan, R 1991 demonstrated that recombinant expression of Dimethylallylpyrophosphate:5'-AMP transferase in cultures of *E.coli* containing sorbitol and glycyl betaine in the culture medium produced a soluble active protein instead of an insoluble protein. It is believed that the *E.coli* cytoplasm took up the sorbitol and glycyl betaine

osmolytes such that they generated a major proportion of the cytoplasmic osmotic balance. These two substances can minimise protein-protein contacts, increasing the solubility of the expressed protein.

Section 4.11.8 *In vitro* synthesis of mPPAR α -DBD

His*6 tagged mPPAR α -DBD protein was produced using an *in vitro* transcription / translation reaction. This reaction contained reticulocyte lysate extracts which contain Heat shock proteins. Heat shock proteins can aid the folding of nascent polypeptides in their correct tertiary structure. Evidence to show that Heat shock proteins are required for the folding of transcription factors such as the glucocorticoid receptor came from comparing the production of glucocorticoid receptor in wheat germ extracts that lack heat shock proteins and in reticulocyte lysate extracts which do contain Heat shock proteins. Glucocorticoid receptor translated in wheat germ extracts could not bind glucocorticoid hormone, whereas receptor produced in reticulocyte lysate extract did show high affinity hormone binding (Dalman, F.*et al* 1989). It was therefore hypothesised that mPPAR α -DBD produced using reticulocyte lysate extracts would produce soluble correctly folded protein. Figure 3.53 shows SDS-PAGE analysis of His*6 tagged mPPAR α , mPPAR α and RXR α proteins produced by *in vitro* transcription translation reactions using reticulocyte lysate extracts.

The reaction extracts containing the *in vitro* translated receptors were assayed for DNA binding in electromobility shift assays. Figure 3.54 shows that mPPAR α -DBD, mPPAR α , mRXR α or combinations of these receptors did not bind to con4A6z PPRE probes in an electromobility shift assay. Independent batches of *in vitro* translated receptors, including human PPAR α , guinea pig PPAR α as well as mPPAR α , mRXR α and mPPAR α -DBD were assayed for binding to wild type and mutant rat acyl-CoA oxidase PPRE as well (data not shown). No specific DNA binding was found for any of the receptors produced by *in vitro* transcription / translation reactions. The

same assay conditions that were used to show specific binding of liver nuclear protein extracts were also used for *in vitro* translated receptors. Thus as no receptor binding was observed it is not possible to conclude if the mPPAR α -DBD protein produced by *in vitro* transcription translation reactions was correctly folded. The reason for the lack of *in vitro* translated receptor binding in the electromobility shift assays was unable to be determined.

Chapter 5 References

Aldridge, T.C., Tugwood, J.D. and Green, S. (1995) Identification and characterisation of DNA elements implicated in the regulation of the CYP4A1 transcription. *Biochemical Journal*, **306**:473-479.

Alegret, M., Cerqueda, E., Ferrando, R., Vazquez, M., Sanchez, R.M., Adzet, T., Merlos, M. and Laguna, J.C. (1995) Selective modification of rat hepatic microsomal fatty acid chain elongation and desaturation by fibrates: relationship with peroxisomal proliferation. *British Journal of Pharmacology*, **114**:1351-1358.

Amri, E.-Z., Bonino, F., Aihaud, G., Abumrad, N.A. and Grimaldi, P.A. (1995) Cloning of a protein that mediates transcriptional effects of fatty acids in preadipocytes. *Journal of Biological Chemistry* **270**,5:2367-2371.

Aperlo, C., Pognonec, P., Saladin, R., Auwerx, J. and Boulukos, K.E. (1995) cDNA cloning and characterization of the transcriptional activities of the hamster peroxisome proliferator-activated receptor haPPAR γ . *Gene* **162**:297-302.

Argos, P. (1985) Evidence for a repeating domain in type-I restriction enzymes. *The Embo Journal*, **4**:1351-1355.

Ashby, J., Brady, A., Elcombe, C.R., Elliott, B.M., Ishmael, J., Odum, J., Tugwood, J. and Purchase, I.F.H. (1994) Mechanistically based human hazard assessment of peroxisome proliferator induced hepatocarcinogenesis. *Human and Experimental Toxicology*, **13**(suppl.2):S19-S33.

Atkinson, H.C. and Waddell, B.J. (1997) Circadian variation in basal plasma corticosterone and adrenocorticotropin in the rat: sexual dimorphism and changes across the estrous cycle. *Endocrinology*, **138**, 9:3842–3848.

Baes, M., Castelein, H., Desmet, L. and Declercq, P.E. (1995) Agonism of COUP-TF and PPAR α / RXR α on the activation of the malic enzyme gene promoter: modulation by 9-*cis* RA. *Biochemical and Biophysical Research Communications*, **215**, 1:338–345.

Bamberger, C.M., Bamberger, A-M., de Castro, M. and Chrousos, G.P. (1995) Glucocorticoid receptor b, a potential endogenous inhibitor of glucocorticoid action in humans. *The Journal of Clinical Investigation*, **95**:2435–2441.

Bardot, O., Aldridge, T.C., Latruffe, N. and Green, S. (1993) PPAR-RXR heterodimer activates a peroxisome proliferator response element upstream of the bifunctional enzyme gene. *Biochemical and Biophysical Research Communications*, **192**, 1:37–45.

Baudhuin, P., Beaufay, H. and De Duve, C. (1965) *Journal of Cell Biology*, **26**:219–43.

Baumgart, E., Volkl, A., Pill, J. and Fahimi, H.D. (1990) Proliferation of peroxisomes without simultaneous induction of the peroxisomal fatty acid β -oxidation. *FEBS Letters*, **264**, 1:5–9.

Beck, F., Plummer, S., Senior, P.V., Byrne, S., Green, S. and Brammer, W.J. (1992) The ontogeny of peroxisome proliferator activated receptor gene expression in mouse and rat. *Proceedings of the royal society of london series B-Biological Sciences*, **247**,1319:83–87.

Bell, A.R., Saovory, R., Horley, N.J., Choudhury, A.I., Dickens, M., Gray, T.J.B., Salter, A.M. and Bell, D.R. (1998) Molecular basis of non-responsiveness to peroxisome proliferators: the guinea pig PPAR α is functional and mediates peroxisome proliferator-induced hypolipidaemia. *Biochemical Journal*, in press.

Bell, D.R., Bars, R.G., Gibson, G.G. and Elcombe, C.R. (1991) Localization and differential induction of cytochrome P450IVA and acyl-CoA oxidase in rat liver. *Biochemistry Journal*, **275**:247-252.

Bell, D.R., Plant, N.J., Rider, C.G., Na, L., Brown, S., Ateitalla, I., Acharya, S.K., Davies, M.H., Elias, E., Jenkins, N.A., Gilbert, D.J., Copeland, N.G. and Elcombe, C.R. (1993) Species specific induction of cytochrome P450 4A RNAs: PCR cloning of partial guinea-pig, human and mouse CYP4A cDNAs. *Biochemistry Journal*, **294**:173-180.

Bently, P., Calder, I., Elcombe, C., Grasso, P. Wiegand, H.G. and Stringer, D.A. (1993) Hepatic peroxisome proliferation in rodents and its significance for humans. *Food and Chemical Toxicology* , **31**:857-907.

Bhat, M.K., Ashizawa, K. and Cheng, S-Y. (1994) Phosphorylation enhances target sequence dependent dimerisation of thyroid hormone receptor with retinoid X receptor. *Proceedings of the National Academy of Science USA*, **91**:7927-7931.

Bigler, J. and Eisenmann, R.N. (1995) Novel location and function of a thyroid hormone response element. *The EMBO Journal*, **14**, 22:5710-5723.

Bingfang, H., Kosovsky, M.J. and Siddiqui, A. (1995) Retinoid X Receptor a transactivates the hepatitis B virus enhancer 1 element by forming a heterodimeric complex with the peroxisome proliferator-activated receptor. *Journal of Virology*, **69**, 1:547-551.

Bishai, W.R., Rappuoli, R. and Murphy, J.R. (1987) High level expression of a proteolytically sensitive diphtheria toxin fragment in *Escherichia coli*. *Journal of Bacteriology*, **169**:5140-5151.

Blackwell, J.R. and Horgan, R. (1991) A novel strategy for production of a highly expressed recombinant protein in an active form. *FEBS Letters*, **1,2,3**:10-12.

Blaauboer, B.J., Van Holsteijn, C.W.M., Bleumink, R., Mennes, W.C., Van Pelt, F.N.A.M., Yap, S.H., Van Pelt, J.F., Van Iersel, A.A.J., Timmerman, A. and Schmid, B.P. (1990) The effect of beclobric acid and clofibrac acid on peroxisomal β -oxidation and peroxisomal proliferation in primary cultures of rat, monkey and human hepatocytes. *Biochemical Pharmacology*, **40**,3:521-528.

Blumberg, B., Mangelsdorf, D.J., Dyck, J.A., Bittner, D.A., Evans, R.M., De Robertis, E.M. (1992) Multiple retinoid responsive receptors in a single cell: families of retinoid X receptors and retinoic acid receptors in the *Xenopus* egg. *Proceedings of the National Academy of Science USA*, **89**:2321-2325.

Blumcke, S., Schwartzkopf, W., Lobeck, H., Edmondson, N.A., Prentice, D.E. and Blane, G.F. (1983) Influence of fenofibrate on cellular and subcellular liver structure in hyperlipidaemic patients. *Atherosclerosis*, **46**:105-116.

Bocos, C., Gottlicher, M., Gearing, K., Banner, C., Enmark, E., Teboul, M., Crickmore, A. and Gustafsson, J.-A. (1995) Fatty acid activation of peroxisome proliferator-activated receptor (PPAR). *Journal of Steroid Biochemistry and Molecular Biology* **53**,1-6:467-473.

Bogazzi, F., Hudson, L.D. and Nikodem, V.M. (1994) A novel heterodimerisation partner for thyroid hormone receptor. *The Journal of Biological Chemistry*, **269**, 16:11683-11686.

Bourguet, W., Ruff, M., Chambon, P., Gronemeyer, H. and Moras, D. (1995) Crystal structure of the ligand binding domain of the human nuclear receptor RXR α . *Nature*, **375**:377-382.

Braissant, O., Foufelle, F., Scotto, C., Dauca, M. and Wahli, W. (1996) Differential expression of peroxisome proliferator activated receptors (PPARs): Tissue distribution of PPAR- α , - β , - γ in the adult rat. *Endocrinology*, **137**,1:354-366.

Budroe, J.D., Umemura, T., Angeloff, K. and Williams, G.M. (1992) Dose response relationships of hepatic acyl-CoA oxidase and catalase activity and liver mitogenesis induced by the peroxisome proliferator ciprofibrate in C57BL/6N and BALB/c mice. *Toxicology and Applied Pharmacology*, **113**:192-198.

Bulow, H.E., Mobius, K., Bahr, V. and Bernhardt, R. (1996) Molecular cloning and functional expression of the cytochrome P450 11 β -hydroxylase of the guinea pig. *Biochemical and Biophysical Research Communications*, **221**:304-312.

Butterworth, B.E., Smith-Oliver, T., Earle, L., Loury, D.J., White, R.D., Doolittle, D.J., Working, P.K., Cattely, R.C., Jirtle, R., Michalopoulos, G. and Strom, S. (1989) Use of primary cultures of human hepatocytes in toxicology studies. *Cancer research*, **49**:1075-1084.

Camp, H.S. and Tafuri, S.R. (1997) Regulation of peroxisome proliferator activated receptor γ activity by mitogen-activated protein kinase. *The Journal of Biological Chemistry*, **272**, 16:10811-10816.

Cao, Y., Adachi, J., Yano, T. and Hasegawa, M. (1994) Phylogenetic place of guinea pigs: no support of the rodent-polyphyly hypothesis from maximum-likelihood analyses of multiple protein sequences. *Molecular Biology and Evolution*, **11**(4):593-604.

Cao, Y., Okada, N. and Hasegawa, M. (1997) Phylogenetic position of the guinea pigs revisited. *Molecular Biology and Evolution*, **14**(4):461-464.

Castelein, H., Declercq, P.E. and Baes, M. (1997) DNA binding preferences of PPAR α / RXR α heterodimers. *Biochemical and Biophysical Research Communications*, **233**:91-95.

Castelein, H., Gulick, T., Declercq, P.E., Mannaerts, G.P., Moore, D.D. and Baes, M.I. (1994) The peroxisome proliferator activated receptor regulates malic enzyme gene expression. The Journal of Biological Chemistry, **269**,43:26754–26758.

Cathala, G., Savouret, F., Mendez, B., West, B.D., Karin, M., Martial, J.A. and Baxter, J.D. (1983) A method for isolation of intact translationally active ribonucleic acid. DNA, **2**, 4:329–335.

Cattley, R.C. and Glover, S.E. (1993) Elevated 8-hydroxydeoxyguanosine in hepatic DNA of rats following exposure to peroxisome proliferators : relationship to carcinogens and nuclear localisation. Carcinogenesis, **14**:2495–2499.

Cavaillès, V., Dauvois, S., L’Horset, F., Lopez, G., Hoare, S., Kushner, P.J. and Parker, M.G. (1995) Nuclear factor RIP40 modulates transcriptional activation by the estrogen receptor. The EMBO Journal, **14**, 15:3741–3751.

Chance, D.,S., Wu, S-M., and McIntosh, M.K. (1995) Inverse relationship between peroxisomal and mitochondrial β -oxidation in HepG2 cells treated with dehydroepiandrosterone and clofibric acid. Proceedings of the Society for Experimental Biology and Medecine, **208**:378–384.

Chen, F., Law, S.W. and O’Malley, B.W. (1993) Identification of two mPPAR related receptors and evidence for the existence of five subfamily members. Biochemical and Biophysical Research Communications **196**, 2: 671–677.

Chen, H., Huang, C-Y., Wilson, M.W., Lay, L.T., Robertson, L.W., Chow, C.K. and Glauert, H. (1994) Effect of the peroxisome proliferators ciprofibrate and perfluorodecanoic acid on hepatic cell proliferation and toxicity in sprague-dawley rats. Carcinogenesis, **15**, 12:2847–2850.

Chrousos, G.P., Detera-Wadleigh, S.D. and Karl, M. (1993) Syndromes of Glucocorticoid resistance. *Annals of International Medicine*, **119**:1113-1124.

Chu, R., Lin, Y., Rao, S. and Reddy, J.K. (1995) Cooperative formation of higher order peroxisome proliferator activated receptor and retinoid X receptor complexes on the peroxisome proliferator responsive element of the rat hydratase-dehydrogenase gene. *The Journal of Biological Chemistry*, **270**,50:29636-29639.

Ciriolo, M.R., Mavelli, I., Rotilio, G., Borzatta, V., Cristofari, M. and Stanzani, L. (1982) Decreased superoxide dismutase and glutathione peroxidase in liver of rats treated with hypolipidaemic drugs. *FEBS Letters*, **144**:264-268.

Clayson, D.B., Mehta, R. and Iverson, F. (1994) Oxidative DNA damage- The effects of certain genotoxic and operationally non-genotoxic carcinogens. *Mutation Research*, **317**:25-42.

Close, I., Shackleton, G., Goldfarb, P.S., and Gibson, G.G. (1992) Influence of single and concurrent clofibrate and phenobarbital administration on cytochrome P450-dependent mixed function oxidase activities and peroxisome proliferation in male rat liver. *Journal of Biochemical Toxicology*, **7**,3 :193-198.

Cohen, A.J. and Crasso, P. (1981) Review of hepatic response to hypolipidaemic drugs in rodents and its toxicological significance to man. *Food and Cosmetic Toxicology*, **19**:585-605.

Conaway, R.C. and Conaway, J.W. (1993) General initiation factors for RNA polymerase II. *Annual review of Biochemistry*, **62**:161-190.

Conway, J.G., Tomaszewski, K.E., Olson, M.J., Cattely, R.C., Marsman, D.S. and Popp, J.A. (1989) Relationship of oxidative damage to the hepatocarcinogenicity of peroxisome proliferators di(2-ethylhexyl)phthalate and Wy-14,643. *Carcinogenesis*, **10**:513-519.

Cornu, M.C., Lhuguenot, J.C., Brady, A.M., Moore, R. and Elcombe, C.R. (1992) Identification of the proximate peroxisome proliferators derived from di(2-ethylhexyl)adipate and species differences in response. *Biochemical Pharmacology*, **43**, 10:2129-2134.

Cornu-Chagnon, M.-C., Dupont, H., and Edgar, A. (1995) Fenofibrate : Metabolism and species differences for peroxisome proliferation in cultured hepatocytes. *Fundamental and Applied Toxicology*, **26**:63-74.

Cruciani, V., Rast, C., Durand, M.-J., Nguyen-Ba, G. and Vasseur, P. (1997) Comparative effects of clofibrate and methylclofenapate on morphological transformation and intercellular communication of syrian hamster embryo cells. *Carcinogenesis*, **18**, 4:701-706.

Dalman, F., Bresnick, E., Patel, P., Perdew, G., Watson, S. and Pratt, W. (1989) Direct evidence that the glucocorticoid receptor binds Hsp90 at or near the termination of receptor translation. *Journal of Biological Chemistry*, **264**, 33:19815-19821.

De Duve, C. and Baudhuin, P. (1966) *Physiology Review*, **46**:323-57.

De La Inglesia, F.A., Lewis, J.E., Buchanan, R.A., Marcus, E.L. and McMahon, G. (1982) Light and electron microscopy of liver in hyperlipoproteinemic patients under long term gemfibrozil treatment. *Atherosclerosis*, **43**:19-37.

D'Erchia, A.M., Gissi, C., Pesole, G., Saccone, C. and Arnason, U. (1996) The guinea pig is not a rodent. *Nature*, **381**:597-600.

DiRenzo, J., Soderstrom, M., Kurukawa, R., Ogliastro, M.-H., Ricote, M., Ingre, S., Horlein, A., Rosenfeld, M.G. and Glass, C.K. (1997) Peroxisome proliferator-activated receptors and retinoic acid receptors differentially control the interactions of retinoid X receptor heterodimers with ligands, coactivators, and corepressors. *Molecular and Cellular Biology*, **17**, 4:2166-2176.

Dirven, H.A.A.M., Van Den Broek, P.H.H., Peeters, M.C.E., Peters, J.G.P., Mennes, W.C., Blaauboer, B.J., Noordhoek, J. and Jongeneelen, F.J. (1993) Effects of the peroxisome proliferator mono(2-ethylhexyl)phthalate in primary hepatocyte cultures derived from rat, guinea pig, rabbit, and monkey. *Biochemical Pharmacology*, **45**,12:2425–2434.

Dhabhar, F.S., McEwen, B.S. and Spencer, R.L. (1993) Stress response, adrenal steroid receptor levels and corticosteroid-binding globulin levels- a comparison between Sprague-Dawley, Fischer 344 and Lewis rats. *Brain Research*, 616:89–98.

Dowell, P., Peterson, V.J., Zabriskie, M., and Leid, M. (1997) Ligand-induced Peroxisome Proliferator-Activated Receptor a conformational change. *Journal of Biological Chemistry*, **272**,3:2013–2020.

Duclos, S., Bride, J., Ramirez, L.C. and Bournot, P. (1997) Peroxisome proliferation and β -oxidation in fao and MH₁C₁ rat hepatoma cells, HepG2 human hepatoblastoma cells and cultured human hepatocytes:effect of ciprofibrate. *European Journal of Cell Biology*, **72**:314–323.

Ebihara, K., Masuhiro, Y., Kitamoto, T., Suzawa, M., Uematsu, Y., Yoshizawa, T., Ono, T., Harada, H., Matsuda, K., Hasegawa, T., Masushige, S. and Kato, S. (1996) Intron retention generates a novel isoform of the murine vitamin D receptor that acts in a dominant negative way on the vitamin D signaling pathway. *Molecular and Cellular Biology*, **16**, 7:3393–3400.

Edlund, T., Walker, M.D., Barr, P.J. and Rutter, W.J. (1985) Cell-specific expression of the rat insulin gene:evidence for role of two distinct 5' flanking elements. *Science* **230**:912–916.

Elbrecht, A., Chen, Y., Cullinan, C.A., Hayes, N., Leibowitz, M.D., Moller, D.E. and Berger, J. (1996) Molecular cloning, expression and characterization of human peroxisome proliferator activated receptors $\gamma 1$ and $\gamma 2$. *Biochemical and Biophysical Research Communications* **224**: 431-437.

Elcombe, C.R. and Mitchell, A.M. (1986) Peroxisome proliferation due to di(2-ethylhexyl)phthalate (DEHP):species differences and possible mechanisms. *Environmental health perspectives*, **70**:211-219.

Elcombe, C.R. (1985) Species differences in carcinogenicity and peroxisome proliferation due to trichloroethylene: a biochemical human hazard assessment. *Archives of Toxicology*, suppl. **8**:6-17.

Elholm, M., Bjerking, G., Knudsen, J., Kristiansen, K and Mandrup, S. (1996) Regulatory elements in the promoter region of the rat gene encoding the acyl-CoA-binding protein. *Gene*, **173**:233-238.

Elliott, B.M. and Elcombe, C.R. (1987) Lack of DNA damage or lipid peroxidation measured in vivo in the rat following treatment with peroxisome proliferators. *Carcinogenesis*, **8**:1213-1218.

Encio, I.J. and Detera-Wadleigh, S.D. (1991) The genomic structure of the human glucocorticoid receptor. *The Journal of Biological Chemistry*, **266**:7182-7188.

Expandiar, P., Thomas, V.A., Glauert, H.P., O'Brien, M., Noonan, D. and Robertson, L.W. (1995) The herbicide dicamba (2-methoxy-3,6-dichlorobenzoic acid) is a peroxisome proliferator in rats. *Fundamental and Applied Toxicology*, **26**:85-90.

Felgner, P.L., Gadek, T.R., Holm, M., Roman, R., Chan, H.W., Wenz, M., Northrop, J.P., Ringold, G.M. and Danielsen, M. (1987) Lipofection – A highly efficient, lipid-mediated DNA-transfection procedure. *Proceedings of the National Academy of Sciences USA*, **84**, 21:7413–7417.

Felsenstein, J. (1978) Cases in which parsimony and compatibility methods will be positively misleading. *Systematic Zoology*, **27**:401–410.

Fitzgerald, J.E., Sanyer, T.L., Schardein, J.L., Lake, R.S., McGuire, E.J. and De La Iglesia, F. A. (1981) Carcinogen bioassay and mutagenicity studies with the hypolipidaemic agent gemfibrozil. *Journal of the National Cancer Institute*, **67**:1105–1116.

Foliot, A., Touchard, D and Mallet, L. (1986) Inhibition of liver glutathione s-transferase activity in rats by hypolipidaemic drugs related to or unrelated to clofibrate. *Biochemical Pharmacology*, **35**:1685–1690.

Folkers, G.E., van der Burg, B. and van der Saag, P.T. (1996) A role for cofactors in synergistic and cell specific activation by retinoic acid receptors and retinoid X receptor. *Journal of Steroid Biochemistry and Molecular Biology*, **56**,1–6:119–129.

Foxworthy, P.S. and Eacho, P.I. (1994) Culture hepatocytes for studies of peroxisome proliferation: methods and applications. *Journal of Pharmacological and Toxicological Methods*, **31**:21–30.

Foxworthy, P.S., White, S.L., Hoover, D.M. and Eacho, P.I. (1990) Effect of ciprofibrate, bezafibrate and LY171883 on peroxisomal β -oxidation in cultured rat, dog and rhesus monkey hepatocytes. *Toxicology and applied pharmacology*, **104**:386–394.

Forman, B.M., Chen, J. and Evans, R. (1997) Hypolipidaemic drugs, polyunsaturated fatty acids, and eicosanoids are ligands for peroxisome proliferator-activated receptors α and γ . Proceedings of the National Academy of Science USA, **94**:4312-4317.

Frick, H., Elo Haapa, K. and Heinonen, O.P. (1987) Helsinki Heart Study: Primary-prevention trial with gemfibrozil in middle aged men with dyslipidemia. New England Journal of Medicine, **317**:1235-1247.

Freedman, L.P. and Luisi, B.F. (1993) On the mechanism of DNA binding by nuclear hormone receptors: a structural and functional perspective. Journal of Cellular Biochemistry, **51**:140-150.

Fry, M.S. and Blair-Hedges, S. (1995) Monophyly of the order rodentia inferred from mitochondrial DNA sequences of the genes for 12S rRNA, 16S rRNA and tRNA-Valine. Molecular Biology and Evolution, **12**(1):168-176.

Furukawa, K., Numoto, S., Furuya, K., Furukawa, N.T. and Williams, G.M. (1985) Effects of the hepatocarcinogen nafenopin, a peroxisome proliferator on the activities of rat liver glutathione requiring enzymes and catalase in comparison to the action of phenobarbital. Cancer Research, **45**:5011-5019.

Gariot, P., Barrat, P., Drouin, P., Genton, P., Pointer, B., Foliguet, B., Kolopp, M. and Debry, G. (1987) Morphometric study of human hepatic cell modifications induced by fenofibrate. Metabolism, **36**:203-210.

Gearing, K.L., Gottlicher, M., Teboul, M., Widmark, E. and Gustafsson, J-A. (1993) Interaction of the peroxisome proliferator activated receptor and retinoid X receptor. Proceedings of the National Academy of Sciences USA, **90**:1440-1444.

Gebel, T., Arand, M. and Oesch, F. (1992) Induction of the peroxisome proliferator activated receptor by fenofibrate in the rat liver. *FEBS Letters*, **309**, 1:37-40.

Giguere, V., Shago, M., Zirngibl, R., Tate, P., Rossart, J. and Varmuza, S. (1990) Identification of a novel isoform of the retinoic acid receptor gamma expressed in the mouse embryo. *Molecular and Cellular Biology*, **10**:2335-2340.

Gibson, G. and Lake, B. (1993) *Peroxisomes: Biology and Importance in Toxicology and Medicine*. Taylor and Francis Ltd.

Giguere, V., Tini, M., Flock, G., Ong, E., Evans, R.M. and Otulakowski, G. (1994) Isoform-specific amino-terminal domains dictate DNA binding properties of ROR- α , a novel family of hormone nuclear receptors. *Genes and Development*, **8**:538-553.

Gorski, K., Carneiro, M. and Schibler, U. (1986) Tissue-specific in vitro transcription from the mouse albumin promoter. *Cell*, **47**:767-776.

Goto, K., Suzuki, Y., Yoshida, K., Yamamoto, K. and Sinohara, H. (1994) Plasma α -1-antiproteinase from the mongolian gerbil, *Meriones unguiculatus*: Isolation, partial characterisation, sequencing of cDNA, and implications for molecular evolution. *Journal of Biochemistry*, **116**:582-588.

Gaur, D., Hide, W.A. and Li, W.-H. (1991) Is the guinea pig a rodent ? *Nature*, **351**:649-652.

Gray, R.H. and De La Iglesia, F.A. (1984) Quantitative microscopy comparison of peroxisome proliferation by the lipid regulating agent gemfibrozil in several species. *Hepatology*, **4**,3:520-530.

Greene, M.E., Blumberg, B., McBride, O.W., Yi, H.F., Kronquist, K., Kwan, K., Hsieh, L., Greene, G. and Nimer, S.D. (1995) Isolation of the human peroxisome proliferator-activated receptor gamma cDNA: expression in hematopoietic cells and chromosomal mapping. *Gene Expression* **4**: 281-299.

Green, S., Tugwood, J.D. and Issemann, I. (1992) The molecular mechanism of peroxisome proliferator action: a model for species differences and mechanistic assessment. *Toxicology Letters*, **64/65**:131-139.

Green, S. (1992) Peroxisome proliferators: a model for receptor mediated carcinogenesis. *Cancer Surveys*, **14**:221-232.

Haase-Pettingwell, C.A and King, J. (1989) Formation of aggregates from a thermolabile in vivo folding intermediate in P22 tailspike protein. *The Journal Biological Chemistry*, **264**:10693-10698.

Halachmi, S., Marden, E., Martin, G., Mackay, H., Abbondanza, C. and Brown, M. (1994) Estrogen receptor associated proteins: possible mediators of hormone induced transcription. *Science*, **264**:1455-1458.

Hanefeld, M., Kemmer, C. and Kadner, E. (1983) Relationship between morphological changes and lipid lowering action of p-chlorophenoxyisobutyric acid (CPIB) on hepatic mitochondria and peroxisomes in man. *Atherosclerosis*, **46**:239-246.

Harding, H.P., and Lazar, M.A. (1993) The orphan receptor REV-ERBA-alpha activates transcription via a novel response element. *Molecular and Cellular Biology*, **13**, 5:3113-3121.

Hertz, R., Bishara-Shieban, J. and Bar-Tana, J. (1995) Mode of action of peroxisome proliferators as hypolipidaemic drugs: suppression of apolipoprotein C-III. *The Journal of Biological Chemistry*, **270**, 22: 13470-13475.

Hertz, R., Seckbach, M., Zakin, M.M. and Bar-Tana, J. (1996) Transcriptional suppression of the transferrin gene by hypolipidaemic peroxisome proliferators. *The Journal of Biological Chemistry*, **271**, 1:218-224.

Hollenberg, S.M., Wienberger, C., Ong, E.S., Cerelli, G., Oro, A., Lebo, R., Thompson, E.B., Rosenfeld, M.G. and Evans, R.M. (1985) Primary structure and expression of a functional human glucocorticoid receptor cDNA. *Nature (London)*, **318**:635-641.

Holmes, M.C., French, K.L. and Seckl, J.R. (1997) Dysregulation of diurnal rhythms of Serotonin 5-HT_{2C} and Corticosteroid receptor gene expression in the hippocampus with food restriction and glucocorticoids. *The Journal of Neuroscience*, **17**, 11:4056-4065.

Hong, H., Kohli, K., Trivedi, A., Johnson, D.L. and Stallcup, M.R. (1996) GRIP1, a novel mouse protein that serves as a transcriptional co-activator in yeast for the hormone binding domains of steroid receptors. *Proceedings of the National Academy of Science USA*, **93**:4948-4952.

Huang, C-Y., Wilson, M.W., Lay, L.T., Chow, C.K., Robertson, L.W. and Glauert, P. (1994) Increased 8-hydroxydeoxyguanosine in hepatic DNA of rats treated with the peroxisome proliferators ciprofibrate and perfluorodecanoic acid. *Cancer Letters*, **87**:223-228.

Hurley, D.M., Accili, D., Sratakis, C.A., Karl, M., Vamvakopoulos, N., Rorer, E., Constantine, K., Taylor, S.I. and Chrousos, G.P. (1991) Point mutation causing a single amino acid substitution in the hormone binding domain of the glucocorticoid receptor in familial glucocorticoid resistance. *Journal of Clinical Investigation*, **87**:680-686.

Ijpenberg, A., Jeannin, E., Wahli, W. and Desvergne, B. (1997) Polarity and specific sequence requirements of peroxisome proliferator activated receptor (PPAR) / retinoid X receptor heterodimer binding to DNA. *The Journal of Biological Chemistry*, **272**, 32:20108-20117.

Issemann, I. and Green, S. (1990) Activation of a member of the steroid hormone receptor superfamily by peroxisome proliferators. *Nature* **347**: 645-650.

Issemann, I., Prince, R., Tugwood, J. and Green, S. (1992) A role for fatty acids and liver fatty acid binding protein in peroxisome proliferation. *Biochemical Society Transactions*, **20**, 4:824-827.

Issemann, I., Prince, R.A., Tugwood, J.D. and Green, S. (1993) The peroxisome proliferator activated receptor:retinoid X receptor heterodimer is activated by fatty acids and fibrate hypolipidaemic drugs. *Journal of Molecular Endocrinology*, **11**:37-47.

Jacq, X., Brou, C., Lutz, Y., Davidson, I., Chambon, P. and Tora, L. (1994) Human TAF_{II}30 is present in a distinct TFIID complex and is regulated for transcriptional activation by the estrogen receptor. *Cell*, **79**:107-117.

James, N.H. and Roberts, R.A. (1996) Species differences in response to peroxisome proliferators correlate in vitro with induction of DNA synthesis rather than suppression of apoptosis. *Carcinogenesis*, **17**,8:1623-1632.

- Jayakumar, A., Huang, W.Y., Raetz, B., Chirala, S.S. and Wakil, S.J. (1996) Cloning and expression of the multifunctional human fatty-acid synthase and its subunits in *Escherichia coli*. Proceedings of the National Academy of Science USA, **93**,25:14509-14514.
- Jiang, G. and Sladek, F.M. (1997) The DNA binding domain of hepatocyte nuclear factor 4 mediates cooperative, specific binding to DNA and heterodimerization with the retinoid X receptor α . The Journal of Biological Chemistry, **272**,2:1218-1225.
- Jones, D.T., Taylor, W.R. and Thornton, J.M. (1992) The rapid generation of mutation data matrices from protein sequences. Computational and Applied Bioscience, **8**:275-282.
- Jones, P.S., Savory, R., Barratt, P., Bell, A.R., Gray, T.J.B., Jenkins, N.A., Gilbert, D.J., Copeland, N.G. and Bell, D.R. (1995) Chromosomal localisation, inducibility, tissue specific expression and strain differences in three murine peroxisome proliferator activated receptor genes. European Journal of Biochemistry, **233**:219-226.
- Jow, L. and Mukherjee, R. (1995) The human peroxisome proliferator-activated receptor (PPAR) subtype NUC1 represses the activation of hPPAR α and thyroid hormone receptors. The Journal of Biological Chemistry **270**, 8:3836-3840.
- Juge-Aubrey, C., Pernin, A., Favez, T., Burger, A.G., Wahli, W., Meier, C.A. and Desvergne, B. (1997) DNA binding properties of peroxisome proliferator-activated receptor subtypes on various natural peroxisome proliferator response elements. The Journal of Biological Chemistry, **272**, **40**:25252-25259.

Karl, M., Lamberts, S.W., Detera-Wadleigh, S.D., Encio, I.J., Stratakis, A., Hurley, D.M., Accili, D. and Chrousos, G.P. (1993) Familial glucocorticoid resistance caused by a splice deletion in the human glucocorticoid receptor gene. *Journal of Clinical Endocrinology and Metabolism*, **76**:683-689.

Kasai, H., Okada, Y., Nishimura, S., Rao, M.S. and Reddy, J.K. (1989) Formation of 8-hydroxyguanosine in liver DNA of rats following long term exposure to a peroxisome proliferator. *Cancer Research*, **49**:2603-2605.

Kastner, P., Krust, A., Mendelsohn, C., Garnier, J.M., Zelent, A., Leroy, P. Staub, A. and Chambon, P. (1990) Multiple isoforms of retinoic acid receptor gamma with specific patterns of expression. *Proceedings of the National Academy of Science USA*, **87**:2700-2704.

Keller, H., Devchand, P.R., Perroud, M. and Wahli, W. (1997) PPAR α structure-function relationships derived from species specific differences in responsiveness to hypolipidaemic agents. *Biological Chemistry*, **378**:651-655

Keller, H., Dreyer, C., Medin, J., Mahfoudi, A., Ozato, K. and Wahli, W. (1993) Fatty acids and retinoids control lipid metabolism through activation of peroxisome proliferator-activated receptor-retinoid X receptor heterodimers. *Proceedings of the National Academy of Science USA*, **90**:2160-2164.

Kliewer, S.A., Forman, B.M., Blumberg, B., Ong, E.S., Borgmeyer, U., Mangelsdorf, D.J., Umesono, K. and Evans, R.M. (1994) Differential expression and activation of a family of murine peroxisome proliferator-activated receptors. *Proceedings of the National Academy of Sciences USA* **91**:7355-7359.

Kliewer, S.A., Sundseth, S.S., Jones, S.A., Brown, P.J., Wisely, G.B., Koble, C.S., Devchand, P., Wahli, W., Willson, T.M., Lenhard, J.M. and Lehmann, J.M. (1997) Fatty acids and eicosanoids regulate gene expression through direct interactions with peroxisome proliferator-activated receptors α and γ . *Proceedings of the National Academy of Sciences USA*, **94**:4318-4323.

Kluwe, W.M., Haseman, J.K., Douglas, J.F. and Huff, J.E. (1982) The carcinogenicity of dietary di(2-ethylhexyl) phthalate (DEHP) in fischer 344 rats and b6c3f1 mice. *Journal of Toxicology and Environmental Health*, **10**:797-815.

Kozak, M. (1994) Determinants of translational fidelity and efficiency in vertebrate mRNAs. *Biochimie*, **76**:815-821.

Kozak, M. (1995) Adherence to the first- AUG rule when a second AUG codon follows closely upon the first. *Proceedings of the National Academy of Sciences USA*, **92**:2662-2666.

Krey, G., Braissant, O., L'Horsset, F., Kalkhoven, E., Perroud, M., Parker, M.G. and Wahli, W. (1997) Fatty acids, eicosanoids, and hypolipidemic agents identified as ligands of peroxisome proliferator-activated receptors by coactivator-dependent receptor ligand assay. *Molecular Endocrinology*, **11**:779-791.

Krey, G., Keller, H., Mahfoudi, A., Medin, J., Ozato, K., Dreyer, C. and Wahli, W. (1993) *Xenopus* peroxisome proliferator activated receptors: genomic organization, response element recognition, heterodimer formation with retinoid X receptor and activation by fatty acids. *Journal of Steroid Biochemistry and Molecular Biology* **47**, 1-6:65-73.

Krust, A., Green, S., Argos, P., Kumar, V., Walter, P., Bornert, J-M. and Chambon, P. (1986) The chicken oestrogen receptor sequence: homology with *v-erbA* and the human oestrogen and glucocorticoid receptors. *The EMBO Journal*, **5**,5:891-897.

Kuma, K. and Miyata, T. (1994) Mammalian phylogeny inferred from multiple protein data. *Japanese Journal of Genetics*, **69**:555-566.

Kurokawa, R. , Yu, V.C., Naar, A., Kyakumoto, S., Han, Z.H. and Silverman, S. (1993) Differential orientation of the DNA binding domain and carboxy-terminal dimerisation interface regulates binding site selection by nuclear receptor heterodimers. *Genes and Development*, **7**, 7B:1423-1435.

Kurokawa, R., DiRenzo, J., Boehm, M., Sugarman, J., Gloss, B., Rosenfeld, M.G., Heyman, R.A. and Glass, C.K. (1994) Regulation of retinoid signalling by receptor polarity and allosteric control of ligand binding. *Nature*, **371**:528-531.

Kurokawa, R., Soderstrom, M., Horlein, A., Halachmi, S., Brown, M., Rosenfeld, M.G. and Glass, C.K. (1995) Polarity specific activities of retinoic acid receptors determined by a co-repressor. *Nature*, **377**:451-454.

LaVallie, E.R., DiBlasio, E.A., Kovacic, S., Grant, K.L., Schendel, P.F. and McCoy, J.M. (1993) A thioredoxin gene fusion expression system that circumvents inclusion body formation in the *E.coli* cytoplasm. *Bio/Technology*, **11**:187-193.

Lake, B.G., Evans, J.G., Cunninghame, M.E. and Price, R.J. (1993) Comparison of the hepatic effects of nafenopin and Wy-14,643 on peroxisome proliferation and cell replication in the rat and syrian hamster. *Environmental Health Perspectives*, **101** (suppl. 5):241-248.

Lake, B.G. (1995) Mechanisms of hepatocarcinogenicity of peroxisome proliferating drugs and chemicals. *Annual, Review of Pharmacology and Toxicology*, **35**:483-507.

Lake, B.G., Evans, J.G., Gray, T.J.B., Korosi, S.A. and North, C.J. (1989a) Comparative studies on nafenopin-induced hepatic peroxisome proliferation in the rat, syrian hamster, guinea pig and marmoset. *Toxicology and Applied and pharmacology*, **99**:148-160.

Lake, B.G., Gray, T.J.B., Korosi, S.A. and Walters, D.G. (1989b) Nafenopin, a peroxisome proliferator depletes hepatic vitamin E content and elevates plasma oxidised glutathione levels in rats. *Toxicology Letters*, **45**:221-229.

Lake, B.G., Gray, T.J.B. and Gangolli, S.D. (1986) Hepatic effects of phthalate esters and related compounds- in vivo and in vitro correlations. *Environmental Health Perspectives*, **67**:283-290.

Lalwani, N.D., Dethloff, L.A., Haskins, J.R., Robertson, D.G. and De La Iglesia, F.A. (1997) Increased nuclear ploidy, not cell proliferation, is sustained in the peroxisome proliferator treated rat liver. *Toxicologic Pathology*, **25**, 2:165-176.

Lalwani, N.D., Reddy, M.K., Qureshi, S.A. and Reddy, J.K. (1981) Development of hepatocellular carcinomas and increased peroxisomal fatty acid β -oxidation in rats fed [4-chloro-6-(2,3-xylidino)-2-pyrimidinylthio] acetic acid (Wy 14,643) in the semipurified diet. *Carcinogenesis*, **2**:645-650.

Lambe K.G. and Tugwood, J.D. (1996) A human peroxisome-proliferator-activated receptor- γ is activated by inducers of adipogenesis, including thiazolidinedione drugs. *European Journal of Biochemistry* **239**: 1-7.

Latruffe, N., Pacot, C., Passily, P., Petit, M., Bardot, O., Caira, F., Cherkaoui Malki, M., Jannin, B., Clemencet, M.C. and Deslex, P. (1995) Peroxisomes and Hepatotoxicity. *Comparative Haematology International*, **5**:189-195.

Laudet, V., Hanni, C., Coll, J., Catzeflis, F. and Stehelin, D. (1992) Evolution of the nuclear receptor gene superfamily. *The EMBO Journal*, **11**,3:1003-1013.

Lazarow, P.B. and Moser, H.W. (1989) *The metabolic basis of inherited disease*. Sixth edition (ed C.R. Scriver, A.L. Beaudet, W.S. Sly, and D. Valle) New York: McGraw-Hill, pp1479-1509.

Lazarow, P.B. and de Duve, C. (1976) A fatty acyl-CoA oxidising system in rat liver peroxisomes: enhancement by clofibrate, a hypolipidaemic drug. *Proceedings of the National Academy of Science USA*, **73**:2043-2046.

Lee, M.S., Kliewer, S.A., Provencal, J., Wright, P.E., and Evans, R.M. (1993) Structure of the retinoid x receptor alpha DNA binding domain: a helix required for homodimeric DNA binding. *Science* **260**: 1117-1121.

Lee, M.S., Sem, D.S., Kliewer, S.A., Provencal, J., Evans, R.M. and Wright, P.E. (1994) NMR assignments and secondary structure of the retinoid X receptor a DNA-binding domain. *European Journal of Biochemistry*, **224**:639-650.

Lee, S.S.T., Pineau, T., Drago, J., Lee, E.J., Owens, J.W., Kroetz, D.L., Fernandez-Salguero, P.M., Westphal, H. and Gonzalez, F.J. (1995) Targeted disruption of the α isoform of the peroxisome proliferator activated receptor gene in mice results in abolishment of the pleiotropic effects of peroxisome proliferators. *Molecular and Cellular Biology*, **15**, 6:3012-3022.

Lemberger, T., Staels, B., Saladin, R., Desvergne, B., Auwerx, J. and Wahli, W. (1994) Regulation of the peroxisome proliferator activated receptor α gene by glucocorticoids. The Journal of Biological Chemistry, **269**,40:24527-24530.

Lemberger, T., Saladin, R., Vazquez, M., Assimacopoulos, F., Staels, B., Desvergne, B., Wahli, W. and Auwerx, J. (1996) Expression of the peroxisome proliferator- activated receptor α gene is stimulated by stress and follows a diurnal rhythm. The Journal of Biological Chemistry, **271**,3:1764-1769.

Leng, X., Blanco, J., Tsai, S.Y., Ozato, K., O'Malley, B.W. and Tsai, M-J. (1995) Mouse retinoid X receptor contains a separable ligand-binding domain and transactivation domain in its E region. Molecular and Cellular Biology, **15**,1:255-263.

Leroy, P., Krust, A., Zelent, A., Mendelsohn, C., Garnier, J.M., Kastner, P., Dierich, A. and Chambon, P. (1991) Multiple isoforms of the mouse retinoic acid receptor α are generated by alternative splicing and differential induction by retinoic acid. Embo Journal, **10**:59-69.

Lewis, D.F.V. and Lake, B.G. (1993) Interaction of some peroxisome proliferators with the mouse liver peroxisome proliferator-activated receptor (PPAR): a molecular modelling and quantitative structure-activity relationship (QSAR) study. Xenobiotica, **23**, 1:79-96.

Lhuguenot, J.C., Mitchell, A.M. and Elcombe, C.R. (1988) The metabolism of mono-(2-ethylhexyl)phthalate (MEHP) and liver peroxisome proliferation in the hamster. Toxicology and Industrial Health, **4**, 4:431-441.

Luckett, W.P. and Hartenberger, J.-L. (eds.) (1985) Evolutionary relationships among rodents. A multidisciplinary analysis. Plenum Press, New York.

Luisi, B.F., Xu, W.X., Otwinowski, Z., Freedman, L.P., Yamamoto, K.R., and Siegler, P.B. (1991) Crystallographic analysis of the interaction of the glucocorticoid receptor with DNA. *Nature* **352**:497-505.

MacDonald, P.N., Sherman, D.R., Dowd, D.R., Jefcoat, S.C. and DeLisle, R.K. (1995) The vitamin D receptor interacts with general transcription factor IIB. *The Journal of Biological Chemistry*, **270**,9:4748-4752.

Mader, S., Chen, J-Y., Chen, Z., White, J., Chambon, P. and Gronemeyer, H. (1993) The patterns of binding of RAR, RXR and TR homo- and heterodimers to direct repeats are dictated by the binding specificities of the DNA binding domains. *The EMBO Journal*, **12**, 13:5029-5041.

Mansen, A., Guardiola-Diaz, H., Rafter, J., Branting, C. and Gustafsson, J-A. (1996) Expression of the peroxisome proliferator activated receptor (PPAR) in mouse colonic mucosa. *Biochemical and Biophysical Research Communications*, **222**:844-851.

Marcus, S.L., Miyata, K.S., Zhang, B., Subramani, S, Rachubinski, R.A. and Capone, J.P. (1993) Diverse peroxisome proliferator activated receptors bind to the peroxisome proliferator-responsive elements of the rat hydratase / dehydrogenase and fatty acyl-CoA oxidase genes but differentially induce expression. *Proceedings of the National Academy of Science USA*, **90**:5723-5727.

Marcus, S.L., Capone, J.P. and Rachubinski, R.A. (1996) Identification of COUP-TFII as a peroxisome proliferator response element binding factor using genetic selection in yeast: COUP-TFII activates transcription in yeast but antagonises PPAR signalling in mammalian cells. *Molecular and Cellular Endocrinology*, **120**:31-39.

Marmomstein, R. Carey, M., Ptashne, M. and Harrison, S.C. (1992) DNA recognition by GAL4:structure of a protein-DNA complex. *Nature*, **356**:408-414.

Masters, C. and Crane, D. (Eds.) (1995) *The peroxisome: a vital organelle*. Cambridge University Press

Masters, C.J. and Crane, D.I. (1992) The peroxisome: organisation and dynamics. *Advances in Molecular and Cellular Biology*, **4**:133-160.

Mastes, C. (1996) Cellular signalling: The role of the peroxisome. *Cellular Signalling*, **8**, 3:197-208.

McGuire, E.J, Gray, R.H. and De La Iglesia, F.A. (1992) Chemical structure-activity relationships:peroxisome proliferation and lipid regulation in rats. *Journal of the American College of Toxicology*, **11**,3:353-361.

McNae, F., Sharma, R. and Gibson, G.G. (1994) Molecular toxicology of peroxisome proliferators. *European Journal of drug Metabolism and Pharmacokinetics*, **3**:219-223.

Melchiorri, C., Chieco, P., Zedda, A.I., Coni, P., Ledda-Columbano, G.M. and Columbano, A. (1993) Ploidy and nuclearity of rat hepatocytes after compensatory regeneration or mitogen-induced liver growth. *Carcinogenesis*, **14**, 9:1825-1830.

Mierendorf, R., Yaeger, K. and Novy, R. (1994) The pET system:Your choice for expression. *InNovations*, **1**,1:1-3.

Miller, R.T., Glover, S.E., Stewart, W.S., Corton, J.C., Popp, J.A. and Cattley, R.C. (1996) Effect on the expression of *c-met*, *c-myc* and PPAR α in liver and liver tumours from rats chronically exposed to the hepatocarcinogenic peroxisome proliferator Wy-14,643. *Carcinogenesis*, **17**,6:1337-1341.

Miyamoto, T., Kaneko, A., Kakizawa, T., Yajima, H., Kamijo, K., Sekine, R., Hiramatsu, K., Nishii, Y., Hashimoto, T. and Hashizume, K. (1997) Inhibition of peroxisome proliferator signalling pathways by thyroid hormone receptor. *The Journal of Biological Chemistry*, **272**, 12:7752-7758.

Miyata, K.S. McCaw, S.E., Patel, H.V., Rachubinski, R.A. and Capone, J.P. (1996) The orphan nuclear hormone receptor LXR α interacts with the peroxisome proliferator-activated receptor and inhibits peroxisome proliferator signalling. *The Journal of Biological Chemistry*, **271**, 16:9189-9192.

Mochizuki, Y., Furukawa, K. and Sawada, N. (1983) Effect of simultaneous administration of clofibrate with diethylnitrosamine on hepatic tumourigenesis in the rat. *Cancer Letters*, **19**:99-105.

Moser, H.W. (1987) New approaches in peroxisomal disorders. *Developmental Neuroscience*, **9**:1-18.

Moser, H.W. (1993) Peroxisomal Disorders. *Advances in human genetics* (ed H.Harris and K.Hirschhorn). Plenum Press New York, vol. 21, pp 1-106.

Motojima, K. (1993) Peroxisome Proliferator-Activated Receptor (PPAR): Structure, Mechanisms of Action and Diverse Functions. *Cell Structure and Function*, **18**:267-277.

Motojima, K., Peters, J.M. and Gonzalez, F.J. (1997) PPAR α mediates peroxisome proliferator induced transcriptional repression of non-peroxisomal gene expression in mouse. *Biochemical and Biophysical Research Communications*, **230**:155–158.

Muerhoff, A.S., Griffin, K.J. and Johnson, E.F. (1992) Characterisation of a rabbit gene encoding a clofibrate-inducible fatty acid ω -hydroxylase:CYP4A6. *Archives of Biochemistry and Biophysics*, **296**,1:66–72.

Mukherjee, R., Jow, L., Croston, G.E. and Paterniti, J.R. (1997) Identification, characterisation and tissue distribution of human peroxisome proliferator-activated receptor (PPAR) isoforms PPAR γ 2 versus PPAR γ 1 and activation with retinoid X receptor agonists and antagonists. *The Journal of Biological Chemistry*, **272**, 12:8071–8076.

Mukherjee, R., Jow, L., Noonan, D. and McDonnell, D.P. (1994) Human and rat peroxisome proliferator activated receptors (PPARs) demonstrate similar tissue distribution but different responsiveness to PPAR activators. *Journal of steroid Biochemistry and Molecular Biology*, **51**,3–4:157–166.

Myers, K.A., Lambe, K.G., Aldridge, T.C., MacDonald, N. and Tugwood, J.D. (1997) Amino acid residues in both the DNA-binding and ligand-binding domains influence transcriptional activity of the human peroxisome proliferator-activated receptor alpha. *Biochemical and Biophysical Research Communications*, **239**:522–526.

Nagaya, T., Nomura, Y., Fujieda, M. and Seo, H. (1996) Heterodimerisation preferences of thyroid hormone receptor α isoforms. *Biochemical and Biophysical Research Communications*, **226**:426–430.

Nagpal, S., Zelent, A. and Chambon, P. (1992) RAR β 4, a retinoic acid receptor isoform is generated from RAR β 2 by alternative splicing and useage of a CUG iniator codon. Proceedings of the National Academy of Science USA, **89**:2718-2722.

Nakatani, T., Suzuki, Y., Yoshida, K. and Sinohara, H. (1995) Molecular cloning and sequence analysis of cDNA encoding plasma α -1-antiproteinase from syrian hamster: implications for the evolution of rodentia. Biochimica and Biophysica Acta, **1263**:245-248.

Neat, C.E., Thomassen, M.S. and Osmundsen, H. (1980) Induction of peroxisomal β -oxidation in rat liver by high fat diets. Biochemical Journal, **186**:369-371.

Nedergaard, J., Alexson, S. and Cannon, B. (1980) Cold adaptation in the rat: increased brown fat peroxisomal β -oxidation relative to maximal mitochondrial oxidative capacity. American Journal of Physiology (cell physiol. **8**):C208-C216.

Nicholas, K.B. and Nicholas, H.B. Jr. (1997) Genedoc:analysis and visualisation of genetic variation. <http://www.cris.com/~ketchup/genedoc.shtml>

Noguchi, T., Fujiwara, S., Hayashi, S. and Haruhiko, S. (1994) Is the guinea pig (*Cavia porcellus*) a rodent ? Computational Biochemistry and Physiology, **107B**, 2:179-182.

Notredame, C. and Higgins D.G. (1996) SAGA – Sequence alignment by genetic algorithm. Nucleic Acids Research, **24**, 8:1515-1524.

Nunez, S.B., Medin, J.A., Braissant, O., Kemp, L., Wahli, W., Ozato, K. and Segars, J.H. (1997) Retinoid X Receptor and Peroxisome Proliferator Activated Receptor activate an estrogen responsive gene independent of the Estrogen receptor. Molecular and Cellular Endocrinology, **127**:27-40.

Oakley, R.H., Webster, J.C., Sar, M., Parker, C.R. and Cidlowski, J.A. (1997) Expression and subcellular distribution of the β -isoform of the human glucocorticoid receptor. *Endocrinology*, **138**, 11:5028-5038.

Oesch, F., Hartmann, R., Strolin-Benedetti, M., Dosert, P., Worner, W. and Schladt, L. (1988) Time-dependence and differential induction of rat and guinea pig peroxisomal β -oxidation, palmitoyl-CoA hydrolase, cytosolic and microsomal epoxide hydrolase after treatment with hypolipidaemic drugs. *J Cancer Res. Clin. Oncol.* **114**: 341-346.

Ohmura, T., Ledda-Columbano, G.M., Piga, R., Columbano, A., Glemba, J., Katyal, S.L., Locker, J. and Shinozuka, H. (1996) Hepatocyte proliferation induced by a single dose of a peroxisome proliferator. *American J. Pathology.* **148**, 3 :815-824.

Oliver, M.F., Heady, J.A., Morris, J.N. and Cooper, J. (1978) A cooperative trial in the primary prevention of ischemic heart disease using clofibrate. *Heart*, **40**:1069-1118.

Onate, S.A., Tsai, S.Y., Tsai, M-J. and O'Malley, B.W. (1995) Sequence and characterisation of a coactivator for the steroid hormone receptor superfamily. *Science*, **270**:1354-1357.

Osada, S., Tsukamoto, T., Takiguchi, M., Mori, M. and Osumi, T. (1997) Identification of an extended half-site motif required for the function of peroxisome proliferator-activated receptor α . *Genes to cells*, **2**:315-327.

Osumi, T., Wen, J-K. and Hashimoto, T. (1991) Two cis-acting regulatory sequences in the peroxisome proliferator-responsive enhancer region of rat acyl-CoA oxidase gene. *Biochemical and Biophysical Research communications*, **175**,3:866-871.

Osumi, T., Wen, J-K., Taketani, S. and Hashimoto, T. (1993) Molecular mechanisms involved in induction of peroxisomal β -oxidation enzymes by hypolipidaemic agents, in *Peroxisomes: Biology and Importance in Toxicology and Medicine*. eds Gibson, G. and Lake, B. Taylor and Francis Ltd. London. pp149-172.

Pacot, C., Petit, M., Caira, F., Rollin, M., Behechti, N., Gregoire, S., Cherkaoui Malki, M., Cavatz, C., Moisant, M., Moreau, C., Thomas, C., Descotes, G., Gallas, J-F., Deslex, P., Althoff, J., Zahnd, J-P., Lhuguenot, J-C. and Latruffe, N. (1993) Response of genetically obese Zucker rats to ciprofibrate, a hypolipidaemic agent, with peroxisome proliferation activity as compared to Zucker lean and sprague-dawley rats. *Biol. Cell*, **77**:27-35.

Pacot, C., Petit, M., Rollin, M., Behechti, N., Moisant, M., Deslex, P., Althoff, J., Lhuguenot, J-C. and Latruffe, N. (1996) Difference between guinea pig and rat in the liver peroxisomal response to equivalent plasmatic level of ciprofibrate. *Archives of Biochemistry and Biophysics*, **327**, 1:181-188.

Palmer, C.N.A., Hsu, M-H., Griffin, K.J. and Johnson, E.F. (1995) Novel sequence determinants in peroxisome proliferator signalling. *The Journal of Biological Chemistry*, **270**, 27:16114-16121.

Palmer, C.N.A., Hsu, M-H., Muerhoff, A.S, Griffin, K.J. and Johnson, E.F. (1994) Interaction of the peroxisome proliferator-activated receptor α with the retinoid X receptor α unmasks a cryptic peroxisome proliferator response element in the CYP4A6 promoter. *The Journal of Biological Chemistry*, **269**, 27:18083-18089.

Palosaari, P.M. and Hiltunen, J.K. (1990) Peroxisomal bifunctional protein from rat liver is a trifunctional enzyme possessing 2-enoyl-CoA hydratase, 3-hydroxylacyl-CoA dehydrogenase, and Δ^3 , Δ^2 -enoyl-CoA isomerase activities. *the Journal of Biological Chemistry*, **265**, 5:2446–2449.

Permadi, H., Lundgren, B., Andersson, K., Sundberg, C. and DePierre, J.W. (1993) Effects of perfluoro fatty acids on peroxisome proliferation and mitochondrial size in mouse liver: dose and time factors and effect of chain length. *Xenobiotica*, **23**, 7:761–770.

Permadi, H., Lundgren, B., Andersson, K. and DePierre, J.W. (1992) Effects of perfluoro fatty acids on xenobiotic-metabolizing enzymes, enzymes which detoxify reactive forms of oxygen and lipid peroxidation in mouse liver. *Biochemical Pharmacology*, **44**, 6:1183–1191.

Pineau, T., Hudgins, W.R., Liu, L., Chen, L-C., Sher, T., Gonzalez, F.J. and Samid, D. (1996) Activation of a human peroxisome proliferator-activated receptor by the anti-tumour agent phenylacetate and its analogues. *Biochemical Pharmacology*, **52**:659–667.

Pink, J.J., Wu, S-Q., Wolf, D.M., Bilimoria, M.M. and Jordan, V.C. (1996) A novel 80 kDa human estrogen receptor containing a duplication of exons 6 and 7. *Nucleic Acids Research*, **24**, 5:962–969.

Price, R.J. Evans, J.G. and Lake, B.G. (1992) Comparison of the effects of nafenopin on hepatic peroxisome proliferation and replicative DNA synthesis in the rat and syrian hamster. *Food and Chemical Toxicology*. **30**, 11 : 937–944.

Qi, J-S., Desai-Yajnik, V., Greene, M.E., Raaka, B.M. and Samuels, H.H. (1995) The ligand-binding domains of the thyroid hormone/retinoid receptor gene subfamily function in vivo to mediate heterodimerization, gene silencing and transactivation. *Molecular and Cellular Biology*, **15**,3:1817-1825.

Rao, M.S. and Reddy, J.K. (1991) An overview of peroxisome proliferator induced hepatocarcinogenesis. *Environmental Health Perspectives*, **93**:205-209.

Reddy, J.K. and Lalwani, N.D. (1983) Carcinogenesis by hepatic peroxisome proliferators: Evaluation of the risk of hypolipidaemic drugs and industrial plasticizers to humans. *CRC Critical Reviews in Toxicology*, **12**:1-58.

Reddy, J.K., Lalwani, N.D., Qureshi, S.A., Reddy, M.K. and Moehle, C.M. (1984) Induction of hepatic peroxisome proliferation in non-rodent species, including primates. *American Journal of Pathology*, **114**:171-183.

Reddy, J.K., Lalwani, N.D., Reddy, M.K. and Qureshi, S.A. (1982) Excessive accumulation of autofluorescent lipofuscin in the liver during hepatocarcinogenesis by methyldclofenapate and other hypolipidaemic peroxisome proliferators. *Cancer research*, **42**:259-266.

Reddy, J.K. and Rao, M.S. (1986) Peroxisome proliferators and cancer: mechanisms and implications. *Trends in Pharmacological Sciences*, **7**:438-443.

Reddy, J.K. and Rao, M.S. (1977) Development of liver tumours in rats treated with the peroxisome enzyme inducer nafenopin. *American Journal of Pathology*, **86**:249.

Reddy, J.K. and Qureshi, S.A. (1979) Tumourigenicity of the hypolipidaemic peroxisome proliferator ethyl- α -p-chlorophenoxyisobuturate (Clofibrate) in rats. *British Journal of Cancer*, **40**:476.

Reo, N.V., Goecke, C.M., Narayanan, L. and Jarnot, B.M. (1994) Effects of perfluoro-n-octanoic acid, perfluoro-n-decanoic acid and clofibrate on hepatic phosphorous metabolism in rats and guinea pigs in vivo. *Toxicology and Applied Pharmacology*, **124**:165-173.

Rodriguez, J.C., Gilgomez, G., Hegardt, F.G. and Haron, D. (1994) Peroxisome proliferated activated receptor mediates induction of the mitochondrial 3-hydroxy-3-methylglutaryl-CoA synthase gene by fatty acids. *Journal Biological Chemistry*, **269**, 29:18767-18772.

Rousseau, V., Becker, D.J., Ongemba, L.N., Rahier, J., Henquin, J-C. and Brichard, S.M. (1997) Developmental and nutritional changes of *ob* and PPAR γ 2 expression in white adipose tissue. *Biochemical Journal*, **321**:451-456.

Ruyter, B., Anderson, O., Dehli, A., Ostlund-Farrants, A-K., Gjoen, T. and Thomassen, M.S. (1997) Peroxisome proliferator activated receptors in Atlantic salmon (*Salmo salar*): effects on PPAR transcription and acyl-CoA oxidase activity in hepatocytes by peroxisome proliferators and fatty acids. *Biochimica and Biophysica Acta*, **1348**:331-338.

Sabzevari, O., Hatcher, M., O'Sullivan, M., Kentish, P., and Gibson, G. (1995) Comparative induction of cytochrome P4504A in rat hepatocyte culture by the peroxisome proliferators, bifonazole and clofibrate. *Xenobiotica*, **25**,4:395-403.

Sakuma, M., Yamada, J. and Suga, T. (1992) Comparison of the inducing effect of dehydroepiandrosterone on hepatic peroxisome proliferation-associated enzymes in several rodent species. *Biochemical Pharmacology* **43**, 6 : 1269-1273.

Sanes, J.R., Rubenstein, J.L.R. and Nicolas, J.F. (1986) Use of recombinant retrovirus to study post-implantation cell lineage in mouse embryos. *The Embo Journal*, **5**, 12:3133-3142.

Sato, T., Murayama, N., Yamazoe, Y. and Kato, R. (1995) Suppression of clofibrate-induction of peroxisomal and microsomal fatty acid-oxidising enzymes by growth hormone and thyroid hormone in primary cultures of rat hepatocytes. *Biochimica et Biophysica Acta*, **1256**:327-333.

Sausen, P.J., Lee, D.C., Rose, M.L. and Cattley, R.C. (1995) Elevated 8-hydroxydeoxyguanosine in hepatic DNA of rats following exposure to peroxisome proliferators: relationship to mitochondrial alterations. *Carcinogenesis*, **16**, 8:1795-1801.

Savory, R. (1996) PPAR α : inducibility and species differences in expression. Ph.D. Thesis. University of Nottingham, UK.

Schein, C.H. (1989) Production of soluble recombinant proteins in bacteria. *Bio/Technology*, **7**:1141-1149.

Schmezer, P., Pool, B.L., Klein, R.G., Komitowski, D. and Schmahl, D. (1988) Various short term assays and two long term studies with the plasticiser di(2-ethylhexyl)phthalate in the syrian golden hamster. *Carcinogenesis*, **9**:37-43.

Schodin, B.A., Schlueter, C.J. and Kranz, D.M. (1996) Binding properties and solubility of single chain T-cell receptors expressed in *Escherichia coli*. *Molecular Immunology*, **33**,9:819-829.

Schoonjans, K., Watanabe, M., Suzuki, H., Mahfoudi, A., Krey, G., Wahli, W., Grimaldi, P., Staels, B., Yamamoto, T. and Auwerx, J. (1995) Induction of the acyl-coenzyme A synthetase gene by fibrates and fatty acids is mediated by a peroxisome proliferator response element in the C-promoter. *The Journal of Biological Chemistry*, **270**,33:19269-19276.

Schoonjans, K., Peinado-Onsurbe, J., Lefebvre, A-M, Heyman, R.A., Briggs, M., Deeb, S., Staels, B. and Auwerx, J. (1996) PPAR α and PPAR γ activators direct a distinct tissue-specific transcriptional response via a PPRE in the lipoprotein lipase gene. *The EMBO Journal*, **15**,19:5336-5348.

Schulman, I.G., Chakravarti, D., Juguilon, H., Romo, A. and Evans, R.M. (1995) Interactions between the retinoid X receptor and a conserved region of the TATA-binding protein mediate hormone-dependent transactivation. *Proceedings of the National Academy of Science USA*, **92**:8288-8292.

Schrader, M., Muller, K.M., Nayeri, S., Kahlen, J-P. and Carlberg, C. (1994) Vitamin D₃-thyroid hormone receptor heterodimer polarity directs ligand sensitivity of transactivation. *Nature*, **370**:382-386.

Schultz, H. (1991) Beta oxidation of fatty acids. *Biochimica and Biophysica Acta*, **1081**:109-120.

Schutgens, R.B.H., Heymans, H.S.A., Wanders, R.J.A., Van den Bosch, H. and Tager, J.M. (1986) Peroxisomal disorders- a newly recognised group of genetic diseases. *European Journal of Pediatrics*, **144**, 5:430-440.

Schwabe, J.W., Chapman, L., Finch, J.T., and Rhodes, D. (1993) The crystal structure of the estrogen receptor DNA-binding domain bound to DNA: how receptors discriminate between their response elements. *Cell* **75**:567-578.

Schwabe, J.W.R., Neuhaus, D. and Rhodes, D. (1990) Solution structure of the DNA-binding domain of the oestrogen receptor. *Nature (London)* **348**:458-461.

Scotto, C., Keller, J-M., Schohn, H., and Dauca, M. (1995) Comparative effects of clofibrate on peroxisomal enzymes of human (Hep EBNA2) and rat (FaO) hepatoma cell lines. *European Journal of Cell Biology*, **66**:375-381.

Seed, B. and Sheen, J.Y. (1988) A simple phase extraction assay for chloramphenicol acetyltransferase activity. *Gene*, **67**, 2:271-277.

Semenkovich, C.F., Chen, S-H., Wims, M., Luo, C-C., Li, W-H. and Chan, L. (1989) Lipoprotein lipase and hepatic lipase mRNA tissue specific expression, developmental regulation, and evolution. *Journal of Lipid Research*, **30**:423-431.

Shalev, A., Siegrist-Kaiser, C.A., Yen, P.M., Wahli, W., Burger, A.G., Chin, W.W. and Meier, C.A. (1996) The peroxisome proliferator activated receptor α is a phosphoprotein: regulation by insulin. *Endocrinology*, **137**, 10:4499-4502.

Sher, T., Yi, H-F., McBride, W. and Gonzalez, F.J. (1993) cDNA cloning, chromosomal mapping and functional characterisation of the human peroxisome proliferator activated receptor. *Biochemistry*, **32**:5598-5604.

Squires, C.H., Childs, J., Eisenberg, S.P., Polverini, P.J. and Sommer, A. (1988) Production and characterisation of human basic fibroblast growth factor from *Escherichia coli*. *The Journal of Biological Chemistry*, **263**:16297-16302.

Steineger, H.H., Sorensen, H.N., Tugwood, J.D., Skrede, S., Spydevold, O. and Gautvik, K.M. (1994) Dexamethasone and insulin demonstrate marked and opposite regulation of the steady-state messenger RNA level of the peroxisomal proliferator-activated receptor (PPAR) in hepatic cells - Hormonal modulation of fatty-acid-induced transcription. *European Journal of Biochemistry*, **225**,3:967-974.

Sterchele, P.F., Sun, H., Peterson, R.E. and Vanden Heuvel, J.P. (1996) Regulation of peroxisome proliferator-activated receptor- α mRNA in rat liver. *Archives of Biochemistry and Biophysics*, **326**,2:281-289.

Stott, W.T., Yano, B.L., Williams, D.M., Barnard, S.D., Hannah, M.A., Cieslak, F.S. and Herman, J.R. (1995) Species dependent induction of peroxisome proliferation by haloxyfop, an aryloxyphenoxy herbicide. *Fundamental and Applied Toxicology*, **28**:71-79.

Strimmer, K. and von Haeseler, A. (1996) Quartet puzzling-a maximum-likelihood method for reconstructing tree topologies. *Molecular and Biological Evolution*, **13**, 7:964-969.

Styles, J.A., Kelly, M., Pritchard, N.R. and Elcombe, C.R. (1988) A species comparison of acute hyperplasia induced by the peroxisome proliferator methyldclofenopate: involvement of the binucleated hepatocyte. *Carcinogenesis*, **9**,9:1647-1655.

Tabor, S. (1990) Expression using the T7 RNA polymerase / promoter system. In *Current Protocols in Molecular Biology* (Ausubel, F.A., Brent, R., Kingston, R.E., Moore, D.D., Seidman, J.G., Smith, J.A. and Struhl, K. eds.) Greene Publishing and Wiley-Interscience, New York. pp:16.2.1-16.2.11.

Tamura, H., Iida, T., Watanabe, T. and Suga, T. (1990a) Long term effects of peroxisome proliferators on the balance between hydrogen peroxide generating and scavenging capabilities in the liver of Fischer 344 rats. *Toxicology*, **63**:199-213.

Tamura, H., Iida, T., Watanabe, T. and Suga, T. (1990b) Long term effects of hypolipidaemic peroxisome proliferator administration on hepatic hydrogen peroxide metabolism in rats. *Carcinogenesis*, **11**:445-450.

Tamura, H., Iida, T., Watanabe, T., Suga, T. (1991) Lack of induction of hepatic DNA damage on long term administration of peroxisome proliferators in male F344 rats. *Toxicology*, **69**:55-62

Takagi, H., Morinaga, Y., Tsuchiya, M., Ikemura, H. and Inouye, M. (1988) Control of folding proteins secreted by a high expression secretion vector, pIN-III-ompA: 16-fold increase in production of active subtilisin E in *Escherichia coli*. *Bio / Technology*, **6**:948-950.

Takagi, A., Sai, K., Umemura, T., Hasegawa, R. and Kurokawa, Y. (1990) Significant increase in 8-hydroxyguanosine in liver DNA of rats following short term exposure to peroxisome proliferators di(2-ethylhexyl)phthalate and di(2-ethylhexyl)adipate. *Japanese Journal of Cancer Research* **81**:213-215

Takagi, A., Sai, K., Umemura, T., Hasegawa, R. and Kurokawa, F. (1991) Short term exposure to peroxisome proliferators, perfluorooctanoic acid and perfluorodecanoic acid causes significant increases of 8-hydroxydeoxyguanosine in liver DNA of rats. *Cancer Letters*, **57**:55-60.

Thompson, J.D., Higgins, D.G. and Gibson, T.J. (1994) Clustal-W improving the sensitivity of progressive multiple sequence alignment through sequence weighting, position-specific gap penalties and weight matrix choice. *Nucleic Acids Research*, **22**:4673-4680.

Tontonoz, P., Hu, E., Graves, R.A., Budavari, A.I. and Spiegelman, B.M. (1994a) mPPAR γ 2: Tissue-specific regulator of an adipocyte enhancer. *Genes and Development*, **8**:1224-1234.

Tontonoz, P., Graves, R.A., Budavari, A.I., Erdjument-Bromage, H., Lui, M., Hu, E., Tempst, P. and Spiegelman, B.M. (1994b) Adipocyte-specific transcription factor ARF6 is a heterodimeric complex of two nuclear hormone receptors, PPAR γ and RXR α . *Nucleic Acids Research*, **22**,25:5628-5634.

Tucker, M.J. and Orton, T.C (eds). (1995) Comparative toxicology of hypolipidaemic fibrates. London, Taylor and Francis.

Tugwood, J.D., Aldridge, T.C., Lambe, K.G., MacDonald, N. and Woodyatt, N.J. (1996) in Peroxisomes: Biology and role in toxicology and disease (Reddy, J.K., Suga, T., Mannaerts, G.P., Lazarow, P.B. and Subramani, S. Eds.). Annals of the New York Academy of Sciences, **804**:252-265.

Tugwood, J.D., Issemann, I., Anderson, R.G., Bundell, K., McPheat, W.L. and Green, S. (1992) The mouse peroxisome proliferator activated receptor recognises a response element in the 5' flanking sequence of the rat acyl-CoA oxidase gene. The EMBO Journal, **11**,2:433-439.

van den Bosch, H., Schutgens, R.B.H., Wanders, R.J.A. and Tager, J.M. (1992) Biochemistry of peroxisomes. Annual Review of Biochemistry, **61**:157-197.

van der Leede, B.M., van den Brink, C.E. and van der Saag, P.T. (1993) Retinoic acid receptor and retinoid X receptor expression in retinoic acid-resistant human tumour cell lines. Molecular Carcinogenesis, **8**:112-122.

Varanasi, U., Chu, R., Huang, Q., Castellon, R., Yeldandi, A.V. and Reddy, J.K. (1996) Identification of a peroxisome proliferator-responsive element upstream of the human peroxisomal fatty acyl-coenzyme A oxidase gene. The Journal of Biological Chemistry, **271**,4:2147-2155.

Vidal-Puig, A., Jimenez-Linan, M., Lowell, B.B., Hamann, A., Hu, E., Spiegelman, B., Flier, J.S. and Moller, D.E. (1996) Regulation of PPAR γ gene expression by nutrition and obesity in rodents. Journal of Clinical Investigation, **97**,11:2553-2561.

Voegel, J.J., Heine, M.J.S., Zechel, C., Chambon, P. and Gronemeyer, H. (1996) TIF2, a 160 kDa transcriptional mediator for the ligand-dependent activation function AF-2 of the nuclear receptors. *The EMBO Journal*, **15**, 14:3667-3675.

Vom Baur, E., Zechel, C., Heery, D., Heine, M.J.S., Garnier, J.M., Vivat, V., Le Douarin, B., Gronemeyer, H., Chambon, P. and Losson, R. (1996) Differential ligand-dependent interactions between the AF-2 activating domain of nuclear receptors and putative transcriptional intermediary factors mSUG1 and TIF1. *The EMBO Journal*, **15**, 1:110-124.

Vu-Dac, N., Schoonjans, K., Laine, B., Fruchart, J-C., Auwerx, J. and Staels, B. (1994) Negative regulation of the human apolipoprotein A-I promoter by fibrates can be attenuated by the interaction of the peroxisome proliferator activated receptor with its response element. *The Journal of Biological Chemistry*, **269**,49:31012-31018.

Ward, J.M., Diwan, B.A., Ohshima, M., Hu, H., Schuller, H.M. and Rice, J.M. (1986) Tumour-initiating and promoting activities of di(2-ethylhexyl)phthalate *in vivo* and *in vitro*. *Environmental Health Perspectives*, **65**:279-291.

Ward, J.M., Ohshima, M., Lynch, P. and Riggs, C. (1984) Di(2-ethylhexyl)phthalate but not phenobarbital promotes N-nitrosodiethylamine-initiated hepatocellular proliferative lesions after short term exposure in male B6C3F1 mice. *Cancer Letters*, **24**:49-55.

Ward, J.M., Rice, J.M, Creasia, D., Lynch, P. and Riggs, C. (1983) Dissimilar patterns of promotion by di(2-ethylhexyl)phthalate and phenobarbital of hepatocellular neoplasia initiated by diethylnitrosamine in B6C3F1 mice. *Carcinogenesis*, **4**, 8:1021-1029.

Warren, J.R., Simmon, V.F. and Reddy, J.K. (1980) Properties of hypolipidaemic peroxisome proliferators in the lymphocyte [³H]thymidine and *Salmonella* mutagenesis assays. *Cancer Research*, **40**:36–41.

Weiss, P and Bianchine, J.R. (1970) The effect of clofibrate on vitamin E concentrations in the rat. *Atherosclerosis*, **11**:203–205.

Werman, A., Hollenberg, A., Solanes, G., Bjorbaek, C, Vidal-Puig, A.J. and Flier, J.S. (1997) Ligand-independent activation domain in the N terminus of peroxisome proliferator-activated receptor γ (PPAR γ). *The Journal of Biological Chemistry*, **272**, 32:20230–20235.

Williams, G., Ruegg, N., Birch, A., Weber, C., Hofstadter, K., Robinson, J.A., Aguet, M., Garotta, G., Schlatter, D. and Huber, W. (1995) Dissection of the extracellular human interferon-gamma receptor alpha chain into 2 immunoglobulin like domains-Production in an *Escherichia coli* thioredoxin gene fusion expression system and recognition by neutralising antibodies. *Biochemistry*, **34**, 5:1787–1797.

Wilson, T.E., Fahrner, T.J. and Milbrandt, J. (1993) The orphan receptors NGFI-B and steroidogenic factor I establish monomer binding as a 3rd paradigm of nuclear receptor binding. *Molecular and Cellular Biology*, **13**, 9:5794–5804.

Wilson, T.E., Paulsen, R.E., Padgett, K.A. and Milbrandt, J. (1992) Participation of non-zinc finger residues in DNA binding by two nuclear orphan receptors. *Science*, **256**:107–110.

Wisconsin Package version 9.0, Genetics Computer Group, Madison, Wisc. USA.

Xing, G., Zhang, L., Heynen, T., Yoshikawa, T., Smith, M., Weiss, S. and Detera-Wadleigh, S. (1995) Rat PPAR δ contains a CGG triplet repeat and is prominently expressed in the thalamic nuclei. *Biochemical and Biophysical Research Communications* **217**, 3:1015–1025.

Xu, R.B., Liu, Z.M. and Zhao, Y. (1991) A study on the circadian rhythm of glucocorticoid receptor. *Neuroendocrinology*, **53**(suppl. 1):31-36.

Yamada, J., Sugiyama, H., Watanabe, T. and Suga, T. (1995) Suppressive effect of growth hormone on the expression of peroxisome proliferator-activated receptor in cultured hepatocytes. *Research Communications in Molecular Pathology and Pharmacology*, **90**,1:173-176.

Yamaoto, K., Volki, A. and Fahimi, H.D. (1992) Investigation of peroxisomal lipid β -oxidation enzymes in guinea pig liver peroxisomes by immunoblotting and immunocytochemistry. *The Journal of Histochemistry and Cytochemistry*, **40**, 12:1909-1918.

Zechel, C., Shen, X-Q., Chambon, P. and Gronemeyer, H. (1994) Dimerization interfaces formed between the DNA binding domains determine the cooperative binding of RXR/RAR and RXR/TR heterodimers to DR5 and DR4 elements. *The EMBO Journal*, **13**,6:1414-1424.

Zelent, A., Mendelsohn, C., Kastner, P., Krust, A., Garnier, J.M., Ruffenach, F., Leroy, P. and Chambon, P. (1991) Differentially expressed isoforms of the mouse retinoic acid receptor β are generated by usage of two promoters and alternative splicing. *Embo Journal*, **10**:71-81.

Zhang, B., Marcus, S.L., Sajjadi, F.G., Alvares, K., Reddy, J.K., Subramani, S., Rachubinski, R.A. and Capone, J.P. (1992) Identification of a peroxisome proliferator-responsive element upstream of the gene encoding rat peroxisomal enoyl-CoA hydratase/ 3-hydroxyacyl-CoA dehydrogenase. *Proceedings of the National Academy of Sciences USA*, **89**:7541-7545.

Zhang, Q-X., Hilsenbeck, S.G., Fuqua, S.A.W. and Borg, A. (1996) Multiple splicing variants of the estrogen receptor are present in individual human breast tumours. *Journal of Steroid Biochemistry and Molecular Biology*, **59**, 3/4:251-260.

Zhu, Y., Qi, C., Jain, S., Rao, M.S. and Reddy, J.K. (1997) Isolation and characterisation of PBP, a protein that interacts with peroxisome proliferator-activated receptor. *The Journal of Biological Chemistry*, **272**, 41:25500-25506.

Zhu, Y., Qi, C., Korenberg, J.R., Chen, X-N., Noya, D., Rao, S. and Reddy, J.K. (1995) Structural organization of mouse peroxisome proliferator-activated receptor γ (mPPAR γ) gene: Alternative promoter use and different splicing yield two mPPAR γ isoforms. *Proceedings of the National Academy of Sciences USA* **92**: 7921-7925.